Testing the Efficacy of GDF6 as a Biological Therapy for the Treatment of Intervertebral Disc Degeneration

A thesis submitted to the University of Manchester for the degree of Doctor of Philosophy in the Faculty of Medical and Human Sciences

2015

Louise Elizabeth Clarke

School of Medicine

Table of Contents

CHAPTER 2: MATERIALS AND METHODS

CHAPTER 3: DIFFERENTIATION OF HUMAN MESENCHYMAL STEM CELLS TO A NUCLEUS PULPOSUS PHENOTYPE USING MEMBERS OF THE TGF-β SUPERFAMILY

CHAPTER 4: EFFECT OF GDF6, HYPOXIA AND LOAD ON MESENCHYMAL STEM CELL DIFFERNTIATION

CHAPTER 5: A COMPARATIVE STUDY OF THE RESPONSE OF PRE-DIFFERENTIATED MSCS AND MATURE NP CELLS TO THE PRO-INFLAMMATORY NICHE OF THE INTERVERTEBRAL DISC

CHAPTER 7: ASSESSMENT OF THE EFFICACY OF GDF6 AS A BIOLOGICAL THERAPY: DEVELOPMENT OF AN EX VIVO DEGENERATE IVD MODEL AND PRELIMINARY ASSESSMENT OF A MICROPARTICLE GROWTH FACTOR DELIVERY SYSTEM

List of Tables

List of Figures

List of Abbreviations

°C	Degrees Celsius
ΔCt	Delta cycle threshold
µg	Microgram
µl	Microlitre
µm	Micrometer
3D	Three-dimensional
AC	Articular chondrocyte
ACAN	Aggrecan
ADAMTS	A disintegrin and metalloproteinase with thrombospondin motif
AD-MSCs	Adipose derived mesenchymal stem cells
AF	Annulus fibrosus
AFM	Atomic force microscopy
aNPCs	AD-MSCs differentiated with GDF6
BDNF	Brain-derived neurotrophic factor
BMP	Bone morphogenic protein
BM-MSCs	Bone marrow mesenchymal stem cells
bp	Base pair
BSA	Bovine serum albumin
CAXII	Carbonic anhydrase-12
cDNA	Complimentary deoxyribonucleic acid
CEP	Cartilaginous endplate
cm	Centimetre
CO_2	Carbon dioxide
COL2A1	Collagen, type II, alpha 1
COMP	Cartilage oligomeric protein
CS	Chondroitin sulphate
Ct	Cycle threshold
DMEM	Dulbecco's modified eagles medium
dNTP	Deoxyribonucleotide triphosphate
ECM	Extracellular matrix
EDTA	Ethylenediaminetetraacetic acid
EIF2B1	Eukaryotic translation initiation factor 2B
ELISA	Enzyme-linked immunosorbant assay
FBS	Foetal bovine serum
FOXF1	Forkhead box F1
GAG	Glycosaminoglycan
GAPDH	Glyceraldehyde-3-phosphate dehydrogenase
GDF5	Growth Differentiation Factor 5
GDF6	Growth Differentiation Factor 6
HA	Hyaluronic acid
HBSS	Hank's balanced salt solution
H&E	Haematoxylin and eosin
IL-1	Interleukin-1

IL-1R	Interleukin-1 receptor
IL-1RA	Interleukin-1 receptor antagonist
IMS	Industrial methylated spirits
IVD	Intervertebral disc
KRT8	Cytokeratin8
KRT18	Cytokeratin-18
KRT19	Cytokeratin-19
L	Litre
LBP	Low back pain
M	Molar
MCT	Microcentrifuge tube
ml	Millilitre
mm	Millimetre
mM	Millimolar
MMP	Matrix metalloproteinase
MPa	Megapascal
MRI	Magnetic resonance imaging
mRNA	Message ribonucleic acid
MRPL19	Mitochondrial ribosomal protein L19
MSC	Mesenchymal stem cell
NC	Notochordal
ng	Nanogram
NGF	Neural growth factor
nm	Nanometre
NP	Nucleus pulposus
O_2	Oxygen
PBS	Phosphate buffered saline
PG	Proteoglycan
qPCR	Quantitative polymerase chain reaction
RNA	Ribonucleic acid
RT-PCR	Reverse transcription polymerase chain reaction
SAM	Scanning acoustic microscopy
SE	Standard error of the mean
Sox	Sry-related high mobility group box
T	Brachyury (gene notation)
TGF-β	Transforming growth factor-β
TIMP	Tissue inhibitor of metalloproteinase
TNF-α	Tumour necrosis factor-α
VB	Vertebral body
VCAN	Versican
VEGF	Vascular endothelial growth factor
v/v	volume/volume
w/v	weight/volume

Abstract

Intervertebral disc (IVD) degeneration is associated with low back pain (LBP), which affects approximately 80% of the global population and is a huge socioeconomic burden. Presently, conservative and surgical therapies are inadequate and have poor long term outcomes; hence there is a necessity for alternative options, such as cell-based therapies, that will address the underlying pathogenesis. Mesenchymal stem cells (MSCs), specifically bone marrow (BM-MSCs) and adipose derived (AD-MSCs) have been shown to differentiate to a nucleus pulposus (NP) like cell (discogenic differentiation); although to date optimum discogenic differentiation protocols have not been defined. The most common method is the use of a transforming growth factor (TGF-β) however, this growth factor is commonly used to induce chondrogenesis. Thus, there is a need to identify growth factors or small molecules that can induce discogenic differentiation and appropriate matrix formation, particularly when exposed to IVD microenvironmental factors. The initial objective of the study was to investigate the discogenic potential of BM-MSCs and AD-MSCs when cultured with members of the TGF-β superfamily. Results showed growth differentiation factor 6 (GDF6) induced an improved discogenic phenotype in human AD-MSCs (aNPCs) resulting in a proteoglycan rich matrix, compared to growth differentiation factor 5 (GDF5) or TGF-β treatment or BM-MSCs exposed to the same growth factors. AD-MSCs supplemented with GDF6 were also exposed to hypoxia and load to mimic the IVD microenvironment. Whilst hypoxia and load increased discogenic differentiation, matrix synthesis was aberrantly altered resulting in a stiffer matrix than that produced in standard conditions. Another feature of the degenerate IVD environment, to which any implanted cells will be subjected to, is the milieu of cytokines specifically interleukin-1β (IL-1β). Thus, the response of aNPCs to IL-1β was compared to native degenerate NP cells. Interestingly, IL-1β had no detrimental catabolic effect on aNPCs suggesting that these cells may be able to withstand the effects of the IL-1β milieu of the degenerate IVD niche. The effect of GDF6 on native NP cells was also investigated and found to restore a non-degenerate NP phenotype by upregulating NP marker gene expression and increasing ECM synthesis. Furthermore, when NP cells were treated with GDF6 and exposed to IL-1β there was still an upregulation of ECM and suppression of catabolic genes, suggesting GDF6 may have a protective role. Having established the efficacy of GDF6, preliminary experiments were undertaken to assess the feasibility of using GDF6 loaded microparticles to provide sustained delivery of the growth factor; results were comparable to exogenous delivery of GDF6. In addition, initial studies were undertaken to develop an *ex vivo* IVD model in order to test the efficacy of regenerative therapies such as those described throughout the thesis. Taken together, this study shows that GDF6 is a promising biological therapy for IVD regeneration strategies for the treatment of IVD degeneration.

Declaration

No portion of the work referred to in the thesis has been submitted in support of an application for another degree or qualification of this or any other university or other institute of learning

Copyright Statement

Acknowledgements

Firstly I wish to thank my supervisors Professor Judith Hoyland and Dr. Stephen Richardson for their support and advice during this four year course. For all of the hours spent in meetings, going through data, planning experiments, writing abstracts and papers, producing posters, the list is endless and I just want to say thank you for all of the encouragement throughout.

Additionally I would like to thank the technical staff, Pauline, Andy, Sonal and Daman, whose expertise in the techniques used throughout this thesis is second to none. I would particularly like to thank Andy for his patience when teaching me how to utilise the loading rig and how to use a screwdriver. I would also like to thank Dr James McConnell for all of his help and advice for both SAM and AFM techniques.

I would also like to thank all of my colleagues throughout my time here, many of which have come and gone, Francesca, Kim, Jude, Shahnaz, Nicola, Chris, Russell, Julen, Matt, Ricardo, Matt, Hamish, Eric and Mi. Thank you for all of the tea breaks, kebab Fridays and I wish you all the greatest of luck in your future career pursuits.

On a more personal note, I couldn't have done this without the support of my family, particularly my parents, Judith and Paul. Thank you so much for letting me live back at home in order to write my thesis and all of the support, encouragement and the 'you're nearly there's' over the past four years, I owe you big time! Thank you also to Lisa and my fellow Parkvillians who were always on hand for a chat, encouragement and glass of wine, thank you! Finally, thank you to Andy who over the past 19 months has given me great motivation to continue and strive to succeed and hand in my thesis. Thank you so much for your support and now I can finally say 'I've done it!' Thank you to you all!!

Chapter 1

General Introduction

1.1Thesis/Study Overview

Lower back pain (LBP) affects a large proportion of the global population and has been associated with intervertebral disc (IVD) degeneration. At present existing therapeutic options are limited and offer poor long-term efficacy as they do not tackle the underlying pathogenesis and aberrant cell biology of the disorder. Hence, investigation and research into biological therapies has become a focal point to improve clinical treatments and to target treatment at the molecular and cellular level. Imperative to fulfilling this aim is the consideration of the appropriate cell population for tissue engineering strategies, as there are a number of studies investigating different cell sources including human mesenchymal stem cells (MSCs). In addition, the growing understanding of the molecular phenotype of nucleus pulposus (NP) cells and the defining NP marker genes can allow tailored differentiation approaches that are more appropriate to induce discogenic differentiation as opposed to current protocols. Importantly, for cellular therapies to be clinically transferable the response of such therapies to the IVD microenvironment must be elucidated to ensure cells are still functional and react favourably to the degenerate IVD niche. Finally, the delivery of the therapy is also important whether this be a specific biomaterial or direct injection into the IVD. Therefore in consideration of all these aspects, the focus of the study was to develop a biological/cell based therapy for regeneration of the degenerate IVD and tests its efficacy in a degenerate ex vivo model to assess the ability to restore tissue integrity and biomechanical properties.

1.2 Lower Back Pain

The human spinal column is divided into four specific vertebral regions; cervical, thoracic, lumbar and sacral (Figure 1.1A) with lower back pain (LBP) relating directly to the lumbar segment. As one of the most prevalent musculoskeletal diseases in western society (Stewart et al., 2003), LBP is estimated to affect 84% of adults at one point within their lifetime, with 6.3-11.1% of the UK population experiencing chronic LBP (>3 months) (Junpier et al., 2009). As the frequency of LBP has a close association with aging (Papageorgiou et al., 1995) and an ever increasing older population, the disorder poses a huge socioeconomic burden. The collective expenditure in the UK in 2000 totalled £12 billion in costs arising annually

through loss of productivity, social benefit payments and direct and indirect cost to the healthcare system equating to 1-2% of gross national product (GDP). (Maniadakis and Gray, 2000;HS(G)96 2nd Edition.,HMSO 1997) whilst in the U.S LBP is the third most common cause of surgical procedures (Andersson, 1999) with an annual expenditure of approximately $85 billion (Martin et al., 2008). The precise origins of the LBP are unclear and deemed to be multifactorial, however imaging studies have strongly correlated a link between intervertebral disc (IVD) degeneration and LBP in up to 40% of cases (Cheung et al., 2009; Samartzis et al., 2011; Takatalo et al., 2011).

1.3 Intervertebral Disc Structure

The 24 articulating vertebrae of the spine are each separated by an IVD, which act as a fibrocartilaginous cushion. The discs facilitate joint movement, flexibility and enable the spine to withstand and distribute load evenly. The IVD can be separated into three defined regions: the cartilaginous endplate (CEP), the annulus fibrosus (AF) and the nucleus pulposus (NP) (Figure 1.1B and Figure 1.1C). Each region has a distinct structure and function, which all work synergistically enabling the disc to perform efficiently.

1.3.1 The Cartilaginous Endplates

The CEPs are a thin layer of hyaline cartilage which interface between the disc and the vertebral body (VB), located both superiorly and inferiorly (Raj, 2008). They are directly attached to the lamellae of the AF (Inoue, 1981) and in turn confine the NP tissue to its anatomical location (Broberg, 1983). The CEPs also act as a semi-permeable barrier providing nutrients and metabolites into the disc and the removal of waste products from the disc via diffusion between the NP, AF and VB (Roberts et al., 1989).

1.3.2 The Annulus Fibrosus

The AF is comprised primarily of highly organised type I collagen concentric lamella numbering between 10 and 25 (Marchand and Ahmed, 1990) which encompasses the NP. Based on structural and cellular differences, the AF can be divided into the inner and outer part. The outer AF is composed of lamella fibres

which are orientated at a 70^{O} angle and the adjacent lamella alternate in direction (Roughley, 2004) (Figure 1.1C) which facilitates the ability to resist tensile forces. The functionality of the AF is aided by the inclusion of elastin between collagen fibres which aids in recovery of disc shape after mechanical compression, bending or flexing (Urban and Roberts, 2003; Raj, 2008). The inner AF is a transition zone between highly ordered collagenous structure of the outer AF and the hydrated NP, comprised of a mixture of both type I and type II collagen (Bron et al., 2009; Pattappa et al., 2012).

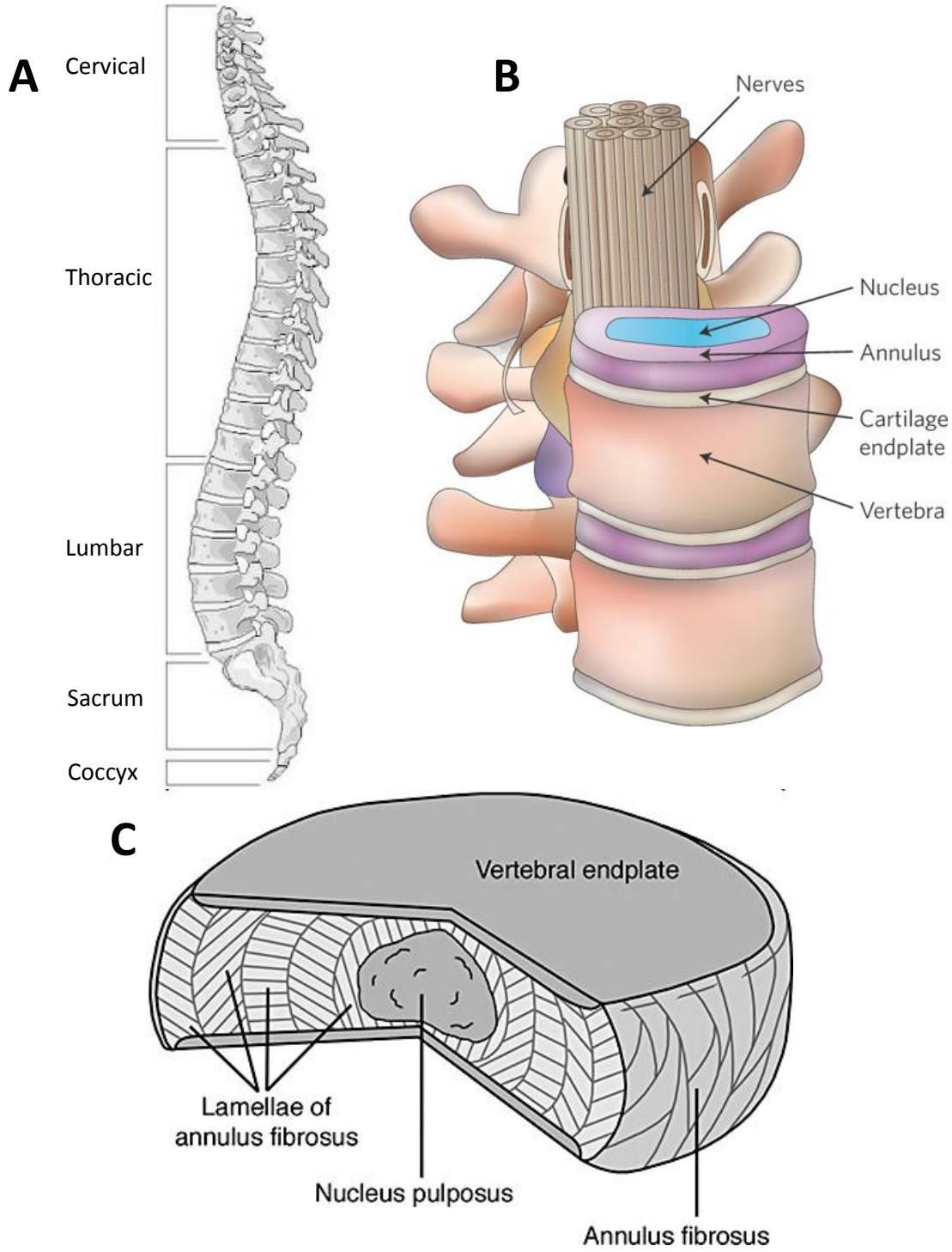

Figure 1.1 A schematic representation of the spine and intervertebral disc. **A.** Four distinct regions of the spinal column (adapted from www.gallery4share.com/v/vertebral-column-unlabelled-lateral-view [accessed 7.1.2016]). **B**. A spinal unit to show the IVD sandwiched between the vertebral bodies, separated by a superior and inferior end-plate (adapted from Hukins, 2005).**C.** The IVD comprised of a centrally located nucleus pulposus encompassed by the lamellae of the annulus fibrosus and separated from the vertebral bodies by the endplate (adapted from Raj, 2008).

1.3.3 The Nucleus Pulposus

The centrally located NP (Figure 1.1C) is morphologically very different than the AF, as it is highly hydrated and gelatinous in nature. The high proteoglycan (PG) content (predominantly aggrecan) is water imbibing and therefore maintains the hydrostatic pressure which helps the disc to resist compressive loads and distribute them uniformly (Adams and Roughley, 2006).

1.4 Cells of the Intervertebral Disc

The different regions of the disc have distinct cell morphologies, even though the IVD is one of the most cell sparse organs in the body .The CEP, AF and NP tissues comprise of approximately 15000, 9000 and 4000 cells/mm^3 respectively (Maroudas et al., 1975). In comparison to a similar cartilaginous joint, articular cartilage (AC) has a cell density of 14000-15000mm^3 (Stockwell, 1971). Irrespective of the low cell density, the cells produce a large amount of extracellular matrix (ECM).

1.4.1 Cells of the CEPs

The CEP is populated by rounded chondrocyte-like cells which are embedded in a matrix consisting of type II collagen, PGs and water (Maroudas et al., 1975, Roberts et al., 1989, Roberts et al., 1991).

1.4.2 Cells of the AF

The cells of the outer AF region are elongated fibroblast-like cells whereas cells toward the inner AF are chondrocyte like (Roberts et al., 2006) both of which align in the same orientation as the collagen fibres (Maroudas et al.,1975) and synthesise mainly type I collagen (Eyre and Muir, 1976).

1.4.3 Cells of the NP

NP cells can be described as chondrocyte-like as they are rounded in morphology and synthesise ECM components including aggrecan, type II collagen and the transcription factor SOX-9 (SRY (Sex determining region Y)-Box-9) (Sieve et al., 2002). Whilst this description is similar to classic chondrocytes of the AC, recent phenotypic studies have been undertaken to distinguish AC and NP cells (Minogue et al., 2010b, Power et al., 2011). This is described in detail in section 1.10.1.

In addition to the small rounded NP cells, a larger cell population also resides within NP tissue. The notochordal cells (NC cells) are morphologically distinct and are characterised by numerous vacuoles within the cells (80% of cell volume (Hunter, 2005)), a larger diameter compared to NP cells (25μm to 8μm (Hunter et al., 2003)) in addition to forming dense cellular networks. In humans the foetal NP is populated with an abundance of NC cells (Boos et al., 2002) that with maturity of the disc gradually disappear by adolescence and are replaced by mature NP cells. The precise mechanisms in which the NC cells are lost from the tissue is unclear, however apoptosis (Kim et al., 2005), biomechanical alterations and insufficient nutrient supply have been thought to contribute (Louman-Gardiner et al., 2011). This transition varies between species, as for humans the alteration is completed before reaching skeletal maturity whereas other smaller animals such as rodents and pigs keep their population of NC cells into adult life (Alini et al., 2008). There has been great debate about the origin of the adult NP cells, with suggestions that cells migrate or are recruited from tissues such as the AF or CEP. However, recent fate-mapping or lineage tracing studies undertaken in mice models demonstrated that adult NP cells are derived from the embryonic notochord. The studies utilised notochord specific Cre recombinase driven by either Sonic hedgehog (Shh) (Choi et al., 2008) or Noto (McCann et al., 2012) promoters. In addition, studies have demonstrated the expression of notochordal cell marker brachyury (T) by adult NP cells, signifying their notochordal origin (Minogue et al., 2010b; Weiler et al., 2010).

1.5 Extracellular Matrix (ECM) Composition of the IVD

As reviewed in section 1.3 the IVD is sparsely populated with cells, however these cells synthesise a large amount of ECM. Whilst the ECM formed is similar to that in cartilage (Figure 1.2), comprising largely of collagens and PGs, the composition of the matrix is different. It has been demonstrated that in a healthy disc that the PG: collagen ratio is 27:1, measured at the protein level (ACAN:COL2A1), in comparison to a ratio of 2:1 in the CEP (Mwale et al., 2004).

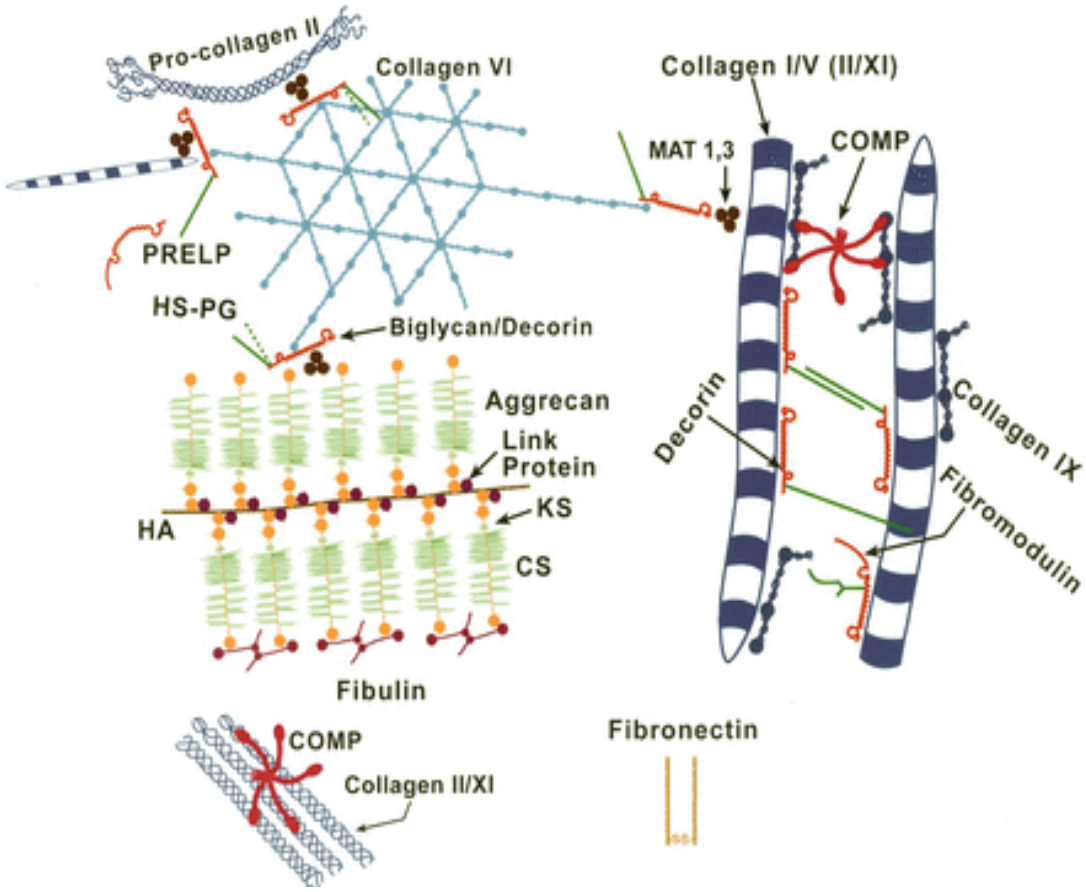

Figure 1.2 Assemblies of matrix proteins within the IVD. COMP = cartilage oligomeric protein; CS = chondroitin sulphate; KS = keratin sulphate; HA = hyaluronic acid; HS-PG = heparin sulphate proteoglycan; MAT = matrillin; PRELP = proline arginine-rich end leucine-rich repeat protein. (Heinegard and Saxne, 2011).

1.5.1 Collagens

Collagens are proteins located in the ECM of all connective tissues and are characterised by the presence of a triple helix domain. In the disc, collagen comprises approximately 70% of its dry weight (Eyre et al., 2002) and there are a variety of isoforms including types I, II, III, V, VI, IX, XI, XII and XIV (Eyre et al., 2002). The most abundant of these are type I and type II collagen. The AF ECM is predominately formed of type I organised collagen fibres which account for 50-60% of its dry weight (Bogduk and Twomey, 1987) whereas, the NP ECM contains type II collagen which are arranged sporadically and only comprised 15-20% of the weight of the dry NP (Le Maitre et al., 2007d). Together type I and II make up 80% of the total collagen found in the disc (Roberts et al., 1991) with the remaining 10-20% consisting of type VI collagen. The other collagens are present in small quantities and contribute to the organisation and mechanical stability of the ECM (Eyre and Muir, 1976, Roberts et al., 1991). Whilst type II collagen is found in both the disc and hyaline cartilage, collagen present in the disc demonstrates increased levels of hydroxylation on the proline and lysine amino acids which is thought to lead to a more protease resistant matrix (Yang et al., 1993). This demonstrates that although NP cells are described as 'chondrocyte-like' they synthesise a unique matrix that is different to that found in cartilage.

In addition to collagens, cartilage oligomeric matrix protein (COMP) is essential in the organisation of collagen fibrils in the AF ECM network and also plays a role in network stability by binding to the globular domain of type IX collagen (Feng et al., 2006, Ishii et al., 2006). Taken together, the collagen network of the disc offers tensile strength and constrains the NP to resist compressive forces.

1.5.2 PGs

In the NP, PGs account for 65% of the dry weight of the tissue, with the predominant PG being aggrecan. The vastly hydrated ECM in the NP can be attributed to the high PG content, which is responsible for attracting water into the tissue due to the negative charge. A PG is typically made up of a core protein that is covalently bonded to side chains of negatively charged GAGs. As shown in Figure 1.3, the

aggrecan core protein is bonded to sulphated GAG chains of keratin and chondroitin sulphate. In addition, aggrecan has a hyaluronan binding globular domain and a C-type lectin motif which allows it to form large aggregates and bind to other proteins (Iozzo and Murdoch, 1996, Wu et al., 2005).

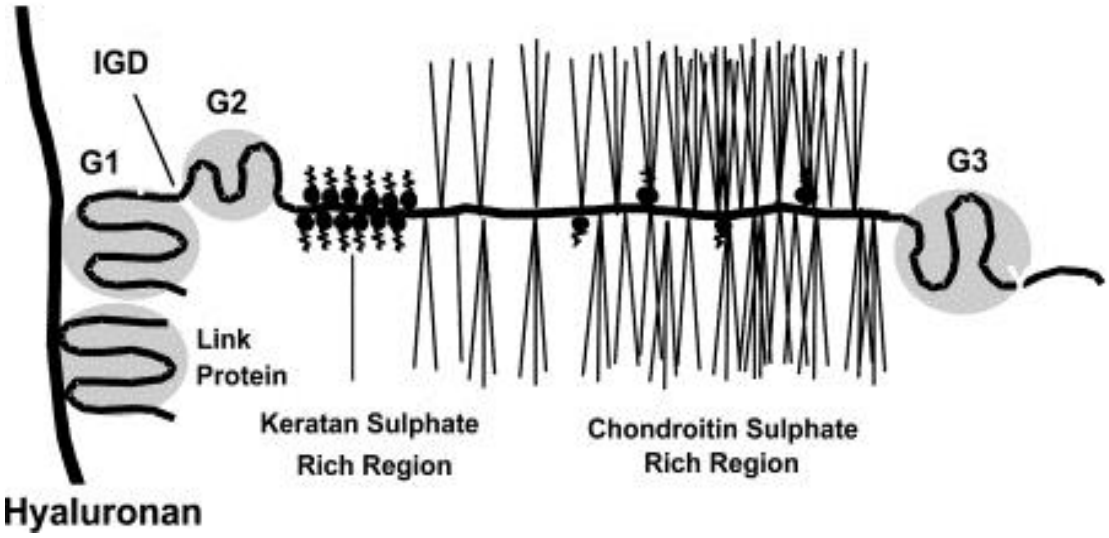

Figure 1.3 A diagrammatic representation of an aggrecan molecule.
It contains two N-terminal globular domains, G1 and G2, separated by an IGD (interglobular domain), followed by a GAG-attachment region and a C-terminal globular domain, G3 (Adapted from Porter et al., 2005).

Another PG present in the ECM of the disc is versican, which is partially homologous to aggrecan however it only contains chondroitin sulphate GAG chains resulting in a lower negative charge hence less potential to bind water (Wu et al., 2005). As such, it is predominately located in the AF as a component of the translamellar crossbridges (Melrose et al., 2008).In addition to the large aggregating PGs, there are a number of small, leucine-rich proteoglycans (SLRPs) found in the disc, including biglycan, decorin, lumican and fibromodulin. These molecules have a smaller protein core and fewer GAG chains and are found in greater amounts in the AF (Inkinen et al., 1998). Their function is to interact with various collagens including type I, II, VI and guide the assembly of the collagen network (Wiberg et al., 2002).

1.5.3 Matrix Degrading Enzymes

In a healthy IVD, the ECM is broken down and remodelled, as part of the homeostatic upkeep; this is undertaken by metalloproteinases and their inhibitors. There are two main families of matrix degrading enzymes, matrix metalloprotinases (MMPs) and a disintegrin and metalloproteinase with thrombospondin motif (ADAMTS') (Vo et al., 2013). The MMPs can be further classified into 'collagenases' (MMP -1, -8 and -13) (Roberts et al., 2000, Le Maitre et al., 2004a), 'gelatinases' (MMP-2 and -9) (Hsieh and Lotz., 2003, Crean et al., 1997), 'stromelysin' (MMP-3) (Le Maitre et al., 2004a) and 'matrilysin' (MMP -7) (Roberts et al., 2000).Additionally 'aggrecanases' that degrade aggrecan are also found in the disc (ADAMTS-1,-4,-5,-9,-15) (Sivan et al., 2013; Pockert et al., 2009). The activity of the enzymes are regulated by a family of proteins termed tissue inhibitors of metalloprotinases (TIMPs), TIMPs -1 and -2 inhibit MMPs and TIMP-3 is an inhibitor of ADAMTS-4 and -5 (Kashiwagi et al., 2001).

1.6 IVD Niche

The IVD milieu can be described as a hostile environment. The cells within the disc require nutritional pathway in order to maintain the cells and to remove metabolic wastes. The foetal and infant disc has an ample blood supply with vessels penetrating into the disc, but as the disc matures the degree of vascularisation decreases immensely with parts of the disc being up to 8mm from the closest blood supply (Roughley, 2004; Urban et al., 2004; Choi, 2009). Hence, the mature disc is the largest avascular and aneural organ in the human body and is reliant on alternative methods of obtaining nutrition. The nutritional pathway is primarily diffusion through the CEPs which is dependent on the solute charge and size. When this route is compromised, for example via either calcification or ossification of the end plates with age, this can result in or contribute to disc degeneration (Urban et al., 2004).

As the disc is hypoxic in nature (1-5% oxygen) the cells within the disc rely on oxygen independent-anaerobic metabolism, through the process of glycolysis in which glucose is metabolised into lactic acid and ATP (Holm et al., 1981). Another factor that influences cell metabolism is the pH levels within the disc. As Figure 1.4

demonstrates in the centre of the IVD the level of lactic acid is increased, due to the distance of diffusion, which results in an acidic pH (Holm et al., 1981).The disc also has a low glucose concentration (1.2nmol/mm^3) (Soukane et al., 2007) and the constant subjection to mechanical load is also homeostatic to the disc; this is described in greater detail in section 1.8.1.2.

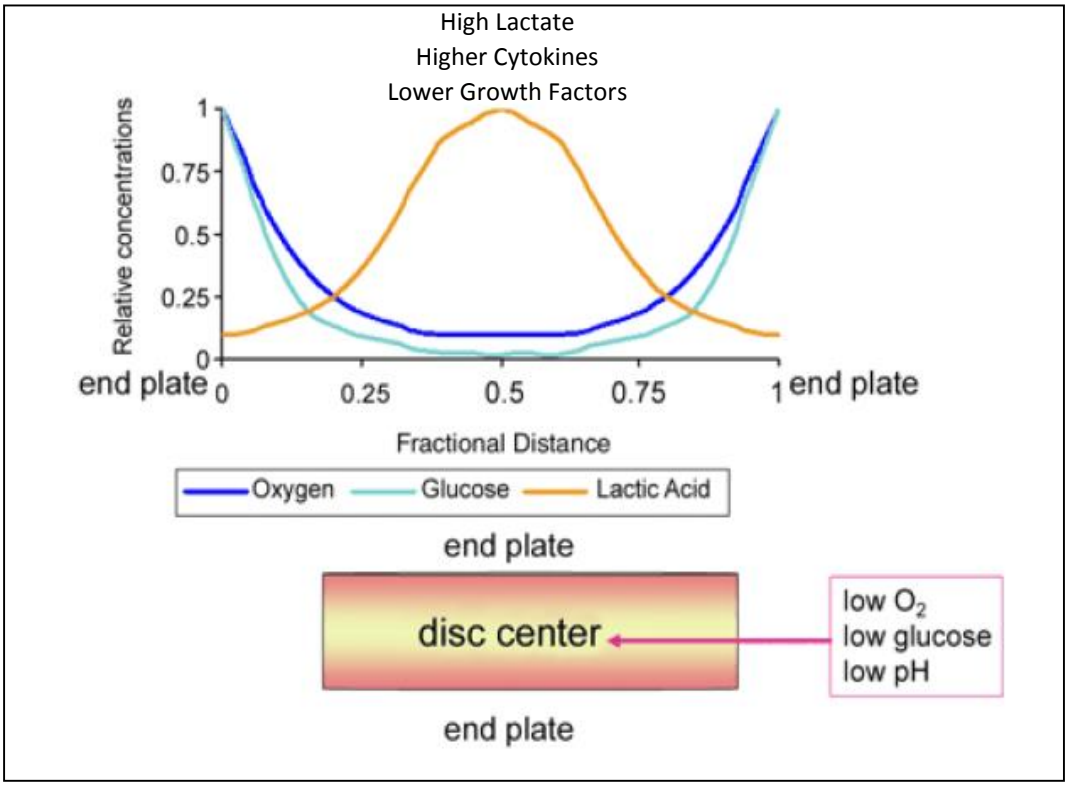

Figure 1.4 Schematic diagram of oxygen, glucose, lactic acid and pH levels within the IVD. The microenvironment of the IVD shows low levels of oxygen and glucose in the centre of the disc whilst there are high levels of lactic acid resulting in a low pH (Adapted from Urban et al., 2004).

Native NP cells have demonstrated a metabolic adaptation to the hypoxic environment, which was highlighted by Risbud and colleagues (Risbud et al., 2006). Hypoxia-inducible factor 1-α (HIF-1α) is an important transcription factor that allows a cell to switch from aerobic to anaerobic metabolism (Firth et al., 1995), hence is degraded under normoxic conditions but stable under hypoxic conditions (Wang et al., 1995). In the study by Risbud et al., it was shown that unlike other cells, there was not a significant upregulation of HIF-1α when NP cells were cultured in hypoxia suggesting that the cells are adapted to the low oxygen environment and that

normoxic stabilisation of HIF-1α is characteristic of NP cells (Risbud et al., 2006). However, whilst NP cells are adapted to this harsh environment, for cell-based therapies to be successful, understanding the interactions between implanted cells and factors within the IVD microenvironment is important in order to understand whether cells will function appropriately

1.7 Aging of the IVD

With the progression of age there are a number of morphological and molecular alterations that occur, which are comparable with changes observed in the degenerate disc. At a cellular level, (discussed in section 1.4.3), within the first decade the distinct NC cell population present in immature discs diminishes to an imperceptible level (Hunter et al., 2004). Subsequently the cells are no longer morphologically identifiable as NC cells and the 'chondrocyte-like' adult NP cells appear simultaneously (Hunter et al., 2004). As the disc ages and matures the density of NP cells reduces significantly to approximately 10% of that in a newborn (Liebscher et al., 2011). At a gross morphological level changes occur such as loss of disc height, dehydration of the tissue and discolouration of the nucleus (Hormel et al., 1991). These alterations are due to fundamental changes in the ECM of the IVD, as with age there is a decrease in both collagen and PG formation (Singh et al., 2009). A decrease in PG reduces the ability of the disc to imbibe water and hydrate the tissue, resulting in a lower water content (Antoniou et al., 1996) and a reduction in disc height as demonstrated by MRI (Frobin et al., 2001). Discolouration of the tissues, as shown in Figure 1.5, has been attributed to an accumulation of products from non-enzymatic glycosylation (Hormel et al., 1991).

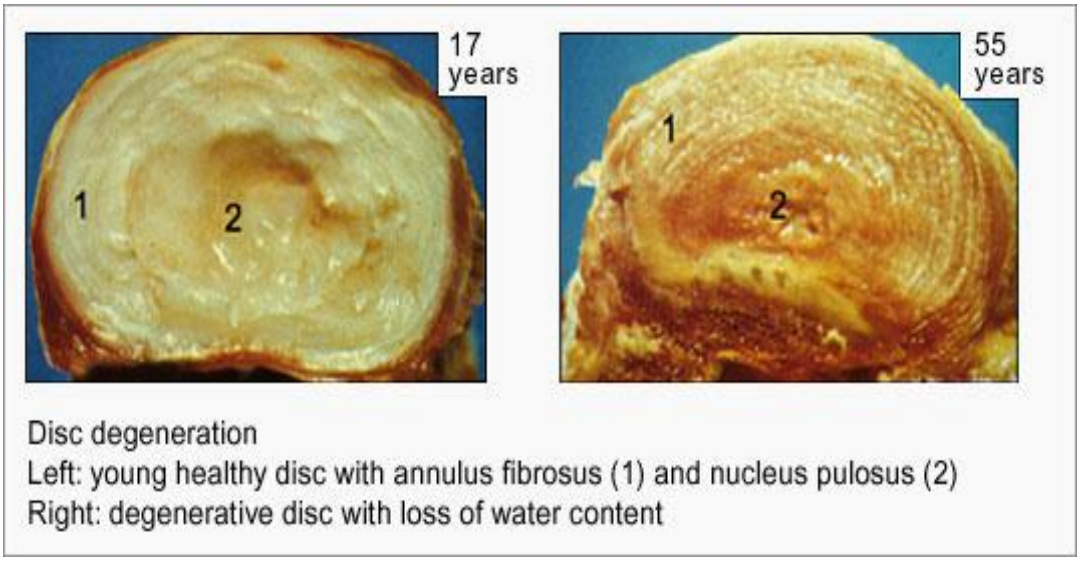

Figure 1.5 A photographic comparison between a healthy and degenerate disc. The image on the left depicts a young healthy disc from a 17 year old patient demonstrating a hydrated NP and ordered lamellae in the AF. The image on the right shows a degenerate disc from a 55 year old patient, with discolouration, granular NP and disordered AF (Adapted from http://www.eurospine.org/motion-preservation.html [accessed 7.1.2016]).

The changes described in the ECM subsequently lead to impaired mechanical function as the disc is unable to distribute load uniformly (Costi et al., 2008). Hence the forces are unevenly reassigned to the AF which progressively disrupts both the AF structure and loading properties (O'Connell et al., 2009).

1.8 Intervertebral Disc Degeneration

1.8.1 Risk factors

The precise aetiology of disc degeneration is not fully understood as it can be deemed as a multifactorial disorder with a range of environmental and genetic factors having been identified. It is considered to be a pathological process comparable to natural age-related changes except it occurs at an accelerated rate.

1.8.1.1Genetic Association

Genetic predisposition to the development of disc degeneration has been well studied at both a familial and protein level. Studies have demonstrated a significant correlation in discogenic pain in relatives of patients with LBP compared to nonrelated controls (Postacchini et al., 1988; Bijkerk et al., 1999). Matsui and colleagues highlighted the increased severity of radiographic markers of degeneration when the patient had a first order relative whom had previously undergone spinal surgery (Matsui et al., 1998). In addition a series of twin studies has illustrated that hereditary predisposition to degeneration has a greater influence than environmental factors. Overall the studies estimate that genetic factors can account for 75% of susceptibly to degeneration (Battie et al., 1995a, Battie et al., 1995b, Battie et al., 2009).

Whilst familial studies show a clear link between genetics and disc degeneration they do not provide candidate genes that are responsible, hence numerous studies have investigated this (summarised in Table 1.1).

Table 1.1 Genes Associated with IVD Degeneration in Human Population

Protein	IVD Function	Alleles with Variants
Type IX Collagen	ECM support	COL9A2 COL9A3
Vitamin D Receptor	Alters GAG structure	TaqI Apa
Type I Collagen	AF support	COL1A1
Aggrecan	NP osmotic gradient	CS1
MMP-3	ECM degradation	5A 6A

(Adapted from Kepler et al., 2013)

Degeneration has been associated with polymorphisms in the SP1 allele of COL1A1 in a number of populations, Dutch (Pluijm et al., 2004), Finnish (Videman et al., 2009) and Greek (Tilkeridis et al., 2005). Alleles of the genes COL9A2 and COL9A3 which encode the matrix protein type IX collagen have been associated with degeneration in two populations (Finnish (Annunen et al., 1999) and Chinese (Jim et al., 2005)). Interestingly the Trp3 allele associated with sciatica in the Finnish population was absent in the Chinese population indicating that genetic risk factors can vary between ethnicities.

A variable number of tandem repeats (VNTR) polymorphism in the CS1 subunit of the aggrecan gene alters the PGs ability to bind to the GAG side chain chondritin sulphate which can change the physical properties and increase the risk of degeneration (Solovieva et al., 2007). This polymorphism has been identified in Japanese (Kawaguchi et al., 1999), Iranian (Mashayekhi et al., 2010) and Turkish (Eser et al., 2010) ethnicities. Similarly polymorphisms in the vitamin D receptor have been linked with insufficient sulphation of GAGs affecting the ECM function (Kepler et al., 2013).

As a degradative enzyme is it no surprise that mutations in the MMP-3 gene have been linked to disc degeneration. A polymorphism in the promoter region of the gene increases protein expression of MMP-3 which leads to increased matrix degradation (Takahashi et al., 2001).

1.8.1.2 Mechanical Load

Due to the upright nature of the torso the disc is constantly subjected to compressive and dynamic loading which is important for disc homeostasis. Matsumoto and colleagues (Matsumoto et al., 1999) have demonstrated that biomechanical loading is essential to maintain both phenotypic and functional characteristics of NP cells in rat studies (Matsumoto et al., 1999). Despite the positive anabolic effects of physiological loading, excessive or altered biomechanics such as increased frequency or magnitude can be detrimental to the disc (MacLean et al., 2004; Stokes and Iatridis, 2004; Walsh and Lotz, 2004). On the other hand, it has been demonstrated that discs exposed to no load, static load or high loading regimes

results in an increase in catabolic gene expression (Paul et al., 2011). In a study by Walter and colleagues (Walter et al., 2011) the importance of evenly distributed load is highlighted by comparison of axial compression applied either asymmetrically or uniformly to an IVD. Results showed a down regulation of anabolic genes and an up regulation of catabolic markers as well as induction of cell death and a loss of ACAN from the tissue (Walter et al., 2011).

1.8.1.3 Lifestyle and Environment

There are a number of lifestyle and environmental factors that can influence the development of disc degeneration. One particular factor is manual labour employment which comprises of heavy lifting, repeatedly bending, twisting and exposure to vibrations. Studies have demonstrated that alterations to the disc exceed those who work in a sedentary environment (Battie et al., 1995b, Videman et al., 1990). Additionally, exposure to vibrations has been found to impair disc nutrition by altering the peripheral circulation in the CEP and AF (Elfering et al., 2002, Kumar et al., 1999). Other lifestyle aspects include smoking which can alter blood flow and vessel walls to affect the nutritional pathway (Ernst, 1993; Miller et al., 2000) and nicotine has been shown to have a detrimental effect on disc cells (Akmal et al., 2004). Additionally obesity and an increased body mass index (BMI) have been identified as positive risk factors for the development of disc degeneration (Deyo and Bass, 1989; Elfering et al., 2002; Weiler et al., 2011).

1.8.2 Characteristic Features of Disc Degeneration

Degeneration of the IVD is progressive in nature and exhibits characteristic alterations that are seen at a macroscopic level (Figure 1.6). Morphological changes include loss of disc height, absence of regional distinction between the NP and AF, formation of fissures and nerve in growth into the AF (Freemont et al., 2002a).

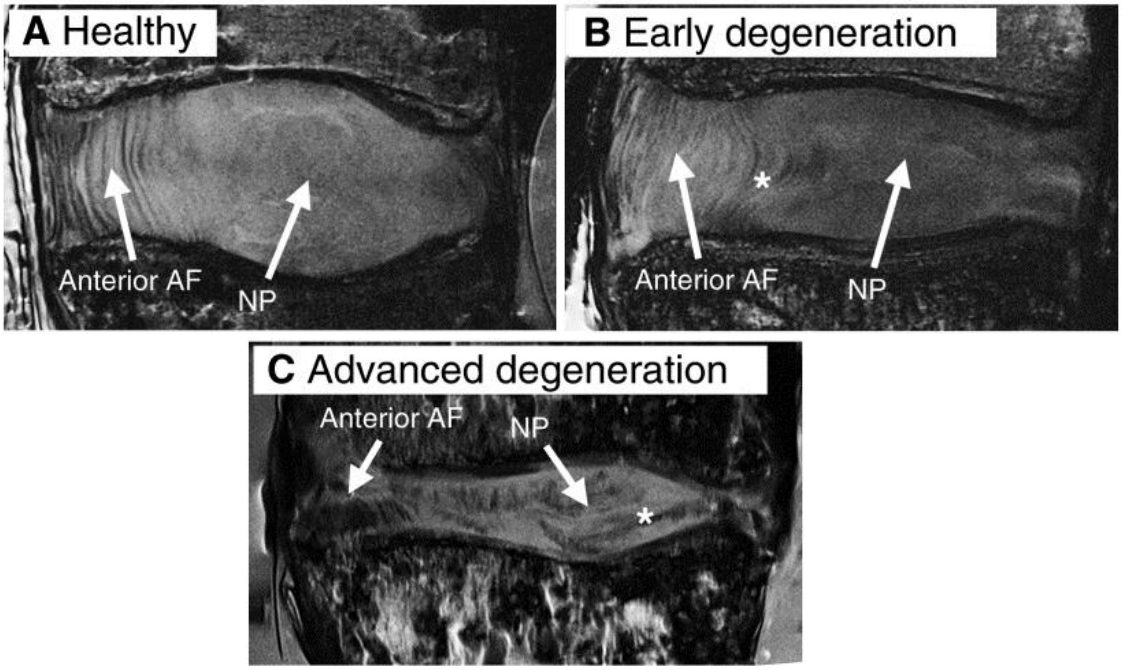

Figure 1.6 Magnetic Resonance Images of the progressive changes during IVD degeneration. A. A healthy disc showing the highly organised lamella of the AF, and intact NP which can be seen as two distinct regions. **B.** Early stages of degeneration, including slight loss of disc height, AF bulging shown by * and loss of signal from the NP region suggesting loss of tissue. **C**. Disc displaying advanced degeneration resulting in extreme structural deterioration, loss of disc height, fissures indicated by * and no distinction between regions (Adapted from Smith et al., 2011).

1.8.2.1 Changes in Cell Density

As discussed in section 1.4 the disc is comprised of a sparse cell population that within a healthy disc are metabolically active and able to maintain a stable cell density. With the onset of degeneration there is an increase in cell death (Trout et al., 1982) observed by both necrotic and apoptotic mechanisms (Sitte et al., 2009; Bertram et al., 2009). Apoptosis is proposed to be the dominate cell death process (Gruber and Hanley, 1998; Zhang et al., 2008; Bertram et al., 2009) and can be linked to a diminished nutritional supply (Horner and Urban, 2001; Bibby and Urban, 2004) caused by the reduction of blood vessels to the vertebral bodies and the calcification of CEPs (Roberts et al., 1996). Additionally, increased cell proliferation and formation of cell clusters is another feature of disc degeneration (Johnson et al., 2001). Cell clusters are primarily located in regions of matrix disorganisation (e.g

fissures or clefts (Johnson et al., 2001; Boos et al., 2002; Zhao et al., 2007) and adjacent to neovascularisation to obtain sufficient nutrients. It has been demonstrated that the cells within the cluster have an altered NP phenotype as they express increased levels of MMPs (Roberts et al., 2000; Roberts et al., 2006a).

1.8.2.2 Cellular Senescence

There are two mechanisms for cellular senescence that contribute differently to natural disc aging and disc degeneration. Replicative senescence is caused by telomere shortening when the cell divides (Campisi, 1997) and can be associated with the natural aging of the disc (Johnson et al., 2001; Roberts et al., 2006a; Gruber et al., 2007). For example cell clusters observed in degenerate discs have been shown to express senescence markers which has been shown to be indicative of replicative senescence (Roberts et al., 2006a; Gruber et al., 2007) Whereas stress-induced premature senescence (SIPS) results from a number of stress factors which can include mechanical load, increased cytokines or reactive oxygen species (Zhao et al., 2007). It has been suggested that the hostile nature of the degenerate disc microenvironment may induce premature senescence (Le Maitre et al., 2005; Le Maitre et al., 2007a). Le Maitre and colleagues demonstrated greater levels of senescent cells in degenerate IVDs in comparison to age-matched controls (Le Maitre et al., 2005) highlighting the differences between aging and degeneration.

1.8.2.3 Changes in ECM Composition

With the progression of age and the onset of degeneration there are alterations in synthesis, composition and breakdown of the matrix. Firstly there is a decrease in the synthesis of PGs primarily aggrecan in addition to other PGs (versican) which results in the disc being less hydrated and providing an insufficient swelling pressure (Buckwalter, 1995; Freemont et al., 2002a). There is also a change in the relative proportions of GAGs attached to the PGs, as chondroitin sulphate is substituted for the less hydrophilic keratin sulphate (Scott et al., 1994; Choi, 2009).

Concurrently, there are also abnormalities in the distribution of the structural protein collagen. In the NP tissue fine type II collagen fibrils are replaced by coarser type I collagen leading to a fibrotic NP, (Boos et al., 1997; Nerlich et al., 1997; Zhang et al., 2009b) whereas in the AF there is increased type II collagen and decreased type I collagen. In severely degenerate discs increased type X collagen has been observed which is associated with the ossification of hypertrophic chondrocytes and can contribute to the decrease in porosity of CEPs (Boos et al., 1997).

In healthy discs the balance between anabolic and catabolic mechanisms is sustained however in degeneration there is a shift toward catabolism resulting in matrix degradation. Degeneration induces an increased production of matrix degrading enzymes particularly MMPs and ADAMTSs. Elevated levels have been demonstrated for a number of enzymes including MMPs -1, -3, -7, -9 and -13 (Roberts et al., 2000; Le Maitre et al., 2004a; Le Maitre et al., 2006a; Weiler et al., 2002) and ADAMTSs -1, -4, -5, -9 and -15 (Le Maitre et al., 2004a; Pockert et al., 2009). The substrates for the enzymes are the collagens and PGs located in the disc as discussed in section 1.5.3. Expression of the regulatory inhibitors TIMP-1 and TIMP-2 are increased during degeneration (Roberts et al., 2000) however TIMP-3 expression is not increased. Therefore there is an imbalance between the expression of ADAMTS and TIMP-3 favouring the degradation enzyme resulting in the breakdown of aggrecan (Le Maitre et al., 2004a; Pockert et al., 2009).

In the musculoskeletal disorder osteoarthritis, similar degenerate changes to those observed in the IVD occur in articular cartilage in which the cytokines interleukin – 1 (IL-1) and tumour necrosis factor α (TNF α) are strongly implicated in driving the catabolic alterations (Igarashi et al., 2000; Koshy et al., 2002). In a series of studies by Le Maitre and colleagues (Le Maitre et al., 2005; Le Maitre et al., 2006b; Le Maitre et al., 2007b; Le Maitre et al 2007c) both cytokines were investigated to determine the role they play in IVD degeneration. With regard to IL-1β the results demonstrate that the cytokine is produced by native disc cells, and during degeneration there is increased expression in comparison to non-degenerate discs (Le Maitre et al., 2005). However, the increase in IL-1β is not reciprocated by an increase in the IL-1 inhibitor, IL-1 receptor antagonist (IL-1Ra) meaning the greater expression of IL-1β will cause damage to the disc. Treatment of the disc with the cytokine resulted in a downregulation of anabolic molecules and upregulated levels

of MMP and ADAMTS enzymes, leading to a catabolic shift in matrix synthesis. Additionally, Le Maitre and colleagues investigated the cytokines simultaneously in non-degenerate, degenerate and herniated human discs to determine the most predominant cytokine. Gene expression of IL-1β was detected in 79% of discs compared to TNF-α expression in only 59%, with the degenerate and herniated showing the highest levels. It was also shown that whilst the IL-1R expression increased with degeneration compared to non-degenerate discs, this was not seen with TNF-α receptor I at either a gene or protein level. This suggests that IL-1β may play a more substantial role in the pathogenesis of IVD degeneration than TNF-α, although both cytokines are produced (Le Maitre et al., 2007b). As a pro-inflammatory mediator IL-1β acts a key initiator as it regulates the expression of a number of other cytokines and chemokines which are secondary inflammatory mediators. Stimulation of IVD cells with IL-1β has demonstrated significant upregulation of cytokines IL-6, IL-8 and IL-17 (Jimbo et al., 2005; Klawitter et al., 2014; Studer et al., 2011; Gruber et al., 2013). Likewise IL-1β has recently been described as the master regulator of catabolic processes by Phillips and colleagues (Phillips et al., 2015) who demonstrated that treatment of human NP cells with IL-1β resulted in significant upregulation of a number of chemokines including CCL2, CCL3, CCL4, CCL5, CCL7, CXCL1, CXCL8, CXCL9, and CXCL10. This is significant as chemokines have also demonstrated the ability to promote catabolism by increasing levels of MMP3 and MMP13 (Borzi et al., 2000; Hsu et al., 2004).

The ECM in normal discs is maintained with a careful balance between anabolic and catabolic processes. The degradative enzymes MMPs and ADAMTSs are primarily the enzymes that are involved in the breakdown of the ECM and have also been shown to be influenced by stimulation with IL-1β (Millward-Sadler et al., 2009; Kim et al., 2013; Wei et al., 2013; Phillips et al., 2013; Wang et al., 2011) which in turn enhances the catabolic processes leading to matrix degradation and IVD degeneration.

Another pathology induced by IL-1β is the induction of apoptosis. In a number of studies NP cells exposed to IL-1β undergo morphological changes, upregulation of MMP3 and MMP13 and increased apoptotic rate (Zhang et al., 2013; Orrenius et al., 2015; Yang et al., 2014; Yang et al., 2015). The ability of IL-1β to increase apoptosis leads to the loss of NP cells which is associated with the degeneration of

the disc (Liebscher et al., 2011). The mechanisms underlying how IL-1β induces apoptosis are not fully elucidated and continued research is necessary to determine if this could be a potential target for therapy.

1.8.2.4 Vascularisation and Innervation

Another characteristic of disc degeneration is an increase in vascularisation and innervation of the NP and inner AF which is coupled with increased pain (Freemont et al., 2002; Ratsep et al., 2013). Firstly the decrease of hydrostatic pressure and aggrecan from the matrix is an important factor in the innervation of the disc. Evidence suggests that aggrecan from normal discs has the ability to inhibit the growth of neuritis and endothelial cells *in vitro*; hence the decrease in aggrecan during degeneration allows in growth (Johnson et al., 2005; Johnson et al., 2002). IL-1 has also been reported as having the ability to increase the expression of vascular endothelial growth factor (VEGF) and neurotrophic factors nerve growth factor (NGF) and brain- derived neurotrophic factor (BDNF) (Lee et al., 2011a). This was highlighted by Lee and colleagues (Lee et al., 2011a) in which immunohistohemical stains demonstrated a positive correlation between IL-1 and VEGF, NGF and BDNF. Such results imply that IL-1 is the driving force behind angiogenesis and innervations (Lee et al., 2011a). Also both NGF and BDNF have been identified in degenerate discs; however only BDNF was significantly upregulated with the severity of degeneration (Purmessur et al., 2008). In addition this study also demonstrated that treatment of NP cells with exogenous IL-1 significantly increased expression of NGF and BDNF which corroborates work undertaken by Lee et al (Purmessur et al., 2008; Lee et al., 2011a).

1.8.2.5 Consequences of Disc Degeneration

As there are significant changes at both a morphological and molecular level during degeneration, this impairs the ability of the disc to undertake its function as a fibrocartilaginous cushion. The loss and disorganisation of matrix proteins results in the disc being unable to distribute load uniformly. Hence the forces are reassigned to the AF and therefore a change of force from tensile to compressive forces (Adams et

al., 1996). This can result in annular tears and NP herniation. Figure 1.7 summarises the changes at both a macroscopic and molecular level. The histological images in this figure demonstrate the comparison between a normal and degenerate IVD in which there is no distinction between the NP and AF. In addition the hydrated NP is lost and the vertebral bodies are closer together resulting in abnormal movement which can lead to LBP (Freemont, 2009).

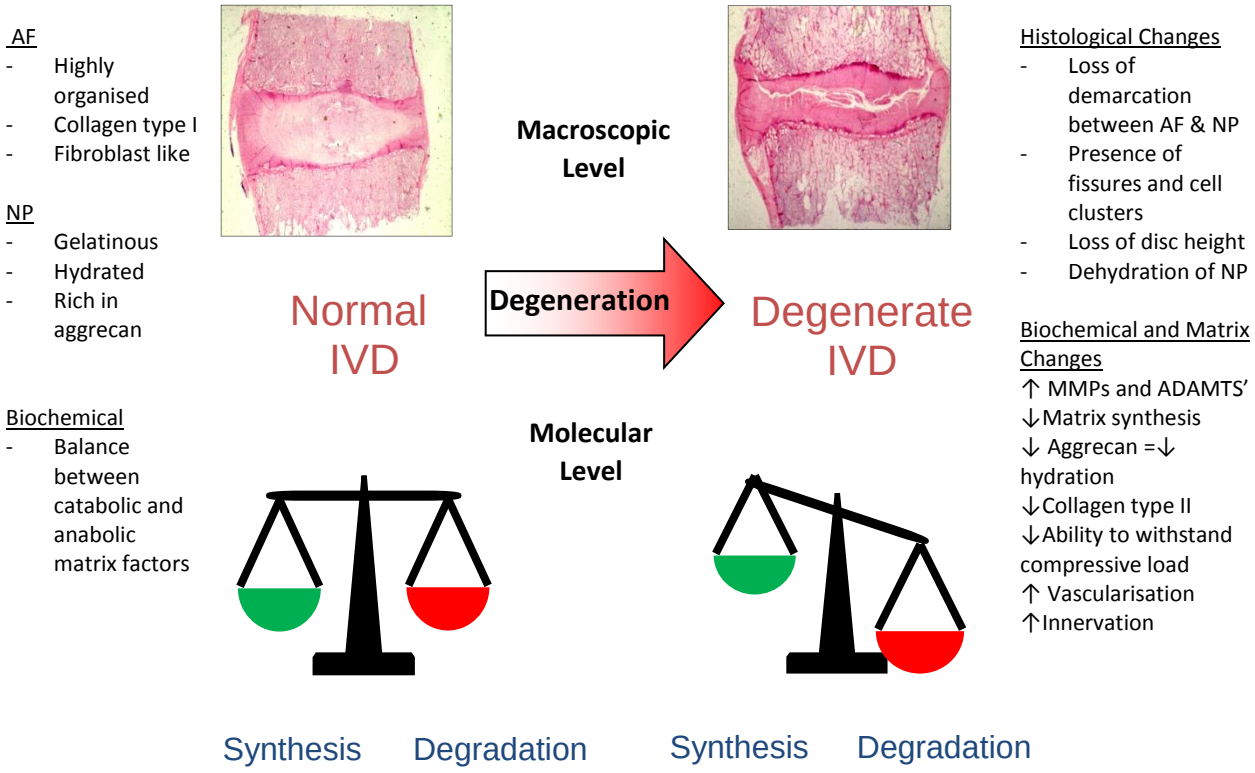

Figure 1.7 A summary of characteristic alterations shown in disc generation at a macroscopic and molecular level. Disc degeneration is characterised by a number of histological changes including loss of regional demarcation, fissures and cell clusters and loss of disc height. The morphological alterations are resultant from biochemical and synthesis changes including increases in MMPs and ADAMTSs, decrease in aggrecan and collagen type II, altered biomechanics and increased vascularisation and innervation (Adapted from Freemont, 2009).

1.9 Current Treatments for LBP

At present the treatment regimes in place for LBP are conservative and associated with symptomatic pain relief. The options for discogenic pain include conventional methods such as anti-inflammatory drugs, physical therapy and muscle relaxants

(Chou et al., 2007). Other methods target lifestyle aspects which may further induce pain, such as weight loss and core strengthening exercises, which have shown to relieve symptoms (Slade and Keating, 2007). Non-traditional therapies such as acupuncture, spinal manipulation and massage have also been shown to alleviate painful symptoms of LBP (Chou and Huffman, 2007). Surgical treatments are therefore only recommended to patients when all conservative methods have been exhausted. The clinical postoperative goals are to relieve pain and to improve function and mobility, with disc arthroplasty or spinal fusion the standard operative procedures (Zhang et al., 2008). Ultimately fusion is regarded as the ‘‘gold standard’’ in surgical treatment, however this procedure may in fact induce and accelerate degeneration in adjacent segments due to altered biomechanical properties and unevenly distributed load (Lee, 1988; Gillet, 2003; Berg et al., 2011). Consequently alternative methods of therapy are a necessity and should target the underlying pathogenesis of LBP, essentially aiming to restore/ repair the IVD rather than solely focusing on pain reduction.

1.10 Regenerative Strategies

Biological and novel therapeutic approaches to treat disc degeneration are essential in medical progression in order to target the fundamental pathogenesis of the disease and essentially aim to restore the IVD. There have been a wide range of approaches aimed at investigating how to reinstate the balance between anabolism and catabolism.

A number of *in vitro* studies have focused on the stimulation of existing native tissue cells through the administration of growth factors including transforming growth factor-β (TGF-β) (Gruber et al., 1997; Hayes and Ralphs, 2011), osteogenic protein-1 (OP-1) (Masuda et al., 2003, Imai et al., 2007a), bone morphogenic protein 2 (BMP-2) (Tim Yoon et al., 2003) and growth differentiation factor 5 (GDF5) (Li et al., 2004). The factors have been shown to increase matrix synthesis and upregulate PGs and type II collagen expression. OP-1 has an ability to stimulate ECM production as demonstrated by both human and rabbit IVD cells (Masuda et al., 2003; Imai et al., 2007b).

Similarly *in vivo* and *ex vivo* studies have investigated direct injection of OP-1 (Imai et al., 2007b; Miyamoto et al., 2006), TGF-β (Thompson et al., 1991), GDF5 (Walsh et al., 2004), insulin-like growth factor (IGF) (Osada et al., 1996) and growth differentiation 6 (GDF6) (Wei et al., 2009). Whilst both sets of studies have demonstrated positive results and it boasts the advantage of being minimally invasive, there are a number of limitations that restrict the clinical potential of these therapies. Firstly the short half-life of the molecules would lead to the necessity of multiple applications which would also add to the expense of the treatment. Also there are a low number of healthy cells located in the degenerate disc which could respond to exogenous stimulation. However despite the limitations, a phase I/II clinical trial has been undertaken to assess the safety of intradiscal GDF5 in early disc degeneration and the results are currently being analysed (Advanced Technologies and Regenerative Medicine, 2012; Zhang et al., 2011a).

Another approach that has been investigated is the employment of gene therapy. This proposed method provides enhanced durability and sustainability in comparison to the injection or stimulation with growth factors. Studies have investigated a variety of anti-inflammatory molecules including; SOX-9, BMPs (Paul et al., 2003; Zhang et al., 2006b), TGF-β3 (Nishida et al., 1999); TIMP-1 (Wallach et al., 2003) and latent membrane protein 1 (LMP1) (Kuh et al., 2008). Studies by Le Maitre and colleagues (Le Maitre 2006b; Le Maitre 2007b) demonstrate the adenovirus mediated transfer of IL-1Ra which aimed to prevent the detrimental nature of IL-1β. Importantly the results highlighted a reduction in matrix degradation and elevated levels of IL-1Ra for prolonged time periods (2 weeks), and that the native cells were immune to the actions of IL-1β (Le Maitre 2006b; Le Maitre 2007c).Gene manipulation has shown promising results however there are a number of safety concerns which can obstruct clinical translation. This includes transfection to other cells, patient specific dose responses or immune reactions (Maerz et al., 2013); therefore cellular based therapies may be a more appropriate therapy.

1.10.1 Choice of Cell Type

Cellular based therapies are aimed at replacing the degenerate cells within the disc that display irregular cluster formation, apoptotic and necrotic characteristics

(Johnson et al., 2001; Urban and Roberts, 2003). Degenerate cells also develop a senescent phenotype that results in a reduced cell replication potential (Le Maitre et al., 2007a) and also display increased catabolic activity in the form of MMPs and ADAMTS's (Le Maitre et al., 2004a; Le Maitre 2006a); hence replacement with viable cells is an essential therapeutic treatment. There is great debate as to the most appropriate cell source and a number have been investigated as summarised in Figure 1.8.

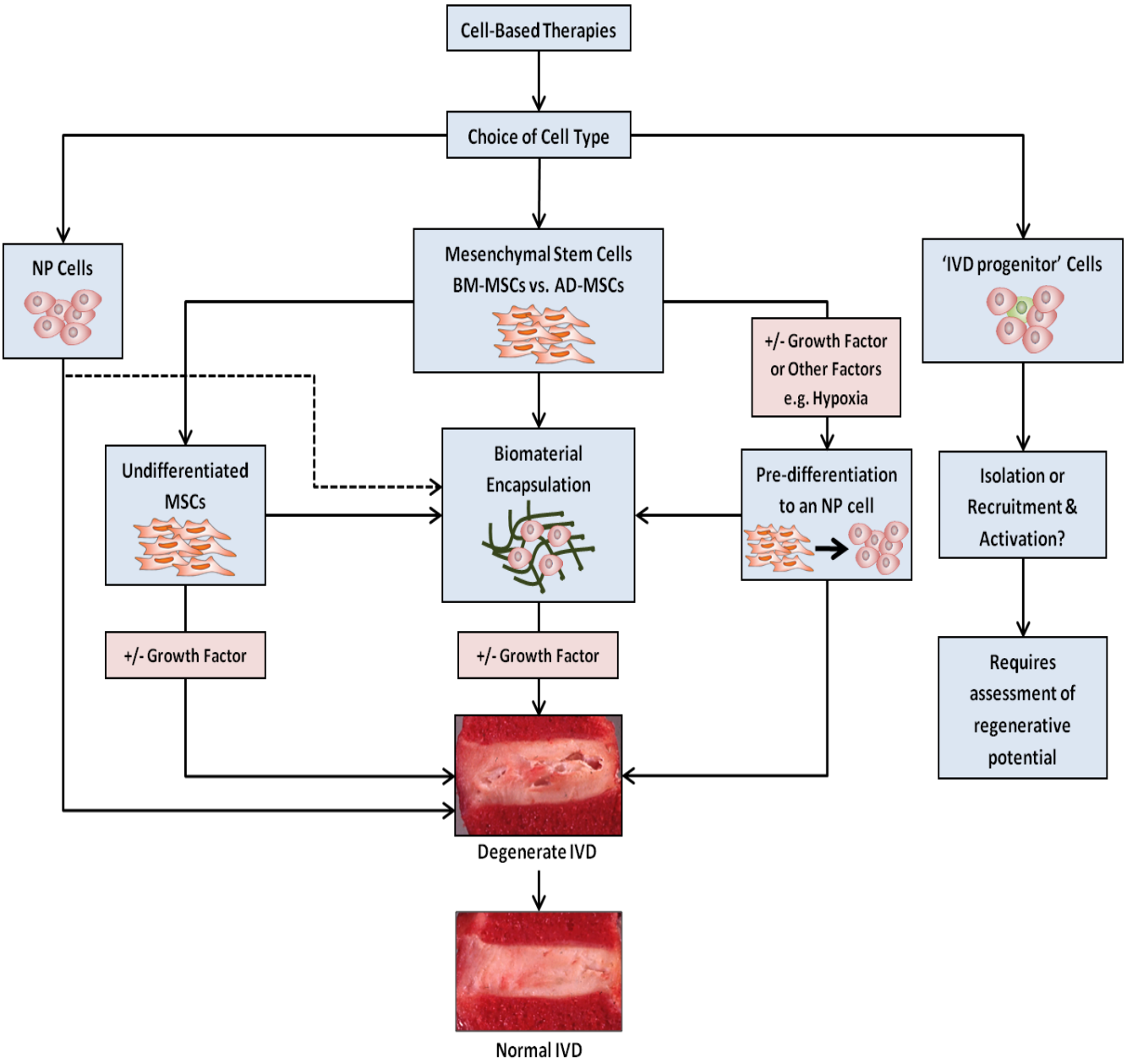

Figure 1.8 A schematic flow diagram to show the different cell types that can be utilised in cell based therapies. The diagram depicts different cell choices autologous NP cells, BM-MSCs or AD-MSCs or IVD progenitor cells. Cell based therapies can then either employ either a biomaterial, a growth factor or other environmental factors such as hypoxia in order to repair the degenerate IVD (Clarke et al., 2015).

1.10.1.1 NP Cells

The first proposed option is to utilise a population of NP cells, with studies investigating both autologous and allogenic cells. A number of *in vitro* and *in vivo* studies using several different animal models (Nishimura and Mochida, 1998; Nomura et al., 2001; Okuma et al., 2000; Watanabe et al., 2003) have demonstrated that NP cells can increase PG synthesis and cell viability. In addition, a multicentre clinical study undertaken by *EuroDisc* demonstrated in a canine model that following autologous NP cell transplantation, cells remained viable, ECM was similar to normal IVD tissue and there was retention of disc height. As such a randomised trial was undertaken in humans. Results indicated that after 2 years patients who received autologous NP transplants had a greater reduction in pain and significantly greater water content in comparison to patients who underwent discectomy surgery alone (Meisel et al., 2007; Hohaus et al., 2008). Although studies have demonstrated the ability to improve degeneration *in vivo* there are a number of disadvantages that prevent the potential of clinical translation. Firstly, in order to perform autologous re-implantation there is a need for two separate surgeries to harvest and then implant the cells; this increases the risk of infection and damage to the spine (Maidhof et al., 2012). Also the hypocellular nature of the disc implies that a number of discs must be disrupted in order to obtain a sufficient number of cells. This can lead to accelerated degeneration and induce degeneration in adjacent non-degenerate motion segments (Richardson et al., 2008). Furthermore genetic predisposition to IVD degeneration suggests that the cells are already susceptible to degeneration and should not be utilised as a regenerative tool (Gruber et al., 2006). Finally, as discussed degenerate cells exhibit senescence along with an altered phenotype and thus do not show normal cell function (Le Maitre et al., 2007a; Gruber et al., 2007; Le Maitre et al., 2004a; Le Maitre et al., 2005) hence an alternative cell source would be more appropriate.

1.10.1.2 IVD Progenitor Cells

A number of recent studies have postulated that a native stem cell/progenitor population resides in the disc which could contribute to the repair of the tissue and could be used as a regenerative tool. A progenitor population has been identified in cells isolated from both NP and AF tissue, expressing characteristic stem cell markers CD105, CD166, CD63, CD49a, CD90, p75 and CD133/1. This population also has the ability to differentiate to classic mesenchymal lineages including chondrogenic, osteogenic and adipogenic (Risbud et al., 2007). Furthermore, Blanco and colleagues (Blanco et al., 2010) isolated an MSC population from degenerate NP samples; however this population was unable to differentiate to an adipogenic lineage, which questions how MSC-like this population is (Blanco et al., 2010). Another study (Henriksson et al., 2009) undertaken in four species (rabbits, rats, minipigs and human IVD tissue) isolated a stem cell niche at the boundary of the outer AF and perichondrium region. This population of highly proliferative cells expressed the stem cell markers Notch1, Delta4, Jagged1, C-KIT and STRO-1 (Henriksson et al., 2009). Following this study the authors investigated the migratory ability of this cell population (Henriksson et al., 2012) with the results suggesting the cells may respond to tissue damage. The final study in this series was extended to degenerate human IVD samples and a small population was found to express OCT3/4, NOTCH1, CD105, CD90 and STRO-1 suggesting they are progenitor in nature (Brisby et al., 2013). In a recent key study carried out by Sakai and colleagues (Sakai et al., 2012) a multipotent population of cells was identified in both mice and human discs. The cells were able to sequentially alter the cell surface markers from Tie2+ to GD2+ to CD24+, however with the increase of age and degeneration this progenitor population (Tie2+) decreased in frequency. The presence of a progenitor population has also been identified in the CEPs of the disc in two separate studies (Liu et al., 2011; Huang et al., 2012). Taken together the studies demonstrate that the population of the disc is heterogeneous (Gilson et al., 2010, Rutges et al., 2010) and a percentage of this is a progenitor population. Further studies however are required to determine the regenerative potential of the progenitor cells and also to elucidate a protocol to acquire and culture such cells for regenerative application. Therefore an alternative cell source that has been thoroughly investigated would be of greater potential to IVD regeneration.

1.10.1.3 MSCs

The employment of MSCs as a potential cell source for cell based therapy of IVD degeneration has been of intense focus in recent years. MSCs were first identified in 1970 by Friedenstein and colleagues (Friedenstein et al., 1968) when the presence of a non-haematopoietic cell population in bone marrow was described. MSCs have the capacity to self-renew and also to differentiate to a number of mesenchymal lineages (Pittenger et al., 1999) (Figure 1.9). Along with bone marrow (BM-MSCs) (Kolf et al., 2007), MSCs can be isolated from a number of sources including adipose tissue (AD-MSCs) (Zuk et al., 2001), synovial membrane, muscle and blood (Zuk et al., 2010; De Bari et al., 2003; Bosch et al., 2000; Zvaifler et al., 2000. A number of studies have shown the potential of MSCs to differentiate to an NP phenotype (Risbud et al., 2004; Richardson et al., 2006; Minogue et al., 2010a; Clarke et al 2014).

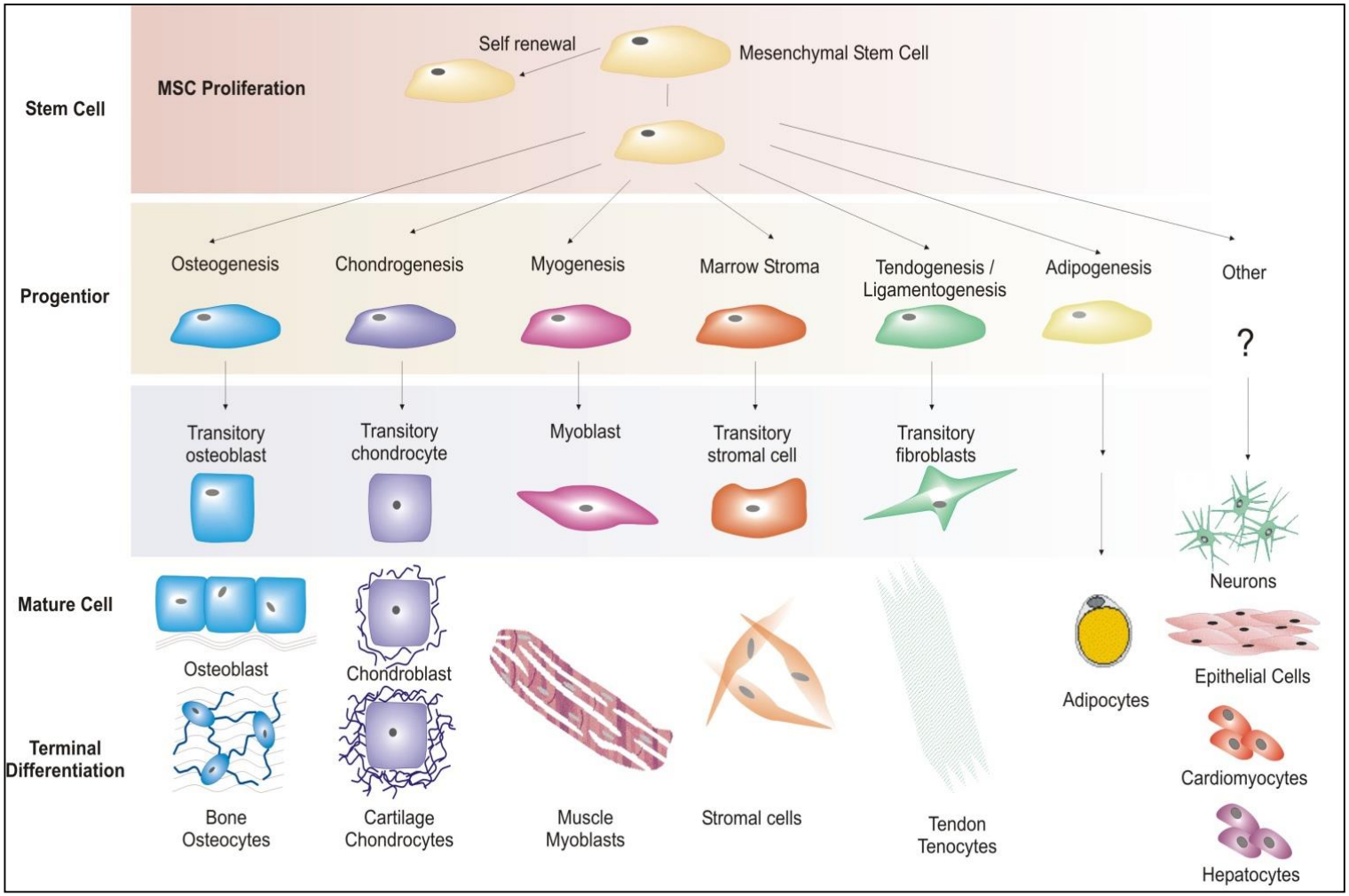

Figure 1.9 A schematic diagram to show differentiation potential of MSCs. MSCs are able to undergo self-proliferation and are able to differentiate into a range of mesenchymal tissues including bone, cartilage, muscle, stroma, tendon and adipose. Evidence has also suggested a greater plasticity including liver, heart, skin and nerve tissues. (Adapted from Caplan 1994).

Different *in vitro* methods have been implemented in order to differentiate MSCs toward the NP linage. These include a co-culture system in which MSCs are directly cultured with NP cells in order to adopt the NP phenotype (Richardson et al., 2006b). This particular study demonstrated an increased expression in MSCs of classic ECM genes (Richardson et al., 2006b). This study highlighted that if partially differentiated MSCs were re-implanted into the disc, the native NP cells would help them to retain the NP phenotype. Another method explored by Risbud and colleagues (Risbud et al., 2004) showed that under hypoxic conditions and with the addition of TGF-β1 to culture media, the MSC cells were directed toward an NP phenotype, shown by upregulation of ECM genes (Risbud et al., 2004). Whilst BM-MSCs are the most widely investigated cell source there have recently been studies from this laboratory and others that suggest AD-MSCs maybe a more appropriate cell source for IVD regeneration (Minogue et al., 2010a; Clarke et al., 2014; Zhang et al., 2014).

1.10.2 Injection of MSCs

The ability of the MSCs to differentiate to an NP phenotype is fundamental to ensure that this regenerative strategy can facilitate reparative treatment. Several studies have assessed the potential of directly injecting MSCs into the disc (Sakai et al., 2005; Hiyama et al., 2008; Jeong et al., 2009; Le Maitre et al., 2009a; Feng et al., 2011b) to investigate if the IVD microenvironment would promote differentiation and repair the disc. Sakai and colleagues (Sakai et al., 2005) injected autologous MSCs into a degenerative rabbit model and assessed following a 48 week period. The results demonstrated that the microenvironment of the NP induced site- dependent differentiation as the fluorescently labelled MSCs, expressed classic ECM markers aggrecan and type II collagen. In addition there was significant restoration of total PG content, in comparison to untreated discs (Sakai et al., 2005). Similarly using a rabbit model, Feng and colleagues (Feng et al., 2011b) compared results from transplanting autologous MSCs and NP cells separately into the disc. Results demonstrated an increase in disc height, GAG content and no significant difference between the two cell populations (Feng et al., 2011b). However, one specific limitation with a rabbit model is that this species retains an NC population, which

may support a regenerative response (Alini et al., 2008). A study using human MSCs was undertaken by Le Maitre and colleagues (Le Maitre et al., 2009a), in which undifferentiated MSCs were injected into bovine tissue explants. The cells remained viable for a 4-week culture period and displayed an NP phenotype by the expression of common matrix molecules, signifying the ability to differentiate in situ.

As a whole these studies highlight the promising potential of MSCs as a therapeutic treatment, due to the increase in GAG and enhanced matrix production. This in turn has led to a recent Phase I clinical study (Orozco et al., 2011) in which 10 patients with chronic LBP were injected with autologous BM-MSCs into the NP region. After 1 year 90% of patients showed improved pain relief which was attributed to the potential induction of anti-inflammatory cytokines (Chanda et al., 2010; Orozco et al., 2011). In addition there was a significant increase in the water content of the discs however no improvement in disc height was seen. Another trial began in 2012 at the Washington Centre for Pain Management which aimed to study 100 patients for 3 years following the injection of BM-MSCs in a hyaluronic acid carrier (Wash, 2012).

The work undertaken to date focuses on the capacity of MSCs to differentiate to repair the disc, to improve GAG formation and ECM synthesis. It must be ensured that the correct cell phenotype and matrix is produced to form an appropriate functional tissue.

1.10.3 NP Cell Phenotype

1.10.3.1 Classic NP Phenotype

Classically NP cells are described as ‘chondrocyte like’ as they are rounded in morphology and form a matrix rich in type II collagen and aggrecan and express the master chondrogenic transcription factor SOX9 (Sieve et al., 2002). However whilst the matrix components may be the same there are distinct differences between NP and articular cartilage particularly in terms of the ratio of PG to collagen (Mwale et al., 2004). The NP cells produce a PG rich matrix with a PG: collagen ratio of 27:1 compared to cartilage which is only 2:1. The difference in ratio has implications on a number of factors including the stiffness of the matrix and thus the tissue as a whole

and also the hydration capability. In addition the majority of studies previously undertaken to assess the differentiation of cells to an NP phenotype only analyse the classic ECM molecules (Sakai et al., 2005; Richardson et al., 2006). Therefore investigations were undertaken to elucidate novel markers that will allow NP cells to be distinguished from other cartilaginous cells. This will also facilitate the development of MSC based therapies to ensure they adopt the correct phenotype and produced a PG rich matrix.

1.10.3.2 Clarification of NP Novel Markers

Microarray studies allow for thousands of gene expression levels to be determined concurrently; hence there have been a number of studies that have aimed to identify a panel of unique NP markers to distinguish NP cells using this method (Lee et al., 2007, Minogue et al., 2010a, Minogue et al., 2010b, Power et al., 2012, Sakai et al., 2009).

Initial investigations were undertaken in small animal models including canine (Sakai et al., 2009), rat (Lee et al., 2007) and rabbit (Clouet et al., 2009). In each study a panel of markers were identified that were differentially expressed between NP and AC/AF cells which confirms the hypothesis that NP cells are distinct in their gene expression profile (Mwale et al., 2004). A study from this group (Minogue et al., 2010b) then looked at the differential gene expression between NP, AF and AC tissues isolated from bovine which is a larger animal model. The results highlighted inter-species variation as there was no correlation between this study and the smaller animal models. As such a microarray was carried out using human IVD tissue (Minogue et al., 2010a) comparing differential expression between NP and AC cells. Crucially, the genes identified in this experiment confirmed and correlated with analysis from the bovine model (Minogue et al., 2010a; Minogue et al., 2010b). The results from both experiments demonstrated that a number of genes were differentially expressed in both models, in particular FOXF1 and KRT18. Interestingly, Powers et al consequently confirmed a number of these finding particularly expression of CA12. This study also identified cell surface markers expressed by the NP cells which may enable direct isolation. A summary of novel markers identified by the microarrays' is found in Table 1.2.

In most circumstances initial experiments are carried out using small animal models, however in this type of investigation it is not entirely appropriate. This is due to the fact that some animal species, (rat, rabbit and some dogs) are populated by NC cells, which are lost during infancy in humans. Therefore the differences observed in the small animal, bovine and human analyses may be due to the fact that the microarray was undertaken with NC rich tissue rather than smaller NP cells. It must be noted that the species of dog utilised in Sakai et al (Sakai et al., 2009) was in fact a chondrodystrophic breed which mirrors human development with the loss of NC cells. The only animal model to show a distinct overlap with human markers was the bovine model. This is possibly due to the fact that bovine discs provide a model where the load, structure and microenvironment is similar to that observed in humans (Miyazaki et al., 2009; Showalter et al., 2012).

In addition to the microarray studies a recent review paper by Risbud and colleagues (Risbud et al., 2015) has evaluated the current consensus of the NP phenotype. Following the spine research interest group at the 2014 orthopaedic research society meeting a working definition of an NP cell phenotype has been proposed. This is to ensure consistency across publications and to ensure that researchers are following the same criteria. The phenotypic markers suggested are: HIF-1α, GLUT-1, Shh, T, KRT18, KRT19, CA12 CD24 and aggrecan:collagen ratio>20 at the protein level.

Table 1.2 A Summary of Highly Differently Expressed NP Marker Genes Identified in Four Different Species by Microarray Analysis.

Species	Top Differentially Expressed Genes	Gene	Confirmation in alternate models	Gene or Protein Expression	Ref
Rat	Cytokeratin-19	KRT19	Bovine, Human	Gene/Protein	(2,3)
	Annexin A3	ANXA3	-	Gene	(2)
	Glypican 3	GPC3	-	Gene/Protein	(2)
	Pleiotrophin	PTN	-	Gene	(2)
	Vimentin	VIM	Human	Gene	(2)
Canine	Cytokeratin- 18	KRT18	Bovine, Human	Gene/Protein	(1,3)
	a 2-macroglobulin	A2M	Human	Gene/Protein	(1)
	Neural cell adhesion molecule-1	NCAM1/CD56	Bovine	Gene/Protein	(1,3)
	Desmocollin-2	DSC2	Human	Gene/Protein	(1)
Bovine	Cytokeratin- 8	KRT8	Human	Gene	(3)
	Synaptosomal associated protein 25	SNAP25	-	Gene	(3)
	N-cadherin	CDH2	Human	Gene	(3)
	Forkhead box protein F1	FOXF1	Human	Gene	(3)
	Brain acid soluble protein 1	BASP1	Human	Gene	(3)
Human	β-globin	HBB	Bovine	Gene	(3)
	Ovostatin 2	OVOS2	Bovine	Gene	(3)
	Paired box protein 1	PAX1	Bovine	Gene	(3)
	Carbonic anhydrase 12	CA12	Bovine	Gene/Protein	(3,4)
	C-type lectin domain family 2 member B	CLEC2B	-	Gene	(4)
	ϒ- sarcoglycan	SGCG	-	Gene	(4)
	Tyrosine protein kinase receptor 3	TYRO3	-	Gene	(4)

(Adapted from: Ludwinski et al., 2013). References: (1) Sakai et al., 2009; (2) Lee et al., 2007; (3) Minogue et al., 2010b (4) Power et al., 2011.

1.10.3 Directing Differentiation of MSCs

There have been a number of different approaches applied in order to differentiate MSCs to an NP phenotype. The most common methodology *in vitro* is the use of a differentiating media supplemented with a growth factor. Components of differentiating media include a number of nonproteinaceous supplements including; insulin, transferring, selenite (ITS-X) and linoleic acid, which act as a replacement for foetal calf serum and promote proliferation and ECM synthesis. Ascrobate-2-phosphate has demonstrated the upregulation of ECM marker genes (Altaf et al., 2006) and the synthetic glucocortocoid dexamethasone which stimulates the expression of SOX9 (Sekiya et al., 2002). Whilst the nonproteinaceous supplements aid in the differentiation of MSCs, growth factors are considered to be the most potent inducer.

A wide variety of growth factors have been assessed including TGF-β, IGF-1, FGF-2 and OP-1 (Buckley and Kelly, 2012; Yu et al., 2012; Longobardi et al., 2006; Steck et al., 2005). However these studies demonstrate the chondrogenic differentiation of MSCs as the genes investigated were limited to chondrogenic matrix markers. Therefore with the elucidation of the novel NP markers this has allowed a more accurate phenotype to be assessed. More recent studies have utilised this set of unique markers to define differentiation. Growth differentiation factor 5 (GDF5/BMP-14/ CDMP-1) and growth differentiation factor 6 (GDF6/BMP-13/ CDMP-2) are members of the TGF super-family and have been associated with skeletal development (Karsenty et al., 2002; Settle et al., 2003; Asai-Coakwell et al., 2009). The group have previously demonstrated that both growth factors are expressed by human NP cells (Le Maitre et al., 2009c). GDF5 has also recently been shown to enhance differentiation of BM-MSCs to an NP-like phenotype (i.e. discogenic differentiation) compared to TGF-β1, as shown by the enhanced expression of a panel of novel markers including CA12, KRT19 and FOXF1 (Gantanbien-Ritter etal., 2011; Stoyanov et al., 2011; Peroglio, 2013). However, in this series of studies treatment with GDF5 failed to produce a more PG-rich matrix than cells treated with TGF-β. This suggests that whilst the discogenic markers are upregulated, the cells are not producing the correct PG-rich matrix. Conversely GDF5 has more recently been utilised to induce chondrogenic differentiation in embryonic stem cells (ESCs) (Oldershaw et al., 2010) and is extensively used for

regenerative strategies in the tendon (Ozasa et al 2014). Hence this growth factor may not be the appropriate choice for discogenic differentiation.

GDF6 on the other hand, has been shown to play an important role in spinal column development and interestingly a congenital mutation in this gene leads to Klippel-Fieil syndrome, resulting in numerous skeletal and developmental defects, including spinal fusion (Tassabehji et al., 2008) implying that it may have a pivotal role in IVD development and homeostasis. Additionally injection of GDF6 ,at the time of injury, in an experimentally degenerate ovine disc model reversed histological changes compared to control discs and retained greater hydration after 4 months (Wei et al., 2009). Taken together, GDF6 may be a superior growth factor to induce discogenic differentiation than TGF-β which, to date has been the most commonly used growth factor.

Other methods used to differentiate MSCs are environmental conditions including 3-dimensional (3D) cultures, low oxygen levels (hypoxia) and low glucose levels. Culture in a 3D system has been shown to be superior to conventional 2D monolayer when differentiating MSCs (Malda et al., 2003, Gruber and Hanley, 2000) as they maintain the differentiated phenotype. Additionally culture in hypoxia has been shown to enhance discogenic differentiation (Risbud et al., 2004; Stoyanov et al., 2011). Finally co-culture systems are a useful method to study cell-cell interactions which may occur in vivo and can also be used to induce differentiation of MSCs when cultured with NP cells (Richardson et al., 2006).

Overall it can be concluded that there is no standard protocol to differentiate MSCs to an NP phenotype, however the most frequently used method is 3D culture, with a differentiating media and supplementation with a growth factor.

1.10.4 Biomaterials/Scaffold

The principle of a biomaterial is to help to repair or maintain target tissue and to mimic the properties of the native ECM. Regarding the IVD, ultimately the material should attain mechanical capability, support in the delivery of cells to the disc and act as a scaffold for cells to produce their own functional matrix. Additionally the material should be biocompatible, hence without inducing an inflammatory reaction

or any detrimental cytotoxic effects that could accelerate degeneration (Pereira et al., 2011).

The fabrication of biomaterials can be from either natural components or synthetic polymers and there are a number of tunable properties such as, pore size, self-assembly and polymer content that can be modified in order to optimise the biomaterial function (Ratner and Bryant, 2004). As a heterogeneous and complicated organ there have been a number of regenerative approaches taken. This includes targeting tissues individually either NP or AF (Silva-Correia et al., 2011; See et al., 2011; Guillaume et al., 2014) or a biphasic method (Nesti et al., 2008; Lazebnik et al., 2011).

These approaches are also dependent upon the severity of degeneration. In early degeneration, in which tissue integrity is still viable, approaches using hydrogel biomaterials to deliver a new cell population is a popular method. In a moderately degenerated disc, an injected hydrogel would also have to provide mechanical stability and to mimic the role of the ECM. Finally in advanced degeneration, a total disc replacement maybe necessary, therefore a material mimetic of both the NP and AF tissues respectively and simultaneously would be required. The approach that has been investigated most intensely is the fabrication of cellular hydrogels for the replacement of NP tissue. Table 1.3 details a range of biomaterials that have been investigated for MSC-based NP regeneration.

Table 1.3 MSC seeded scaffolds for IVD tissue engineering

Cell Type	Cell Source	Biomaterial	Method	Outcome	Reference
BM-MSCs	Adult Rat	15% hyaluronan gel	- Cells were seeded into scaffolds at 1 x 10^7 cells/ml - Cellular and acellular gels were then injected into healthy rat disc model	- Significant decrease in BM-MSC number at day 7 and only 67% viability. - BM-MSC viability was restored to 100% and increase in cell number in the NP by day 28 - Disc height was increased in discs injected with BM-MSC seeded gels	Crevensten et al., 2004
BM-MSCs	Rabbit	Type I atelocollagen (CELLGEN)	- BM-MSCS were embedded into atelocollagen at a density of 1 X10^6 - Cell seeded- gels were then injected into a degenerative rabbit model.(2 weeks after NP aspiration)	- BM-MSCs differentiated to NP like cells shown by chondrogenic gene expression - BM-MSC transplantation recovered COL2A1 and ACAN expression and decreased COL1 compared to non-treated discs - Restoration of PG content by cell seeded gels to 83%+/- 13% of normal tissue compared to 52% +/- 16% of non-treated discs	Risbud et al., 2004
NP Cells ACs BM-MSCs	Human	Chitosan glycerophosphate	- Cells were encapsulated separately into gels at a density of 4x 10^6 cells/ml - Constructs were cultured in standard DMEM for 28 days.	- Chondrogenic gene analysis demonstrated BM-MSCs adopt a phenotype similar to AC and NP cells. - BM-MSCs secreted PG and collagen at a ratio similar to that of NP cells compared to ACs.	Richardson et al., 2008
BM-MSCs	Human	Water-soluble azide-functionalised chitosan was crosslinked with propiolic acid ester-functional poly- (ethylene glycol)	- Cells were encapsulated at 4 x10^6 cells/ml - Constructs were cultured for 24 hours to assess viability - Cells were also cultured in 2D on the surface of the gel for 7 days	- In 3D after 24h cells had 95% viability. - In 2D cells viable after 7 days showing that the gel is not cytotoxic to cells	Truong et al., 2015

BM-MSCs	8-12 week old Rats	Type II collagen and hyaluronic acid (HA) Cross linked with different concentrations of: 1-ethyl-3(3-dimethyl aminopropyl) carbodiimide(EDC) and N-hydroxysuccinimide (NHS)	- Cells were seeded into hydrogels at a density of 50,000 - Constructs were cultured for 7 days	- Type II collagen/ HA crosslinked with 8mM EDC/NHS was able to support a viable population of rBM-MSCs - The cells also could differentiate to a chondrogenic lineage as shown by COL2, ACAN.	Calderon et al., 2010
BM-MSCs NP Cells	Human	Four different sponge-shaped matrixes: 1. Equine collagen 2. Porcine collagen 3. Gelatin 4. Chitosan Alginate as a control	- Cells were seeded into different matrixes at $4x10^6$ cells/ml - Constructs were cultured in chondrogenic media (+TGF-b) for 7 and 35 days.	- In collagen and gelatin matrixes BM-MSCs produced higher mRNA and protein level of COL1, COL2A1, and ACAN and a higher PG content and cell survival rate than chitosan or alginate groups. - BM-MSCs in porcine collagen expressed a similar COL2A1:ACAN ratio as NP cells - BM-MSC expression of novel NP markers KRT19, PAX-1 and FOXF1 was lower than in NP cells	Bertolo et al., 2012
BM-MSCs NP cells	Porcine	Alginate hydrogels Chitosan hydrogels	- Cells were seeded in alginate and chitosan gels separately at densities of 4×10^6 and 8×10^6 cells/ml. Also at a 1:1 ratio BM-MSCs:NP to yield 8×10^6 cells/ml - Cells were cultured in a chondrogenic media (+TGF-b) for 21 days.	- NP cells remained viable in both biomaterials whereas BM-MSC viability was diminished in chitosan. - sGAG and COL2A1 deposition was superior in alginate for both cell types compared to chitosan. - Co-cultures demonstrated a decrease in BM-MSC number and an increase in NP cells.	Naqvi et al., 2014

AD-MSCs	Rabbit	Type II collagen/HA/4S-Star PEG	- Cells were seeded into gels with different concentrations of collagen - Constructs were cultured for 21days in differentiating media	- After 21 days of culture AD-MSCs maintain +/-80% viability - Higher concentrations of collagen maintain a rounder shaped cell along with high levels of COL2A1, ACAN, SOX9 and low levels of COL1.	Fontana et al., 2014
BM-MSCs	Rabbit	Type I collagen microspheres	- $2.5x10^5$ cells were encapsulated in collagen and 2uL pipetted to form microspheres. - Cell seeded microspheres were then injected into a degenerative rabbit model.(1 month after NP aspiration)	- BM-MSCs in collagen microspheres maintained the dynamic mechanical behaviour greater than MSCs in saline alone. - Delivery in collagen microspheres also reduced the risk of osteophyte formation compared to saline controls.	Li et al., 2014
BM-MSCs	Human	Photocrosslinked carboxymethylcellulose (CMC)	- Cells were encapsulated at 20 x 10^6 cells/ml - Constructs were cultured with and without TGF-b for 7 and 21 days	- Constructs treated with TGF-b resulted in significantly higher GAG and COL2A1 content	Gupta et al., 2011
BM-MSCs	Bovine	20% teleostean, 3% N-carboxyethyl chitosan and 7.5% oxidized dextran	- Cells were encapsulated at 20 x 10^6 cells/ml - Constructs were cultured for 0, 14 and 42 days with or without TGF-b	- Hydrogel maintained cell viability up to 42 days - Upregulation of COL2A1 and ACAN expression demonstrates differentiation - Increased collagen and aggrecan content	Smith et al., 2014

(Adapted: Clarke et al., 2015)

A hydrogel can be defined as a hydrophobic insoluble polymer network that swells in an aqueous medium. This presents an environment that resembles the vastly hydrated nature of the NP tissue, which makes them an excellent candidate for NP reparative treatment (Ratner and Bryant, 2004). There are numerous methods that can activate the initial liquid component toward hydrogel formation such as self-assembly, thermoresponsive, pH sensitivity and photo cross-linking. Enabling the hydrogels to be tuned accordingly, this is extremely important property that allows a minimally invasive approach rather than a surgical implant.

The particular biomaterial selected for hydrogel formation, intended for NP regeneration, would act as an encapsulation vehicle for MSCs. The addition of the material is beneficial to both structural and mechanical properties, which can act as a temporary ECM, while the new cell population lays this down. There have been numerous studies using a variety of materials that have investigated the feasibility of NP regeneration using hydrogels. The majority of studies have explored the potential of collagen and hyaluronic acid as a basis for hydrogels, due to their natural presence in the native disc (Sakai et al., 2006b; Lee et al., 2011b; Crevensten et al., 2004; Moss et al., 2011; Peroglio et al., 2011; Halloran et al., 2008; Calderon et al., 2010; Collin et al., 2011; Huang et al., 2011).Studies from our group have illustrated that a thermoresponsive hydrogel chitosan glycerophosphate (C/Gp) can aid in the differentiation of MSCs and maintain a discigenic phenotype (Richardson et al., 2008). A more recent study has fabricated a chitosan-based hydrogel with a variety of tuneable properties which also allows MSC attachment and proliferation (Truong et al., 2015).

A different technique undertaken by Pereira and colleagues (Pereira et al., 2014) assessed the potential of the chemoattractant stromal cell derived factor -1 (SDF-1) encapsulated in a hyaluronan based hydrogel to recruit MSCs. When injected to the degenerate NP region the combination of the hydrogel and SDF-1 increased the number of migrating MSCs to the area. This study highlights the multifunctional uses for biomaterials and shows that they can enhance endogenous cell migration.

Biomaterials therefore offer a support to the differentiation of MSCs, recruitment of endogenous cells and also provide an environment to enhance matrix production. In particular for IVD regeneration an advantage of a biomaterial is that it can offer

protection from the native IVD niche which is hostile and could be detrimental to implanted cells and halt the regenerative capabilities.

1.11 Implanted Cells in the IVD Niche

The interaction between the implanted cells and the IVD milieu is significant to clinical translation as it is necessary to understand whether the cells can function within such a harsh environment. As previously described in section 1.6 there are a number of factors that accumulate to provide the IVD niche, hence a studies have investigated these different aspects.

Firstly Wuertz et al (Wuertz et al.,2008) assessed how low glucose, osmolarity and acidic pH, signifying the degenerate environment affects BM-MSCs. Whilst low glucose conditions actually increased proliferation and matrix (ACAN, COL1) production, treatment with the other conditions resulted in significantly decreased proliferation and matrix expression. Similarly a combination of all treatments resulted in decreased matrix, suggesting that a low pH and high osmolarity have the greater deleterious effect to the viability of the BM-MSCs than glucose concentration alone. A comparable study (Liang et al., 2012) was also undertaken to assess the response of human AD-MSCs to the same conditions. The results from this study also confirmed that high osmolarity and low pH also have the greatest detrimental effects. In a study (Wuertz et al.,2009) solely focused on the effects of pH on MSCs the results showed an inhibition of ACAN, COL1 and TIMP-3 expression in addition to an altered morphology and decrease in proliferation and viability.

On the other hand, researchers have investigated in the effect of hypoxia whilst culturing cells which demonstrate enhanced matrix production and differentiation of MSCs (Stoyanov et al., 2011; Felka et al., 2009; Markway et al., 2010; Li et al., 2013). Notably Stoyanov and colleagues highlighted an increase in CA12 expression which has been described as an NP novel marker and also associated with pH regulation. Therefore upregulation of this particular gene may allow the MSCs to adapt to the degenerate environment and increase cell survival.

As studies have highlighted both positive and negative responses of MSCs to the IVD niche, it is important for investigations to integrate environmental aspects into experiments to test the efficacy of the proposed cell based therapy and also to elucidate the interaction with the microenvironment.

1.12 Models of IVD

Whilst *in vitro* experiments are essential to investigate cellular interactions, signalling mechanisms and the responses of cells to individual variables, larger model systems are essential to ensure clinical transferability and to assess multiple variables in system that mimics the native environment. One particular method to investigate this is to use animal or human models of IVD degeneration. The focus of recent studies is to utilise an 'ex vivo' model whereby degeneration can be induced by a number of different methods, in order to test the efficacy of potential therapies.

1.12.1 Animal Models

With current tissue acts and ethical regulations in place, the ability to obtain human IVD tissues is limited. Hence there are numerous animal models that have been used to investigate the pathogenesis of IVD degeneration and for testing of potential treatments.

When considering the use of animal models there a number of factors to consider; including the particular anatomy of the different species in relation to a human, loading and mechanical differences, size of the animal which may contribute to nutritional diffusion differences and finally induction of degeneration (Alini, 2008).

Common small animals that are regularly employed to generate IVD models include the use of rats, mice and rabbits. While the cost of using a small animal can be considered as relatively cheap, there are a number of other factors that distinguish them from the human. The small spinal structures and disc diameters may not be feasible to study physiological biomechanical properties. Another difference is the presence of NC cells, which are not seen in larger skeletally mature animals such as bovine and ovine and may also induce responses that would not be seen in humans (An and Masuda, 2006).

Larger animals that are employed as model systems range from sheep, pigs, dogs and cows. A larger animal is a more expensive model; however the bovine IVD in particular has been shown to have a similar size and matrix composition in comparison to the human IVD, providing a reliable model (Oshima et al., 1993). As an exclusively bipedal species, the ability to mimic physiological loading in a quadruped, during an *in vivo* experiment is not possible. This is due to the different muscle contractions acting horizontally as opposed to vertically; this could mean however that load experienced in bovine discs is higher than that experienced in a human (Alini, 2008). Another aspect to consider when creating the degenerative model is how to induce the degeneration within the disc. There are essentially two methods to do so, either using an animal that undergoes spontaneous degeneration such as a sand rat or specific canine breed, or induce the degeneration artificially (Lotz, 2004). Due to the complexity of animal models and the issues discussed above, more focus is being directed towards the development of organ culture models as the effect of specific treatment strategies can be studied in a controlled environment and individual factors can be studied.

1.12.2 Whole Organ Culture

The utilisation of a whole IVD organ culture system allows an accurate *ex vivo* model, which permits native cells to remain in their microenvironment whilst controlling more aspects, such as load, than in an *in vivo* system. With regard to the three dimensional IVD culture model one particular anatomical feature that can be varied is the presence or absence of endplates (Jim et al., 2011), additionally whole organ culture enables culture for extensive time periods to test therapies, as opposed to in vitro culture. There have been various approaches taken with some studies implementing a loading regime and others concentrating on other variables within the disc.

1.12.3 IVD Models without Load

Although all the studies described in this section do not utilise a loading system, they also differ in variables such as retention of end plates, culture period length and

species of animal. In studies by Risbud and colleagues (Risbud et al., 2003) and Haschtmann and colleagues (Haschtmann et al., 2006), the two groups employed small animal organ culture models, in rat and rabbit respectively. Risbud and colleagues (Risbud et al., 2003) excised discs from the lumbar region of the rat which were then cultured in osmotic media, in multi-well plates for 1 or 3 weeks. The cells remained viable for 7 days; however the PG content and expression of matrix molecules type II collagen and aggrecan were decreased in comparison to freshly harvested discs, this suggests that whilst cells remain viable there is a change in phenotype in the cells as shown by the decrease in ECM synthesis. In the model system described by Haschtmann and colleagues (Haschtmann et al., 2006), discs were excised and cultured in normal media conditions, again in multi-well plates and were cultured up to 7 weeks. Here the cells retained an 81 +/- 7% viability which did not alter over a 49 day period; however q-PCR analysis showed a significant down regulation in both aggrecan and type II collagen gene expression, together with a non-significant decrease of PG content after 7 days. The significance of this study is that cells could remain viable for an extended time period, which is important when testing the efficacy of potential therapies to examine long term effects. Both groups have utilised different methods and different species however a limiting factor to both studies is that they were undertaken in small animal models in which NC cells are present and this is not representative of human IVDs.

In a larger bovine culture system (Jim et al., 2011) three isolation techniques were compared in order to determine the optimum protocol for long term culture. The discs were excised either with bony endplates (BEP), with cartilage endplates (CEP) or removal of endplates (NEP) and cultured for up to 4 weeks. After only 10 days BEP cultured cells showed only 27 +/- 23% viability and the NEP disc showed extreme deformation due to free swelling. Conversely the CEP excision method was able to maintain cells for 4 weeks and also kept cell and structural morphology. The same group (Gawri et al., 2011) also demonstrated the identical excision methods, using human intervertebral discs. Again the results reflected the previous study as the NEP disc excessively swelled and the BEP method lead to reduced cell viability due to reduced nutrient flow. However the CEP culture method maintained cell viability and matrix composition for 4 weeks in both high and low nutrient conditions. The experiment was then further extended over a 4 month period in

which cells remained 95% viable. This suggests that culture with CEP is necessary in order to maintain long term culture in IVD whole organ culture systems. The different results obtained between the small animal (Risbud et al., 2003; Haschtmann et al., 2006) and larger animal models (Jim et al., 2011; Gawri et al., 2011) maybe due to difference between species in, for example, disc size or nutritional influences. It must also be noted that there was no implementation of a loading regime which has been implicated in the maintenance of NP phenotype (Matsumoto et al., 1999). Therefore a culture system that can incorporate loading dynamics would be beneficial.

1.12.4 Loaded Systems

The function of the IVD is to act as a fibrocartilaginous cushion and to equally distribute load and maintain mechanical stability. Therefore it is an essential necessity to incorporate load into a model system to exert the forces experienced in the native environment; this has been demonstrated by a number of groups using a variety of techniques, summarised in table 1.4.

Table 1.4 Summary of Loaded IVD Organ Culture Systems

Loading regime	Preparation of Discs	Model	Outcome	Ref.
Static loading 0,0.2,0.4,0.8 and 1MPa for 24 hours	With CEP	Mouse	Apoptosis increased with increased load and was absent in discs without load.	Ariga et al., 2003
Static loading ~0.25MPa for 7 days	With and without CEP	Bovine	Discs with endplates maintained hydration and GAG levels, but ↓ cell viability. Without endplates cell viability maintained.	Lee et al., 2006
Diurnal loading 0.2MPa for 16h and 0.8MPa for 8h for 7 days	With BEP	Ovine	Under both conditions nutrients were transported into the disc, which enabled maintenance of cell viability for 7 days. ↑of catabolic genes and ↓ of anabolic molecules.	Gantenbien et al., 2006
Static 0.2MPa and diurnal loading (0.1 and 0.3MPa alternating at 12h for 4 and 8days	NEP	Bovine	Static loading ↑ cell viability than diurnal. No changes in GAG content or cell metabolism.	Korecki et al., 2007
Hydrostatic physiological loading (table 6.2) for 14 days	Perspex ring culture (Le Maitre et al., 2004b)	Bovine	↑ Metabolic activity and PG content compared to unloaded controls.	Le Maitre et al., 2009b
Stimulated physiological loading. Diurnal axial load (0.2/0.6MPa, 8/16h) with cyclic sinusoidal load during the 0.6MPa active phase (0.2Hz ± 0.2MPa, 2x4hours) 7 and 21 days under high or low glucose.	With CEP	Ovine	Explants could be maintained for up to 21 days. A combination of high frequency and low glucose resulted in cell death and increases in MMP 13 gene expression.	Junger et al., 2009; Illien-Junger et al., 2010
7 days in an unloaded environment, followed by a static load for 48 hours at 0.1 MPa. Three dynamic loads were then compared 0.1–0.3MPa (low), 0.1–0.6MPa (medium), and 0.1–1.2MPa (high).	With CEP	Bovine	High cell viability was maintained in low load 93.2+/- 3.4%, whereas medium and highly loaded groups decreased cell viability significantly to 36.0+/- 15.1% and 29.3 +/- 16.2% respectively	Haglund et al., 2011
Control or wedge (15^{o}) group, static load 0.2MPa for 7 days	NEP	Bovine	Asymmetric compression had a deleterious effect, ↑ MMP-1, ADAMTS-4, IL-1, IL-6, ↓aggrecan	Walter et al., 2011
Combined loading of 20N static compression and either 0, 2, 5 or 10^{o} torsion at 1.0Hz 1hour/day for 4 days.	With BEP	Bovine	↑ Cell viability in 2^{o} torsion than static. Increasing torsion magnitude	Chan et al., 2011a

Unloaded, continuous low dynamic load (LDL; 0.1–0.2 MPa, 1 Hz) or Diurnal simulated physiological load consisting of a sinusoidal load (1 Hz) alternating in magnitude every 30 minutes (0.1–0.2 MPa and 0.1–0.6 MPa) for 16 h/day, followed by 8 hours of low dynamic load (0.1–0.2 MPa).	With BEP	Caprine	Unloaded and LDL ↓ cell viability, density. SPL preserved native properties during 21 day period.	Paul et al., 2012
Four modalities: unloaded, cyclic compression, cyclic torsion, combined compression and torsion.8h/day for 14 days.	With CEP	Bovine	↓ NP cell viability in combined group (10%), in other group's ↑ 70%. NP cell morphology also changed in combined group.	Chan et al., 2013
Physiological- 1Hz alternating 0.1MPa and 0.1-0.6MPa 16h/day and 8h LDL-0.1-0.2MPa 1Hz High dynamic- 1Hz alternating 0.1MPa and 0.4-0.8MPa 16h/day and 8h LDL. High static – 0.1MPa and 0.4-0.8MPa 16h/day and 8h LDL.	With BEP	Caprine	Dynamic overloading caused cell death in all regions, static overload affected AF. ↑ Catabolic and inflammation genes, ↓ water content and GAG.	Paul et al., 2013
1Hz sinusoidal load for 4.5h following preload 'high' 130±20N, 'low' 50±10N	With BEP	Caprine	Linear relationship between compression and intradiscal pressure.	Vergroesen et al., 2014
Cyclinc compression, 1 Hz, 1 MPa, 2500 cycles per day	With hemi-vertebrae	Rabbit	Persistent degenerative changes after spinal trauma with dynamic loading	Dudli et al., 2015

As detailed in table 1.4 the majority of studies exposed the discs to either a static, diurnal loading regime or a combination, which do not mimic the physiological ranges experienced by the human spine. In a study by Le Maitre and colleagues (Le Maitre et al., 2009b), a daily loading regime (Table 1.5) was designed which incorporated the forces exerted on the disc during daily tasks such as sitting, standing, jogging and lying down, taken from studies by (Wilke et al., 1999), which is more representative of a physiologically relevant *in vivo* loading regime than models that only apply a diurnal dynamic load.

Table 1.5 Dynamic Daily Loading Regime Designed to Mimic Physiological Load

Step	Load (MPa)	Frequency (Hz)	Duration (h)
Lying 1	0.09-0.11	0.2	4
Lying 2	0.23-0.25	0.2	4
Walking	0.53-0.65	0.5	2
Sitting/Standing	0.49-0.51	0.2	4
Jogging	0.35-0.95	1.0	2
Sitting/Standing	0.49-0.51	0.2	4
Walking	0.53-0.65	0.5	2
Sitting/Standing	0.49-0.51	0.2	2

1.12. 5 Biomechanical Parameters

As a bipedal species there is a constant application of force exerted on the IVD, which is a homeostatic feature for the maintenance of normal disc function. Figure 6.1 demonstrates the difference forces that can be experienced within the disc due to normal everyday movement.

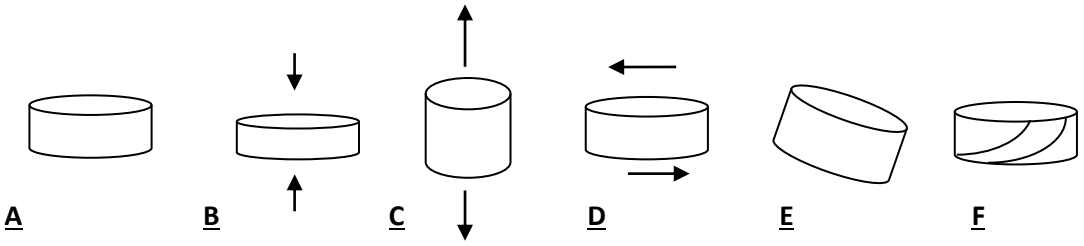

Figure 1. 10 A schematic diagram to highlight the different methods force can be applied to a disc. (A) No force, (B) Compressive Force, (C) Tensile Force, (D) Shear Force, (E) Bending Moment, (F) Torsional Moment (Torque).

1.12.6 Models of Degeneration

In order to use such *ex vivo* models to test efficacy of novel therapies, the models must present accurate features of degeneration. To date there have been a number of methods to artificially induce degeneration and mimic the progressive degenerative changes as seen in the human disease.

Enzymatic degradation is the procedure to selectively degrade ECM in the NP tissue, with the overall aim being to reduce disc volume, induce instability in biomechanics and ultimately create a void of tissue in order to reinsert a reparative biomaterial. This has been demonstrated using a number of digestive enzymes including, chondroitinase ABC, trypsin, elastinase, collagenase and papain (Imai et al., 2007b; Barbir et al., 2010; Chiba et al., 2007; Norcross et al., 2003; Roberts et al., 2008; Jim et al., 2011).

As previously mentioned the bovine model in particular been reported to have a similar size and matrix composition (Oshima et al., 1993) to human IVD and therefore can be used to induce degenerative changes that may more closely mimic the human disorder. The studies undertaken by some groups (Roberts et al., 2008 and Jim et al., 2011) both used 1, 5, 10, 20 mg/ml or 0.05 mg/ml concentrations of the digestive enzyme trypsin respectively to induce change, with a 24 hour treatment. In addition Roberts and colleagues used another enzyme papain at a concentration of 20 mg/ml as a comparison. The treated discs resulted in an enzymatically produced cavity in which a reparative treatment can be inserted. In the study carried out by Jim

and colleagues GAG levels were reduced by 70% after 14 days illustrating loss of PG (a feature of disc degeneration).

One major concern about this method is that it does not mimic the progressive nature of the disease and in reality serves as an advanced degeneration model with loss of tissue integrity, rather than mimicking early degenerative changes. Other methods that have also been trialled include a needle puncture injury which has been demonstrated in studies by (Korecki et al., 2008 and Zhang et al., 2011b). Korecki and colleagues (Korecki et al., 2008) presented data that suggested the insertion of both 25G and 14G needle sizes into a bovine disc model induced short term localized degeneration, whilst Zhang and colleagues (Zhang et al., 2011b) demonstrated that insertion of a 4.5-mm drill bit resulted in a significantly higher degenerative histological score compared to smaller scalpel blades used and uninjured controls. The studies suggest that disruption of the disc by instruments such as a needle tip can also induce degenerative changes. Therefore this must be taken into account when considering regenerative delivery methods, as an injection to the disc could also induce degeneration.

Recent studies have also investigated the ability of IL-1 and TNFα to induce early degenerative changes in normal discs, in order to mimic the progressive changes reported in human IVD degeneration and to initiate the deleterious cascade of catabolic events characteristic of disc degeneration (Purmessur et al., 2013; Ponnappan et al 2011). Purmessur and colleagues demonstrated that addition of 200ng/ml TNFα to the cell media surrounding bovine IVD explants for a 7 day period induces a catabolic shift in matrix synthesis and loss of PG content in comparison to fresh discs (Purmessur et al., 2013). Limitations of this study however stem from the removal of end plates during culturing. This allows greater nutrient diffusion and increases the capability of the TNFα to enter the disc, which does not truely mimic physiological conditions. On the other hand Ponnappan and colleagues added a combination of 100ng/ml TNFα and 10ng/ml IL-1 to the culture media surrounding rat IVD explants and analysed discs after 3 or 10 days of treatment. The results also demonstrated a down regulation of matrix genes such as collagen and aggrecan, a significant up regulation of MMP enzymes and increased NGF expression (Ponnappan et al 2011). Limitations of this study however arise as loading conditions were lacking, and whilst the osmolarity was raised to counteract

free swelling, this cannot replicate true mechanical loading conditions. Both studies are beneficial however to pinpoint the deleterious effects of both cytokines during disc degeneration and highlight the aberrant cell biology that occurs initially in disc degeneration.

1.13 Aim of the Project

LBP is a musculoskeletal disease that is associated with IVD degeneration. At present treatments are conservative and focus on the elimination of pain rather than addressing the underlying pathology. Therefore, new cellular based therapies have been proposed to aid in the repair of the degenerate IVD. The choice of cell to be used as a regenerative tool is critical as it is essential to form a functional and appropriate matrix. The elucidation of novel NP markers allows a distinct NP phenotype to be defined, and thus can be used to ensure that MSCs are appropriately differentiated to the correct phenotype. However at present there is no standard protocol to differentiate MSCs to an NP cell.

In addition to this proposed therapies need to be exposed to the IVD microenvironment to test the efficacy of the therapy. This can be undertaken in both *in vitro* and *ex vivo* studies. With these omissions in the literature in mind the aims of each chapter are detailed below.

Chapter 3

1) To characterise cell differentiation and biochemical composition induced by different exogenous growth factors, (TGF-β, GDF5 and GDF6) on MSCs (both BM-MSCs and ADMSCs) seeded in a type I collagen hydrogel.
2) To investigate the biomechanical properties of the ECM in the resultant tissue engineered constructs.
3) To compare the discogenic potential of patient matched BM-MSCs and AD-MSCs to determine a superior cell source.

Chapter 4

1) To characterise discogenic differentiation of AD-MSCs supplemented with GDF6 encapsulated in type I collagen hydrogels following culture in

different conditions (normoxia, hypoxia, normoxia and load, hypoxia and load).

2) To investigate the biochemical composition of AD-MSC seeded constructs supplemented with GDF6 and exposed to normoxia, hypoxia, normoxia and load and hypoxia and load.
3) Investigate the biomechanical properties of the ECM in the resultant tissue engineered constructs.

Chapter 5

1) To investigate the effect of IL-1β on aNPCs
2) To investigate the effect of IL-1β on mature NP cells in order to ascertain whether there are any differential responses. This will be assessed in terms of anabolic and catabolic gene expression, proteoglycan and ECM synthesis.

Chapter 6

1) Investigate the effect of GDF6 on mature NP cells assessed by gene expression of ECM, novel NP, catabolic and anti-catabolic markers and sGAG quantification.
2) Investigate whether pre-treatment with GDF6 protects NP cells when exposed to IL-1β assessed by gene expression of ECM, catabolic and anti-catabolic markers, sGAG quantification and histological localisation.
3) Assess whether a sustained presence of GDF6 is necessary in order to protect NP cells from the catabolic actions of IL-1β.

Chapter 7

1) Establish an ex vivo IVD degeneration model utilising the bovine IVD
2) Establish a compressive testing protocol to assess the biomechanical properties of IVDs
3) Compare the biomechanical properties of normal, experimentally induced degenerate and discs injected with hydrogel.
4) Optimise a microparticle delivery system to allow sustained delivery of the growth factor GDF6

5) Assess whether GDF6 loaded microparticles induce a similar degree of discogenic differentiation in AD-MSCs as exogenous GDF6 supplementation.

Chapter 2

Materials and Methods

2.1 General Human Cell Culture

All reagents are purchased from Sigma Aldrich unless otherwise stated.

2.1.1Isolation of MSCs

Human BM-MSCs and AD-MSCs were isolated from bone marrow aspirates and subcutaneous fat respectively, removed from the proximal femur during hip-replacement surgery in accordance with the North West Research Ethics Committee, Human tissue Act (HTA) legislation and fully informed written consent of all patients. All processing of human samples was performed at room temperature in a laminar flow hood class-II with sterile instruments. Cells were incubated at 37 ºC with 5% CO2 and 20% Oxygen unless otherwise stated.

2.1.1.1 Bone Marrow Samples

BM-MSCs were isolate by Histopaque-1077 gradient centrifugation with simultaneous application of RosetteSep (STEMCELL Technologies) to negatively sort for unwanted blood cells. The sample removed from the proximal femur was diluted to 50 ml with α-MEM supplemented with antibiotics and antimycotics (100 U/ml penicillin, 100 μg/ml streptomycin and 250 μg/ml amphotericin B), centrifuged at 500 x *g* for 10 minutes and the supernatant removed. The cell pellet was resuspended in 5 ml α-MEM supplemented with 20% (v/v) FBS (Life Technologies), antibiotics and antimycotics (subsequently termed initial MSC medium). Two hundred and fifty microliters RosetteSep per 5 ml sample was added to remove unwanted blood cells and incubated for 20 minutes at room temperature. Subsequently, the sample was diluted with 5 ml Hank´s Buffered Salt Solution (HBSS) containing 2% (v/v) FCS and 1mM ethylenediaminetetraacetic acid (EDTA) and with care layered onto 5 ml Histopaque (density: 1.077 g/ml) and centrifuged at 500 x *g* for 30 minutes without applying the brakes in order not to destroy the gradient. Finally, mononuclear cells from the plasma-density gradient interface were seeded into a T75 cell culture flask (BD Biosciences) with 10 ml of initial MSC medium. After 5 days the medium was changed and non-adherent cells were discarded. Adherent cells were cultured to confluence as detailed in section 2.1.2 to be used in future experiments.

2.1.1.2 Adipose Derived Samples

Adipose tissue was dissected from non-adipose tissue, minced into small pieces and incubated at 37^{o}C in 15 ml HBSS containing 0.2% (w/v) type I collagenase and 20 mM calcium chloride for 2 hours with gentle agitation to allow digestion of the tissue. The digested solution was filtered through a 70 μm cell strainer, neutralized with initial MSC medium, and centrifuged for 5 minutes. Finally, the supernatant was aspirated, cells resuspended in initial MSC medium and cultured to confluence in T75 cell culture flask with non-adherent cells discarded.

2.1.1.3 NP Cell Extraction

Degenerate NP cells were isolated from human IVD tissue obtained from surgical samples following informed consent of patients undergoing discectomy and local ethical committee approval. NP tissue was macroscopically dissected from AF tissue, cut into small pieces and incubated at 37^{o}C with 300-350 PUK/ml pronase solution for 30 minutes. Subsequently, the tissue was enzymatically digested with 0.25% (w/v) collagenase type II and 0.1% (w/v) hyaluronidase in serum-free medium containing antibiotics until almost all tissue was digested. The digested tissue/cell suspension was filtered through a 40 μm cell strainer (Fisher Scientific) to remove tissue debris. Cells were then centrifuged at 400 x *g* for 5 minutes, counted and cultured to confluence in a T75 flask in complete NP medium. Representative portions of IVD tissue samples were also embedded in paraffin wax for histological assessment/grading (by a histopathologist Professor Antony Freemont) on the basis of morphological changes (Sive et al., 2002).

2.1.2 Maintenance of Cells

Both BM-MSCs and AD-MSCs were maintained in Minimum Essential Medium α-Modification (α-MEM) including non-essential amino acids, 110 mg/L sodium pyruvate, 1000 mg/L glucose and further supplemented with final concentrations of 10% (v/v) foetal bovine serum (FBS), 2 mM GlutaMAX ^{TM} (Life Technologies), 50 μg/ml ascorbate, 100 U/ml penicillin, 100 μg/ml streptomycin and 0.25 μg/ml amphotericin, (subsequently termed complete MSC medium).

NP cells were maintained in Dulbecco's Modified Eagles Medium (DMEM) including Glutamax and 4500 mg/L D-glucose and supplemented with 10% (v/v) FBS, 50 μg/ml ascorbate, 1 mM sodium pyruvate, 100 U/ml penicillin, 100 μg/ml streptomycin and 0.25 μg/ml amphotericin (subsequently termed complete NP medium). All cells were fed 2-3 times a week.

2.1.3 Passaging and Counting of Cells

To prevent cell contact inhibition of growth, cells were trypsinised when ~80% confluent as determined by phase contrast microscopy. The medium was aspirated and the cells washed in phosphate buffered saline (PBS) prior to addition of 5 ml 0.25% (w/v) trypsin/EDTA solution. Flasks were then returned to the incubator to aid cell detachment. Cells were then transferred to a 15 ml Falcon tube containing 5 ml of MSC medium in order to inactivate the trypsin and pelleted by centrifugation at 400 x *g* for 5 minutes. The supernatant was aspirated and the pellet resuspended in an adequate volume of respective complete medium. Cell counts were undertaken by taking a 10 μl aliquot of the cell suspension and applying to a chamber of a Neubauer haemocytometer. An average count of viable cells located within 4 corner squares (4 x 1 mm^2) and multiplied by 10^4 (conversion factor for Neubauer) was undertaken to give the cell number/ml. The total cell number was then determined by multiplying the cell number/ml by the total volume of cell suspension. Cells were seeded into flasks at a density of 3000 cells/cm^2.

2.1.4 Cryopreservation of Cells

For long-term storage, cells were frozen down and stored in liquid nitrogen. Briefly, following trypsinisation and counting of cells, cells were centrifuged at 400 x *g* for 5 minutes and supernatant removed. The cell pellet was re-suspended in 1 ml Recovery™ cell culture freezing medium (Life Techmologies) and transferred to labelled 1.8 ml cryogenic vials (Fisher Scientific) where they were frozen down at -80°C in a rate controlled Nalgene™ Mr. Frosty™ container (Fisher Scientific) (1°C/min). After 24 hours cryovials were transferred into liquid nitrogen for long-term storage. To thaw cells, cryovials were removed from the liquid nitrogen and

placed in a 37ºC water bath until defrosted. The cell suspension was transferred to a tissue culture flask containing complete medium and left for 24 hours to allow cell attachment. After 24 hours the media was removed and replaced with fresh complete media.

2.1.5 Encapsulation of Cells into Type I Collagen Hydrogels

To encapsulate cells into a type I collagen hydrogel, cells were counted to give a final density of 4 x 10^6/ml and resuspended in the respective complete media. Following this, cells were pelleted via centrifugation at 400 x *g* for 5 minutes. The supernatant was aspirated and the cells were resuspended in 1 part complete media prior to the addition of the 8 parts type I collagen (Devro) (pH 2) and 1 part phosphate buffer (0.2 M sodium phosphate, 1.3 M sodium chloride, pH 11). The solution was vortexed briefly to distribute the cells evenly and a volume of 100 µl was transferred into 0.4 µm high density translucent membrane cell culture inserts (BD Biosciences), within a 24 well plate (BD Biosciences). The culture inserts were maintained with 750 µl media within the well of the plate and the plates transferred to the incubator at 37ºC for 1 hour before 500 µl media was pipetted on top of the hydrogel itself to ensure adequate diffusion of nutrients.

2.1.6 Cell Samples Utilised in Study

The samples listed in table 2.1, were isolated from patients undergoing hip replacement surgery or discectomy surgery as described in sections 2.1.1.1, 2.1.1.2 and 2.1.1.3. Cells were passaged and maintained in respective media (2.1.2) prior to experimental use.

Table 2.1 Details of Cells Utilised Throughout the Study

Sample	Sample ID	Sex	Age	Cell type	Chapter	Analysis
1	WH026	F	32	Patient matched BM-MSCs and AD-MSCs	Chapter 3	• Gene Expression (collagen, pellet)
2	WH035	F	44	Patient matched BM-MSCs and AD-MSCs	Chapter 3	• Gene Expression (collagen, pellet) • DMMB (collagen, pellet) • Safranin-O (collagen, pellet) • Picrosirius Red • SAM
3	WH023	M	40	Patient matched BM-MSCs and AD-MSCs	Chapter 3	• Gene Expression (collagen) • Growth Factor Optimisation
4	WH067	F	22	Patient matched BM-MSCs and AD-MSCs	Chapter 3	• Gene Expression (collagen, pellet) • DMMB (collagen, pellet) • Safranin-O (collagen, pellet) • Picrosirius Red • SAM
5	WH076	M	44	Patient matched BM-MSCs and AD-MSCs	Chapter 3	• Gene Expression (collagen) • Growth Factor Optimisation
6	WH066	F	78	Patient matched BM-MSCs and AD-MSCs	Chapter 3	• Gene Expression (collagen, pellet) • DMMB (collagen, pellet)

						• Safranin-O (collagen, pellet) • Picrosirius Red • SAM
7	WH080	M	66	Patient matched BM-MSCs and AD-MSCs	Chapter 3	• Gene Expression (collagen) • Growth Factor Optimisation
8	WH017	F	52	AD-MSCs	Chapter 4	• Gene Expression • DMMB • Picrosirius Red AFM
9	WH019	F	76	AD-MSCs	Chapter 4 Chapter 5 Chapter 7	• Gene Expression • DMMB • Picrosirius Red • AFM
10	WH020	M	69	AD-MSCs	Chapter 4 Chapter 5 Chapter 7	• Gene Expression • DMMB • Picrosirius Red • AFM
11	WH018	M	67	AD-MSCs	Chapter 4	• Gene Expression • DMMB • PCR • Saf-O
12	WH021	M	55	AD-MSCs	Chapter 4 Chapter 5	• Gene Expression • DMMB • Saf-O
13	HH549	M	55	NP Cells	Chapter 5 Chapter 6	• Gene Expression • DMMB • PCR • Saf-O
14	HH563	F	43	NP Cells	Chapter 5 Chapter 6	• Gene Expression • DMMB • PCR • Saf-O

15	HH294	M	47	NP Cells	Chapter 5 Chapter 6	• Gene Expression • DMMB • PCR • Saf-O
16	HH681	F	41	NP Cells	Chapter 5 Chapter 6	• Gene Expression • DMMB • Saf-O
17	HH518	F	48	NP Cells	Chapter 6	• Gene Expression • DMMB
18	HH572	M	49	NP Cells	Chapter 6	• Gene Expression • DMMB
19	HH370	F	38	NP Cells	Chapter 6	• Gene Expression • DMMB
20	HH367	M	29	NP Cells	Chapter 6	• Gene Expression • DMMB

2.2 General Molecular Biology

2.2.1 Total RNA Extraction

In all experiments detailed in subsequent chapters cells were cultured in a three dimensional systems therefore constructs were fragmented to release the cells and allow them to be lysed. All work was performed under RNase-free conditions. Constructs were transferred to individual 1.5 ml microcentrifuge tubes (MCT's), followed by the addition of 40 µl molecular grinding resin and 400 µl TRI-Reagent. The structures were then ground using a pestle in order to break up the constructs and release the cells. A further 560 µl of TRI-Reagent was added and incubated for 10 minutes before centrifugation at 12000 x *g* for 15 minutes at 4^{o}C to remove debris and the resin. Subsequently 200 µl of chloroform was added to the supernatant and incubated for 3 minutes prior to another centrifugation step at 12000 *g* for 15 minutes at 4^{o}C. The upper aqueous phase was transferred to a fresh MCT supplemented with 2 µl Glycoblue and 500 µl isopropanol before incubation for 10 minutes. A further centrifugation step for 20 minutes resulted in a pellet which was then washed in ice cold 75% (v/v) ethanol and centrifuged for a final time for 5 minutes at 12000 x *g* at 4^{o}C. The ethanol was removed and the pellets air dried to allow evaporation of excess ethanol, prior to resuspension in 21.2 µl Tris-EDTA buffer (pH 7.4).

2.2.2 Purification of RNA Samples

Preliminary experiments undertaken to assess the feasibility of using collagen hydrogels demonstrated that due to the three dimensional culture, samples showed enhanced absorption at 270 nm due to the carryover of phenol when compared to samples cultured in monolayer. Therefore, an additional process was required to facilitate the removal of TRI-Reagent retained within the RNA solution and to ensure the RNA was of an appropriate quality (Krebs et al., 2009).

A water saturated butanol solution was prepared at a 1:1 ratio and vortexed for 10 seconds to allow the phases to separate. Subsequently 500 µl of the upper phase was added to the 21.2 µl RNA solution and vortexed for 5 seconds to mix. This was followed by centrifugation for 1 minute at 12000 x *g*. The butanol layer was carefully removed and replaced with 500 µl of water saturated diethyl ether which had been prepared in the same way as the butanol. This was vortexed for 5 seconds followed by a further centrifugation step for 1 minute at 12000 x *g*. After the

centrifugation step the samples separated into two phases, the upper organic phase was discarded and the remaining ether was evaporated by leaving the samples open under a fume hood for 10 minutes at 37ºC.

2.2.3 Quantification of Total RNA

The RNA concentration and purity was quantified using a NanoDrop® ND-1000 spectrophotometer and software v3.8.1. The A260/280 and A260/230 identified RNA purity; samples with a ratio of 1.8 or higher were considered appropriate for downstream gene expression analysis.

2.2.4 Reverse Transcription

cDNA was synthesised from pure RNA samples using the High Capacity Reverse Transcription Kit. RNA samples were diluted to 200 ng/µl final concentration. Where samples had smaller quantities of RNA (<200 ng/µl) the maximum possible volume was added. An assay 2X master mix was prepared on ice comprising of the reagents detailed n table 2.2:

Table 2.2 Reverse Transcription Master Mix

Master Mix Reagents X1	Volume added (µl)
10X RT Buffer	2
25X dNTP mix (100mM)	0.8
10X RT Random Primers	2
MultiScribe™ Reverse Transcriptase	1
RNAse Inhibitor	1
Molecular biology grade H_2O	3.2

The master mix was mixed at 1:1 ratio with RNA 10 µl:10 µl in RNAse free 0.5 ml MCT. The tubes were placed in a MJ Research PTC-200 Peltier thermal cycler and incubated under the following conditions: 10 minutes at 25ºC, 120 minutes at 37ºC,

5 seconds at 85ºC, followed by cooling to 4ºC. The cDNA samples were diluted to 5 ng/µl based on the RNA concentrations taken after purification of RNA with H_2O and stored at -20ºC.

2.2.5 Quantitative Real-Time Polymerase Chain Reaction

In order to analyse the gene expression profiles of different cDNA samples qPCR reactions were undertaken using the TaqMan qPCR system. FAM-BHQ1 probes were utilised at a concentration of 450 mM and optimal primer concentration determined empirically. QRT-PCR reactions were performed in 96-well optical reaction plates, sealed with optically clear adhesive film and run on an Applied Biosystems StepOne Plus Real Time PCR System. Each reaction consisted of a total volume of 10 µl, incorporating 8 µl master mix and 2 µl cDNA. The master mix was prepared containing 5 µl 2X Lumino Ct qPCR Readymix, 1 µl forward primer, 1 µl reverse primer, and 0.5 µl probe and 0.5 µl 40X ROX internal reference dye. Mastermix was vortexed and 8 µl pipetted into each well of the 96-well plate. Biological samples were examined in triplicate and 2 µl of cDNA was pipetted into each well. A positive and negative sample was run for each gene examined to ensure no false positives; total human RNA and molecular grade H_2O replaced cDNA respectively. The reactions were cycled under the following conditions: 95°C for 20 seconds followed by 40 cycles of 95°C for 1 second and 60°C for 20 seconds. Optimised primer concentrations and primer/probe sequences for the genes utilised throughout this study are detailed in Table 2.3.

The two different methods to detect gene expression by qPCR are shown in Figure 2.1, these are either SYBR Green or the TaqMan probe methods. Throughout this study the latter method is used.

The SYBR Green method uses a highly specific, double-stranded DNA binding dye to detect PCR product as it accumulates during PCR cycles. However, dsDNA dyes such as SYBR® Green will bind to all dsDNA PCR products, including nonspecific PCR products. This can potentially interfere with or prevent accurate quantification of the intended target sequence. Whereas, the TaqMan chemistry uses a fluorogenic probe to enable the detection of a specific PCR product (containing the probe sequence) as it accumulates during PCR cycles. Hence, significantly increasing

specificity, and allowing accurate quantification even in the presence of some non-specific DNA amplification. The probes are flanked with a fluorescent reporter (FAM) at one end and a quencher (MGB) at the opposite end of the probe and the close proximity of the reporter to the quencher prevents detection of its fluorescence (Figure 2.1). During the annealing stage of the reaction both probe and primers anneal to the DNA target. Polymerisation of a new DNA strand is initiated from the primers, and once the polymerase reaches the probe, its 5'-3-exonuclease degrades the probe, separating the fluorescent reporter from the quencher, resulting in an increase in fluorescence. Fluorescence is then detected and measured in the real-time PCR thermocycler, and its geometric increase corresponding to exponential increase of the product is used to determine the threshold cycle in each reaction. The probes also contain a minor groove binder at the 3´ end which increases the melting temperature of probes, allowing the use of shorter probes which exhibit greater differences in melting temperature values between matched and mismatched probes.

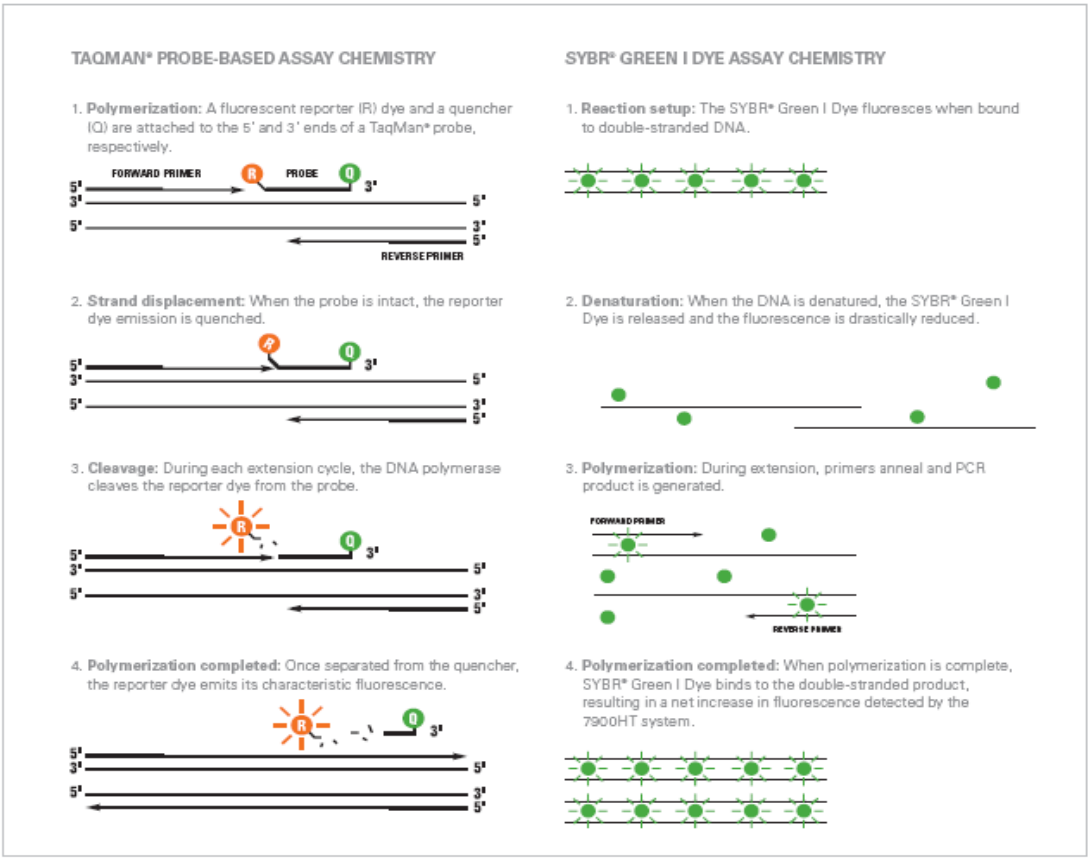

Figure 2.1 Comparison of TaqMan probe and SYBR green qPCR systems. (ThermoScientific, https://www.thermofisher.com/uk/en/home/life-science/pcr/real-time-pcr/qpcr-education/taqman-assays-vs-sybr-green-dye-for-qpcr.html [accessed: 4.02.2016])

Table 2.3 Primer and Probe details

Gene	Accession Number	Forward Primer Sequence 5'-3'	Reverse Primer Sequence 5'-3'	Probe Sequence 5'-3'	Optimal Primer Concentration
MRPL19	NM_014763	CCACATTCCAGAGTTC TA	CCGAGGATTATAAAGTTCAAA	CAAATCTCGACACCTTGTCCTTCG	900mM
EIF2B1	NM_001414	TCCCAGATAAGTTTAAGTATAA G	AGCAGAGTGATTAAGGAA	CGCAGACTGGACAAGA CCTCA	600mM
GAPDH	NM_002046	CTCCTCTGACTTCAACAG	CGTTGTCATACCAGGAAA	CACCCACTCCTCCACCTTTGA	600mM
SOX9	NM_000346	GCTCTGGAGACTTCTGA A	GGTACTTGTAAT CC GGGTG	TCCTCCTTGTGCTGCACG CG	450mM
ACAN	NM_001135	GGCTTCCACCAGTG TGA C	GTGTCTC GGATGCC ATACG	TGACCAGACTGTCAGATACCCCATCC A	900mM
COL2A1	NM_033150	CAGTGGTAGGTGATGTT C	GGCTTCC ATTTCAG CTATG	CCAACACTGCCAACGT CCAG	450mM
KRT8	NM_002273	TGACCGACGAGAT CAACTTCC	TGGACAGCACCAC AGATGTGT	CAGCTATATGAAGAGGAGATC	600mM
KRT18	NM_0002242	GCGAGGACTTTAA TCTTGGTGATG	TGGTCTTTTGGATG GTTTGCA	CAGCA ACTCCATGCAAA	600mM
KRT19	NM_002276	GGTCATGGCCGAG CAGAA	TTCAGTCCGGCTG GTGAAC	CGGAAGGATG CTGAAG	450mM
FOXF1	NM_001451	CCGTATCTGCACCAGAAC	TGGCGTTGAAAG AGAAGA	CCGAGCTGCAAGGCATCCCG	900mM
CAXII	NM_001218	CCAGCAACAAGTCAGAAG	TCCTGGCCTTTGTACTTTA	TCGCTGTCCTGGCTGTTCTC	600mM
T	NM_003181	TTCTCCAACCTATT CTGACAACTCA	ATTCCAAGGCTGG ACCAATTG	TTTATCCATGC TGCAATC	300mM
MMP3	NM_002422	GTGGAGTTCCTGATGTTG	GCATCTTTTGGCAAATCTG	AATTCACAATCCTGTATGTAAGGT	900mM
MMP13	NM_002427	CCCCAGGCATCAC CATTCAAG	GACAAATCATCTT CATCACCACCAC	CTGCCTTCCTCTTCTTGA	900mM

ADAMTS4	NM_005099	TCAGGAAATTCAGGTACG	CGTGTATTCACCATTGAG	CATAGGAGCCATCTGGC	900mM
ADAMTS5	NM_007038	CGCTTAATGTCTTCCATCCTTA	GGATCTGCTTTCGTGGTAG	CAGCAAACAGTTACCATGGCCATCATC	900mM
TIMP1	NM_003254	GACACCAGAGAACCCA	GACGAGGTCGGAATTG	CTGGCTTCTGGCATCCT	900mM
TIMP2	NM_003255	TGCAGATGTAGTGATCAG	TGCCATAAATGTCGTTTC	ACTTCCTTCTCACTGAC	600mM

The Specificity of primers and probe were confirmed by DNA Sequencing. PCR products were purified using QIAquick PCR purification kit (Qiagen UK) according to manufacturer's instructions. Sequencing analysis of PCR products was undertaken by the Stopford Building DNA sequencing facility. Sequencing results were evaluated on NCBI blast to confirm amplicon sequences (appendix 1).

2.2.6 Data Analysis

The data was analysed according to the ΔCt method outlined by (Livak and Schmittgen., 2001) in which gene expression values are normalised to combined internal reference genes, in this study MRPL19, EIF2B1 and GAPDH. Further calculations were undertaken to obtain values used for graphs and statistical analysis, outlined in table 2.4.

Table 2.4 Calculations for qPCR analysis

Value	Calculation for 2-ΔCt	Calculation for 2-ΔΔCt
Average Ct of sample	Average of triplicate	Average of triplicate
ΔCt of sample average	Average Ct (target gene)- Average Ct (ref. gene)	Average Ct (target gene)- Average Ct (ref. gene)
Standard error of the mean (SE)	STDEV((average ΔCt)/SQRT(n))	STDEV((average ΔCt)/SQRT(n))
2-ΔCt	2^- (ΔCt average)	
ΔΔCt		=(ΔCt average sample)- (ΔCt average control)
2- ΔΔCt		=2^-(ΔΔCt)
+ Standard error	2^- (ΔCt average +SE)	2^- (ΔCt average +SE)
- Standard error	2^- (ΔCt average -SE)	2^- (ΔCt average -SE)
+ Error bars	(-SE)- 2-ΔCt	(-SE)- 2-ΔCt
- Error bars	2-ΔCt – (+SE)	2-ΔCt – (+SE)

2.2.7 Statistical Analysis

Statistical analysis was performed with GraphPad InStat and Prism software using a non-parametric Mann-Whitney Test to assess significance with p values equal to <0.05 were deemed significant.

2.3 General Histology and Protein analysis

2.3.1 Embedding and Sectioning

At an end time point constructs were washed in PBS and transferred to a 1.5 ml MCT and stored at -80°C until embedded. The constructs were placed in ~2 ml optimal cutting temperature compound (OCT) (Thermo Scientific) in a square plastic mould and snap frozen in liquid nitrogen for 30 seconds. Blocks were cut into 5 µm sections using a cryostat (Thermo Scientific) and transferred onto positively charged microscope slides (Thermo Scientific). Sections were left to dry overnight then subsequently washed in RNA-free water to remove OCT prior to specific staining.

2.3.2 Haematoxylin and Eosin Staining

In order to determine the morphology demonstrated by tissue samples a haematoxylin and eosin stain was undertaken. Sections were stained with Harris's modified haematoxylin stain for 2 minutes. Sections were then 'blued' in running water for 5 minutes and counterstained in eosin-ploxin (BDH) for 10 seconds. Sections were dehydrated in IMS (Fisher Scientific), cleared in xylene (Fisher Scientific) and mounted (Thermo Scientific).

2.3.3 Safranin-O/ Fast Green staining

In order to assess the proteoglycan/GAG content of a specific sample, a safranin-O / fast green stain was performed. Sections were stained with Weigerts haematoxylin parts A and B (50:50) (TCS Biosciences) for 3 minutes. Sections were then washed in running water for 10 minutes, followed by staining in 0.1% (w/v) aqueous fast green (Difco) for 5 minutes. Sections were then briefly washed in 1% (v/v) acetic acid (Fisher Scientific), counterstained in 0.1% (w/v) aqueous safranin-O for 4 minutes and finally rinsed in IMS. Sections were dehydrated in IMS (4 x 1 minute), cleared in xylene (3 x 5 minutes) and mounted.

2.3.4 Imaging

All slides were visualised using a Leica RMDB microscope and images captured using a digital camera and Bioquant Nova image analysis system.

2.3.5 Dimethylmethylene Blue Assay

At the end of a timepoint, constructs were washed in PBS and stored at -80°C until the assay was performed. The dimethylmethylene blue (DMMB) assay comprised of three steps;

1) Papain digestion for the removal of interfering proteins and glycoproteins.
2) Analysis of sulphated proteoglycans and glycosaminoglycans (sGAG).
3) DNA quantification with PicoGreen kit.

Constructs were removed from storage and transferred into 1.5 ml MCTs containing 0.5 ml papain extraction reagent (200 mM sodium phosphate buffer at pH 6.4, 100 mM sodium acetate, 10 mM EDTA, 5 mM L-Cysteine HCL, 125 µg/ml papain from papaya latex). The MCTs were placed into a thermally regulated heated block at 65^{o}C and left to digest overnight.

Standard curves were made using chondroitin sulphate C sodium salt from shark cartilage. Standards were prepared at concentrations of 1 µg/ml, 5 µg/ml, 10 µg/ml, 20 µg/ml, 30 µg/ml, 40 µg/ml, and 50 µg/ml and a blank using RNAse free water. Forty microlitres of each standard was pippetted in quadruplicate into the 96 well plate. Subsequently, samples were centrifuged at 10000 x *g* for 10 minutes, the supernatant transferred to a new MCT and 40 µl of each sample transferred to the plate in quadruplicate. The colour reagent dye was prepared with 40 mM glycine, 40 mM sodium chloride, 40 mM hydrochloric acid and 0.0016% (w/v) dimethymethylene blue. The colour reagent dye was added, 200 µl to each well, using a multichannel pipette and the absorbance read (Thermo Scientific Multiskan FC) immediately at a wavelength of 540 nm.

Analysis of the results involved subtraction of the average blank value reading from all standard and sample values. Average absorbance readings of the GAG standard dilutions were used to produce a standard curve and GAG concentration values for the unknown samples calculated using the trendline equation. The quadruplicate readings for each sample were averaged and GAG concentration calculated.

2.3.6 DNA Concentration

For normalisation of GAG concentration, DNA concentration was analysed using the Quant-IT PicoGreen dsDNA assay kit (Life Technologies) and was performed using the remaining papain digested solution. One hundred microlitres of each sample was transferred into wells of a black 96-well microplate in triplicate. One hundred microlitres of each standard curve dilution in triplicate were also run alongside the samples, with 1x TE buffer used for blanks (see table 2.5).

Table 2.5 DNA standard preparation

	DNA Concentration (ng)	**Stock DNA (2 µg/ml) (µl)**	**1 xTE Buffer**
A	1000	200 of stock DNA	200
B	100	40 of A	360
C	10	40 of B	360
D	1	40 of C	360
E	0.1	40 of D	360

Using a multichannel pipette, 100 µl of PicoGreen® working solution (diluted 1:200 with 1x TE buffer) was added, mixed and incubated for 4 minutes at room temperature protected from light. Fluorescence was measured using a BioTek® FLx800 fluorescence plate reader with filters 485 nm (excitation) and 538 nm (emission) wavelength. The average blank value was subtracted from all standard and sample values and standard DNA dilutions were used to produce a standard curve. DNA concentration values for the unknown samples were calculated using the trendline equation. The triplicate readings for each sample were averaged and DNA concentration calculated. GAG concentration was normalised to µg DNA through

division of the average GAG concentration (µg) by the average DNA concentration (µg).

2.3.7 Histological Characterisation of ECM deposition

Collagen constructs were embedded and sectioned as described in section 2.3.1 and safranin-O/FastGreen stains were undertaken to localise sGAG outlined in section 2.3.3. Additionally picrosirius red staining and polarised light microscopy was used to assess fibrillar collagen content. Sections were washed prior to staining in Harris haematoxylin for 5 minutes and differentiating with 1% (v/v) hydrochloric acid (HCL) in 70% (v/v) ethanol. Sections were then "blued" in tap water for 5 minutes before counterstaining in 0.1% (w/v) Sirius Red F3BA in saturated aqueous picric acid, for 1 hour. Sections were then dipped twice into 0.1% (v/v) acetic acid before dehydrating and mounting. The fibrillar collagen content was assessed by imaging the same area under bright-field and cross-polarised light microscope and the total area compared to the birefringent area allowing the percentage fibrillar collagen to be assessed based on intensity of staining. Three areas were assessed per section and three sections per cell type and growth factor treatment.

2.4 Chapter 3 Methods

2.4.1 Experimental Design

The ability of TGF-β superfamily members to differentiate MSCs to an NP-like cell was investigated by differentiation of both BM-MSCs and AD-MSCs in type I collagen hydrogel with differentiating media for 14 days. Differentiation was assessed by gene expression, ECM analysis and assessment of micromechanical stiffness. To assess the effect of the growth factor, and distinguish any effect of the type I collagen hydrogel on MSC differentiation the cells were also cultured in three-dimensional pellets

2.4.2 Differentiation of MSCs with TGF-β, GDF5 and GDF6

At P3 MSCs were encapsulated in type I collagen hydrogels as described in 2.1.5 and cultured in a differentiating media detailed in table 2.6.

Table 2.6 Differentiating Media components

Reagent	Final Concentration
ITS-X (Insulin, Transferrin and Selinium) (Life Technologies)	Insulin 10 μg/ml Transferrin 5.5 μg/ml Selinium 6.7 ng/ml
Antibiotics and Antimycotics	100 U/ml Penicillin 100 μg/ml Streptomycin 0.25 μg/ml Amphotericin
Ascorbic acid 2- Phosphate	100 μM
Bovine Serum Albumin (BSA)	1.25 mg/ml
Dexamethasone	10^{-7} M
FBS	1% (v/v)
Linoleic acid	5.4 μg/ml
L-proline	40 μg/ml
Sodium pyruvate	1 mM

To assess optimal growth factor concentration, media was further supplemented with one of the following conditions, listed in table 2.7, and constructs were cultured for 14 days. The respective growth factor was added prior to use and the media was changed every 2 days.

Table 2.7 Optimisation of Growth Factor Concentrations

Growth Factor	Concentrations (ng/ml)
No Growth Factor	Control
TGF-β3- (Life Tecnologies)	1,10,100
GDF5-(PeproTech)	10, 100, 1000
GDF6- (PeproTech)	10, 100, 1000

These particular concentrations were selected based on previously published work (Stoyanov et al., 2011; Purmessur et al., 2011; Shen et al., 2009) and manufacturer's recommendations. Optimal concentrations were determined following qPCR analysis of ECM (COL2A1, ACAN) and novel NP marker genes (KRT8, KRT18, KRT19).

Following the initial optimisation the experiment was repeated with no growth factor as a control and optimal concentrations of respective growth factors for 14 days. Media was changed every 48 hours and retained for subsequent analysis of sulphated glycosaminoglycan (sGAG).

2.4.3 Pellet Culture

To ensure the biomaterial had no effect on the differentiation of MSCs, cells were also cultured in a 3D pellet culture system. Four samples of the same patient-matched BM-MSC and AD-MSC samples detailed in table 2.1 were cultured in monolayer utilised for this study. The cells were dispensed into a 15 ml falcon tube at a density of 250,000 cells in 2 ml of complete media. This was followed by centrifugation at 400 x *g* for 5 minutes to form a pellet. The Falcon tubes were incubated at 37^{o}C for 24 hours. During culture, caps were loosened to allow gas exchange. Subsequently the media was aspirated and replaced with differentiating media containing the respective growth factor. The media was changed every 48 hours and the respective growth factor was added just prior to use.

2.4.4 Downstream Analysis

After 14 days gene expression levels were assessed using qPCR. The genes investigated were categorised as ECM and novel NP marker genes to assess both the ECM and discogenic potential of MSCs within the constructs. Values were normalised to the housekeeping genes MRPL19, EIF2B1 and GAPDH, then further normalised to normoxic samples to determine the sole effects of the environmental conditions using $2^{-\Delta\Delta Ct}$ method (Livak and Schmittgen, 2001). Statistical analysis was performed by means of a Mann Whitney test with significance defined as $p<0.05$.

sGAG production of both construct and media components was assessed as described in section 2.3.5. Values were normalised to dsDNA content of the constructs which was undertaken as outlined in section 2.3.6.

Collagen constructs and pellets were embedded, sectioned and respective staining undertaken to assess sGAG localisation and fibrillar collagen content as described in sections 2.3.3 and 2.3.7.

2.4.5 Micromechanical Characterisation Using SAM Analysis

Cryro-sections of the constructs were analysed using scanning acoustic microscopy (SAM) KSI 2000 microscope with bespoke data acquisition and control systems to assess micromechanical stiffness. The SAM imaging technique uses ultra-high frequency acoustic energy which is then reflected back to form an image. Figure 2.1 is a schematic representation of the SAM used. The SAM images were collected in triplicate using Multi-Layer Phase Analysis (MLPA) method (Graham et al., 2011; Zhao et al., 2012). The size scan was 200 μm and a frequency of 77 MHz to construct acoustic wave speed maps for a total of 3 samples per treatment.

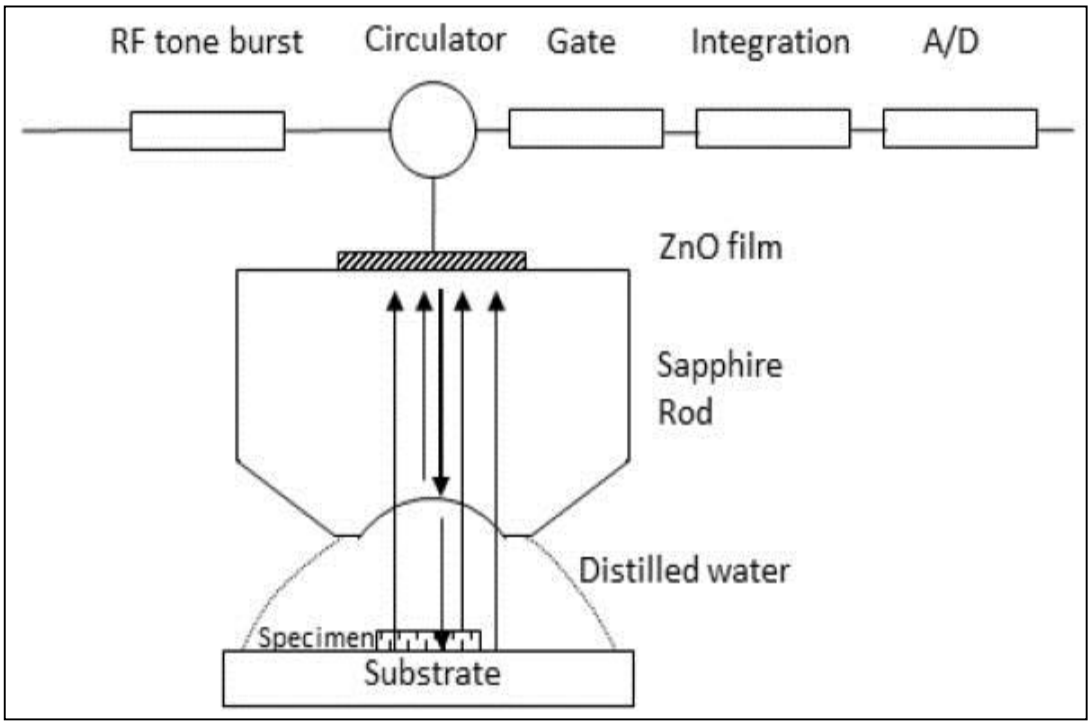

Figure 2.2 Schematic representation of the Scanning Acoustic Microscope (SAM). This illustrates that when a sound wave is generated it propagates through the acoustic lens, medium and specimen with reflections from numerous interfaces (Adapted from Zhao et al., 2012).

2.5 Chapter 4 Methods

2.5.1 Experimental Design

To investigate the effects of the microenvironmental factors on the ability of AD-MSCs supplemented with GDF6 to undergo discogenic differentiation, cells were divided into four treatment groups:

1) Normoxia (20%) (as shown in chapter 3)
2) Hypoxia (2%)
3) Normoxia and Load (20% and 0.04 MPa, 1 Hz, 1 hour per day)
4) Hypoxia and Load (2% and 0.04 MPa, 1 Hz, 1 hour per day)

2.5.2 Application of Compressive Load: Seeding into BioFlex Plates

AD-MSCs listed in table 2.1, were isolated from patients undergoing hip replacement surgery as described in section 2.1.1.2. Cells were passaged and maintained in complete MSC media. At P3 AD-MSCs were encapsulated in type I collagen hydrogels as described in section 2.3.1.5, although in this experiment 100 µl of cell-seeded hydrogel was plated into 13 mm foam rings of BioFlex culture plate at a density of $4x10^6$/ml (Figure 2.2A).

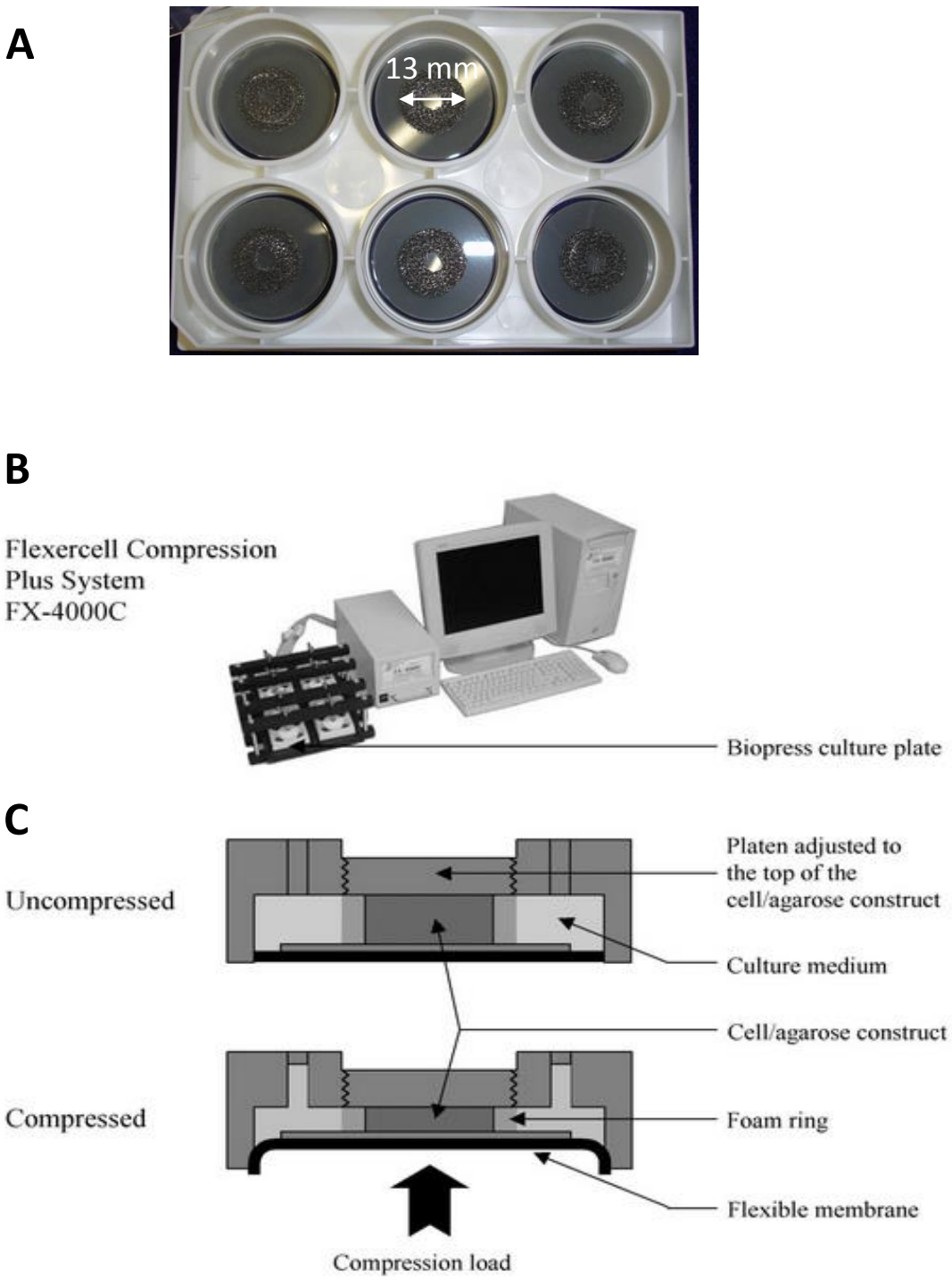

Figure 2.3 Equipment and materials used to apply load. A. Photograph of BioFlex culture plate with flexible membrane bases to allow compression of hydrogels. **B**. A diagram of Flexercell compression system FX-4000C. **C**. A schematic diagram to illustrate how hydrogels were compressed using the Flexercell system (Adapted from www.biomedcentral.com [accessed 10.1.2016]).

Stationary platens were fixed into place in the top of the wells to hold the hydrogels in place. Platens were adjusted using sample thickness and volume of hydrogel calculations to ensure the samples were exposed to the correct compression pressure. All samples had stationary platens fixed to ensure consistency between samples irrespective of whether cells were exposed to load or not. In this experiment a compression regimen of 0.04 MPa at a frequency of 1 Hz for 1 hour per day was used as previously reported by (Bougault et al 2009).

Cells were cultured in one of 4 culture conditions (normoxia, normoxia and load, hypoxia, hypoxia and load) in differentiating media as shown in table 2.6 supplemented with 100 ng/ml GDF6 for 14 days. The media was changed every 48 hours and retained for subsequent analysis of sGAG.

2.5.3 Downstream Analysis

After 14 days gene expression levels were assessed using qPCR. GAPDH was not used in this experiment due to its role in glycolysis which can be affected during hypoxic culture. Statistical analysis was performed by means of a Mann Whitney test with significance defined as $p<0.05$.sGAG production of both construct and media components was assessed as described in section 2.3.5. Values were normalised to dsDNA content of the constructs which was undertaken as outlined in section 2.3.6.

Collagen constructs were embedded and sectioned as described in section 2.3.1 and picrosirius red staining was used to assess fibrillar collagen content as described in 2.3.8.

2.5.4 Micromechanical Characterisation using AFM

The micromechanical stiffness of cyro-sections of the construct were assessed using Atomic Force Microscopy (AFM) (Bauker Catalyst) micro-indentation which assesses the reduced modulus of the tissue (Er). The Er is a mechanical measurement of stiffness that accounts for the indenter compliance (i.e the strength of the cantilever tip used). The Er can be defined as (Choi, 2008):

$$\frac{1}{E_r} = \frac{1 - \nu_i^2}{E_i} + \frac{1 - \nu_s^2}{E_s}$$

E_r= Reduced modulus

E_i = Young's modulus of the indenter **V_i= Poisson's ratio of indenter**

E_s = Young's modulus of the sample **V_s = Poisson's ratio of the sample**

This was performed using a spherically tipped cantilever of nominal radius 1 μm and spring constant of 3 Nm^{-1}. The local reduced modulus, hence tissue stiffness, was determined for each of 100 points in a 20x20 μm region, indented at a frequency of 1 Hz with lateral spacing of 2 μm. For each construct, 3 areas were assessed and a total of 2394 force curves collected per sample and analysed using a Herzian (spherical) model and a maximum force fit of 70%.

In the previous chapter SAM was utilised to measure the stiffness of the tissue; however wavespeed can only be utilised as a surrogate measure for stiffness. Whereas AFM measures the reduced modulus of the tissue which is an actual measurement of stiffness, in addition the AFM has a greater mechanical resolution which allows a larger number of measurements to be made per sample. Hence, AFM can be described as a more precise method to analyse tissue micromechanics and was optimised at a late stage of the PhD.

2.6 Chapter 5 Methods

2.6.1 Experimental Design

To investigate the effects of IL-1β on aNPCs and NP cells, AD-MSCs were initially differentiated to aNPCs with GDF6 for 14 days, whilst NP cells were cultured with no growth factor. The cells were then divided into the following groups:

1) Mature NP cells + No IL-1β for 7 days
2) Mature NP cells + IL-1β for 7 days
3) aNPCs + No IL-1β for 7 days
4) aNPCs + IL-1β for 7 days

2.6.2 AD-MSC Samples

AD-MSCs (table 2.1) were isolated from patients undergoing hip replacement surgery as described in section 2.1.1.2. Cells were maintained in complete MSC media (2.1.2) and passaged to P3 (2.1.3). Following this cells were encapsulated in type I collagen hydrogel as described in 2.1.5 and cultured in differentiating media (table 2.6) supplemented with 100 ng/ml GDF6 to induce discogenic differentiation and media changed every 48 hours.

2.6.3 Mature NP Samples

Native NP cells (table 2.1) were isolated from patients undergoing discectomy surgery as described in section 2.1.1.3. Cells were maintained in complete MSC media (2.1.2) and passaged to P3 (2.1.3). Following this cells were encapsulated in type I collagen hydrogel as described in 2.1.5 and cultured in differentiating media (table 2.6) which was not supplemented with any growth factor and media changed every 48 hours.

2.6.4 Conventional PCR

Following differentiation of AD-MSCs to aNPCs and culture of mature NP cells for 14 days, cells were assessed to ensure they express the IL-1 receptor using conventional PCR. Initially cDNA was generated from extracted total RNA using protocols described in 2.2.1, 2.2.2, 2.2.3 and 2.2.4.

Forward and reverse primers were selected using the nucleotide database with parameters set at a product size of 200-1000, melting temperatures between 58-62ºC with a maximum difference of 2ºC, primers spanning an exon-exon junction and separated by at least one intron. The primer details for GAPDH and IL-1R are listed in table 2.8.

Table 2.8 Primer details for GAPDH and IL-1R for Conventional PCR

Receptor	Accession Number	Forward Primer	Reverse Primer	Product Length	Annealing Temperature ºC
GAPDH	NM_002046	GTTCGACAGTCAGCCGCAT	GGACTGTGGTCATGAGTCCTT	595/687	57
IL-1R	NM_000877	GCCGTCCGTCCAGGTAGA	ACTGGCCGGTGACATTACAG	856	64

The optimal annealing temperature was optimised using total human cDNA and was tested along a spectrum of temperatures starting at 56ºC and increasing by 1ºC to a maximum of 66ºC.

Conventional PCR reactions were performed in 0.2 ml thin-walled PCR reaction tubes and run on an ABI Veriti 96-well Thermal Cycler PCR machine. Each reaction consisted of a total volume of 25 µl, incorporating 2.5 µl cDNA sample and 22.5 µl of master mix which is detailed in table 2.9.

Table 2.9 Conventional PCR Master Mix

Reagent	Volume
10X PCR Buffer +$MgCl_2$	2.5 µl
10mM dNTP mix	0.5 µl
100µM forward primer	0.25 µl
100µM reverse primer	0.25 µl
Taq Enzyme	0.5 µl
Molecular Biology Grade H_2O	18.5 µl

Biological samples were run in triplicate and reactions were cycled under the conditions detailed in table 2.10.

Table 2.10 Cycling conditions for Conventional PCR

Stage	Temperature	Time	
Stage 1	94°C	1 minute	
Stage 2	94°C	30 seconds	40X cycles
	56-66°C	30 seconds	
	72°C	1 minute	
Stage 3	72°C	1 minute	
	4°C	infinite	

Following completion of the cycling reaction 5 µl of loading buffer was added and samples were stored at 4°C.

The PCR products were visualised by gel electrophoresis using 2% agarose gels. The gels were formed by dissolving 4 g of electrophoresis grade agarose in 200 ml of 1x Tris-acetate- EDTA (TAE) buffer and 20 µl of Gel Red was thoroughly mixed into the solution. The solution was then poured into a 100 well gel mould; combs were

placed into the gel and left at room temperature in order to set. After the gel had set combs were removed, the gel placed into an electrophoresis tank and covered with 1xTAE. Samples were pipetted into individual wells at a volume of 15 µl, and next to each gene of 5 µl Hyperladder IV was added to ensure the presence of correct sized bands. Electrophoresis was undertaken at voltages between 50-125 v and the gel observed to ensure samples did not run into adjacent channels. When travelled an appropriate distance the electrophoresis was stopped and the gel placed into the SYNGENE camera and images of the bands were taken under ultraviolet fluorescence using GeneSnap software.

2.6.5 Treatment of Samples with IL-1β

Following analysis of the receptor profile, cells were divided into the groups described in section 2.6.1. Each group was cultured with or without 10 ng/ml IL-1β for a further 7 days with media changes every 48 hours.

2.6.6 Downstream Analysis

After a total of 21 days in culture which included 7 days treatment with or without IL-1β treatment gene expression levels were assessed using qPCR as outlined in section. The genes investigated were categorised as classic ECM, catabolic and anti-catabolic genes to assess the effect of IL-1β on the ECM and catabolic potential of the cells within the constructs. Values were normalised to the housekeeping genes MRPL19, EIF2B1 and GAPDH then further normalised to the respective cell sample not treated with IL-1β to determine the sole effects of the cytokine using $2^{-\Delta\Delta Ct}$ method (Livak and Schmittgen, 2001). Statistical analysis was performed by means of a Mann Whitney test with significance defined as $p<0.05$.

sGAG production of both construct and media components was assessed as described in section 2.3.5. Values were normalised to dsDNA content of the constructs which was undertaken as outlined in section 2.3.6.

Constructs were embedded and sectioned as described in section 2.3.1 and safranin-O stained to show the sGAG localisation as described in section 2.3.3.

2.7 Chapter 6 Methods

2.7.1 Experimental Design

The first stage of this study was to examine the response of mature NP cells to treatment with exogenous GDF6 for 7 and 14 days.

Following this a larger study was undertaken to investigate whether an initial pre-treatment of NP cells with GDF6 or sustained/continued treatment protected NP Cells from or prevented the catabolic effects of IL-1 β The groups for this experiment are detailed in table 2.11.

Table 2.11 Experimental design detailing culture and treatment regimens for NP cells for an initial 14 day period, followed by treatment with or without IL-1β or GDF6

Group	Initial 14 day Culture	Treatment for 7 days
1	No GDF6	No GDF6 No IL-1β
2	No GDF6	No GDF6 10ng/ml IL-1β
3	100ng/ml GDF6	No GDF6 No IL-1β
4	100ng/ml GDF6	No GDF6 10ng/ml IL-1β
5	100ng/ml GDF6	100ng/ml GDF6 No IL-1β
6	100ng/ml GDF6	100ng/ml GDF6 10ng/ml IL-1β

2.7.2 Mature NP Samples

NP cells listed in table 2.1 were isolated from patients undergoing discectomy surgery as described in section 2.1.1.3, the cells were maintained in complete MSC

media (2.1.2) and passaged to P3 (2.1.3) prior to experimental use N=4 for both experiments.

2.7.3 Culture of NP Cells with Exogenous GDF6 and IL-1β

To investigate the effects of GDF6 on mature NP cells, cells were encapsulated in type I collagen hydrogel as described in 2.1.5. The cells were then cultured in differentiating media (Table 2.6) which was either supplemented with or without 100ng/ml of GDF6 for 7 and 14 days.

In addition NP cells were divided into six experimental groups outlined in table 2.11. The cells were encapsulated in type I collagen hydrogel and cultured in differentiating media (Table 2.6.). The supplementation regimen of growth factors and cytokines is detailed in table 2.11 and media was changed every 48 hours. Following a total of 21 days of culture, constructs were collected for downstream analysis including qPCR, quantification of sGAG and histology.

2.8 Chapter 7 Methods

2.8.1 Experimental Design

In this chapter the overall study was divided into a number of sections. The initial study focused on the development of a degenerate ex vivo model, followed by the assessment of the biomechanical properties. Finally preliminary experiments were undertaken to assess the potential of microparticles as a growth factor delivery system for IVD regeneration therapies.

2.8.2 Establishment of the Ex Vivo IVD model: Disc Isolation

Immature (approx 18 months) bovine tails were obtained from a local abattoir within 1 hour of death and caudal discs were isolated within 24hrs of slaughter. The first two largest and the smaller discs of the tail were discarded in accordance with the recent harvesting protocol published by Chan and Gantenbein- Ritter (Chan and Gantenbien- Ritter, 2012) with the remaining discs of similar size used for experimentation (Figure 2.3) .

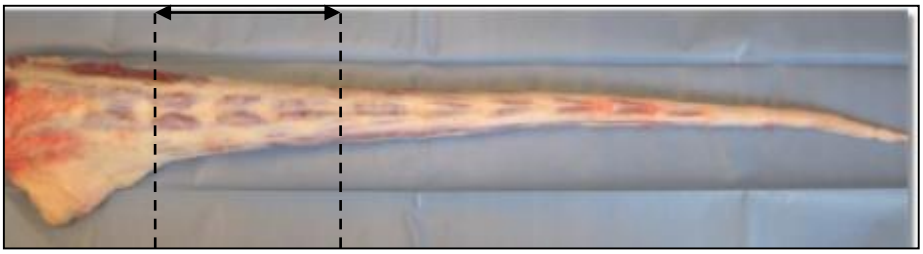

Figure 2.4.**The Bovine tail**. The region between the dotted black lines depicts the region of the tail from which the discs were isolated, hence discarding the larger and smaller discs. This ensured that the discs used for experimental purposes were of a similar size.

The tails were dissected free of skin, muscles and ligaments with a #24 scalpel blade, before parallel axial cuts were made into the vertebral bone using a Medizine 4000 autopsy saw. The incisions were made such that intact bony endplates were maintained across the surface of the NP. The isolated discs were washed in heparin solution (20U/ml) (Sigma) to prevent blood clots, followed by a further wash in antiseptic (dilute mouthwash (1:10) with PBS) to prevent infection and finally washed in PBS before culturing.

2.8.3 Whole Organ Culture

Following excision the discs were transferred to Whirl-pak® bags (Nasco) containing disc culture media which consisted of: 100ml of DMEM/F12 supplemented with 0.2M HEPES (to maintain pH in absence of CO_2), 10% FCS, 2.5mg/ml ascorbic acid, 0.1% Gentamycin and 100 U/ml penicillin, 100 µg/ml streptomycin, 2.5µg/ml amphotericin B (Sigma). Air was then removed from the bag, sealed and discs were incubated at 37^o C under non- loaded conditions.

2.8.4 Development of ex vivo Model

2.8.4.1 Optimisation of Trypsin Concentration

In order to determine an appropriate protocol to induce sufficient matrix degradation in the nucleus pulposus, discs were injected with a range of concentrations of trypsin based on previous work undertaken by Roberts and colleagues (Roberts et al., 2008).

A total of 4 discs from one bovine tail were assigned as a control disc (no injection) or injected with 15, 25, 35 mg/ml trypsin in PBS (12,238U/mg protein, Sigma). Prior to injection an x-ray was taken of the discs at 50kV for an exposure period of 10 seconds, to ensure the 21G needle was adequately located in the NP tissue. An estimated total volume of 200 µl of enzyme solution was then injected

The discs were cultured in Whirl-pak® bags containing disc culture media, at 37°C in unloaded conditions. After 24 hours the trypsin reaction was inactivated by injection of an aprroximately 200 µl of FCS, followed by the transfer of discs to new Whirl-pak® bags containing fresh media and cultured for a further 48 hours.

2.8.4.2 Histology

The degree of matrix degradation/loss was assessed via histological methods. The discs were fixed for 48 hours in 100ml 4% PFA and then immersed in 20% EDTA solution at pH 7.4 for 48 hours in order to decalcify the endplates before processing. Following this the discs were cut sagitally, placed into individual processing cassettes and processed on an extended tissue processing procedure (66 hours). The discs were then embedded in paraffin wax and 5µm sections cut using a rotary microtome. Sections were mounted and dewaxed and rehydrated in xylene and IMS respectively before staining with H&E to assess gross morphology as previously described in section 2.3.2.

2.8.5 Biomechanical Assessment

2.8.5.1 Loading System

The loading system, as previously described by Le Maitre and colleagues (Le Maitre et al., 2009b) is a commercial hydraulic biomechanical testing system, which is comprised of a bench mounted HC5 loading frame (Zwick Testing Machines Ltd) and a load cell that manages the piston (Figure 2.4). For this particular set of experiments, a piston with a flat bottomed surface was attached in order to apply a uniform uni-axial compressive load to the experimental discs. This was partnered with the use of Toolkit 96 Software which in turn generated a controlled and specific loading regime.

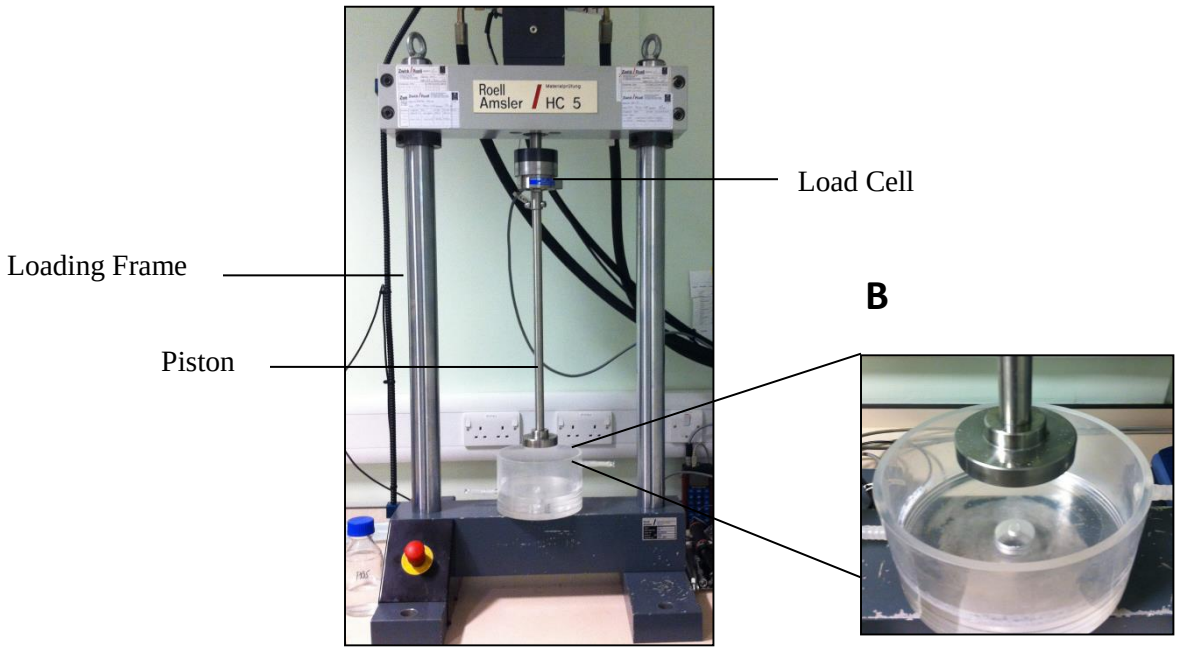

Figure 2.5 Photograph of the loading apparatus used to apply compressive force. Bovine disc tissue explants were excised and separated into three groups, control, induced degenerate and injected with hydrogel. Discs were then biomechanically tested by being placed directly below the flat bottomed piston in a fitted container (Image B) and exposed to the specific loading regime.

2.8.5.2 Experimental Groups

This study focused on investigating three experimental groups:

1) Control disc
2) Experimentally induced degenerate disc
3) Experimentally induced degenerate disc + injection of type I collagen hydrogel

For each experimental group 10 discs were excised as described in section 2.8.2, from a total of 5 different tails, to eliminate inter-animal variation. The diameter and the thickness of the discs were measured for analysis purposes.

The 10 control discs were transferred into individual Whirl-pak® bags containing 100ml of disc culture media as described in 2.8.3. Following this air was removed from the bag, sealed and discs were incubated at 37º C under non- loaded conditions.

For the other 2 groups, discs were injected with 200 µl of 35 mg/ml trypsin to induce a degenerative change, X-rayed to ensure the needle had accurately entered the NP tissue and incubated for 24 hours in Whirl-pak® bags in the same conditions as the control discs. Following 24 hour culture period enzymatic digestion was stopped by

200 µl of FCS. Discs in group 3 then had a further injection of 200 µl type I collagen hydrogel (made up as described in section 2.1.5, which was stained with Inidain ink in order to visualise the hydrogel within the NP tissue. All discs were cultured for another 2 hours, prior to application of compressive load

2.8.5.3 Application of Compressive Load

In a review by Chan et al., (Chan et al., 2011a), it is proposed that the magnitude of physiological loading is between 0.2-0.8 MPa. Therefore initial experiments were undertaken to investigate the loading range in kilograms (kg) that relate to this magnitude. Discs were placed into the plastic container shown in Figure 2.4 and the piston moved at a speed of 0.02 mm/s to a maximum load of 35 kg and results recorded every 2 seconds.

2.8.5.4 Analysis of the Compression Data

The data obtained from the compression experiment was expressed as the force in kN and the position of the piston in a range from 50 mm to -50 mm. Therefore, the following formulas were used in order to obtain presentable data (Table 2.12).

Table 2.12 Formulas used to obtain data from the loading rig

Load	Force(kN) x 100= Load in Kg
Displacement	Original position of the piston – Position of piston at final point = Displacement value (cm)
Strain	Change in thickness (displacement value)/original thickness = Strain
Stress	Force/cross sectional area (using π x r^2) = Stress

2.8.6 Development and optimisation of a Microparticle Delivery System for GDF6

This study was undertaken in collaboration with the Shakesheff laboratory at the University of Nottingham. They have demonstrated the ability to fabricate different size microparticles either 20-50 μm or 50-100 μm (White et al., 2013). Hence, an initial experiment was carried out to determine which microparticles would be suitable for use with the type I collagen hydrogel system and not disrupt the formation of the hydrogel.

2.8.7 Fabrication of Microparticles

2.8.7.1 PLGA-PEG-PLGA Triblock Copolymer Preparation

The triblock copolymer was produced using methods detailed in studies by Zentner and Hou (Zentner et al., 2001; Hou et al., 2008). PEG (1500kDa, Sigma) was heated to 120^{o}C under vacuum, the temperature was then raised to 150^{o}C for 30 minutes under a nitrogen atmosphere and D, L-lactide (Lancaster synthesis, Alfa Aesar) and glycolide (Purac, Netherlands) were added. Following this the catalyst stannous octoate (Sigma) was added and allowed to react for 8 hours. The resulting copolymer was dissolved and precipitated in water in order to remove unreacted reagents and dried under vacuum

2.8.7.2 Microparticle Preparation

PLGA (PLGA 85:15 DLG HCA, MW: 53kDa Lakeshore Biomaterials) microparticles were formed using a water in oil in water, double emulsion method. An aqueous solution of HSA (Sigma) was added to a solution of PLGA and PLGA-PEG-PLGA (9:1 ratio respectively) in dichloromethane (Fisher Scientific). The phases were homogenised (Silverson L5M homogeniser) for 2 minutes at 4000 rpm to form the water in oil emulsion. This was then added to 200mL aqueous solution of polyvinyl alcohol (PVA 0.3%). In order to produce different size microparticles the solution was homogenised for 2 minutes at 9000 rpm for 20-50 μm or 2000 rpm 50-100 μm. The double emulsion was magnetically stirred for 4 hours at 300 rpm and then filtered, washed and lyophilised.

2.8.7.3 Assessment of Small and Large Microparticles in Type I Collagen

AD-MSC seeded type I collagen hydrogels were prepared as previously described in section 2.3.1.5, and loaded with either small or large microparticle at different weights 0mg (control), 1mg, 2mg or 4mg as recommended by Dr Lisa White at the University of Nottingham. The loaded hydrogels were pipetted into cell culture inserts and cultured in differentiating media supplemented with GDF6 (section 2.3.1.7) for 7 days.

2.8.7.4 Histology

Following 7 days in culture hydrogels were snap frozen in liquid nitrogen, embedded in OCT and H and E staining was performed as described in sections 2.3.3.1 and 2.3.3.2.

2.8.7.5 Fabrication and Characterisation of GDF6 Microparticles

Following the size determination experiment 2 batches of microparticles were fabricated as described in 6.3.5.1.2:

1) 0.7g PLGA, 0.3g triblock – 9mg Human Serum Albumin (HSA) – HSA Control
2) 0.7g PLGA, 0.3g triblock – 9mg HSA:1mg GDF6 – GDF6 Microparticles

2.8.7.6 Protein Release Kinetics

Aliquots (25 mg) of the microparticles (triplicate samples from each batch) were suspended in 1 ml PBS and samples were incubated on a 3-dimensional shaker (Gyrotwister, Fisher Scientific UK Ltd) at 5 rpm in a humidified incubator at 37 °C. At defined time intervals, the PBS was removed from the microparticles and replaced with fresh PBS; all liquid above the particles was collected without removing particles. The removed supernatants were stored frozen until required and were then assayed for total protein content using the Micro BCA assay kit with a standard curve of HSA. Sample (150µl) and BCA working reagent (150µl) were mixed and incubated for 2 hours at 37 °C and the absorbance at 540 nm measured using a plate reader.

2.8.7.7 GDF6 ELISA

In order to ensure the release kinetics of HSA protein matched the GDF6 protein a GDF6 ELISA (amsbio) test was performed. Samples were diluted within the 0-50ng/ml range and the ELISA kit protocol was followed. Briefly, 100µl of standards (0ng/ml, 2.5ng/ml, 5ng/ml, 10ng/ml, 25ng/ml, and 50ng/ml) and samples were pipetted into the antibody pre-coated Microtiter plate. Ten microlitres and 50µl of balance solution and conjugate was added respectively, mixed and incubated for 1 hour at 37ºC. Following this the plate was washed x5 with wash solution. A combination of substrate A and B were added to each well and incubated for 15 minutes at 37ºC. Finally 50µl of stop solution was added to each well and the optical density was read at 450nm. The concentrations of samples were then determined using the standard curve.

2.8.7.8 Assessment of Discogenic Differentiation utilising GDF6 loaded microparticles

The results from the ELISA plate determined the total amount of GDF6 that could be incorporated into the hydrogel to replicate the concentration administered exogenously. An experiment was set up to investigate if the microparticles could induce the same degree of discogenic differentiation as exogenous treatment using cells detailed in table 2.1. This was separated into 3 experimental groups:

1) AD-MSC seeded hydrogels +No MP + Exogenous GDF6

2) AD-MSC seeded hydrogels + MP HSA only + Exogenous GDF6

3) AD-MSC seeded hydrogels + MP GDF6 + No Exogenous GDF6

All hydrogels were cultured for 14 days and assessed for discogenic gene expression, GAG content and histological analysis undertaken.

Chapter 3

Differentiation of human mesenchymal stem cells to a nucleus pulposus phenotype using members of the TGF-β superfamily

Work from this chapter is published as:

Clarke, L.E., McConnell, J.C., Sherratt, M.J., Derby, B., Richardson, S.M. and Hoyland, J.A. Growth differentiation factor 6 and transforming growth factor-beta differentially mediate mesenchymal stem cell differentiation, composition, and micromechanical properties of nucleus pulposus constructs. Arthritis Res Ther, 2014. **16**:R67.

See appendix 2

3.1 Overview

Cell-based therapies have been vastly investigated for novel therapeutic applications to treat IVD degeneration. As discussed in chapter 1, BM-MSCs and AD-MSCs have demonstrated the capacity to proliferate *in vitro* and to differentiate into multiple connective tissue lineages, including an NP phenotype (Pittenger et al., 1999; Richardson et al., 2006, Minogue et al., 2010a). Unlike chondrogenic, adipogenic and osteogenic protocols, the methodology to differentiate cells to an NP phenotype has not been clearly defined or standardised. Hence, for MSCs to be utilised in regenerative strategies it is important to accurately identify the differentiated cell phenotype and ensure appropriate and functional ECM synthesis. Recent publications from this group (Minogue et al., 2010b) and others (Sakai et al., 2009; Gilson et al., 2010; Rutges et al., 2010; Power et al.,2011) on the discovery of novel human NP cell markers has allowed a clear distinction to be made between the chondrocyte and NP cell phenotype. This elucidation has allowed a more defined set of markers (KRT8, KRT18, KRT19, FOXF1 and CA12) which in turn have been used to identify appropriate differentiation of both BM-MSC and AD-MSC to an NP like cell (Minogue et al., 2010a, Clarke et al., 2014). Whilst TGF-β has been commonly used by several groups (Risbud et al., 2004; Richardson et al., 2006; Yu et al., 2012) to induce NP-like differentiation, the majority of these studies only used ECM markers (COL2A1, SOX9 and ACAN) to define differentiation (Risbud et al., 2004). Therefore alternative growth factors such as GDF5 and GDF6 should be investigated, using the novel NP markers to define differentiation.

3.1.1 Assessment of Matrix Stiffness

In current literature the main focus of studies aiming to regenerate the IVD is to assess gene and protein marker expression to illustrate that the biochemical composition is similar to that of native NP tissue (Risbud et al., 2004; Richardson et al., 2006; Minogue et al., 2010b). However there is little information published about the biomechanical properties of synthesised ECM in the disc. This is important as the behaviour of ECM-rich tissues is not determined solely on the biochemical composition but also the assembly of these structures. In biological materials there are biomechanical differences between tissue types but more importantly changes with age and the development of disease. For example age related changes in the

mechanical properties of other tissues such as lungs (Lai-Fook and Hyatt, 2000; Nanssens et al., 1999; Meyer et al., 1998) and aorta (Cattell et al., 1996; Graham et al., 2011) are associated with increased stiffness leading to mortality. In particular a study undertaken by Graham and colleagues (Graham et al., 2011) investigated micro-mechanical stiffness of the aorta in an aging sheep model. Using scanning acoustic microscopy (SAM), results showed that the older aorta sample was stiffer than the young sample highlighting the age related changes. In addition this study also demonstrated that SAM is a useful technique to assess stiffness of biological samples. Hence in Stoyanov et al, whilst the supplementation of MSCs with GDF5 induced discogenic differentiation by upregulation of NP markers, the matrix was not PG rich. Therefore information about the stiffness of the matrix would be valuable to see how this corresponds with native tissue but also to the samples treated with TGF-β. Thus, in this study we have combined both the biochemical composition and biomechanical properties to highlight the overall behaviour of resulting constructs.

3.2 Hypothesis

This study was designed to investigate the effects of media conditioned with different exogenous growth factors from the TGF-β superfamily on the discogenic differentiation of both BM-MSCs and AD-MSCs.

For this work it was hypothesised that the choice of exogenous growth factor and MSC source would influence cell differentiation, ECM composition and mechanical stiffness of the resulting construct.

The more specific hypotheses proposed from analysing recent literature and our own work are:

1) GDF6 induces superior discogenic differentiation compared to other TGF-β superfamily members.
2) AD-MSCs are a more appropriate cell choice (as defined by differentiation and matrix formation) for cell based regenerative therapies for the IVD.

3.3 Results

3.3.1 Optimisation of Growth Factor Concentrations

Both BM-MSCs and AD-MSCs were seeded into type I collagen hydrogels and stimulated for 14 days with different concentrations of either: no growth factor (control), TGF-β, GDF5 and GDF6 to determine optimum concentrations to be used in future experiments. qPCR analysis of a selection of ECM and novel NP markers was undertaken. All values were normalised to housekeeping genes and then normalised to the no growth factor controls using the $2^{-\Delta\Delta Ct}$ method as described in table 2.6. Both BM-MSCs (Figure 3.1) and AD-MSCs (Figure 3.2) showed a dose-dependent response to all growth factors when compared to control samples. ECM markers COL2A1 and ACAN demonstrated significantly increased gene expression with exposure to all growth factors, while novel NP marker gene expression was significantly upregulated following stimulation with GDF6, particularly in AD-MSCs. This identified optimal concentrations of 10 ng/ml TGF-β and 100 ng/ml of GDF5 and GDF6. Therefore these concentrations were subsequently used.

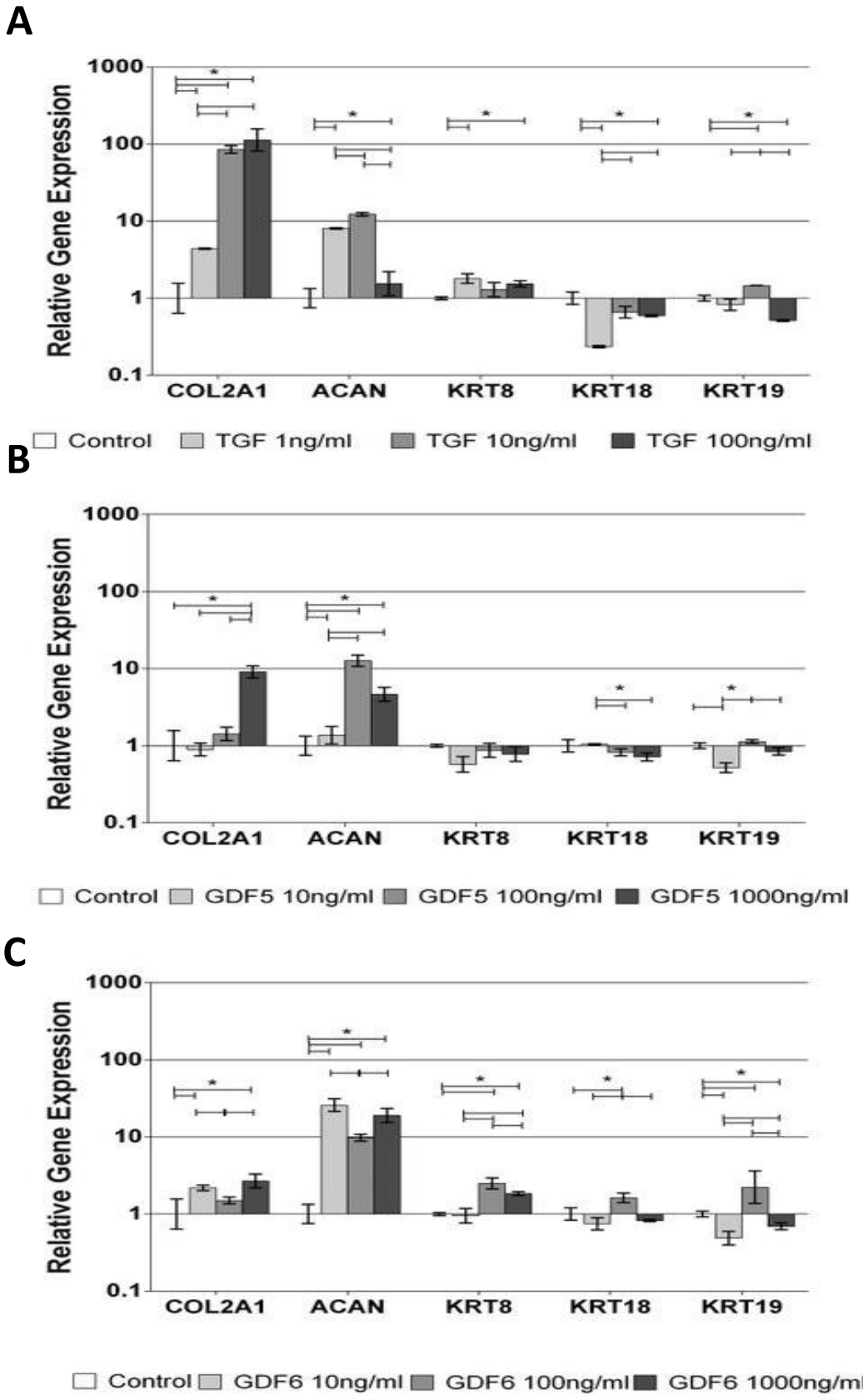

Figure 3.1 Optimisation of growth factor concentrations. BM-MSCs were seeded in type I collagen hydrogels and stimulated with varying concentrations of **A**. TGF-β, **B**. GDF5, or **C**. GDF6 for 14 days. Relative gene expression was normalised to housekeeping gene expression and cells cultured with no growth factor stimulation and plotted on a log scale. N = 3; data represent mean ± SEM. *P < 0.05.

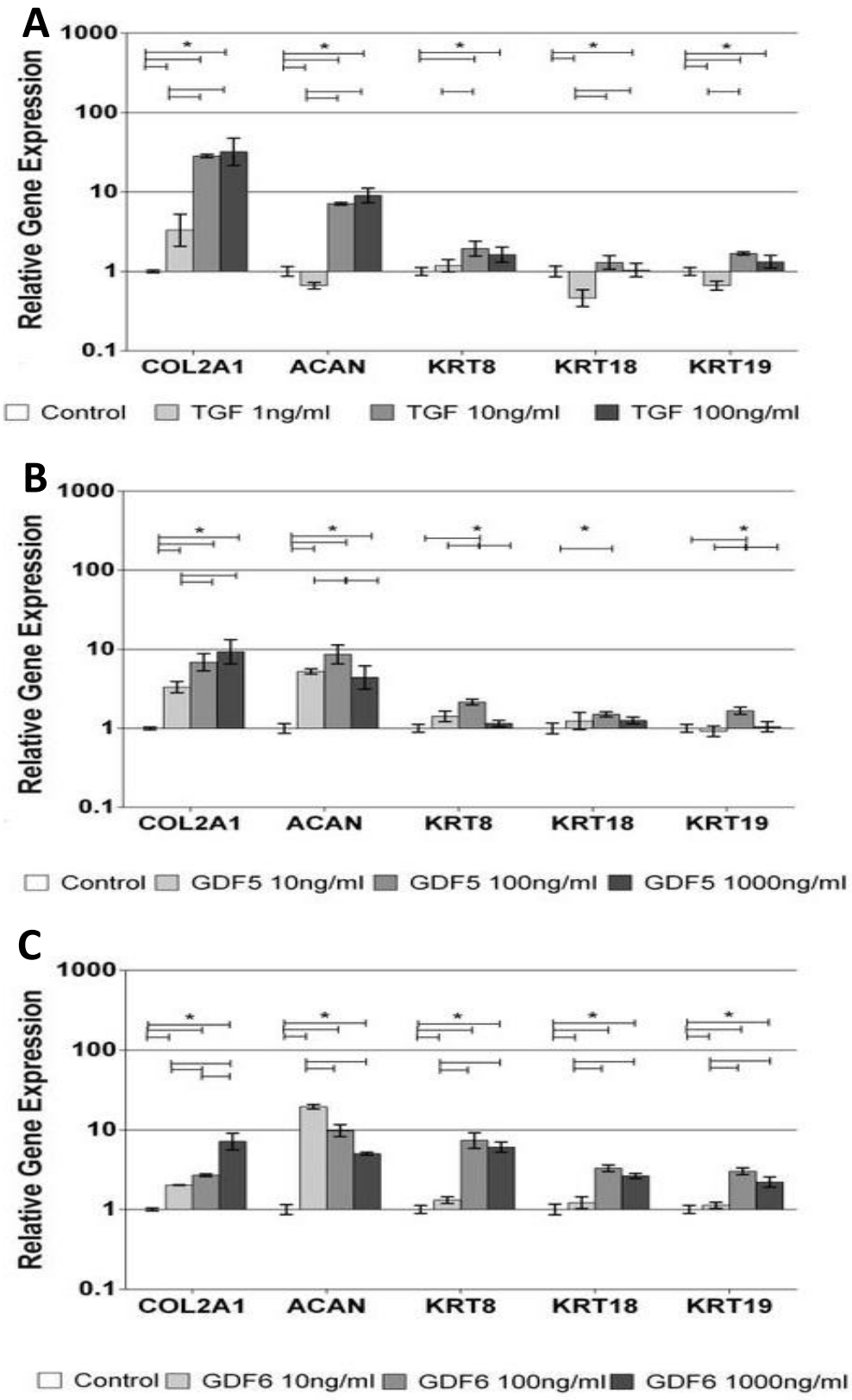

Figure 3.2 Optimisation of growth factor concentrations. AD-MSCs were seeded in type I collagen hydrogels and stimulated with varying concentrations of **A**. TGF-β, **B**. GDF5, or **C**. GDF6 for 14 days. Relative gene expression was normalised to housekeeping gene expression and cells cultured with no growth factor stimulation and plotted on a log scale. N = 3; data represent mean ± SEM. *P < 0.05.

3.3.2 ECM Marker Expression in Type I Collagen Hydrogels

After 14 days of culture in type I collagen hydrogels BM-MSC and AD-MSC ECM gene expression was normalised to housekeeping genes and then to the control sample to assess the effect of each growth factor. BM-MSCs (Figure 3.3 A) cultured in the presence of all growth factors resulted in significant upregulation of SOX9 and ACAN; the largest increase of ACAN (13.1-fold) was in the GDF6 stimulated cohort compared to other treatments (GDF5 8.7-fold and TGF-β 9.0-fold). Cells cultured with TGF-β demonstrated significant upregulation of all ECM markers, as has previously been shown (Risbud et al., 2004; Richardson et al, 2006) with the greatest increase of expression in COL2A1 (66.0-fold) compared to control and also GDF5 (1.5-fold) or GDF6 (2.5-fold). Culture of AD-MSCs (Figure 3.3 B) in the presence of all growth factors resulted in a significant increase in ACAN compared to the control. Similarly to BM-MSCs, the GDF6 stimulated cohort caused a significantly greater increase in ACAN (20.7-fold) than the other growth factor treatments (GDF5 11.0-fold and TGF-β 11.1-fold) compared to the control. Cells cultured with TGF-β demonstrated significant upregulation of all ECM markers, again with the largest upregulation of COL2A1 (34.2-fold) compared to other treatments (GDF5 4.0-fold and GDF6 2.7- fold).

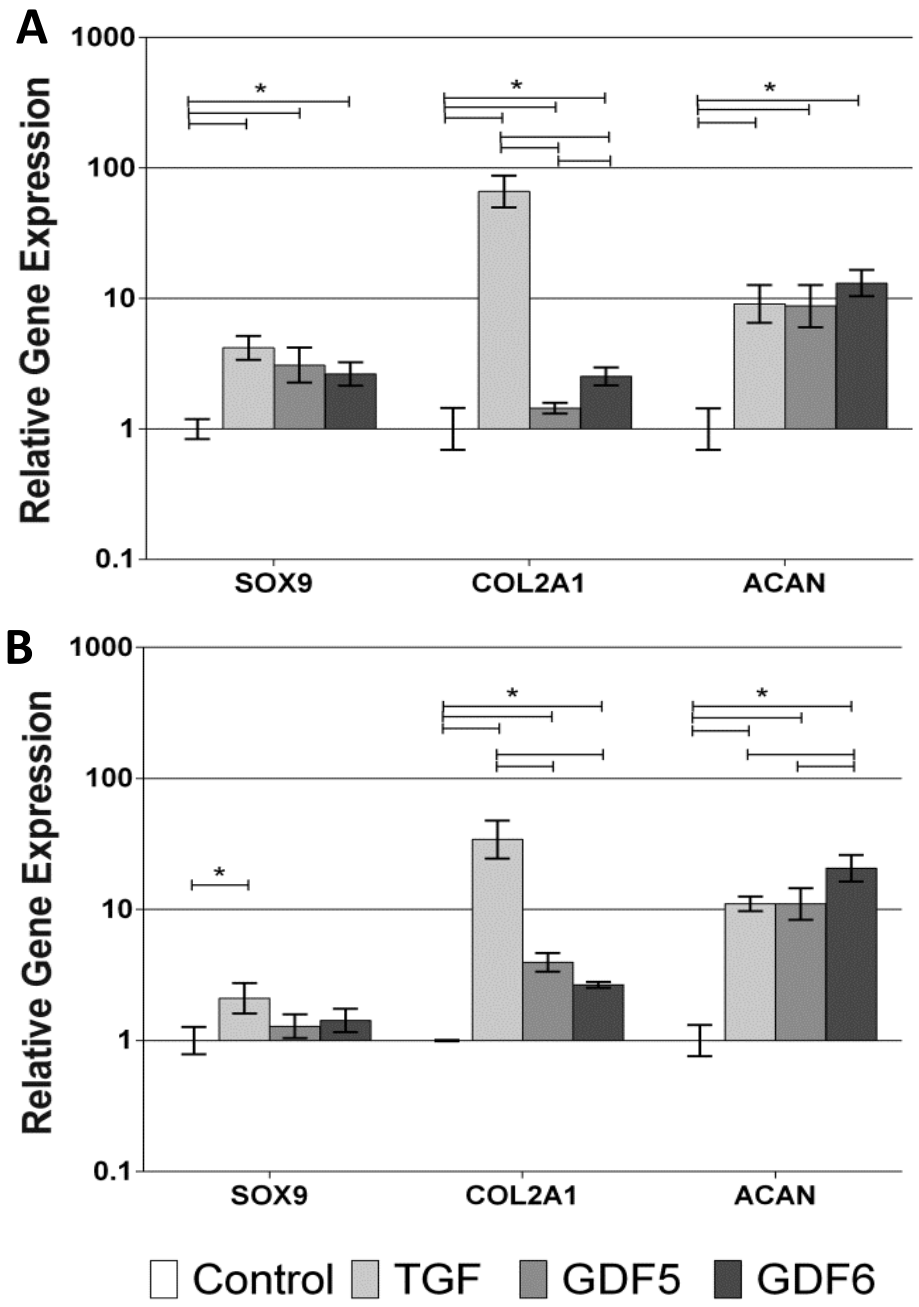

Figure 3.3 qPCR analysis of ECM gene expression. **A.** BM-MSCs and **B**. AD-MSCs were cultured for 14 days in type I collagen hydrogels and stimulated with optimal concentrations of TGF-β, GDF5, or GDF6. Relative gene expression was normalised to mean housekeeping gene expression and cells without growth factor stimulation and plotted on a log scale. $N = 7$; all data represent mean ± SEM. *$P < 0.05$.

3.3.3 ACAN:COL2A1 Gene Expression Ratio

To demonstrate the PG-rich nature of the NP tissue Mwale et al (Mwale et al., 2004) concluded the PG:collagen ratio was 27:1 at the protein level. Similarly this has been undertaken at the gene expression level focusing on the most abundant PG ACAN and COL2A1 (Gantenbien-Ritter et al., 2011; Peroglio, 2013). Hence we looked at the ACAN to COL2A1 relative gene expression to look at the ratio within the constructs. This was analysed using the following formula:

$$(2^{-\Delta CtACAN-\Delta CtCOL2A1})$$

BM-MSCs (Figure 3.4) cultured in the presence of no growth factor, TGF-β, GDF5 and GDF6 demonstrated ratios of 8:1, 0.7:1, 25:1 and 28:1 respectively. Hence cells stimulated with GDF6 had the highest ACAN:COL2A1 ratio, whilst cells treated with TGF-β demonstrated the lowest ratio.

AD-MSCs (Figure 3.4) cultured in the presence of no growth factor, TGF-β, GDF5 and GDF6 demonstrated ratios of 15:1, 4:1, 29:1 and 75:1 respectively. Thus, similar to BM-MSCs, cells stimulated with GDF6 had the highest ACAN:COL2A1 ratio, whilst cells treated with TGF-β demonstrated the lowest ratio.

Overall AD-MSCs treated with GDF6 demonstrated the highest ratio at 75:1, whilst BM-MSCs treated with TGF-β demonstrated the lowest ratio at 0.7:1.

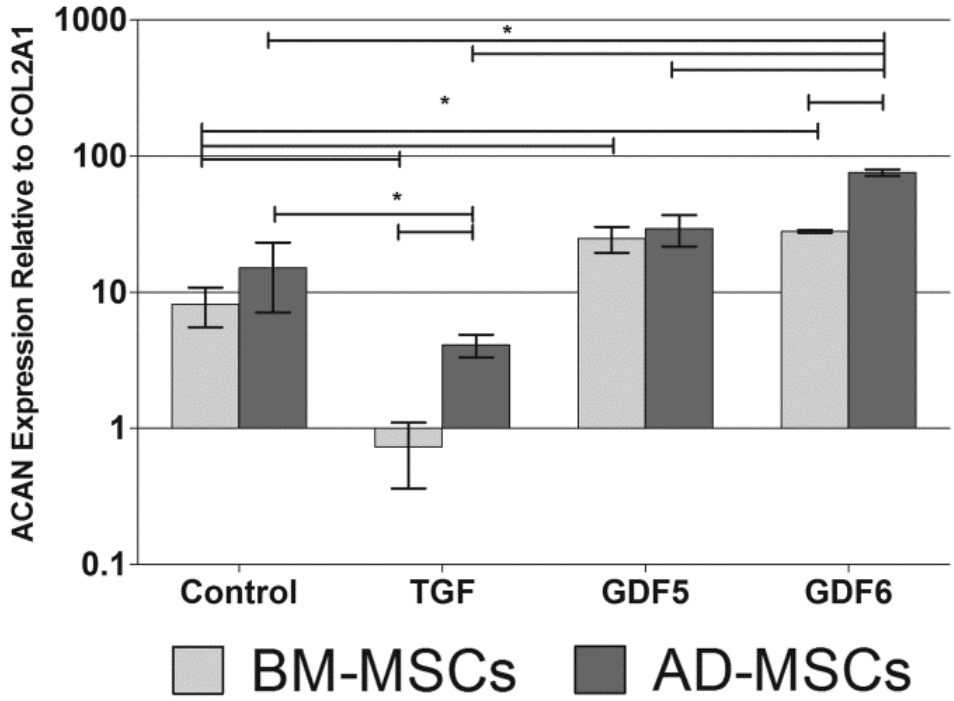

Figure 3.4 ACAN:COL2A1 gene expression ratio in BM and AD-MSCs. Following culture of BM and AD-MSCs in type I collagen hydrogels for 14 days with either no growth factor, or optimal concentrations of TGF-β, GDF5, or GDF6 ratios were determined using the formula (2-ΔCtACAN-ΔCtCOL2A1). N = 7; all data represent mean ± SEM. *P < 0.05.

3.3.4 Novel NP Marker Expression in Type I Collagen Hydrogels

Following microarray studies (Minogue et al., 2010a, Minogue et al., 2010b) a set of defined novel NP markers (KRT8, KRT18, KRT19, CAXII, FOXF1 and T) were used to assess the discogenic differentiation of both BM-MSCs and AD-MSCs. Therefore following 14 days of culture in type I collagen hydrogels BM-MSC and AD-MSC gene expression of novel NP markers was normalised to housekeeping genes and then to the control sample.

Culture of BM-MSCs (Figure 3.5 A) in the presence of TGF-β and GDF5 caused no significant change in KRT8 (0.9 and 0.9- fold respectively), and KRT19 (1.1 and 1.2-fold respectively). There was a significant downregulation of KRT18 (0.7 and 0.5-fold respectively), FOXF1 (0.4 and 0.3- fold respectively) and T (0.6 and 0.6-fold respectively). In contrast, BM-MSCs treated with GDF6 significantly upregulated KRT8 (2.2-fold), KRT18 (2.0- fold), KRT19 (3.0-fold), CAXII (2.9-fold) and T (2.0- fold), with no significant differences noted in FOXF1 (1.2- fold).

Treatment of AD-MSCs (Figure 3.5 B) with GDF6 resulted in significant upregulation of all novel marker genes compared with controls (KRT8 (7.2-fold), KRT18 (3.6-fold), KRT19 (3.3-fold), FOXF1 (3.1-fold), CAXII (2.2-fold) and T (3.5- fold). Stimulation with GDF6 also showed significant increases in comparison to treatment with TGF-β and GDF5 in the case of KRT8, KRT18, KRT19 and T expression. Evaluation of both cell types showed a differential response to the growth factors and demonstrated that expression levels were consistently upregulated to a greater extent in AD-MSCs than in BM-MSCs.

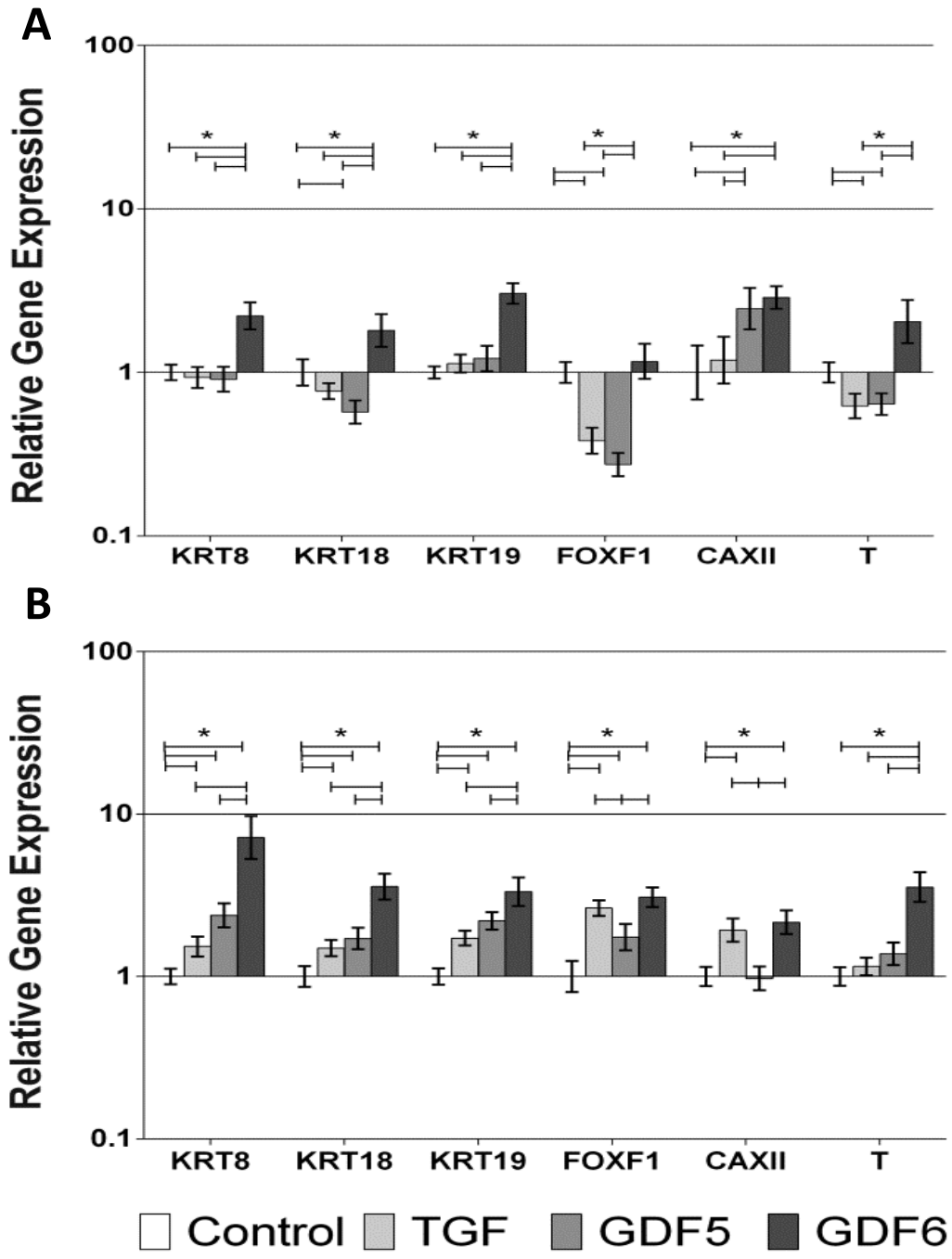

Figure 3.5 qPCR analysis of novel NP marker gene expression changes in response to growth factor stimulation.A. BM-MSCs and B. AD-MSCs were cultured for 14 days in type I collagen hydrogels and stimulated with optimal concentrations of TGF-β, GDF5, or GDF6. Relative gene expression was normalised to mean housekeeping gene expression and cells without growth factor stimulation and plotted on a log scale. N = 7; all data represent mean ± SEM. *P < 0.05.

3.3.5 Assessment of sGAG content

3.3.5.1 Quantification of sGAG synthesis

The quantification of sGAG was further divided into construct and media components and the combined total. AD-MSCs (Figure 3.6A) cultured in type I collagen hydrogels demonstrated significant increases in the sGAG/DNA content within the constructs after stimulation with TGF-β (265.0 μg/μg DNA ±27.7) and GDF6 (243.5 μg/μg DNA ± 13.9) compared to control constructs (123.7 μg/μg DNA ± 19.9). Conversely BM-MSCs (Figure 3.6 A) displayed significant increases in sGAG/DNA content within the constructs compared to the control in only TGF-β stimulated cells, (124.6 μg/μg DNA ± 12.7 and 215.6 μg/μg DNA ± 28.7 respectively). Comparison of the cell types demonstrated that AD-MSCs produced consistently higher levels of sGAG/DNA than BM-MSCs in constructs, particularly in the GDF6 stimulated cohort which was statistically significant (149.6 μg/μg DNA ±17.0 in BM-MSCs versus 243.5 μg/μg DNA μg ± 13.9 in AD-MSCs).

Over the 14 day culture period media was collected every 48 hours and replaced with fresh media. This was then analysed for cumulative release of sGAG into the media. As this does not contain a cellular component it was not normalised to DNA (Figure 3.6 B). After 14 days the sGAG was greatest in AD-MSCs treated with GDF6 (103.7 μg ± 8.5). Both BM-MSCs and AD-MSCs treated with either TGF-β (83.8 μg ± 2.0 and 88.8 μg ± 6.5 respectively) or GDF6 (92.9 μg ± 2.8 and 103.7 μg ± 8.5, respectively) demonstrated significant increases in released sGAG compared with the respective control (59.6 μg ± 2.2 and 66.5 μg ± 3.5).

When total sGAG/DNA combined from both construct and media were analysed this demonstrated that AD-MSCs (Figure 3.6 C) treated with GDF6 produced the most sGAG in the study (3,228.6 μg/μg DNA ± 185.9). This result was significantly greater than both the control (1,703.7 μg/μg DNA ± 72.9) and all other treatment groups (TGF-β 2,414.9 μg/μg DNA ± 180.8 or GDF5 2,512.9 μg/μg DNA ± 134.4). Additionally BM-MSCs treated with GDF6 synthesised the more sGAG (2,799.3 μg/μg DNA ±92.3) than other BM-MSC treatment groups; however this was lower than that produced by AD-MSCs.

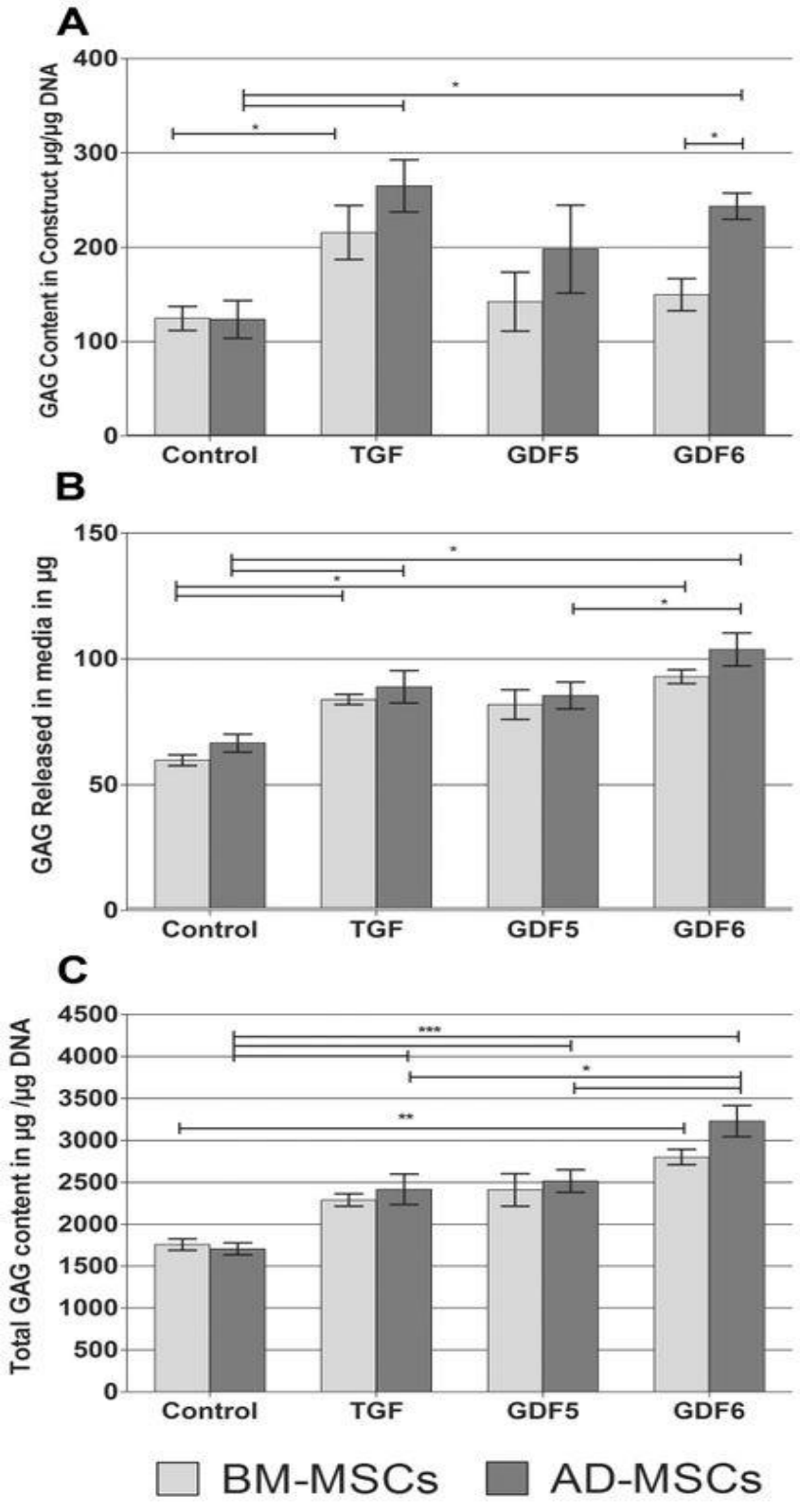

Figure 3.6 Quantification of sGAG in BM and AD-MSC seeded constructs. A. Quantification of sGAG retained within hydrogel constructs, normalised to DNA content within the construct. **B.** DMMB quantification of sGAG released cumulatively into the media throughout the culture period. **C.** Quantification of total sGAG content in the construct and media normalised to DNA content within the construct at day 14. $N = 3$, data represent mean ± SEM. $*P < 0.05$.

3.3.5.2 Histological localisation of sGAG

As discussed, the most commonly utilised growth factor to differentiate MSCs to an NP phenotype in current literature is TGF-β. However, taking both qPCR and quantification of sGAG results from this study together the greatest significant differences were between TGF-β and GDF6. Results have also confirmed that GDF5 demonstrated similar sGAG and qPCR results as TGF-β. Therefore histological assessment was undertaken to highlight the differential response of BM-MSCs and AD-MSCs treated with TGF-β and GDF6.

BM-MSCs (Figure 3.7) treated with TGF-β shows staining confined to the periphery of the construct and regardless of growth factor the BM-MSC samples are less intensely stained compared to the AD-MSC samples. Staining of AD-MSCs (Figure 3.7) stimulated with GDF6 demonstrated a homogenous widespread distribution of sGAG this is a greater extent than AD-MSCs treated with TGF-β.

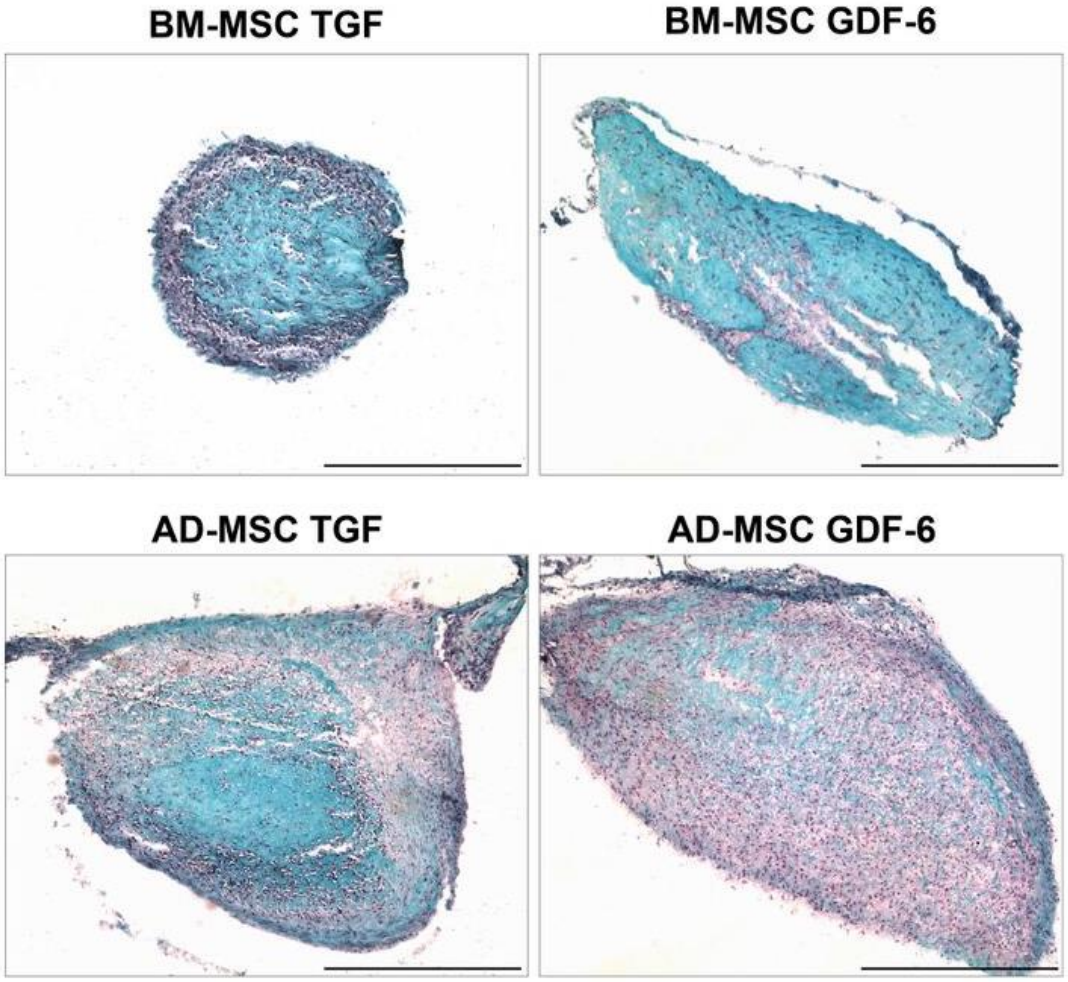

Figure 3.7 Histological localisation of sGAG of BM-MSCs and AD-MSCs treated with TGF-β or GDF6. Safranin O staining of MSC-seeded collagen hydrogels demonstrating deposition of sGAG throughout the constructs, with AD-MSCs stimulated with GDF6 having the highest and most homogeneous sGAG deposition. Scale bars, 500 μm.

3.3.6 Fibrillar Collagen Content

Fibrillar collagen content was assessed using a picrosirus red stain and polarised light microscopy; the histological stains (Figure 3.8 A) were quantified to assess any differential response (Figure 3.8 B). There was no difference in fibrillar collagen deposition between BM-MSCs supplemented with either TGF-β (15.4% ± 0.6%) or GDF6 (16% ± 1.1%). However AD-MSCs treated with TGF-β (19.5% ± 0.9%) showed significantly greater fibrillar collagen content than AD-MSCs treated with GDF6 (16.2% ± 0.7%).

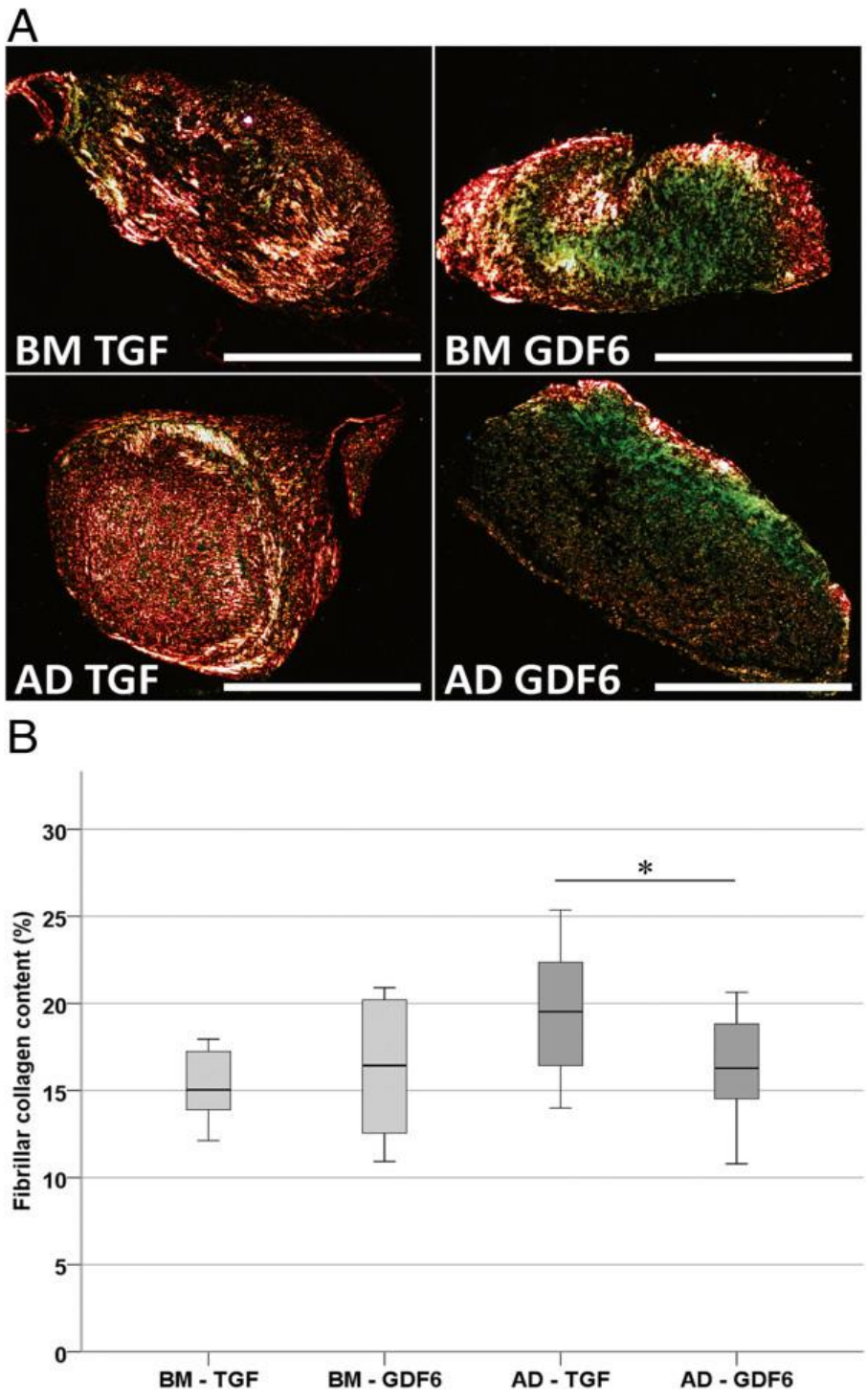

Figure 3.8 Fibrillar collagen content. A. Picrosirius red staining of MSC-seeded type I collagen hydrogels stimulated with TGF-β or GDF6, demonstrating enhanced fibrillar collagen deposition in AD-MSC-seeded constructs stimulated with TGF-β compared with GDF6-stimulated constructs. Scale bar, 500 μm. **B.** Quantification of percentage fibrillar collagen content in BM-MSC and AD-MSC-seeded constructs after stimulation with TGF-β or GDF6. AD-MSC-seeded constructs stimulated with TGF-β demonstrated a significantly higher percentage of fibrillar collagen content compared with GDF-6-stimulated constructs; $N = 3$.

3.3.7 Micromechanical Stiffness of Constructs

Micromechanical stiffness was assessed using scanning acoustic microscopy, which uses acoustic wave speed as a surrogate measurement for stiffness (Figure 3.9) As with the deposition of collagen fibrils, BM-MSCs treated with either TGF-β or GDF6 showed no significant differences in acoustic wave speed (TGF-β, 1,629 $ms^{-1} \pm 8\ ms^{-1}$; GDF6, 1,642 $ms^{-1} \pm 17\ ms^{-1}$). Conversely AD-MSCs treated with TGF-β demonstrated a significantly higher acoustic wave speed 1,644 $ms^{-1} \pm 1\ ms^{-1}$ compared to GDF6 stimulated constructs, 1,599 $ms^{-1} \pm 4\ ms^{-1}$ (Figure 3.9 B and C).

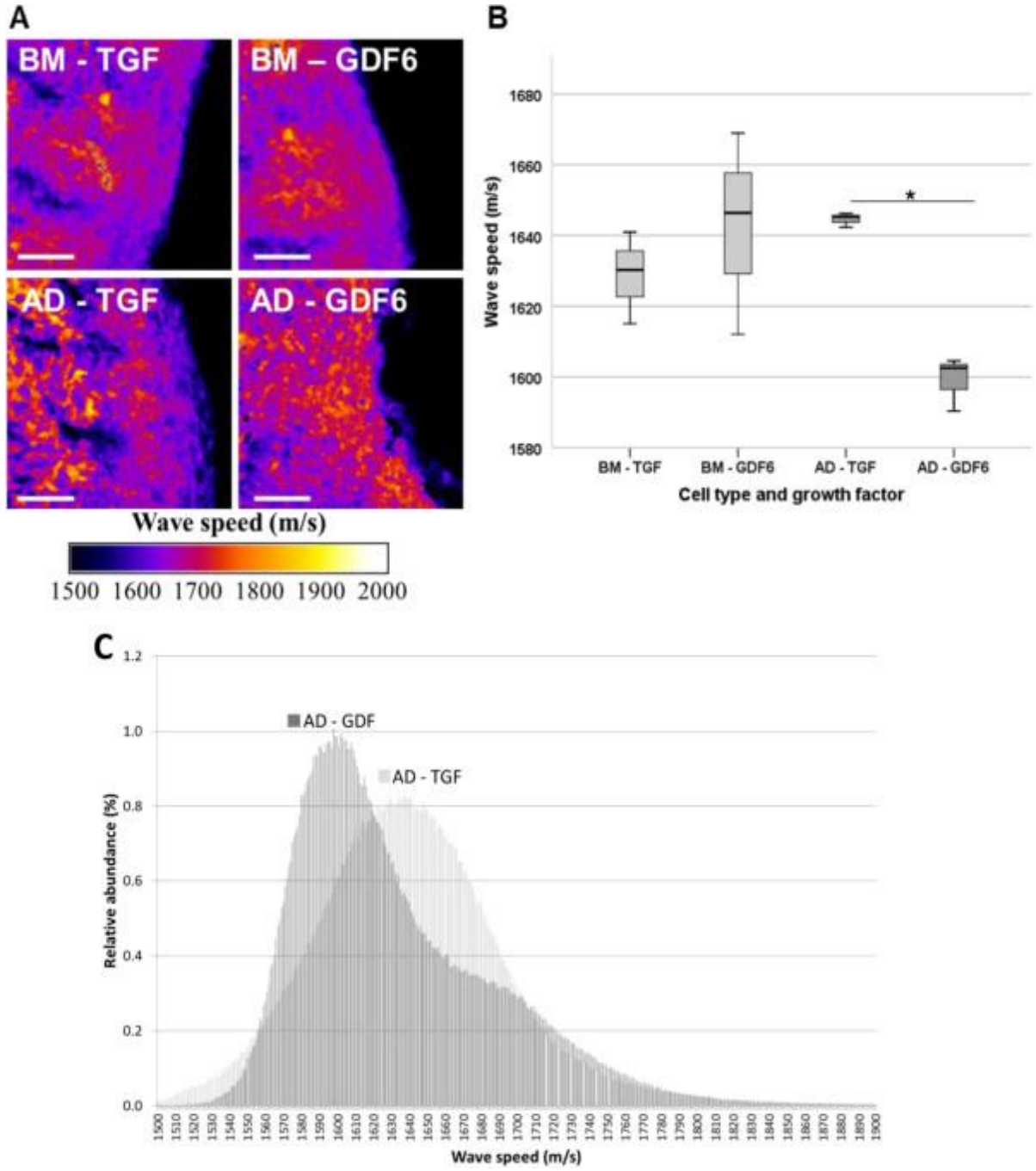

Figure 3.9 Mean acoustic wave speed (a surrogate measure of tissue stiffness) assessed with scanning acoustic microscopy. A. Acoustic wave-speed distribution maps of BM-MSC and AD-MSC-seeded type I collagen hydrogels stimulated with TGF-β or GDF6. Scale bar, 50 μm. **B.** Quantification of wave speed in BM-MSC and AD-MSC-seeded constructs after stimulation with TGF-β or GDF6. $N = 3$. $^{*}P < 0.05$. **C.** Wave-speed distribution in AD-MSC-seeded constructs after stimulation with either TGF-β or GDF6. The GDF6-stimulated construct shows significantly reduced mean wave speed of 1,599 ms^{-1} compared with the TGF-β-stimulated counterpart, 1,644 ms^{-1}.

3.3.8 MSC differentiation in Pellet Culture

To ensure that the results demonstrated in type I collagen hydrogels are true and that the collagen hydrogel does not have any influence on the differentiation of MSCs¸ the study was also performed in three-dimensional pellets. Pellets were prepared as described in section 2.1.8 and qPCR of conventional ECM and novel NP markers was undertaken, along with quantification of sGAG produced.

3.3.9 ECM Marker Expression in Pellet Culture

Following culture for 14 days in pellets and supplementation with respective growth factors gene expression of ECM genes was analysed. As with the previous experiment, expression levels were normalised to housekeeping genes and then to the control sample to assess the effect of each growth factor. Similarly to cells seeded in type I collagen hydrogel, AD-MSCs (Figure 3.10B) demonstrated the highest upregulation of ACAN following GDF6 treatment compared to control sample (11.0-fold) and compared to GDF5 (6.4-fold) and TGF-β (3.5-fold). Whereas BM-MSCs (Figure 3.10A) treated with all three growth factors demonstrated significant upregulation of ACAN compared to the control, but demonstrated no differences between treatment groups (GDF5: 5.8-fold, TGF-β: 6.6-fold, GDF6:6.6-fold).Both BM-MSCs and AD-MSCs supplemented with TGF-β demonstrated the largest gene expression upregulation in COL2A1 (7.8- fold and 4.0- fold respectively). The level of conventional ECM expression was therefore similar to that seen when cells were cultured in type I collagen hydrogels.

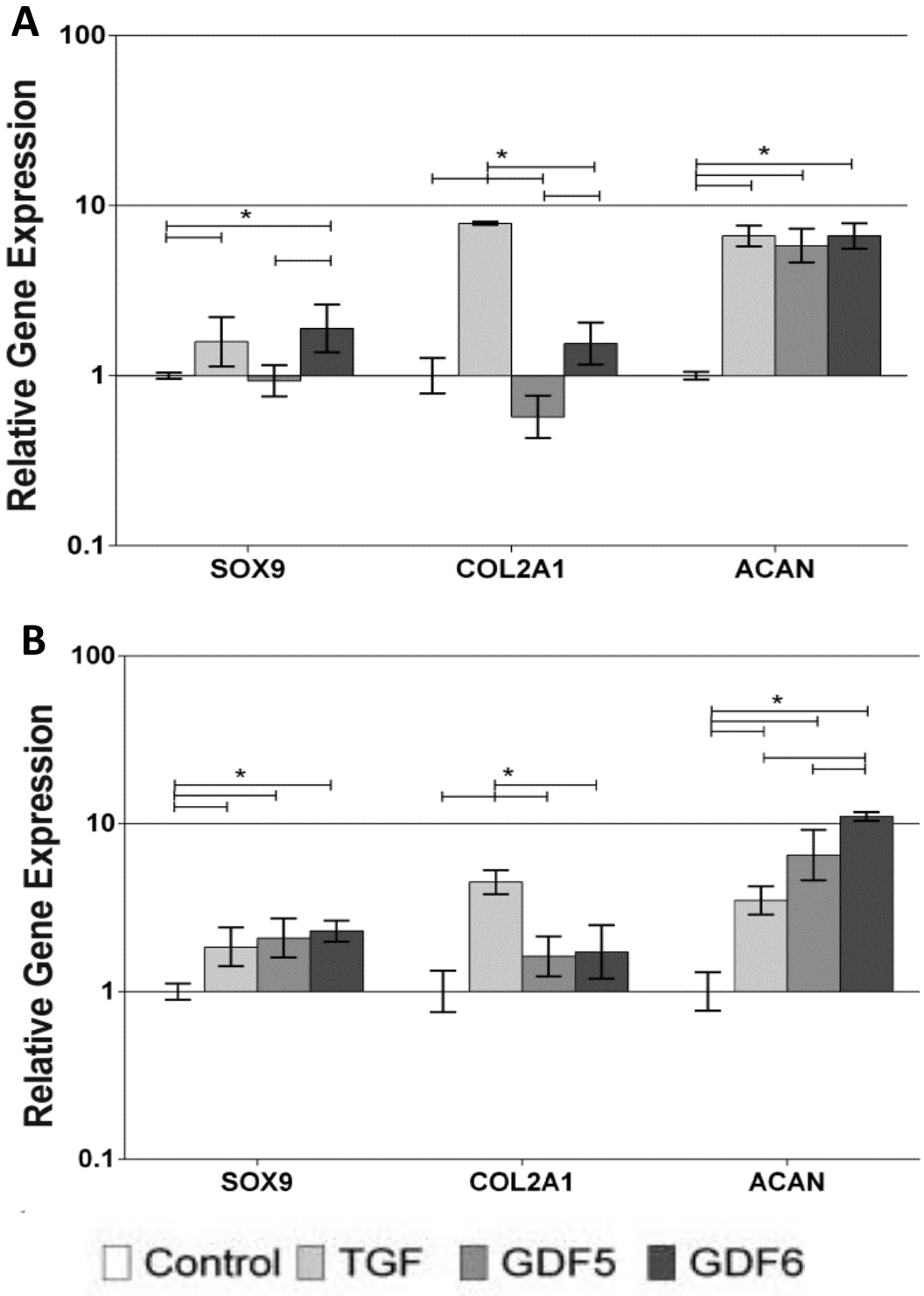

Figure 3.10 Analysis of BM-MSC and AD-MSC response to growth-factor stimulation in pellet culture. qPCR analysis of ECM gene expression changes in **A.** BM-MSCs and **B.** AD-MSCs in pellets in the absence or presence of TGF-β, GDF5, or GDF6. Relative gene expression was normalised to mean housekeeping gene expression and cells without growth-factor stimulation and plotted on a log scale. For all analyses, $N = 4$; data represent mean ± SEM. $*P < 0.05$.

3.3.10 ACAN:COL2A1 Gene Expression Ratio

The ACAN:COL2A1 ratio in the pellets was determined using the same formula outlined in section 2.4.3. BM-MSCs (Figure 3.11) cultured in the presence of no growth factor, TGF-β, GDF5 and GDF6 demonstrated ratios of 16:1, 6.5:1, 92:1 and 88:1 respectively. Hence cells stimulated with GDF5 had the highest ACAN:COL2A1 ratio, whilst cells treated with TGF-β demonstrated the lowest ratio. Whereas, culture of AD-MSCs (Figure 3.11) showed ratios of control: 9.8:1, TGF-β 6.6:1, GDF5: 41:1 and GDF6: 62:1. Hence cells treated with TGF-β demonstrated the lowest ratio, whilst the highest ratio was seen when cells were treated with GDF6. Overall there was no significant difference identified between the two cell types after stimulation with any of the growth factors.

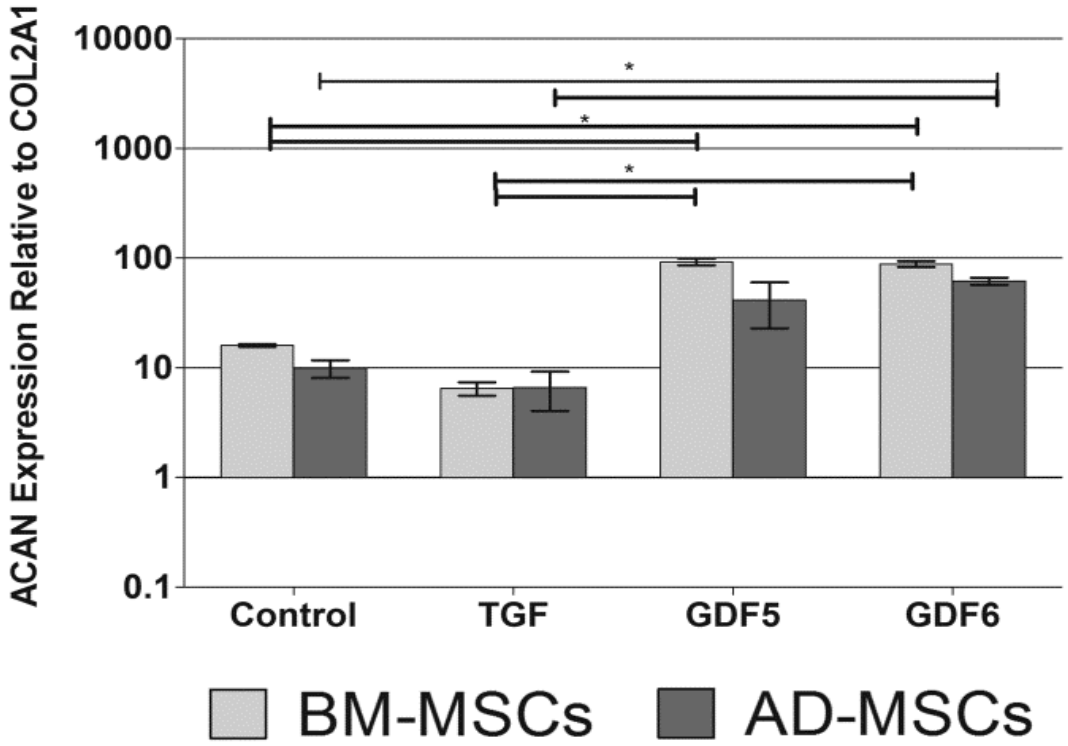

Figure 3.11 ACAN:COL2A1 gene expression ratio in BM-MSCs and AD-MSCs in pellet culture. Cells were cultured in three-dimensional pellets for 14 days with either no growth factor, or optimal concentrations of TGF-β, GDF5, or GDF6. ACAN:COL2A1 ratios were then determined using the formula ($2^{-\Delta CtACAN-\Delta CtCOL2A1}$). $N = 4$; all data represent mean ± SEM. $*P < 0.05$.

3.3.11 Novel NP marker Expression in Pellet Culture

The novel NP markers were used to assess the discogenic differentiation of BM-MSCs and AD-MSCs cultured in pellets after 14 days following exposure to no growth factor, TGF-β, GDF5 and GDF6.

When BM-MSCs (Figure 3.12A) were cultured in the presence of TGF-β and GDF5 there was no significant difference or a downregulation compared to the control in all genes assessed, KRT8 (0.9-fold and 1.1-fold), KRT18 (0.4-fold and 0.3-fold), KRT19 (1.3-fold and 1.1-fold), FOXF1 (1.3-fold and 0.4-fold) CAXII (0.3-fold and 0.3-fold) and T (0.65-fold and 0.65-fold). On the other hand, BM-MSCs cultured with GDF6 significantly upregulated KRT8 (2.0-fold), KRT19 (2.0-fold), FOXF1 (1.5-fold), CAXII (1.8-fold) and T (2.1-fold), compared to the control samples. This

followed the same gene expression pattern as seen when cells were cultured in type I collagen hydrogels.

AD-MSCs (Figure 3.12B) that were supplemented with GDF6 demonstrated significant upregulation of all marker genes compared with controls, which was also observed with cells cultured in type I collagen hydrogels, KRT8 (10.5-fold), KRT18 (3.5-fold), KRT19 (9.9-fold), FOXF1 (2.0-fold), CAXII (3.4-fold) and T (12.8-fold). This increase in gene expression levels was also significantly greater than AD-MSCs exposed to TGF-β and GDF5 in the case of KRT8, KRT18, KRT19, CAXII and T. Hence, as was demonstrated when cells were cultured in type I collagen hydrogels the expression levels were consistently upregulated to a greater extent in AD-MSCs compared to BM-MSCs, suggesting that the growth factors have the same response irrespective of three dimensional culture system.

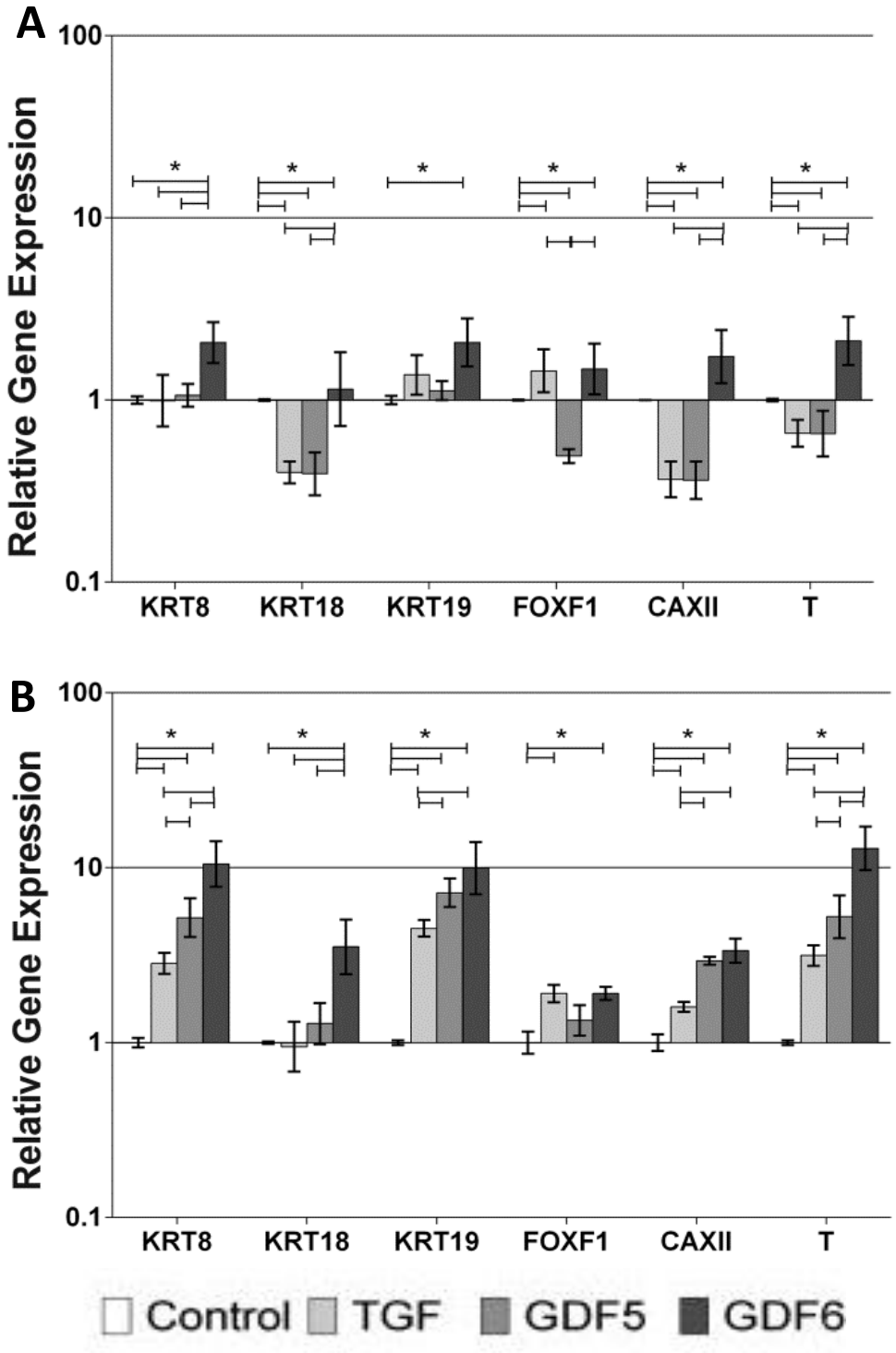

Figure 3.12 Analysis of BM-MSCs and AD-MSCs response to growth-factor stimulation in pellet culture. Quantitative real-time PCR analysis of NP marker gene-expression changes in **(A)**, BM-MSCs and **(B)**, AD-MSCs in pellets in the absence or presence of TGF-β, GDF5, or GDF6. Relative gene expression was normalised to mean housekeeping gene expression and cells without growth-factor stimulation and plotted on a log scale. For all analyses, $N = 4$; data represent mean ± SEM. $*P < 0.05$.

3.3.12 Assessment of sGAG content

3.3.12.1 Quantification of sGAG Synthesis

The construct and media were analysed for sGAG synthesis over the 14 day culture period (Figure 3.13) and the total sGAG/DNA showed that AD-MSCs cultured in the presence of GDF6 formed the most sGAG (3,556.31 μg/μg DNA ± 133.1). This was significantly greater than all other treatment groups groups (TGF-β 2,540.32 μg/μg DNA ± 32.8 or GDF5 2,512.97 μg/μg DNA ± 134.4) including the control (2,206.34 μg/μg DNA ± 267.5). Likewise BM-MSCs supplemented with GDF6 synthesised the greatest sGAG (2,886.65 μg/μg DNA ±225.76). This result also mirrors the data produced when cells were cultured in type I collagen hydrogels, as AD-MSCs cultured in the presence of GDF6 produced the greatest sGAG.

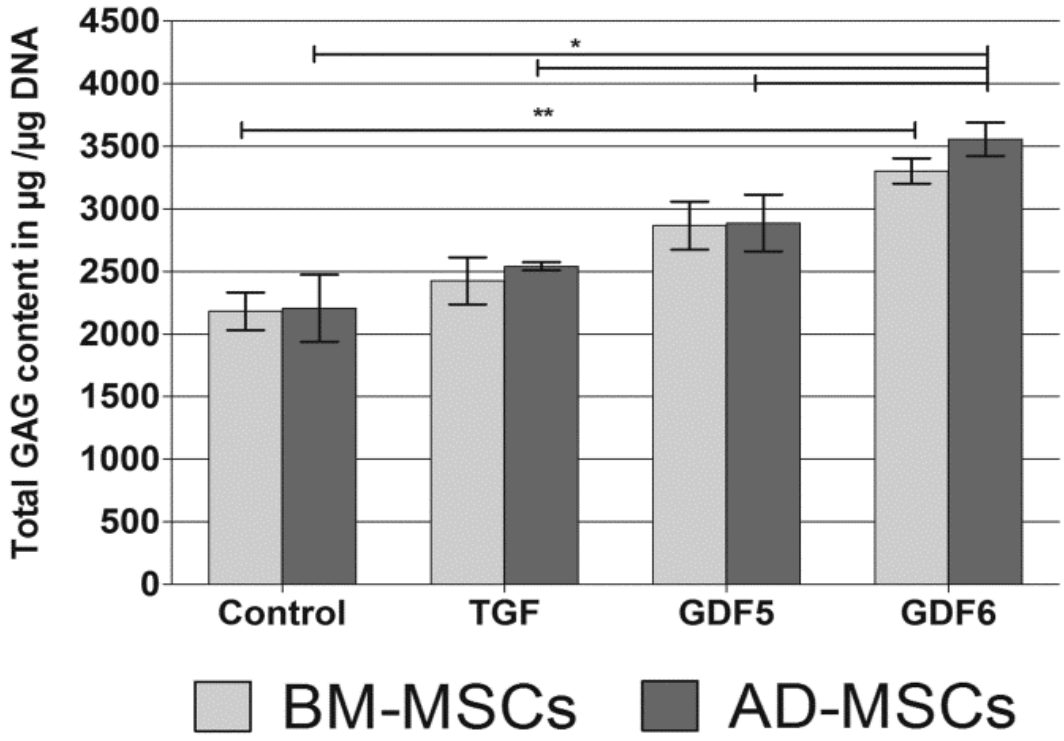

Figure 3.13 Total sGAG synthesis of BM-MSCs and AD-MSCs cultured in pellets. BM and AD-MSCs were seeded in pellets and cultured in the absence or presence of TGF-β, GDF5, or GDF6. Quantification of total sGAG content in the construct and media normalised to DNA content within the construct at day 14. $N = 4$, data represent mean ± SEM. $*P < 0.05$.

3.3.12.2Histological localisation of sGAG

Staining of BM-MSCs (Figure 3.14) stimulated with TGF-β or GDF6 shows little overall sGAG staining and the intensity compared to AD-MSCs is reduced. In contrast, AD-MSCs stimulated with GDF6 demonstrated a homogenous distribution of sGAG which is also demonstrated when cultured in type I collagen hydrogels. The intensity of staining in AD-MSCs treated with TGF-β is also increased compared to BM-MSC samples.

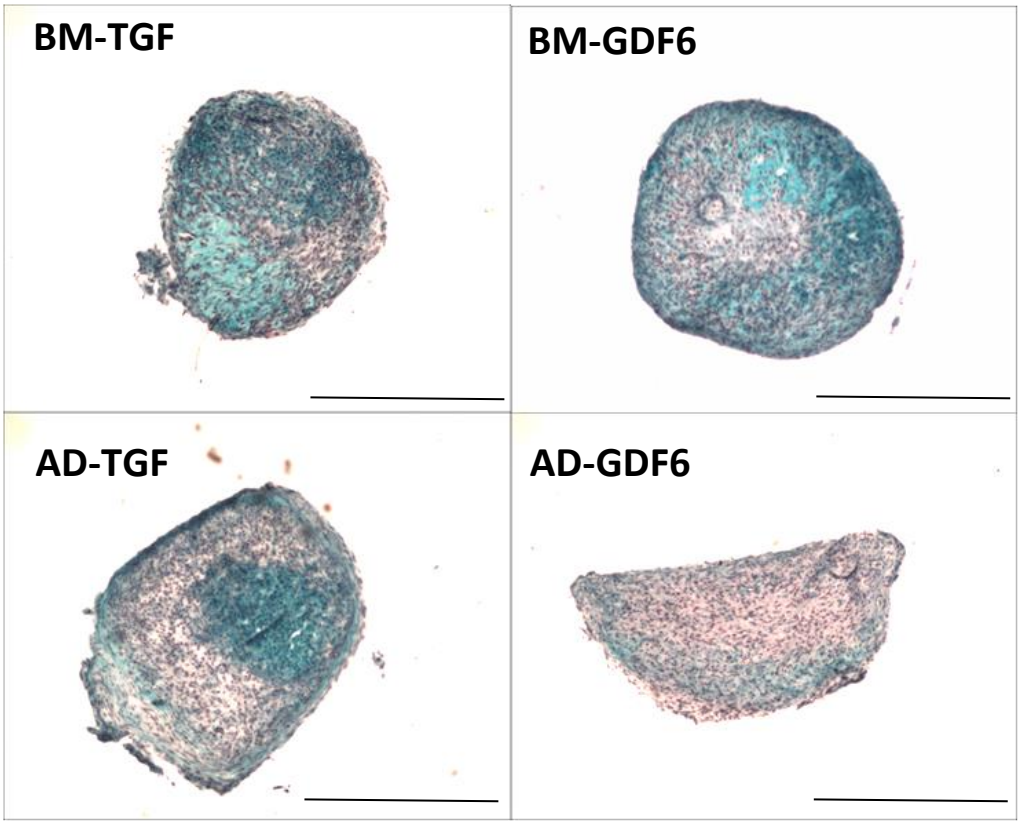

Figure 3.14 Histological localisation of sGAG in BM-MSC and AD-MSC pellet culture. Safranin O staining of MSC-seeded pellet cultures demonstrating deposition of sGAG throughout the constructs, with AD-MSCs stimulated with GDF6 having the highest and most homogeneous sGAG deposition. Scale bars, 500 μm.

3.4 Discussion

Increasingly, there is significant focus to investigate the potential of MSCs to regenerate the IVD. However to date, techniques applied are more widely used to induce chondrogenic differentiation, in particular culture in a 3D environment and differentiating media containing TGF-β. At present, experiments are analysed using gene and protein expression, specifically expression of SOX9, COL2A1 and ACAN to depict an NP like tissue. Recent phenotypic profiling studies suggest that these outcome measures are insufficient to define the end-stage differentiated cell and that more analyses are needed. Thus, with an increased understanding of the NP cell phenotype and distinction of unique phenotypic markers this allows for alternative culture systems to be assessed to optimise discogenic differentiation.

The objective of this study was to compare different growth factors, with the aim of optimising MSC discogenic differentiation and ensuring synthesis of an ECM with appropriate biochemical and biomechanical properties. Additionally comparisons were made between BM-MSCs and AD-MSCs to assess their discogenic potential and which cell source maybe more appropriate for regenerative therapies.

3.4.1 Novel NP Marker Expression

Treatment of both BM-MSCs and AD-MSCs with GDF6 resulted in increased expression of KRT8, KRT18, KRT19, FOXF1 and CAXII compared to control samples and also to cells treated with TGF-β or GDF5. This was more apparent in AD-MSCs as the levels of expression change were greater. As these unique phenotypic markers have previously been used to portray adequate differentiation (Minogue et al 2010a Minogue et al 2010b), the enhanced gene expression demonstrated in this study suggests that both MSC cell types have the capacity to undergo discogenic differentiation , which is improved by GDF6 stimulation.

Expression of the notochordal and mesodermal marker brachyury (T) was also investigated as it has been shown to be expressed by adult NP cells (Minogue et al 2010b). As with other results, stimulation with GDF6 induced the greatest gene expression of T particularly in AD-MSCs.

The study was undertaken in two different three dimensional systems, type I collagen hydrogel and pellet cultures, to ensure that the biomaterial did not influence differentiation. Importantly NP marker expression was consistent across both systems, suggesting that it is growth factor choice that has the predominant effect on differentiation rather than a biomaterial.

3.4.2 Conventional ECM Markers

The NP ECM is predominantly comprised of an abundance of aggrecan and type II collagen molecules with a greater aggrecan to type II collagen ratio. This has previously been shown at both gene transcription (Gantenbein-Ritter et al., 2011) and protein level (Mwale et al., 2004) and is more indicative of NP ECM than AC ECM.

Analysis of both BM-MSCs and AD-MSCs treated with TGF-β demonstrated that this growth factor is driving differentiation toward a more chondrocyte-like cell rather than discogenic differentiation. This is highlighted by a number of results; firstly TGF-β resulted in the highest COL2A1 gene expression and significantly increased expression of SOX-9 (major transcription factor for chondrogenesis) in both cell types. Secondly the ACAN:COL2A1 ratio was lowest compared to both controls and other treatment groups in both cell types and in both culture systems. Lastly when this is combined with the decrease or small upregulation of novel NP marker genes in BM-MSCs and AD-MSCs respectively, the overall results suggest that TGF-β induces chondrogenesis rather than discogenesis.

Results from this study corroborate previous studies (Gantenbien-Ritter et al., 2011; Stoyanov et al., 2011) which reported that GDF5 increased ACAN gene expression and resulted in a greater ACAN:COL2A1 ratio in comparison to TGF-β. Whilst BM-MSCs treated with GDF6 resulted in a similar response to GDF5, AD-MSCs treated with GDF6 produced significantly higher levels of ACAN and gave the highest ACAN:COL2A1 ratio, which as previously mentioned is indicative of an NP-like phenotype.

The overall gene expression analysis in both cell types and culture systems has shown that GDF6 promotes discogenic differentiation in both BM-MSCs and AD-

MSCs. The expression levels are consistently greater in AD-MSCs suggesting that this cell source maybe more appropriate for regenerative therapies.

3.4.3 Assessment of sGAG Synthesis

In order to determine if changes in gene expression were replicated at the protein level and to further characterise differences in cell differentiation analysis of sGAG synthesis was undertaken. This was assessed by two different means a DMMB assay and histological staining.

DMMB assay quantification showed that cells cultured in all conditions synthesised detectable levels of sGAG. There were significant increases in the sGAG/DNA within the constructs compared to the controls in BM-MSCs treated with TGF-β and AD-MSCs treated with either TGF-β or GDF6. During this study there was a substantial amount of sGAG released into the media that was collected over the 14 day time period. All cells released sGAG into the media with treatment of TGF-β or GDF6 resulting in significant increases compared to the control. Similar results of newly synthesised sGAG released into the media have been documented in comparable studies (Peroglio et al., 2013; Buckley et al., 2012). This may be accounted for by the remodelling of the matrix of the collagen hydrogel which may affect the retention capability (Buckley et al., 2012).

The total sGAG was significantly higher in AD-MSCs treated with all three growth factors in comparison to BM-MSCs, in particular treatment with GDF6. However treatment with GDF5 showed no significant sGAG increase which has previously been reported (Stoyanov et al., 2011). Similarly the gene expression profile was reflected in both culture systems; DMMB assay demonstrated similar results with AD-MSCs stimulated with GDF6 synthesising the largest amount of sGAG.

Histological analysis in both collagen constructs and pellets highlighted differences between cell type and growth factor treatment. AD-MSCs treated with GDF6 demonstrated a homogenous distribution throughout and demonstrated more intense staining than BM-MSCs, which supports the DMMB quantification results. Taken together, GDF6-stimulated AD-MSCs produce the greatest level of sGAG and demonstrate a homogenous matrix deposition suggesting that this maybe a more

appropriate cell type and growth factor to regenerate a PG-rich matrix akin to native NP tissue.

3.4.4 Micromechanical Stiffness of Constructs

As discussed, current studies utilise molecular and biochemical methods alone to determine the capacity of cells to differentiate to target cells and produce appropriately functioning tissues. However; if tissue engineering strategies are to be employed in the future, micro and hence macromechanical behaviour of the constructs should be characterised in order to investigate the ability to mimic native tissue properties. Therefore, in this study we quantified the acoustic-wave speed (Zhao et al., 2012), which is proportional to the square root of the materials Young's modulus (Turner 1999). This technique has previously been utilised to localise age-related changes in vascular stiffness (Graham et al., 2011). Our aim was to determine cell and growth factor-specific effects on the resultant micromechanical behaviour of constructs. In concordance with our other findings, AD-MSC constructs supplemented with GDF6 showed significantly lower fibrillar collagen compared to TGF-β counterparts. In addition AD-MSC GDF6 treated samples demonstrated a less stiff matrix demonstrated by a lower acoustic wave speed; this maybe more indicative of a gelatinous NP tissue.

3.4.5 Differences in MSC source

This study has demonstrated differences in the discogenic potential of BM-MSCs and AD-MSCs. In current literature the majority of studies have investigated BM-MSCs as an appropriate cell source for IVD regeneration. However, data from this study by means of conventional and novel NP marker gene expression, protein analysis, histological analysis and micromechanical behaviour studies, suggest that AD-MSCs have the greater capacity to undergo discogenic differentiation and produce an appropriate matrix. It was previously reported that AD-MSCs have a reduced capacity to differentiate to a chondrogenic lineage compared with BM-MSCs (Hennig et al., 2007) because of differences in receptor expression

(specifically, TGF-β receptor I) compared with BM-MSCS suggesting that BM-MSCs may be more appropriate for chondrogenic differentiation.

3.4.6 Conclusion

This study demonstrated that AD-MSCs in collagen hydrogels treated with GDF6 produced a less-stiff, PG rich matrix and expressed both novel NP markers and conventional marker at high levels. The characterisation of not only cell phenotype and ECM composition but the mechanical behaviour of the resultant constructs is important for clinical translation particularly for NP regeneration as the NP is a gelatinous tissue and it is important that an appropriate and functional tissue is formed.

As AD-MSCs have demonstrated a discogenic like phenotype, these cells can be described as AD-MSC derived NP cells (aNPCs).

3.4.7 Implication for Following Chapters

The results from this section of the overall study have proposed an appropriate cell source and growth factor to drive discogenic differentiation for use in IVD regenerative therapies. However, as described in chapter 1, the disc is a hostile environment; therefore how aNPCs respond to this microenvironment needs to be elucidated if this is to be proposed as a successful cell-based biological therapy.

Chapter 4

Effect of GDF6, Hypoxia and Load on Mesenchymal Stem Cell Differentiation

4.1 Overview

The results in chapter 3 showed that a combination of AD-MSCs and GDF6 demonstrated a superior discogenic phenotype in comparison to treatment with alternative TGF-β super family members and to BM-MSCs. Therefore, future experiments will utilise AD-MSCs and GDF6 to elucidate whether they have the potential for a cell-based therapeutic strategy for IVD regeneration.

4.1.1 IVD Microenvironment and Interaction with Potential Therapies

As reviewed in chapter 1 the IVD microenvironment can be described as a hostile environment which is characterised by low oxygen, low glucose and low pH levels (Bartels et al. 1998; Urban, 2002; Grunhagen et al. 2006). Therefore any regenerative therapies targeted at repairing the disc maybe hindered by the harsh IVD niche. Figure 1.4 outlines that as you move to the centre of the disc the oxygen concentration decreases and this has been found to be in the region of 1-5% (Mwale et al., 2011), the pH ranges from 7.1 to levels as low as 6.5 (Urban et al., 2002) and glucose levels range from 5mM and lower (Bibby et al., 2005). Additionally at a biomechanical level the IVD is constantly subjected to physical and dynamic loading which has also been demonstrated to play an essential role in the maintenance of IVD homeostasis (Matsumoto et al., 1999). Hence, a number of studies have investigated different aspects of the microenvironment including pH, low glucose, hypoxia and osmolarity (Wuertz et al., 2008; Liang et al, 2012, Wuertz et al., 2009, Stoyanov et al., 2011). The focus of this particular study is the effects of hypoxia, load and a combination of the two factors.

4.1.2 The Role of Hypoxia in MSC Differentiation

Previous studies have demonstrated that when MSCs are cultured in hypoxic conditions there is an enhancement of ACAN and COL2A1 gene expression and increased sGAG production, demonstrating enhanced matrix synthesis (Markway et al., 2010, Baumgartner et al., 2010, Risbud et al., 2004). A more recent study by Stoyanov and colleagues (Stoyanov et al., 2011) investigated the effects of different growth factors in combination with hypoxia. The study showed that MSCs cultured in hypoxic conditions treated with GDF5 and TGF-β demonstrated the most increased ACAN, COL2A1 and sGAG accumulation. In addition there was also an

upregulation of novel NP markers KRT19 and CA12 under hypoxic conditions, CA12 in MSCs has been shown to play a role in pH regulation (Chiche et al., 2009), hence improving MSC survival. This also suggests that hypoxia may induce discogenic differentiation. This was also demonstrated in a study by Feng et al., (Feng et al., 2011a) who showed that under hypoxic conditions and supplementation of TGF-β BM-MSCs could be differentiated to an NP like cell shown by the upregulation of ACAN, SOX9, COL2A1, increased ECM and continuous expression of HIF-1α. Interestingly, Felka et al., demonstrated that culture of MSCs in hypoxia could reduce the detrimental effect of IL-1β compared to cells not cultured in hypoxia (Felka et al., 2009). In a combination study examining hypoxia and glucose levels Naqvi and Buckley (Naqvi and Buckley. 2015) showed that when BM-MSCs were exposed to hypoxia (5%) and 5mM glucose concentration there was increased accumulation of sGAG and collagen. However when the glucose was reduced to 1mM in the same hypoxic conditions this resulted in cell death and a lack of ECM synthesis. This study highlights that is important to study multiple environmental factors to assess the potential of therapeutic treatments.

4.1.3 The Role of Load in MSC Differentiation

The unique design of the spinal column results in the constant loading of the IVD and studies have shown that discs that are not exposed to load or static load results in a deleterious effect demonstrated by an upregulation of catabolic molecules (Stokes and Iatridis., 2004; Paul et al., 2011; MacLean et al., 2004). Hence load is essential for appropriate function of matrix molecules in the IVD. A study investigating the effect of 10% cyclic compressive load at a frequency of 1Hz for 4 hours a day on rabbit BM-MSCs demonstrated increased gene expression of ACAN and COL2A1 and this showed no significant difference to TGF-β. This suggests that compressive load can induce differentiation alone (Huang et al., 2004). Studies have also demonstrated that AD-MSCs can be differentiated to a chondrgenic phenotype by the upregulation of ACAN and COL2A1 by compressive loading (Ogawa et al., 2009; Dai et al., 2014).

Therefore to test the efficacy of aNPCs as a potential therapy, the response to environmental factors must be elucidated. Testing all factors simultaneously is not feasible as it would not be possible to distinguish which factor was eliciting a response. Therefore, for the following study two factors were chosen for

investigation: hypoxia due to the growing evidence demonstrating its enhanced differentiation of MSCs and load as the disc is constantly subjected to dynamic loading.

4.2 Hypotheses

This study was designed to investigate whether exposing AD-MSCs, supplemented with GDF6, to hypoxia, load or a combination of the two enhances discogenic differentiation and matrix formation and whether the environmental factors act synergistically.

For this work it was hypothesised that in GDF6-stimulated AD-MSCs:

1) Hypoxia would induce a superior discogenic phenotype and ECM compared to cells cultured in normoxia.
2) Loaded conditions would enhance discogenic differentiation and increase synthesis of ECM.

4.3 Experimental Design

To investigate the effects of the microenvironmental factors on the ability of AD-MSCs supplemented with GDF6 to undergo discogenic differentiation, cells were divided into four treatment groups:

5) Normoxia (20%) (as shown in chapter 2)
6) Hypoxia (2%)
7) Normoxia and Load (20% and 0.04 MPa, 1 Hz, 1 hour per day)
8) Hypoxia and Load (2% and 0.04 MPa, 1 Hz, 1 hour per day)

Three patient samples were seeded into type I collagen hydrogels in BioFlex plates for 14 days. Analysis was undertaken by means of gene expression, ECM analysis and assessment of micromechanical stiffness using AFM.

4.4 Results

4.4.1 Discogenic Differentiation of AD-MSCs

AD-MSCs supplemented with GDF6 present a superior NP phenotype than current protocols. Therefore AD-MSCs were seeded into type I collagen hydrogels and supplemented with GDF6 for 14 days. Cells were exposed to: normoxia, normoxia and load, hypoxia or hypoxia and load to assess whether the environmental factors can enhance the discogenic differentiation of the AD-MSCs. A defined set of novel NP markers (Minogue et al 2010a, Clarke et al 2014) were used to assess this. Values were normalised to housekeeping genes and then to the normoxic values to assess the differences compared to standard culture conditions.

Cells cultured in the presence of normoxia and load (Figure 4.1) significantly upregulated KRT8 (3.6-fold), KRT18 (2.8-fold), KRT19 (2.9-fold) and FOXF1 (2.8-fold) compared to cells cultured in normoxia alone. With regard to the expression of CA12, which is associated with pH regulation, this was downregulated, although not to a significant extent.

Cells cultured in hypoxia (Figure 4.1) also showed a significant upregulation in expression of KRT8 (8.6-fold) compared to normoxia and significant CA12 upregulation (4.8-fold) compared to both normoxia and normoxia and load. Whilst there was increased expression in KRT18, KRT19 and FOXF1 this did not reach significance due to greater variation between samples.

Cells cultured in hypoxia and load (Figure 4.1) demonstrated significant upregulation of KRT8 (8.8-fold), KRT18 (6.9-fold) and FOXF1 (7.5-fold) compared to cells cultured in normoxia. Both KRT19 and CA12 gene expression was significantly greater than all other treatment groups (11.2-fold and 10.6-fold, respectively).

Taken together the results show that load, hypoxia and a combination of the two enhance novel NP marker expression compared to culture in normoxia alone.

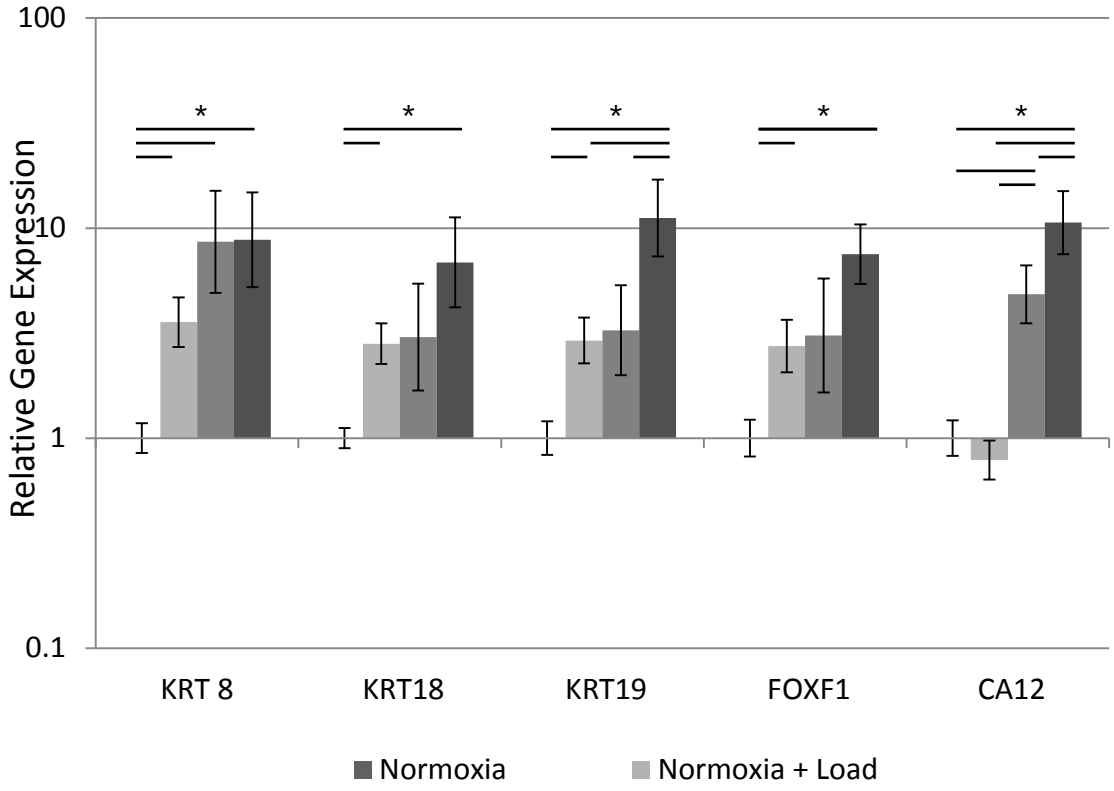

Figure 4.1 qPCR analyses of novel NP gene expression changes during culture in different conditions. AD-MSCs were cultured for 14 days in type I collagen hydrogels, stimulated with 100ng/ml GDF6 and exposed to hypoxia, load or a combination. Relative gene expression was normalised to mean housekeeping gene expression and to normoxic samples. N= 3, all data represent mean +/- SE. *P<0.05.

4.4.2 Increased Proteoglycan Formation

The addition of load, hypoxia or a combination demonstrated enhanced gene expression when analysing the NP novel markers. Therefore to ensure an appropriate and functional phenotype the ECM components of the constructs were investigated.

4.4.2.1 ACAN expression

Cells cultured in the presence of hypoxia resulted in a significant upregulation of ACAN (2.9-fold) (Figure 4.2). A combination of hypoxia and load demonstrated the greatest expression of ACAN (8.6-fold) and was significantly different to both normoxia and normoxia and loaded treatment groups.

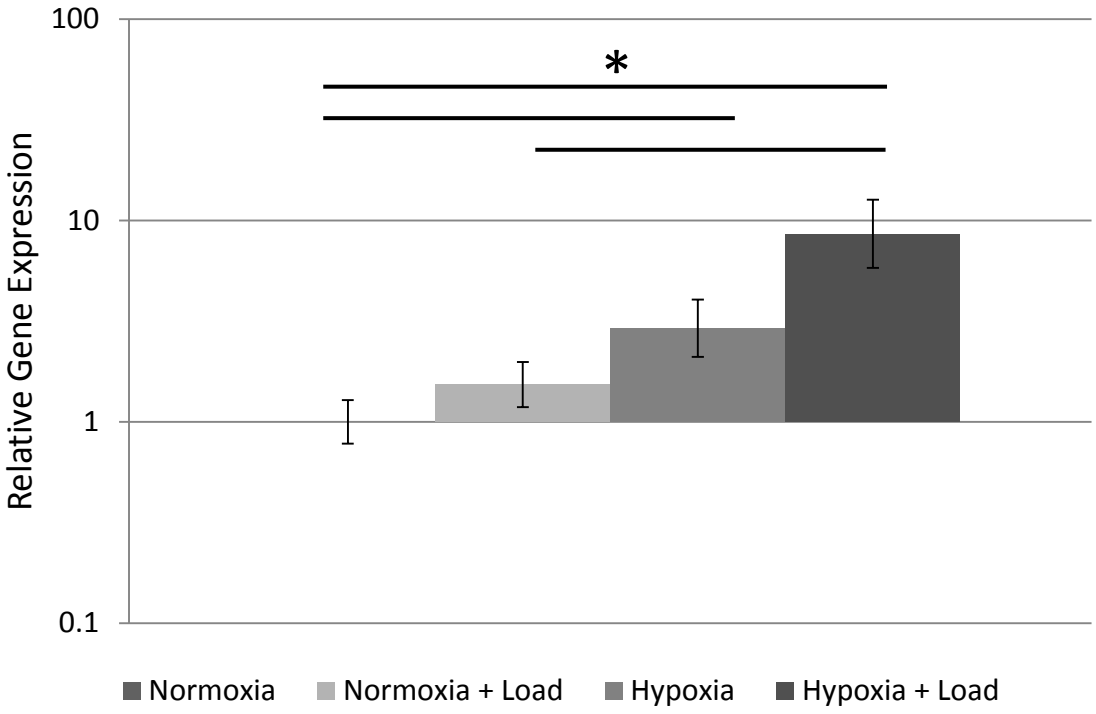

Figure 4.2 qPCR analyses of ACAN gene expression changes during culture in different conditions. AD-MSCs were cultured for 14 days in type I collagen hydrogels, stimulated with 100ng/ml GDF6 and exposed to hypoxia, load or a combination. Relative gene expression was normalised to mean housekeeping gene expression and to normoxic samples. N= 3, all data represent mean +/- SE. *P<0.05.

4.4.2.2 Quantification of sGAG Content

Following 14 days of culture, hydrogels were digested and appropriate assays undertaken (DMMB and PicoGreen) to assess sGAG content; in addition media collected over the 14 days was also analysed. Constructs exposed to hypoxia and load (Figure 4.3A) demonstrated the greatest PG content retained within the construct (250.2 µg/µg DNA± 37.8) compared to other groups and was significantly greater than normoxia and normoxia and load (126.9 µg/µg DNA± 5.5 and 141.6 µg/µg DNA± 8.8, respectively). Hypoxic conditions also significantly increased PG content (178.3 µg/µg DNA± 25.8) compared to culture in normoxia (126.9 µg/µg DNA± 5.5).

Analysis of the media components demonstrated no significant differences between any of the treatment groups (Figure 4.3B); normoxia (104.1 µg ± 6.9), normoxia and load (109.7 µg ± 3.9), hypoxia (119.1 µg ± 6.5), hypoxia and load (113.4 µg ± 4.8).

Total sGAG content demonstrated that constructs cultured in hypoxia and load (Figure 4.3C) had the highest PG content (2750.7 µg ± 179.9) and was significantly greater than both normoxia and normoxia and load groups (2049.2 µg ± 242.2 and 2272.3 µg ± 111.5, respectively).

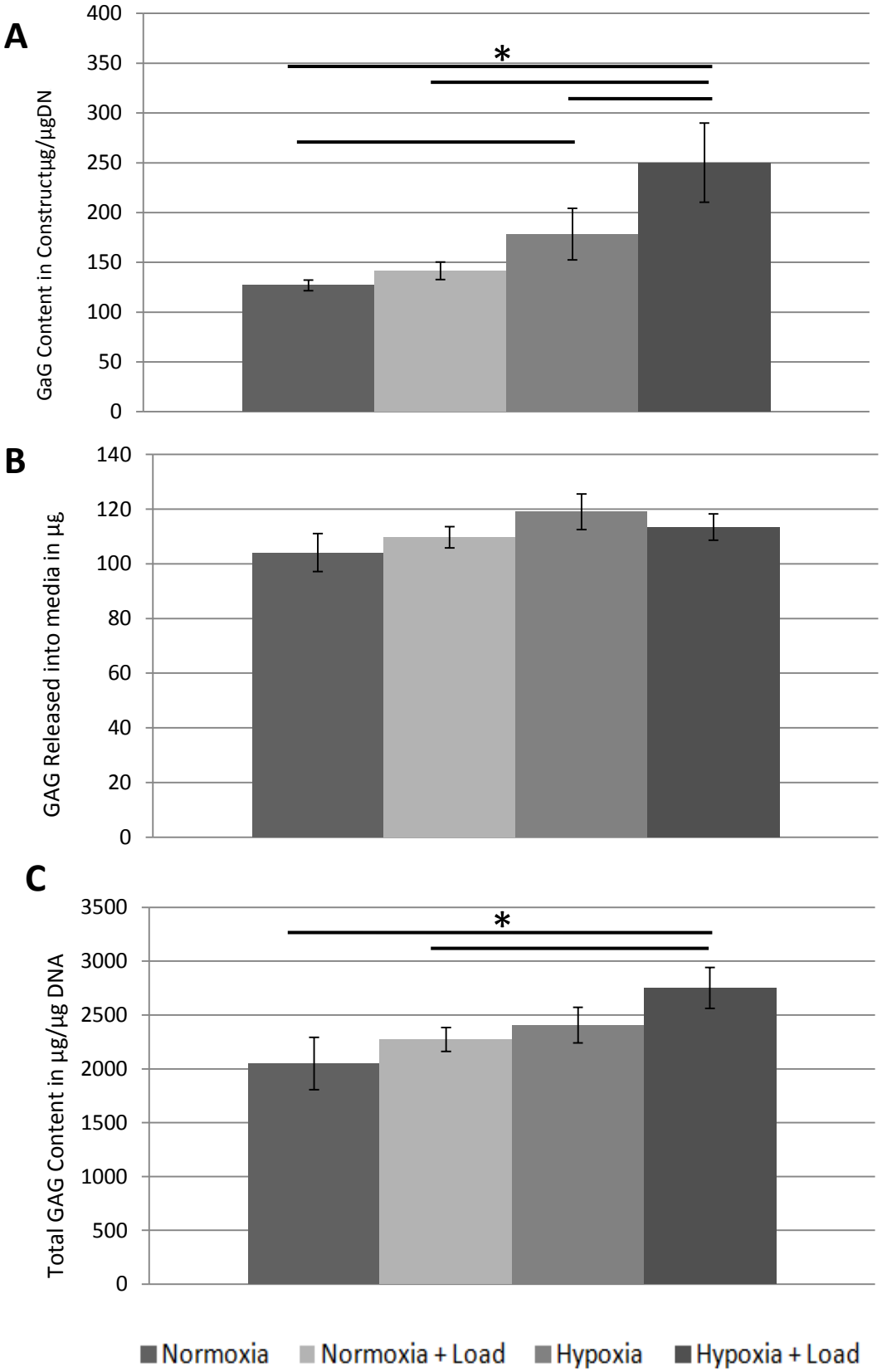

Figure 4.3 Quantification of sGAG by DMMB analysis. After 14 days constructs were papain digested and a DMMB assay used to assess sGAG and Pico Green assay used to assess DNA content. **A.** sGAG retained in the construct. **B.** sGAG released into the media **C.** Total sGAG. N= 3, all data represent mean +/- SE. *P<0.05.

4.4.3 ECM Composition

4.4.3.1 COL2A1 Expression

Cells cultured in the presence of hypoxia and load resulted in a significant upregulation of COL2A1 (24.1-fold) (Figure 3.5) compared to all treatment groups (normoxia: 1.0-fold, normoxia and load: 3.0-fold and hypoxia: 3.6-fold). This demonstrated that a combination of hypoxia and load results in the greatest COL2A1 expression.

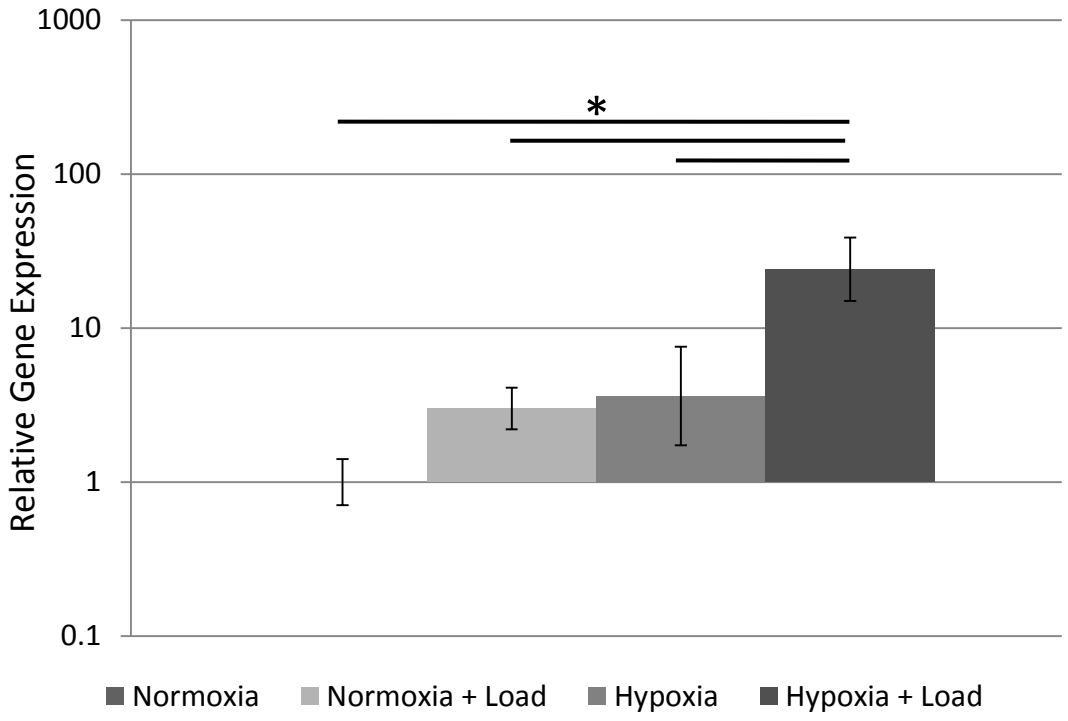

Figure 4.4 qPCR analyses of COL2A1 gene expression changes during culture in different conditions. AD-MSCs were cultured for 14 days in type I collagen hydrogels, stimulated with 100ng/ml GDF6 and exposed to hypoxia, load or a combination. Relative gene expression was normalised to mean housekeeping gene expression and to normoxic samples. N= 3, all data represent mean +/- SE. *P<0.05.

4.4.3.2 ACAN:COL2A1 ratio

As described in chapters 1 and 3, the ratio of ACAN:COL2A1 is extremely important for a gelatinous and functional matrix. Therefore using the formula depicted in 3.3.3 gene expression ratios were determined to establish the ACAN:COL2A1 ratio (Figure 4.5). Cells cultured in normoxia demonstrated the highest ACAN:COL2A1 ratio at 67.9:1, whereas cells cultured in hypoxia and load demonstrated the lowest ratio at 17.10:1. Other treatment groups display ratios of 24.53:1 and 38.75:1 (normoxia and loand: hypoxia, respectively). Culture of cells in normoxia resulted in a significantly greater ratio compared to all other treatment groups. Additionally cells cultured in hypoxia showed a significantly greater ratio than hypoxia and load.

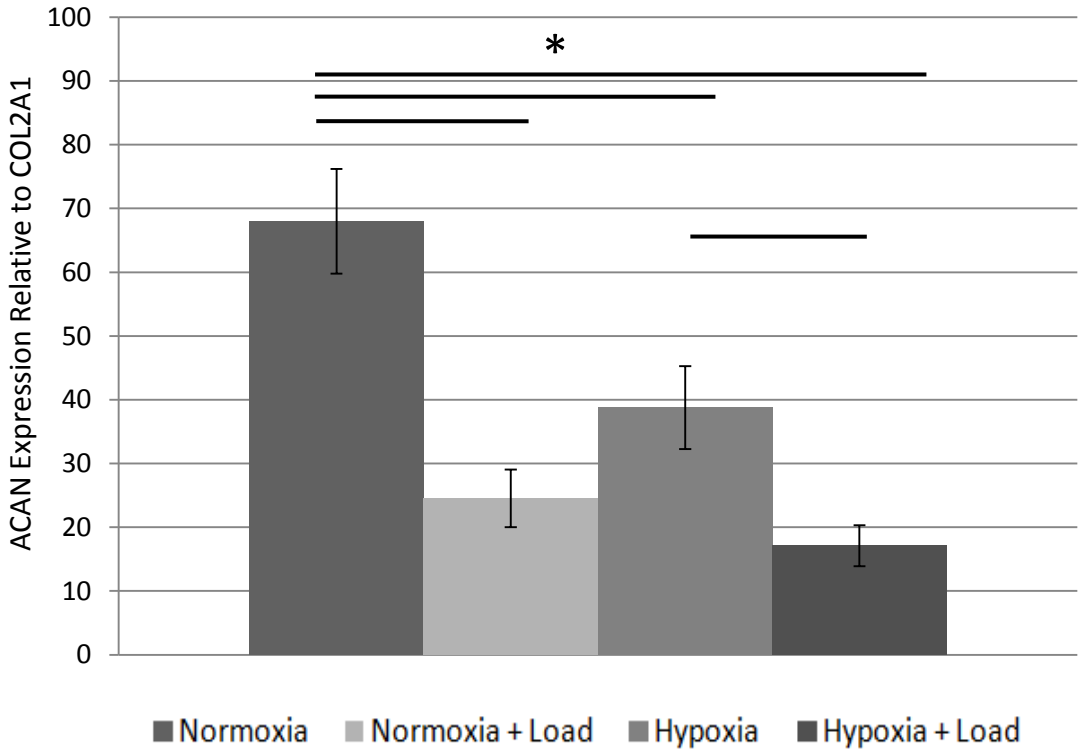

Figure 4.5 ACAN:COL2A1 gene expression ratio in AD-MSC constructs cultured in different conditions. Gene expression of both ACAN and COL2A1 were entered into ($2^{-\Delta CtACAN-\Delta CtCOL2A1}$) forumla to give the gene expression ratio of the constructs. N= 3, all data represent mean +/- SE. *P<0.05.

4.4.3.3 Fibrillar Collagen Content

As throughout the experiment the greatest differences were between cells cultured in normoxia and cells cultured in hypoxia and load these two groups were further analysed to assess for differences in ECM composition. The fibrillar collagen content was assessed using a picrosirus red stain and polarised light microscopy. The histological stains (Figure 4.6A and B) were quantified (Figure 4.6C) and although organised fibrillar content showed a trend towards increased levels in cells cultured in hypoxia and load (51.48% (SD 7.39)) this did not reach statistical significance compared to constructs cultured in normoxic conditions (45.11% (SD 8.67)) ($p=0.41$).

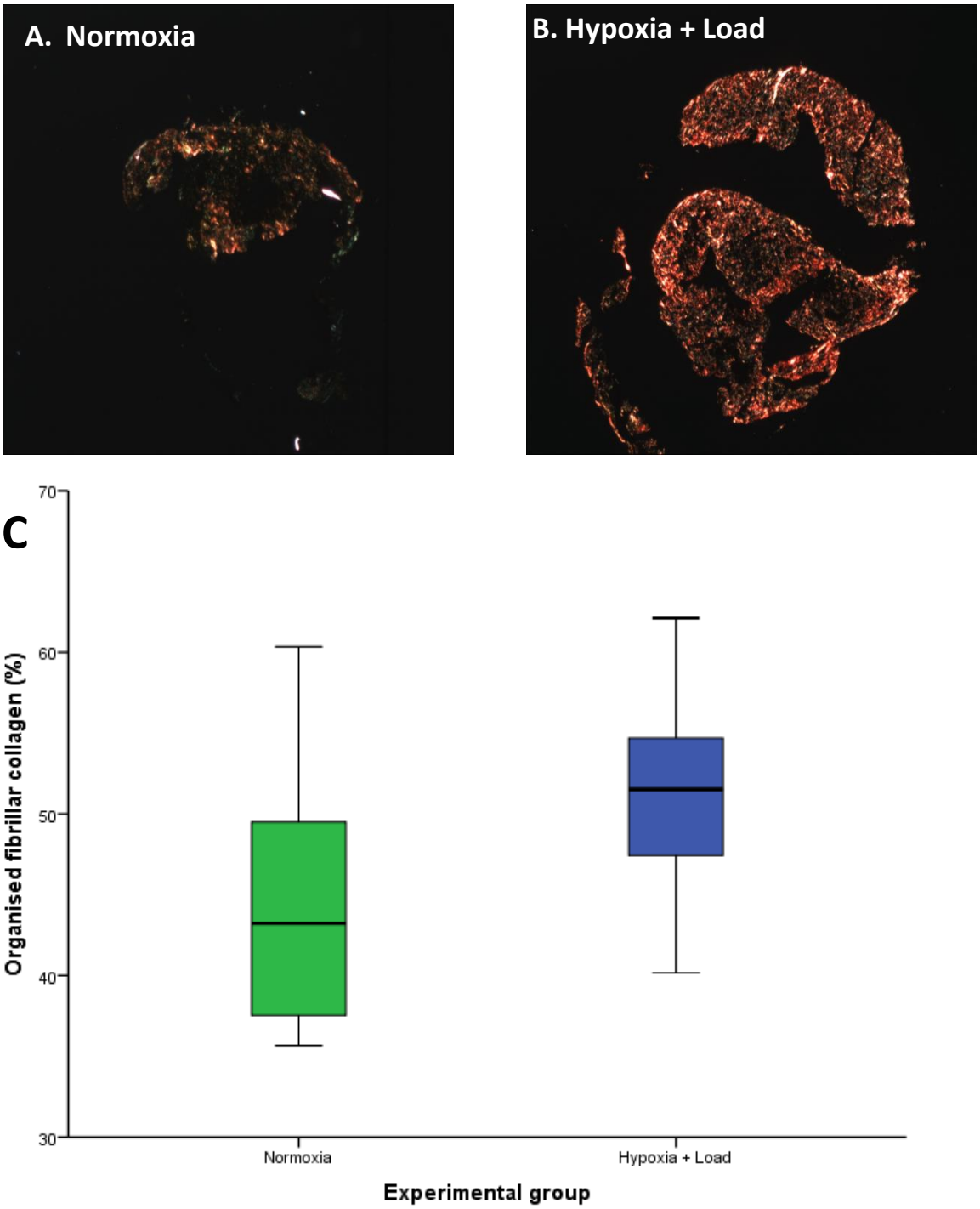

Figure 4.6 Fibrillar collagen content. Picrosirius red staining of AD-MSC seeded type I collagen hydrogels stimulated with GDF6 cultured in either **A**. Normoxia **B**. Hypoxia or load. **C.** Quantification of percentage fibrillar collagen content in AD-MSC-seeded constructs after stimulation with GDF6 and culture in normoxia or hypoxia and loaded conditions. N=3, all data represent mean +/- SD. *P<0.05

4.4.4 Micromechanical Stiffness

Micromechanical stiffness was assessed using AFM micro-indentation, which determines the reduced modulus of the tissue and hence its stiffness. As previously discussed in chapter 2 it is important to assess not only the biochemical components of the constructs but also the biomechanical properties. The mean reduced modulus was significantly higher in the constructs cultured in hypoxia and load (0.917 MPa (SD 0.072)) than compared to constructs cultured in normoxia alone (0.824 MPa (SD 0.086)) ($p<0.001$) (Figure 4.7A). Additionally when the distribution of mean reduced moduli was compared between the two groups, with a total of N= 2394 points for each condition, there was a clear shift toward a higher reduced modulus in constructs exposed to hypoxia and load (Figure 4.7B).

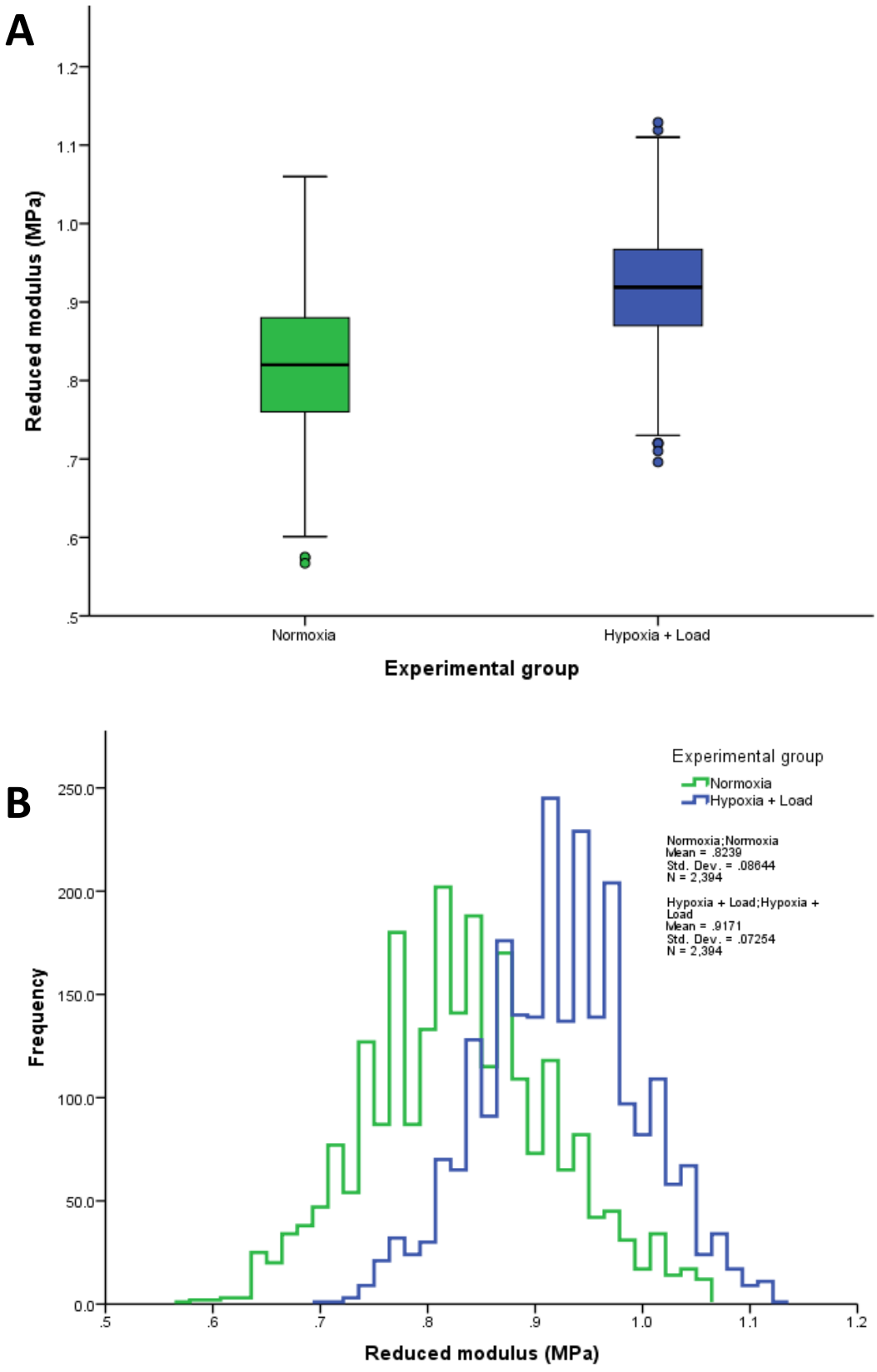

Figure 4.7 Mean reduced modulus assessed with Atomic Force Microscopy. A. Quantification of mean reduced modulus in AD-MSC-seeded constructs in either normoxia or hypoxia and loaded conditions. **B.** Distribution of the mean demonstrates a shift toward a higher reduced moduli for samples cultured in hypoxia and load. N=3, all data represent mean +/- SD. *P<0.05.

4.5 Discussion

For cell-based therapies to be utilised in potential clinical treatments, the interaction of the implanted cells with the native microenvironment must be elucidated. As reviewed in the introduction the IVD microenvironment encompasses a number of unique environmental features such as hypoxia and load. The overall objective of this study was to compare constructs that had been cultured in different microenvironments including normoxia, hypoxia, exposed to load or in combination. The aim was to establish whether exposure to these different factors could enhance discogenic differentiation and if the factors play a role in ECM synthesis. In addition to this, the resulting constructs were analysed to ensure the correct ECM was produced by assessing the biomechanical properties. This was analysed using a combination of qPCR, sGAG quantification, histology and AFM to assess micromechanics.

4.5.1 Enhanced NP Marker Gene Expression

As demonstrated in chapter 3 (and Clarke et al., 2014) AD-MSCs supplemented with GDF6 show a superior NP phenotype when compared to alternative growth factors and cell sources. Therefore to determine the effects of the different environmental factors, all samples were supplemented with GDF6 and data normalised to values obtained under normoxic conditions. The addition of load significantly upregulated KRT8, KRT18, KRT19 and FOXF1, whereas when cells were cultured in hypoxia there was a significant upregulation of KRT8 and CA12 compared to normoxia. The combination of hypoxia and load however demonstrated a significant upregulation of all NP markers, with KRT19 and CA12 gene expression significantly greater than all other conditions suggesting there may be a synergistic effect.

Interestingly, there was a distinction between the cells cultured in normoxia and those cultured in hypoxia when assessing the CA12 gene. In normoxia and normoxia in combination with load there were no fold changes observed, whereas there was a significant increase in CA12 expression when exposed to hypoxic conditions. Similar results were demonstrated in a study by Stoyanov and colleagues (Stoyanov et al.2011) in which a CA12 expression increase was seen in hypoxic conditions.

This corroborates with studies in the cancer field which have also demonstrated an increased expression of CA12 and CA9 when exposed to hypoxic conditions, in a range of tumour cell lines, including bone, breast, cervical and lung. (Wykoff et al., 2000; Ivanov et al., 1998; Supuran et al., 2008). CA12 is membrane bound and is upregulated in von Hippel-Lindau defective renal tumours, however unlike CA9 the dependence on HIF-1 regulation is not clear (Wykoff et al., 2000). In a study by Chiche and colleagues (Chiche et al., 2009) results showed that CA9 and CA12 are able to regulate intracellular pH of LS174Tr tumour cells in hypoxia, hence promoting cell survival. This suggests that upregulation of CA12 by the AD-MSCs may be promoting cell survival in the hypoxic environment. The addition of load also increased discogenic gene expression in both normoxia and hypoxia, in comparison to normoxic treatment alone. Whilst a number of studies have stated that load alone can differentiate MSCs to an 'NP-like' cell, the studies have only examined gene expression of ECM markers SOX9, ACAN and COL2A1 (Jung et al., 2009, Dai et al., 2014, Ogawa et al., 2009). Therefore a recent study by Guggisberg et al., (Guggisberg et al., 2015) also investigated mechanical loading of constructs supplemented with the growth factor GDF5 and in addition to ECM markers, novel NP markers FOXF1 and KRT19 were investigated. BM-MSCs were encapsulated in PEG gels, cultured with GDF5 for 13 days followed by loading for 5 days at 15% strain, 1 Hz. Whilst ACAN and COL2A1 were upregulated the discogenic markers FOXF1 and KRT19 showed no change. This suggests that our study GDF6 is also contributing toward the differentiation of AD-MSCs, in addition to load and hypoxia or a combination of the two. Also in the study undertaken by Guggisberg et al, cells were pre-conditioned for 13 days prior to loading which essentially splits the experiment into two different sections. In comparison to our experiment cells were cultured for 14 days with GDF6 and were either loaded or not loaded to investigate the combinatorial effects of the growth factor and the condition.

Our study showed that culture in hypoxia, with load or a combination of the two can result in enhanced expression of novel NP marker genes compared to culture in normoxia alone.

4.5.2 Increased ECM Composition

The ECM of the NP is gelatinous and comprised primarily of the PG ACAN, which is negatively charged and enables the disc to imbibe water to hydrate the disc. Hence

increased expression of ACAN is beneficial for cell-based therapies. Culture in the presence of both hypoxia groups resulted in the significant upregulation of ACAN compared to normoxia, which corresponds with previous studies (Stoyanov et al 2011; Gantenbein-Ritter et al., 2013). The addition of load in a hypoxic environment further upregulates the expression of ACAN, whereas the addition of load in a normoxic environment induces no significant changes. This suggests that hypoxia is the most important factor when considering upregulation of ACAN, and as such has been shown by a number of studies to be upregulated by MSCs in hypoxic conditions (Cicione et al., 2013, Lee et al., 2013, Risbud et al., 2004).

To ensure the increase of PG was replicated at a protein level a DMMB and PicoGreen assays were undertaken on both constructs and media components. Like ACAN expression, constructs exposed to hypoxia and load demonstrated the greatest sGAG/DNA content retained in the construct compared to other treatment groups.

Taking both the ACAN expression and sGAG content together, results demonstrate that cells cultured in a combination of both hypoxia and load enhance PG formation to the greatest extent. At this point the results suggest that culturing AD-MSCS in both hypoxia, under loaded conditions and further supplemented with GDF6 results in a construct that has enhanced novel marker and ACAN expression in addition to the greatest sGAG content.

Whilst ACAN is the most prominent PG found in NP tissue, there is also an abundance of other ECM components particularly COL2A1. As with previous results in this study constructs cultured under hypoxic and loaded conditions induced the greatest significant upregulation of COL2A1. This result shows that the combination of hypoxia and load significantly increased gene expression of COL2A1. Other studies have demonstrated upregulation of COL2A1 with culture in hypoxia (Risbud et al., 2004) or load (Dia et al., 2014), however this is the first study to show a combination of the two factors.

The disc is recognised as having a distinct ACAN:COL2A1 ratio that has been demonstrated at both a gene transcription (Gantenbein-Ritter et al., 2011) and protein level (Mwale et al., 2004) and is also essential for an appropriate and functional matrix. This ratio is also what distinguishes a chondrogenic matrix to an NP matrix as the ratio of ACAN is much greater. Constructs cultured in normoxia demonstrated the greatest ACAN:COL2A1 ratio whereas the lowest ratio was expressed by cells

cultured in hypoxia and load. Whilst the combination of hypoxia and load increased both ACAN and COL2A1 gene expression to the greatest extent across treatment groups, the greatest increase was observed in collagen expression (ACAN 8.6-fold v 24-fold COL2A1). This suggests that although the genes are being upregulated the ratio of upregulation is not indicative of an NP cell. The cells that were cultured in hypoxia, also demonstrated an increase in ACAN expression although not to the same extent as cells cultured with the combination. However the ACAN:COL2A1 ratio is significantly greater in hypoxic cells than the combination of treatments, as the collagen expression was not significantly greater. This suggests that hypoxia is essential to increase ACAN expression, whilst a combination of hypoxia and load increases COL2A1 expression.

Taken together whilst cells exposed to hypoxia and load display enhanced NP marker expression, increased sGAG formation and increased ACAN and COL2A1 expression, the ratio at which these molecules is produced is not that demonstrated by previous studies (Mwale et al., 2004). Therefore it can be proposed that phenotype induced is correct however the matrix composition may not be appropriate for NP cell-based therapy and as such gene expression and protein profiling may not be sufficient.

4.5.3 Micromechanical Stiffness of Constructs

As shown in chapter 2, use of micromechanical testing is important in addition to biochemical data in order to characterise and depict the construct at a two different levels (biochemical and biomechanical). In chapter 2, SAM was used to analyse the matrix of the resultant constructs, whilst this technique has been used to assess the stiffness of a number of ECM rich tissues including aorta, lungs and skin (Graham et al., 2011) in this study we opted to utilised AFM micro-indentation. This is because although SAM enables a higher spatial resolution than AFM, SAM measures wave speed, which is a surrogate measure of stiffness and not an actual mechanical measurement. In comparison AFM measures the reduced modulus of a tissue which is a mechanical measurement and enables a higher mechanical resolution which means more data can be generated. In this study the aim was to distinguish between constructs exposed to normoxia and constructs cultured in hypoxia and load.

The results from the study so far had shown there to be a significant difference between the, ACAN and COL2A1 gene expression in addition to the vastly different ACAN:COL2A1 ratio. Therefore it was hypothesised that the constructs exposed to hypoxia and load would have a stiffer matrix due to the low ACAN:COL2A1 ratio. Indeed this was the case as the resultant constructs showed that cells cultured in normoxia had a lower reduced modulus (less stiff). In the field of skeletal muscle it has been shown that with increased age, there is increased tissue stiffness and this has been attributed to the increase in collagen content (Feland et al., 2001; Gosselin et al., 1998; Kragstrup et al., 2011). It is also recognised that the collagen fibres are the main structural component of the ECM and the arrangement and organisation of these fibres is important to the mechanical strength, for example in muscle, fibres are aligned and organised (Gao et al., 2008). Although the organised fibrillar collagen content was not significantly different between normoxia and hypoxia and load groups 51.48% of collagen fibres were organised in combined treatment group. In addition the picrosirus red staining appears much more intense in constructs exposed to both hypoxia and load. However in order to assess this result comparison to native tissue would be helpful as at present there are no studies that have produced mechanical data for NP tissue using this AFM micro-indentation technique.

4.5.4 Conclusion

This study demonstrated that AD-MSCs in collagen hydrogels treated with GDF6 exposed to load, hypoxia or a combination results in enhanced expression of NP marker genes compared to normoxic conditions. It can be postulated that hypoxia has the greatest effect on ACAN expression, whilst a combination of load and hypoxia increases COL2A1 expression. Although cells exposed to hypoxia and load had the greatest upregulation of both ACAN and COL2A1, the ratio at which this was produced is incorrect and not appropriate for an NP like ECM, as this resulted in a stiffer matrix compared to culture in normoxia alone. Therefore in terms of clinical application this must be considered as both load and hypoxia are native to the IVD microenvironment. As this is an *in vitro* study it should be extended further and incorporated into disc models to see the effects in a larger ex vivo system.

Once again this has shown that characterisation of phenotype, ECM and micromechanics are important as all aspects must be appropriate for a successful therapy.

4.5.5 Implication for Following Chapters

The results from this section have demonstrated that hypoxia and load have a differential effect on the differentiation of AD-MSCs in the presence of GDF6. However if AD-MSCs together with GDF6 are to be utilised as a potential therapy for IVD regeneration, then native NP cells will also come into contact or be exposed to GDF6. The effect of GDF6 on native degenerate NP cells or its effects whilst in an inflammatory environment has not yet been clarified and needs to be looked at to assess the potential as a biological therapy.

Chapter 5

A comparative study of the Response of Pre-Differentiated MSCs and Mature NP Cells to the Pro-inflammatory niche of the intervertebral disc

5.1 Overview

For regeneration strategies, MSCs will be implanted into this degenerate niche and thus their response to the cytokine milieu needs to be ascertained to ensure that catabolic events are not exacerbated.

5.1.1 The role of Interleukin- 1 in the IVD

IIL-1β has been profoundly implicated in driving the catabolic changes that occur during disc degeneration (Igarashi et al., 2000; Koshy et al., 2002, Le Maitre et al., 2005). A total of 11 cytokines make up the IL-1 family and it is IL-1β that is the predominant cytokine leading to IVD degeneration (Le Maitre et al., 2005). IL-1β has been associated with a number of pathologies that contribute to the development of IVD degeneration; these are illustrated in Figure 5.1.

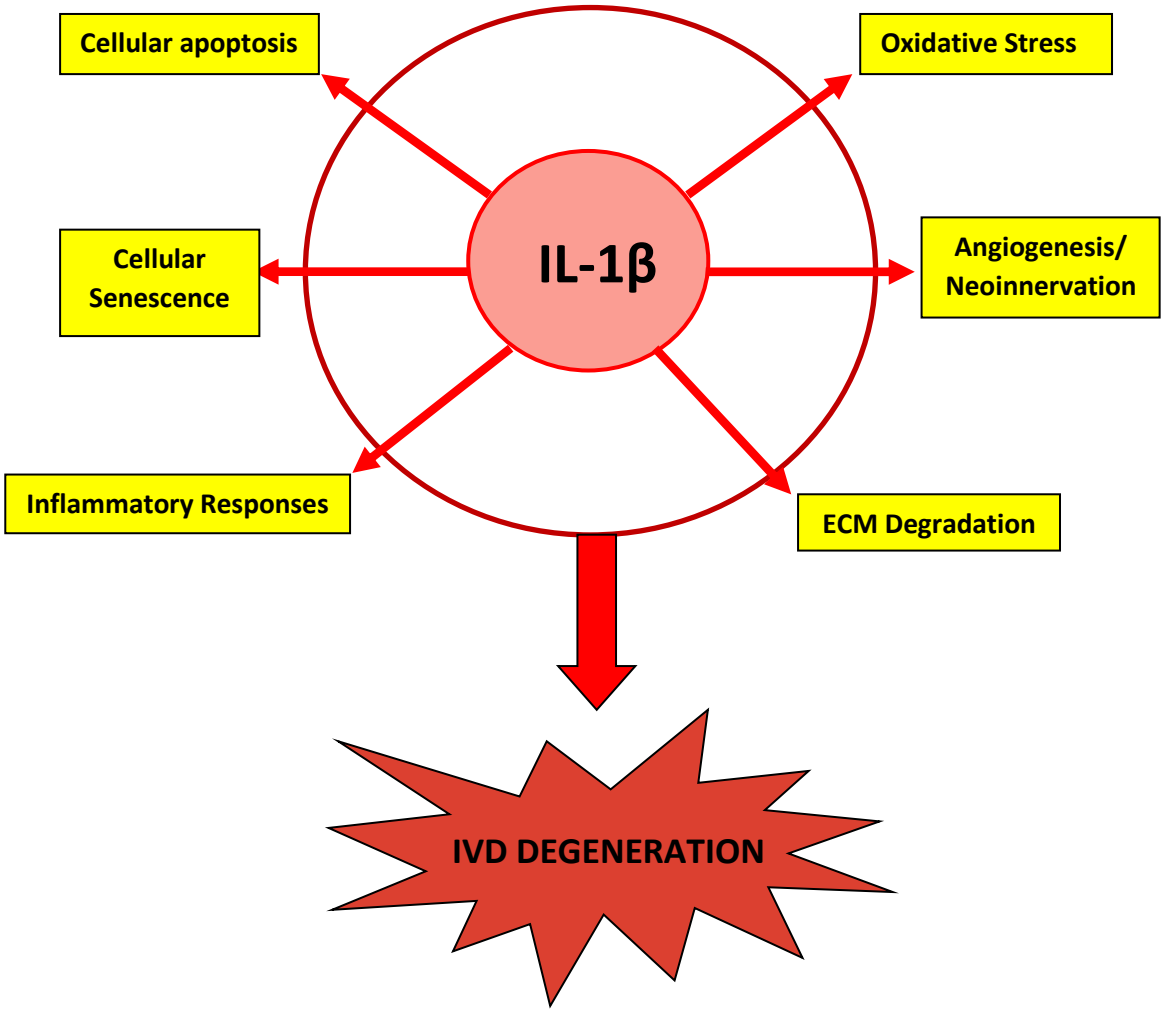

Figure 5.1 A schematic diagram to describe the different pathologies that IL-1β can induce (Adapted from Yang et al., 2015).

Taking all studies discussed in chapter 1 together IL-1β can lead to a number of different pathologies in the disc that can lead to disc degeneration. Hence, it is imperative to understand the effect of IL-1β on implanted cells.

Previous work in this thesis has shown that GDF6 is able to differentiate AD-MSCs to a discogenic phenotype (chapter 3, Clarke et al., 2014) that produces an appropriate matrix, and as such these cells would be suitable for IVD regeneration. However, whilst studies have investigated the effect of IL-1β on native NP cells and MSCS (Le Maitre et al., 2005; Fan et al., 2012), to date no studies have investigated the effect of IL-1β on pre-differentiated cells, i.e. cells that have a discogenic like phenotype, aNPCs. As such if aNPCs are to be utilised as a cell based therapy the response to the degenerate, cytokine rich niche must be assessed.

5.2 Hypotheses

The study was designed to investigate how aNPCs would respond to a pro-inflammatory environment (i.e IL-1β), compared to mature NP cells to determine if any differential responses between the two cell types.

It was hypothesised that aNPCs would respond differently to IL-1β than NP cells, leading to a reduced catabolic profile/response.

5.3 Experimental Design

To investigate the effects of IL-1β on aNPCs and NP cells, AD-MSCs were initially differentiated to aNPCs with GDF6 for 14 days, whilst NP cells were cultured with no growth factor. The cells were then divided into the following groups:

1) Mature NP cells + No IL-1β for 7 days
2) Mature NP cells + IL-1β for 7 days
3) aNPCs + No IL-1β for 7 days
4) aNPCs + IL-1β for 7 days

Analysis was undertaken by means of conventional PCR, gene expression studies utilising QRT-PCR and ECM analysis (histology and SGAG analysis).

5.4 Results

5.4.1 IL-1 Receptor expression in aNPCs and Mature NP cells

To ensure that both cell types would be receptive to IL-1β treatment, the expression of IL-1R was undertaken using RT-PCR. This was carried out after 14 days of culture when AD-MSCs had been differentiated to aNPCs and prior to the 7 day treatment with or without IL-1β. The results demonstrate that both cell types express the IL-1R gene in all three samples tested (Figure 5.2).

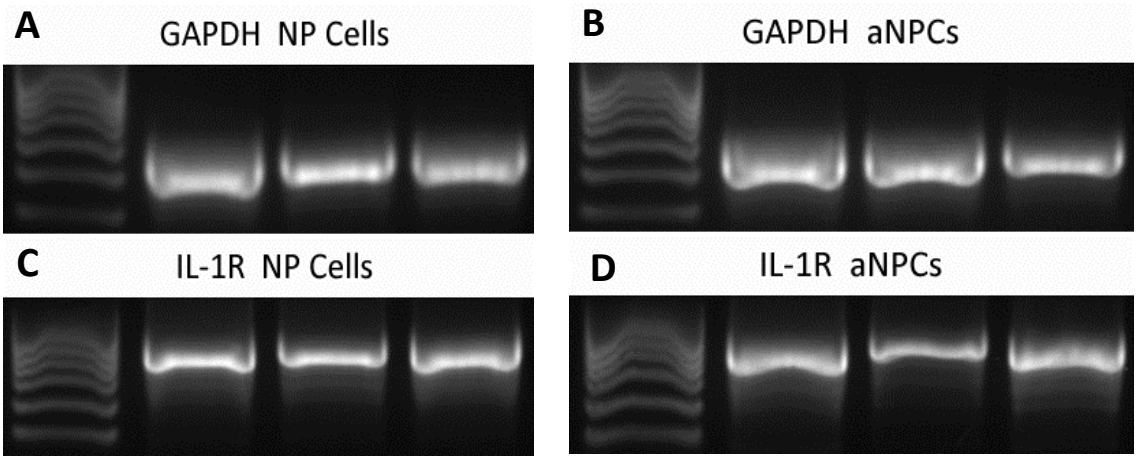

Figure 5.2 RT-PCR analysis of IL-1R. **A**. Mature NP cells **B**. aNPCs housekeeping expression profile of GAPDH. C. Mature NP cells D. aNPCs IL-1R gene expression profile for both cell types following 14 days of culture. N=3.

5.4.2 ECM Gene Expression Profile

After a total of 21 days of culture, aNPCs and NP cells seeded into type I collagen hydrogels were assessed for ECM gene expression. This was normalised to housekeeping genes and then to respective sample that was not treated with IL-1β to assess the effect of the cytokine.

Mature NP cells (Figure 5.3A) cultured in the presence of IL-1β resulted in significant down regulation of all ECM genes. The most significant decrease in expression was observed in COL2A1 (0.13-fold), this was followed by ACAN (0.25-fold) and then SOX9 (0.39-fold). On the other hand aNPCs (Figure 5.3B) showed no significant changes in expression compared to the respective control.

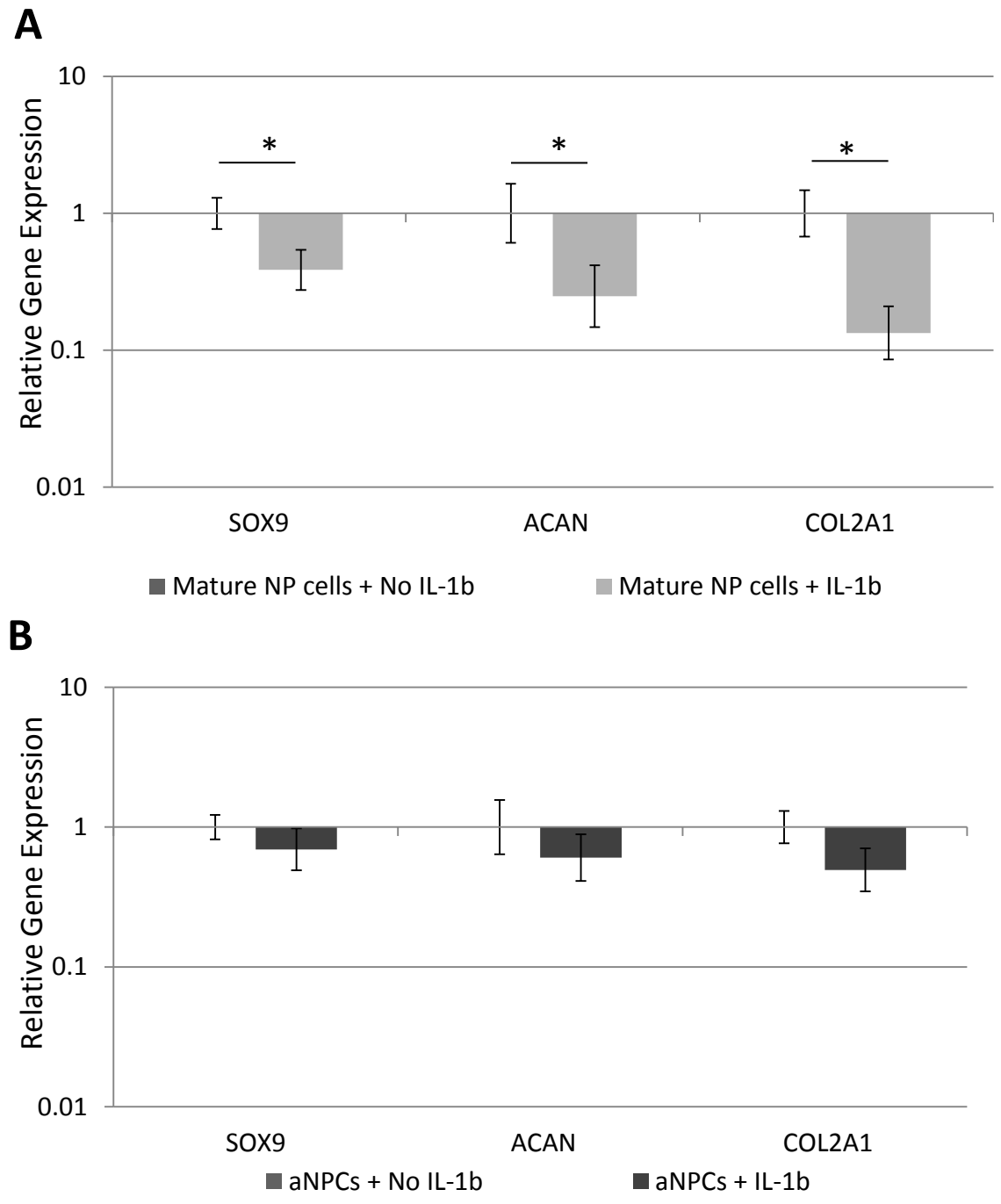

Figure 5.3 qPCR analysis of ECM gene expression of mature NP and aNPC seeded constructs treated with and without IL-1β. **A.** Mature NP cells and **B.** aNPCs. aNPCs were initially differentiated for 14 days using GDF6 as described in chapter 2 whilst NP cells were maintained for 14 days with no growth factor. Following this cells were treated either with or without 10ng/ml IL-1β for a further 7 days. Relative gene expression was normalised to housekeeping gene expression and then to the respective cell type that was not treated with IL-1β and plotted on a log scale. N=4; all data represent mean ± SEM *P<0.05.

5.4.3 Catabolic and Anti-Catabolic Gene Expression Profiles

The catabolic marker genes analysed were stromelysin MMP3, collagenase MMP13 and aggrecanases ADAMTS4 and ADAMTS5, whilst the anti-catabolic markers were the TIMPs -1 and -2 which inhibit the MMPs. Following treatment with IL-1β the two cell types were assessed for the catabolic and anti-catabolic gene profiles.

Mature NP cells (Figure 5.4A) demonstrated a significant upregulation of catabolic markers MMP3 (10.23-fold), MMP13 (7.47-fold) and ADAMTS4 (3.40-fold). There was no significant difference observed in the expression of ADAMTS5 (1.17-fold). With regard to the anti-catabolic markers the results showed a significant decrease in both TIMP1 and TIMP2 (0.36-fold and 0.19-fold, respectively).

On the other hand aNPCs treated with IL-1β for 7 days demonstrated no significant differences across either catabolic or anti-catabolic gene profiles.

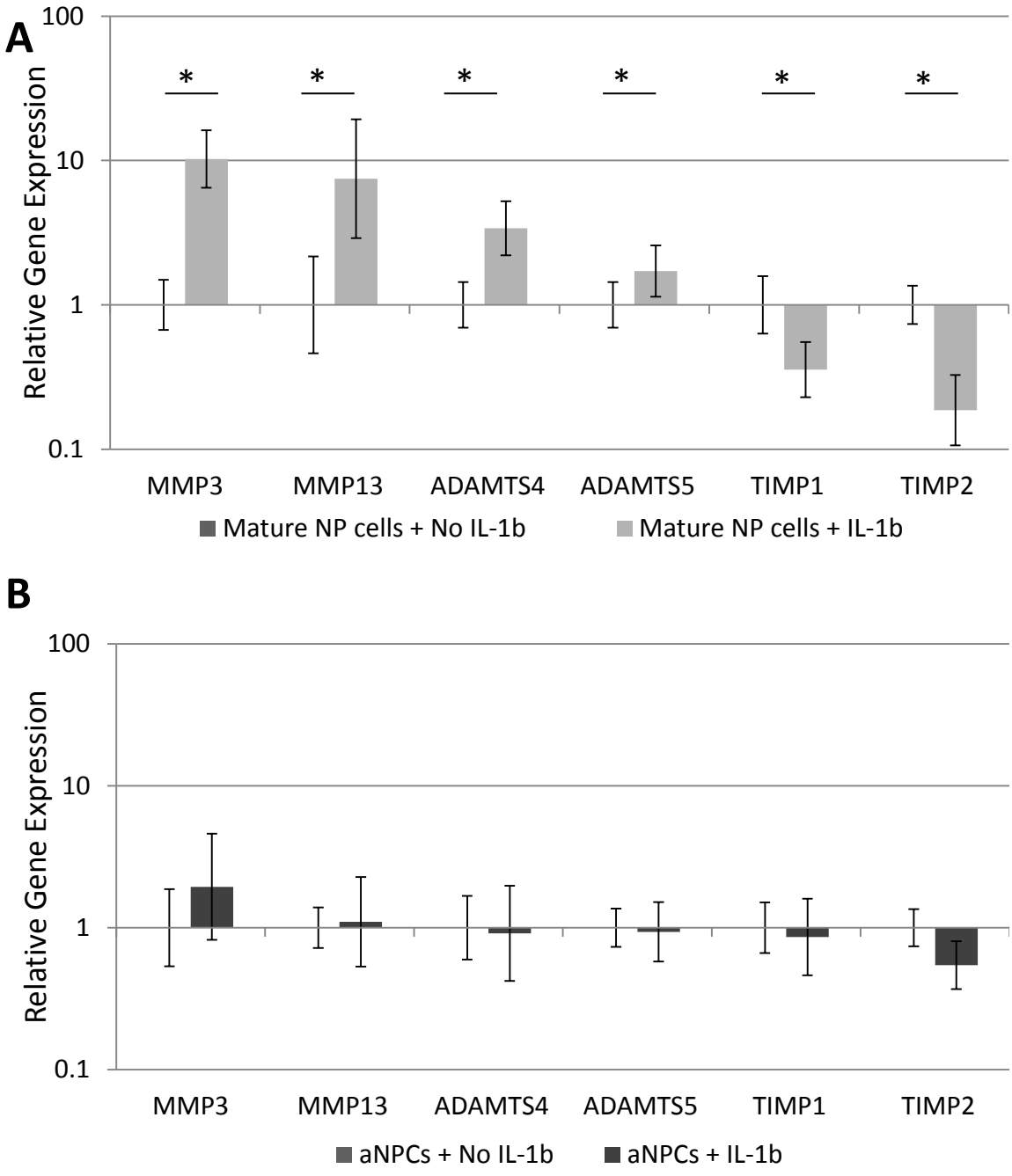

Figure 5.4 qPCR analysis of catabolic and anti-catabolic gene expression of mature NP and aNPC seeded constructs treated with and without IL-1β. **A.** Mature NP cells and **B.** aNPCs. aNPCs were initially differentiated for 14 days using GDF6 as described in chapter 2 whilst NP cells were maintained for 14 days with no growth factor. Following this cells were treated either with or without 10ng/ml IL-1β for a further 7 days. Relative gene expression was normalised to housekeeping gene expression and then to the respective cell type that was not treated with IL-1β and plotted on a log scale. N=4; all data represent mean ± SEM *P<0.05.

5.4.4 Assessment of sGAG content

5.4.4.1 Quantification of sGAG in Mature NP Cells

Mature NP cells (Figure 5.5A) cultured in the presence of IL-1β for 7 days demonstrated a significant decrease in sGAG/DNA content compared to constructs not treated with IL-1β (98.25 μg/μg DNA ±6.67 and 134.47 μg/μg DNA ±16.57, respectively).

Over the 21 day culture period media was collected every 48 hours and analysed for cumulative release of sGAG (Figure 5.5B). As with the sGAG retained in the construct the sGAG was greatest in the control constructs (167.28 μg ±30.62) compared to constructs that had been treated with IL-1β (131.95 μg ±34.39), however this result was not deemed significant.

However when total sGAG/DNA combined from both construct and media (Figure 5.5C) were analysed this demonstrated that NP cells treated with IL-1β produced a significantly lower sGAG content (1764.190 μg/μg DNA ±328.65) compared to cells that were not treated with the cytokine (2846.60 μg/μg DNA ±446.27). This means that cells treated with IL-1β only produce 61.97% of the sGAG that control cells produce over 21 days.

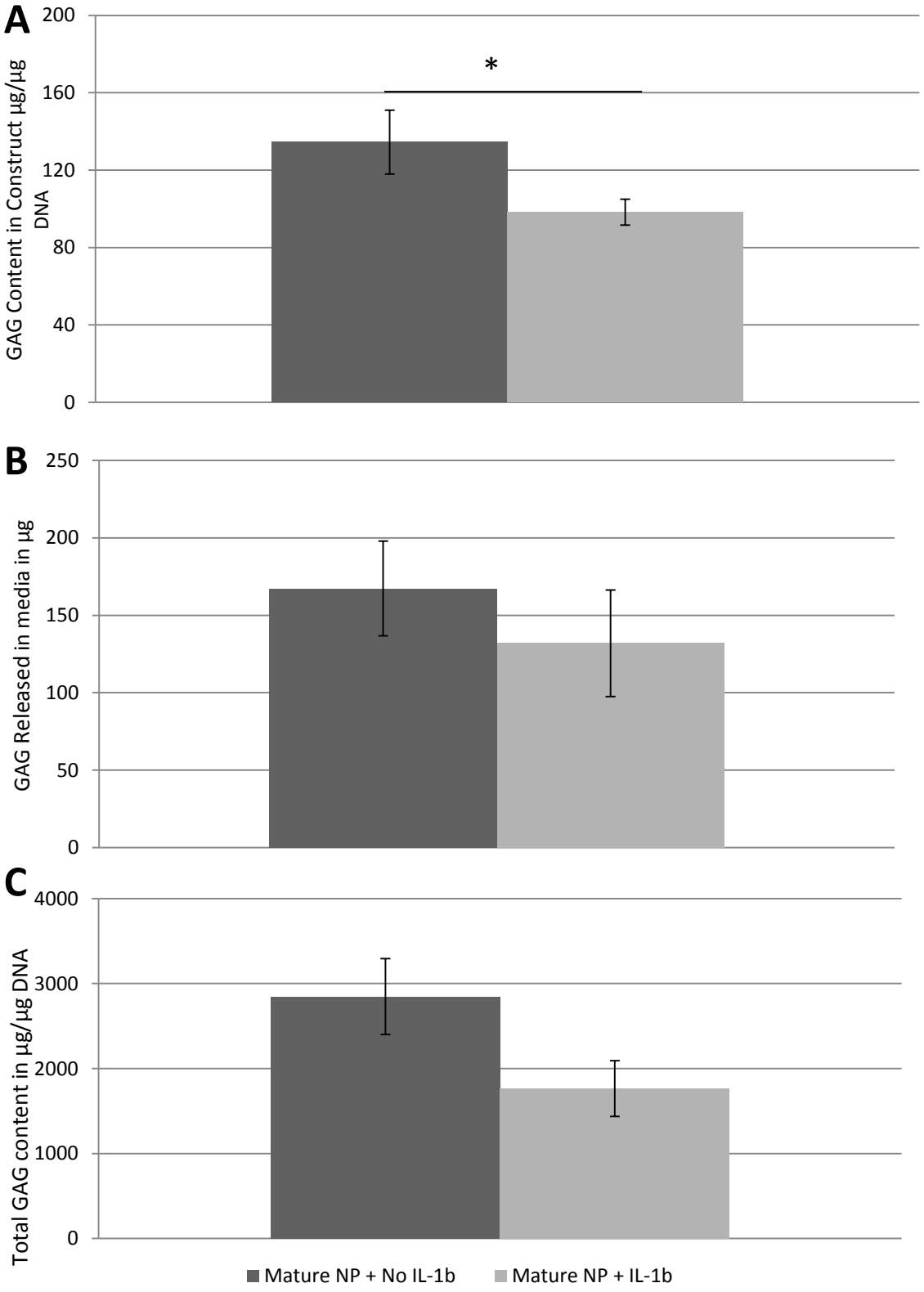

Figure 5.5 Quantification of sGAG in mature NP seeded constructs treated with and without IL-1β. (A) sGAG retained within hydrogel constructs, normalised to DNA content within the construct. **(B)** DMMB quantification of sGAG released cumulatively into the media throughout the 21 day culture period. **(C)** Quantification of total sGAG content in the construct and media normalised to DNA content within the construct at day 21. $N = 4$, data represent mean ± SEM. $^*P < 0.05$.

5.4.4.2 Quantification of sGAG in aNPCs

With regard to aNPCs (Figure 5.6A) cultured in the presence of IL-1β for 7 days the sGAG/DNA retained within the construct was decreased compared to constructs not treated with IL-1β (134.70 μg/μg DNA ±10.72 and 162.85 μg/μg DNA ±10.71, respectively) however this was not significant. The content values in relation to mature NP cells are higher in both treatment groups (IL-1β treatment aNPC vs. NP: 134.70 μg/μg DNA ±10.72 vs. 98.25 μg/μg DNA ±6.67) (No IL-1β treatment aNPC vs. NP 162.85 μg/μg DNA ±10.71 vs. 134.47 μg/μg DNA ±16.57).

The analysis of media (Figure 5.6B) collected over the culture period demonstrated that there was no significant difference in cells treated with and without IL-1β (145.99 μg ± 28.17 and 172.56 μg ±23.30, respectively). Similarly the greatest sGAG content across both cell types was demonstrated in the aNPC controls, (IL-1β treatment aNPC vs. NP: 145.99 μg ± 28.17 vs. 131.95 μg ±34.39) (No IL-1β treatment aNPC vs. NP: 172.56 μg ±23.30 vs. 167.28 μg ±30.62).

The total sGAG/DNA (Figure 5.6C) demonstrated no significant difference between aNPCs treated with and without IL-1β (2791.2 0μg/μg DNA ± 593.28 and 3229.60 μg/μg DNA ±479.21, respectively). This result showed that cells treated with the cytokine produced 86.42% of sGAG content compared to controls over a 21 day period. Therefore, aNPCs demonstrate the ability to produce greater sGAG than NP cells in a catabolic environment.

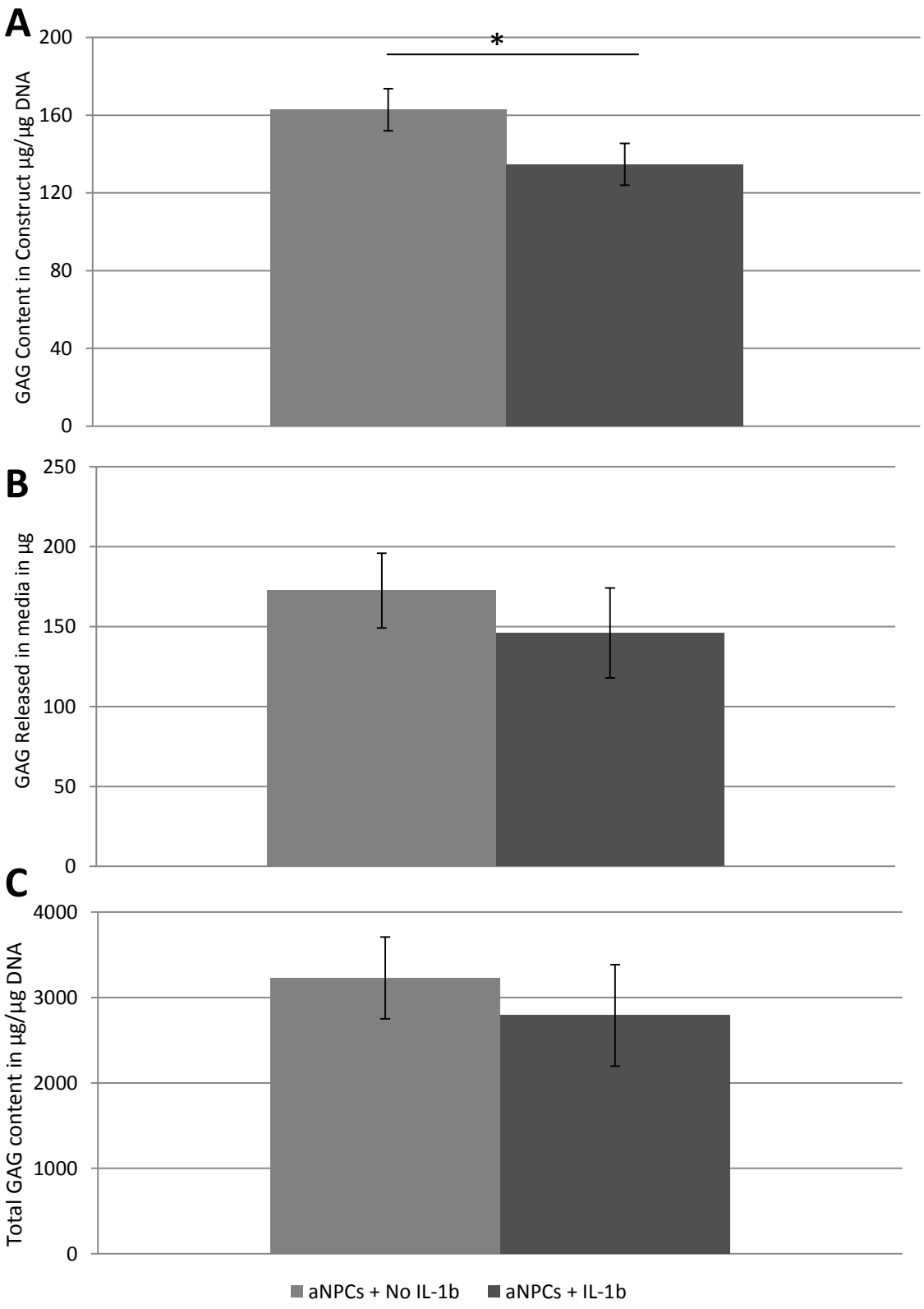

Figure 4.6 Quantification of sGAG in aNPC seeded constructs treated with and without IL-1β. (A) Quantification of sGAG retained within hydrogel constructs, normalised to DNA content within the construct. **(B)** sGAG released cumulatively into the media throughout the 21 day culture period. **(C)** Quantification of total sGAG content in the construct and media normalised to DNA content within the construct at day 21. $N = 4$, data represent mean ± SEM. $^{*}P < 0.05$.

5.4.4.3 Histological assessment of sGAG

Histological assessment sGAG was undertaken by safranin O staining (Figure 5.7). Mature NP cells and aNPCs that were not treated with IL-1β demonstrated homogenous distribution of sGAG throughout the construct. Similarly aNPCs treated with IL-1β showed a large amount of sGAG staining and this was localised to the centre of the construct. In contrast mature NP cells treated with IL-1β demonstrated a lack of staining suggesting that there is less sGAG than in the other treatment groups.

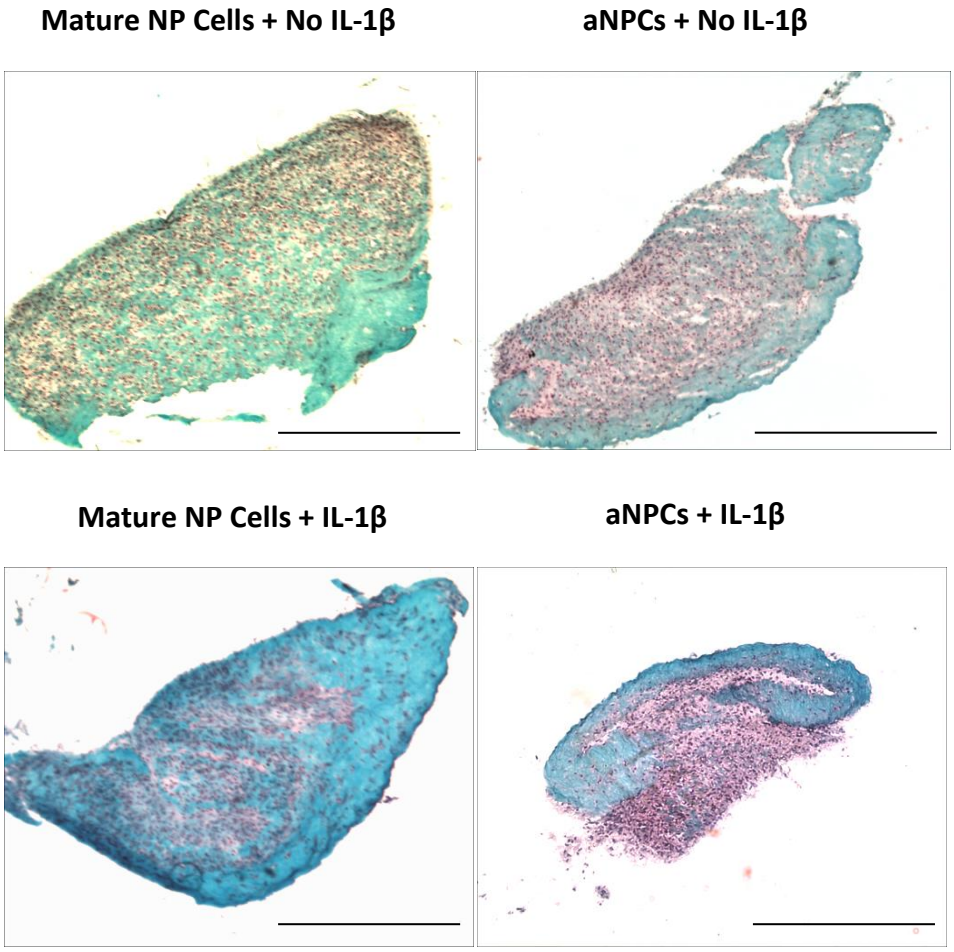

Figure 5.7 Histological localisation of sGAG of mature NP cells and aNPCs treated with or without IL-1β. Safranin O staining of mature NP cells and aNPC seeded constructs demonstrating deposition of sGAG. Scale bars, 500 μm.

5.5 Discussion

The pro-inflammatory cytokine IL-1β has demonstrated the ability to initiate catabolic processes that lead to IVD degeneration. Numerous studies have linked the cytokine to a number of pathologies in the degenerate disc including apoptosis, ECM degradation and angiogenesis amongst others. In addition it has been found that as the severity of degeneration increases in the disc so does the levels of IL-1β. Therefore if cellular based therapies are to be utilised in order to repair the degenerate IVD then the response of the cells to the inflammatory niche should be assessed. The objective of this study was to investigate how AD-MSCs that were pre-differentiated to an NP cell (aNPCs), would respond to treatment with IL-1β compared to mature NP cells. At present there are no studies in the disc biology field that have assessed the potential of pre-differentiating AD-MSCs to an NP like cell and exposing these cells to a catabolic environment to mimic the degenerate disc. In previous studies undertaken by this group (Le Maitre et al., 2005) it was demonstrated that treatment of NP cells with IL-1β resulted in a significant increase of catabolic markers (MMP3, MMP13 and ADAMTS4) in addition to significant decreases in ECM production (ACAN, COL2A1, COL1 and SOX6). Therefore we hypothesised that treatment of mature NP cells would demonstrate similar responses as previously described, however aNPCs would have a differential response and may in fact not respond to IL-1β in the same manner.

5.5.1 IL-1 Receptor Profile

As the study was investigating two different cell types, it was imperative to make sure that both cell types expressed the IL-1 receptor in order to respond to the IL-1β treatment. If one cell type did not have the receptor then it would be unable to respond to the treatment, therefore if any differences were seen between the cells this could be a potential reason. Hence the conventional PCR was undertaken and demonstrated that both cells expressed IL-1R and that cells should respond to treatment.

5.5.2 Differential ECM expression profile of aNPCs and mature NP Cells

As described throughout the thesis thus far, the NP of the disc is rich in ACAN and type II collagen. When the disc is healthy there is a balance between anabolism and catabolism, however with degeneration and the increase of IL-1β this balance is shifted toward a catabolic nature and increase in matrix degradation. Therefore following 7 days of culture with or without IL-1β a range of conventional ECM genes were analysed. When mature NP cells were exposed to IL-1β the expression of COL2A1, ACAN and SOX9 was significantly decreased compared to no treatment which corroborates previous studies (Le Maitre et al., 2005). On the other hand whilst aNPCs did show decreases in all three genes, this was not deemed significant compared to cells that were not treated with IL-1β. This suggests that pre-differentiation of AD-MSCS to aNPCs can protect the cells against the detrimental effects of IL-1β and does not result in matrix breakdown to such an extent as is observed in NP cells.

5.5.3 Differential Catabolic and Anti-catabolic Expression Profile

Expression of MMPs and ADAMTSs are a necessity to the homeostatic turnover of ECM, however during degeneration studies have demonstrated the increase of these catabolic molecules. As previous studies have demonstrated (LeMaitre et al., 2005) there was a significant increase in the catabolic markers and decrease in the anti-catabolic markers, which in turn leads to an imbalance and essentially matrix breakdown. However, this study has demonstrated that pre-differentiation of AD-MSCs for 14 days prior to catabolic treatment leads to no significant upregulation of catabolic markers or down regulation of anti-catabolic markers. Taken together with the gene expression of ECM markers, this is suggesting that pre-differentiation may be protective against the inflammatory environment.

5.5.4 PG Content of the Constructs

As demonstrated throughout the rest of the study mature NP cells and aNPSCs showed differential responses in the production of sGAG. The histological localisation demonstrated no change in the staining of aNPCs with or without IL-1β treatment, however mature NP cells show a severe lack of sGAG staining following treatment with IL-1β. This is also reflected in the quantification of sGAG by a DMMB assay, as aNPCs show no difference treated with or without IL-1β. This suggests that over the 21 day time period mature NP cells produce significantly lower sGAG content when exposed to IL-1β, which is mimicking the degenerate IVD environment. Whereas aNPCs even in a catabolic environment are able to synthesise sGAG, this is beneficial in terms of therapeutic application as these results suggest that aNPCs would have the capacity to produce sGAG in the degenerate IVD.

5.5.5 Conclusion

AD-MSC differentiated NP cells and mature NP cells respond to IL-1β in a differential manner, NP cells responded in the characteristic catabolic manner (as previously reported with decreases in SOX9, COL2A1, ACAN, TIMP1 and TIMP2, and increases in MMP3 and MMP13. Furthermore GAG content in constructs was significantly reduced. Interestingly, IL-1β had no detrimental catabolic effect on AD-MSC differentiated NP cells suggesting that these cells may be able to withstand the effects of the IL-1β milieu of the degenerate IVD niche. Thus, pre-differentiation of AD-MSCs to an NP like cell prior to implantation may improve the success of cell based therapies for IVD regeneration and prevent further catabolic events in the degenerate IVD niche.

Chapter 6

The Effect of GDF6 on Native NP Cells: Restoration of a Non-degenerate NP phenotype

6.1 Overview

As previously discussed GDF6 is a member of the TGF-β superfamily and plays a role in the development of skeletal tissues. Previous studies have shown that mutations in this gene lead to Klippel-Fiel syndrome (KFS), which can be defined as congenital fusion of vertebrae (Tassabehji et al., 2008; Asai-Coakwell et al., 2009). Also, mutations in GDF6 knockout mice (Settle et al., 2003) show fusion of both ankle and wrist joints. In a recent study by Wei and colleagues (Wei et al., 2015) the group detected expression of GDF6 in the human foetal spinal column across of range of ages 8-19 weeks. Interestingly the group detected high levels of GDF6 in the period of early ossification of vertebrae and the development of the IVDs where the growth factor was localised to the NP. As the foetal age increased GDF6 expression decreased with the progression of ossification and was restricted to the cartilaginous region. This work suggests that GDF6 acts as a suppressor to ossification and helps appropriate vertebral segmentation during the development of the spine. This is also supported by previous work (Shen et al., 2009) carried out by this group as they demonstrated that supplementation of exogenous GDF6 to BM-MSCs in fact inhibited osteogenic differentiation.

Work undertaken by our laboratory has also localised GDF6 to the IVD, but in this case adult IVD samples. A comparison of the NP region, inner and outer AF showed that GDF6 was predominately expressed in the NP region of the IVD. Also whilst there was a slight decrease in the percentage of positive cells with the severity of degeneration this was not deemed to be significant, suggesting that reduced expression of GDF6 is not associated with pathogenesis. Likewise in a more recent study (Gulati et al., 2015) localised GDF6 expression in degenerate and scoliotic NP tissues and found no significant difference between the two diseases states. .

6.1.2 Functional effects of GDF6 on IVD cells

There are a limited number of studies that have investigated the effect of GDF6 on disc cells, particularly NP cells. Firstly Wei and colleagues (Wei et al., 2009) used a stab injury degenerative ovine model and injected a single dose of GDF6 at the same time as injury. This resulted in increased collagen and PG production, an increase in number of NP cells and increased disc hydration after 4 months compared to the degenerate control discs. Such data suggests that GDF6 may be a potent therapeutic

option for the treatment of IVD degeneration. Additionally, more recently a study undertaken examined the effect of GDF6 applied exogenously to NP, AF and cartilaginous end plate cells *in vitro* (Gulati et al., 2015). Cells were cultured in alginate beads and exposed to GDF6 for 7 days; this resulted in increased PG content compared to no treatment. Whilst this study demonstrated that GDF6 enhanced PG content and collagen expression no information about the phenotypic nature or the catabolic profile of the cells or whether cells would function differently in a catabolic environment following treatment with GDF6 was provided. Such aspects are important when considered the potential of GDF6 as a biological therapy for IVD degeneration treatment strategies.

6.2 Hypotheses

This study was designed to investigate the effects of exogenous GDF6 on mature human NP cells Two aspects were investigated: firstly the effect of GDF6 treatment on mature NP cells phenotype and function and, secondly the assessment as to whether pre-treatment of mature NP cells with GDF6 is protective against the catabolic environment of the degenerate IVD.

It was hypothesised that:

1) GDF6 would reduce the catabolic profile and thereby restore a normal phenotype in degenerate NP cells.
2) Pre-treatment with GDF6 would protect cells from the catabolic effects of IL-1β.

6.3 Experimental Design

The first stage of this study was to examine the response of mature NP cells to treatment with exogenous GDF6 for 7 and 14 days.

Following this a larger study was undertaken to investigate whether an initial pre-treatment of NP cells with GDF6 or sustained/continued treatment protected NP Cells from or prevented the catabolic effects of IL-1β.

6.4 Results

6.4.1 Gene Expression in NP Cells following 7 days of Culture with GDF6

Mature NP cells (n=4) were cultured for 7 days in differentiating media with and without GDF6 and gene expression analysed with gene expression of target genes normalised to the housekeeping genes and to the day 7 control. Analysis of the conventional ECM genes (Figure 6.1A) demonstrated significantly higher levels of expression for COL2A1 and ACAN (2.11-fold and 1.61-fold, respectively) compared to no treatment with GDF6, whilst expression of SOX9 was increased (1.25-fold), although not significantly. .

With regard to the expression of phenotypic NP markers (Figure 5.1B) treatment of NP cells with GDF6 significantly upregulated the majority of markers assessed including KRT8 (2.68-fold), KRT18 (2.37-fold), KRT19 (2.11-fold) and T (1.88-fold). The expression of FOXF1 and CAXII were not significantly different compared to the controls (1.29-fold and 1.37-fold, respectively).

The final panel of markers that were investigated were the catabolic and anti-catabolic markers (Figure 5.1C). Significant increases were only see in expression levels of MMP13 (2.06-fold) and ADAMTS4 (1.88-fold), with no changes in gene expression for the other genes analysed.

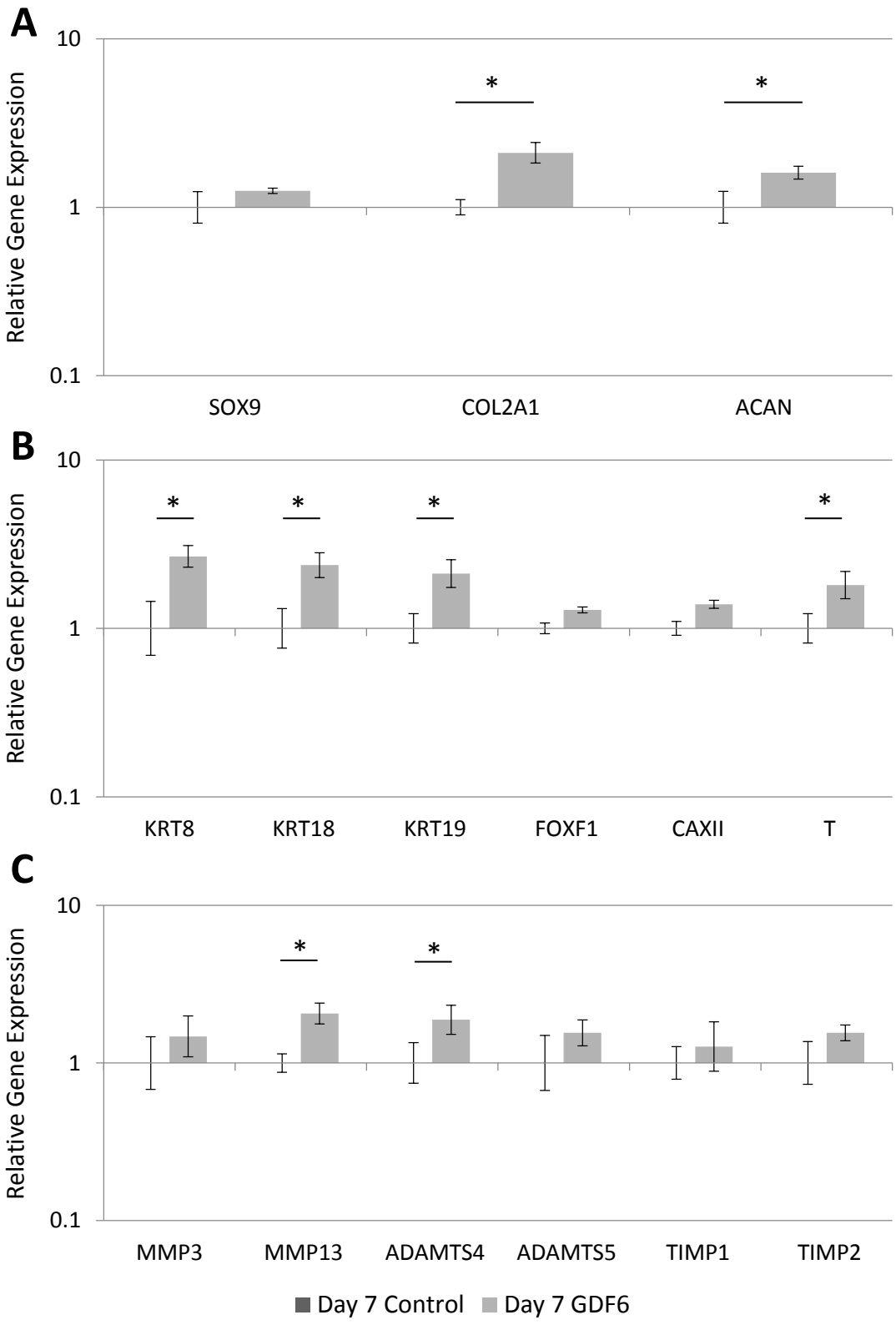

Figure 6.1 Gene expression of mature NP cells cultured with and without GDF6 for 7 days. Cells were encapsulated in type I collagen hydrogels and cultured either with or without 100ng/ml GDF6 for 7 days, q-PCR was then undertaken for **A.** conventional ECM markers **B.** novel NP phenotypic markers **C.** catabolic and anti-catabolic markers. Relative gene expression was normalised to housekeeping gene expression and then to the respective cell type that was not treated with GDF6 and plotted on a log scale N = 4; all data represent mean ± SEM. *P < 0.05.

6.4.2 Gene Expression in NP Cells following 14 days of Culture with GDF6

In addition to the 7 day culture, cells were cultured for 14 days to assess differences in the culture period time. Similarly results were normalised to housekeeping genes and then to day 14 controls, which were cultured with no GDF6. Assessment of conventional ECM genes (Figure 6.2A) showed that treatment with GDF6 for 14 days increased levels of expression for all three genes with the greatest upregulation in ACAN, (SOX9 (2.34-fold), COL2A1 (4.37-fold) and ACAN (9.25-fold). All genes showed increases compared to 7 days in culture when compared to the respective controls, SOX9 (1.25-fold vs 2.34- fold), COL2A1 (2.11-fold vs. 4.37-fold), ACAN (1.61-fold vs. 9.25-fold). This shows that with increased time in culture, there are significant increases in the expression of ECM molecules.

Similarly assessment of NP phenotypic marker expression (Figure 6.2B) demonstrated that exogenous GDF6 increased levels of all genes, KRT8 (3.71-fold), KRT18 (3.22-fold), KRT19 (4.20-fold), FOXF1 (2.47-fold), CAXII (2.64-fold) and T (4.41-fold). As with the ECM genes, the expression of NP marker genes was increased compared to culture over a 14 day period, when compared to the respective controls; KRT8 (2.68-fold vs 3.71-fold), KRT18 (2.37-fold vs 3.22-fold), KRT19 (2.11-fold vs 4.20-fold), FOXF1 (1.29-fold vs 2.47-fold), CAXII (1.37-fold vs 2.64-fold) and T (1.88-fold vs 4.41-fold).

Finally the catabolic and anti-catabolic markers showed no significant differences between samples treated with or without GDF6.

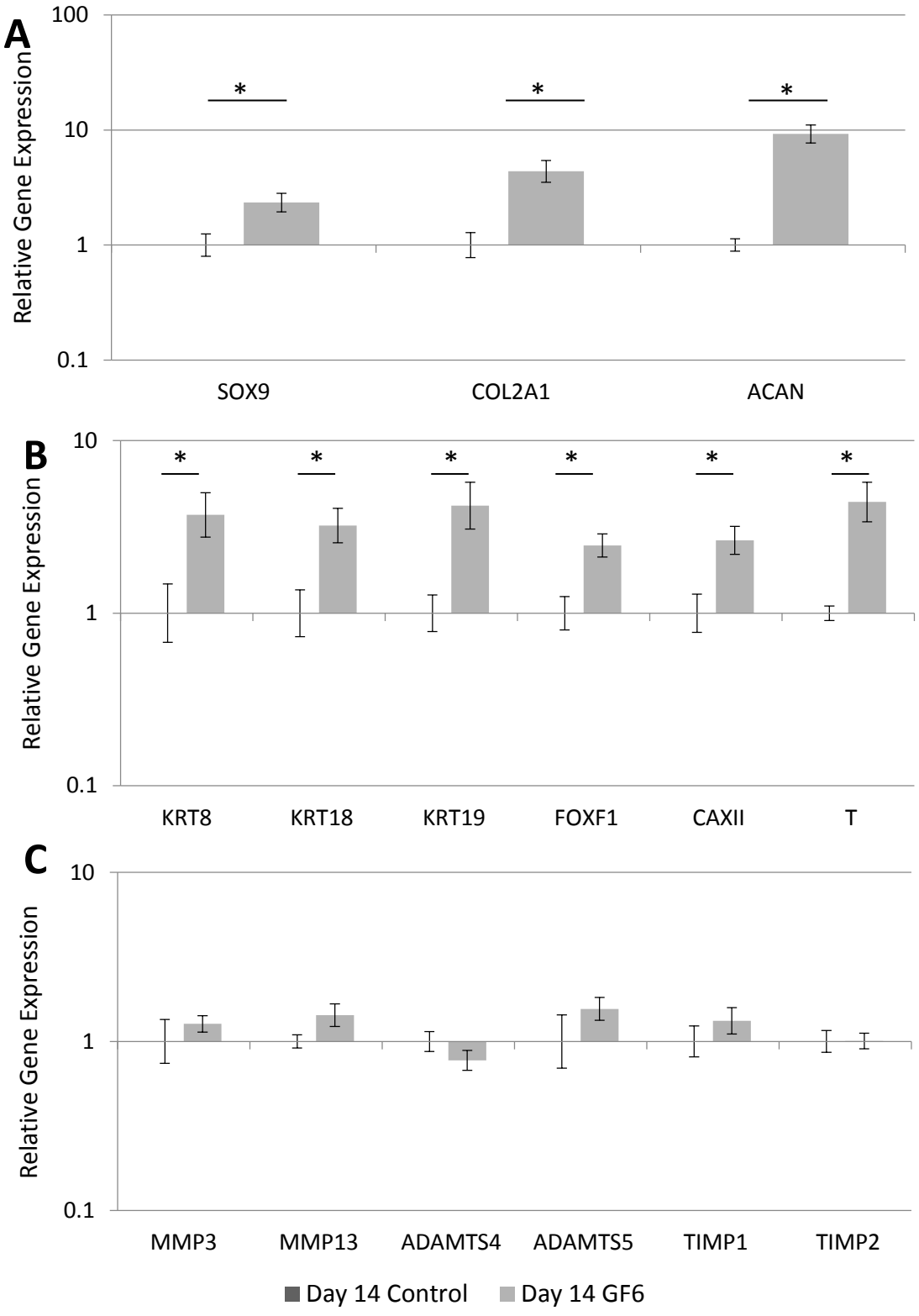

Figure 6.2.Gene expression of mature NP cells cultured with and without GDF6 for 14 days. Cells were encapsulated in type I collagen hydrogels and cultured either with or without 100ng/ml GDF6 for 14 days, q-PCR was then undertaken for **A.** conventional ECM markers **B.** novel NP phenotypic markers **C.** catabolic and anti-catabolic markers. Relative gene expression was normalised to housekeeping gene expression and then to the respective cell type that was not treated with GDF6 and plotted on a log scale N = 4; all data represent mean ± SEM. *P < 0.05

6.4.3 ACAN:COL2A1 Gene Expression Ratio

In order to assess the gene expression ratio of the ACAN and COL2A1, which is a distinguishing feature of the NP tissue, the formula outlined in section 2.4.3 was used (Figure 6.3). Mature NP cells cultured in the presence of GDF6 for 7 and 14 days resulted in a higher ratio of ACAN :COL2A1 compared to the respective controls (Day 7: Control 34:1; GDF6 75:1 and Day 14: Control 192:1 and 525:1). Overall even in culture without GDF6 the ratio of ACAN: COL2A1 increased with increased time in culture, however this was enhanced with the addition of GDF6.

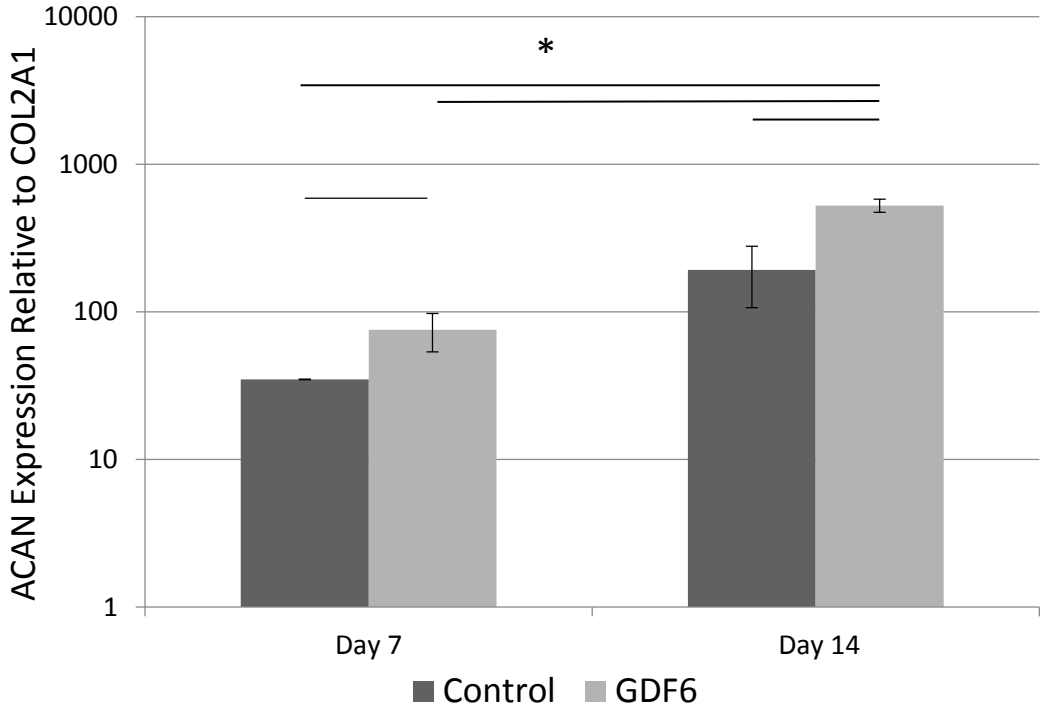

Figure 6.3 ACAN:COL2A1 ratio gene expression ratio in mature NP cells treated with and without GDF6 and cultured for 7 or 14 days. Following culture of NP cells in type I collagen hydrogels for 7 or 14 days with either no growth factor, or GDF6 ratios were determined using the formula (2-ΔCtACAN-ΔCtCOL2A1). N = 4; all data represent mean ± SEM. *P < 0.05.

6.4.4 Quantification of sGAG synthesis

Assessment of the construct, media and combined totals of sGAG were undertaken using a DMMB assay. Similar to the gene expression data, cells that were cultured for a sustained period demonstrated greater sGAG content. In cells cultured with and without GDF6 for 7 days (Figure 6.4A) there were no significant differences observed with contents of 72.56 μg/μg DNA ±5.91 and 61.77 μg/μg DNA ± 7.80, respectively. However, there was a significant difference when cells were cultured for 14 days with GDF6 compared to no treatment (149.54 μg/μg DNA ± 12.93 and 111.94 μg/μg DNA ± 0.53). The results show that sustained culture leads to formation of greater sGAG, which was enhanced with exposure/ stimulation to GDF6.

As media was changed every 48 hours, this was assessed after 7 and 14 days for release of sGAG into the media (Figure 6.4B). Following 7 days there were no differences observed between cells treated with GDF6 and the control cells as they released totals of 56.62 μg/μg ± 2.05 and 51.69 μg/μg ± 2.65, respectively. In a similar manner to the constructs there was a significant increase of sGAG with sustained time in culture. Following 14 days control samples released 95.26 μg/μg ± 3.08 and cells exposed to GDF6 released significantly greater total of 107.82 μg/μg ± 2.66.

When the total sGAG/DNA was combined for both construct and media components and normalised to the DNA content, both day 7 and day 14 NP cells treated with GDF6 were significantly different compared to the respective controls. (Day 7: Control: 897.27 μg/μg DNA ± 151.52 and GDF6 1356.48 μg/μg DNA ± 140.55) (Day 14: Control: 1748.31 μg/μg DNA ± 137.68 and GDF6 2287.89 μg/μg DNA ± 188.52). The highest total content was demonstrated by NP cells cultured for 14 days GDF6.

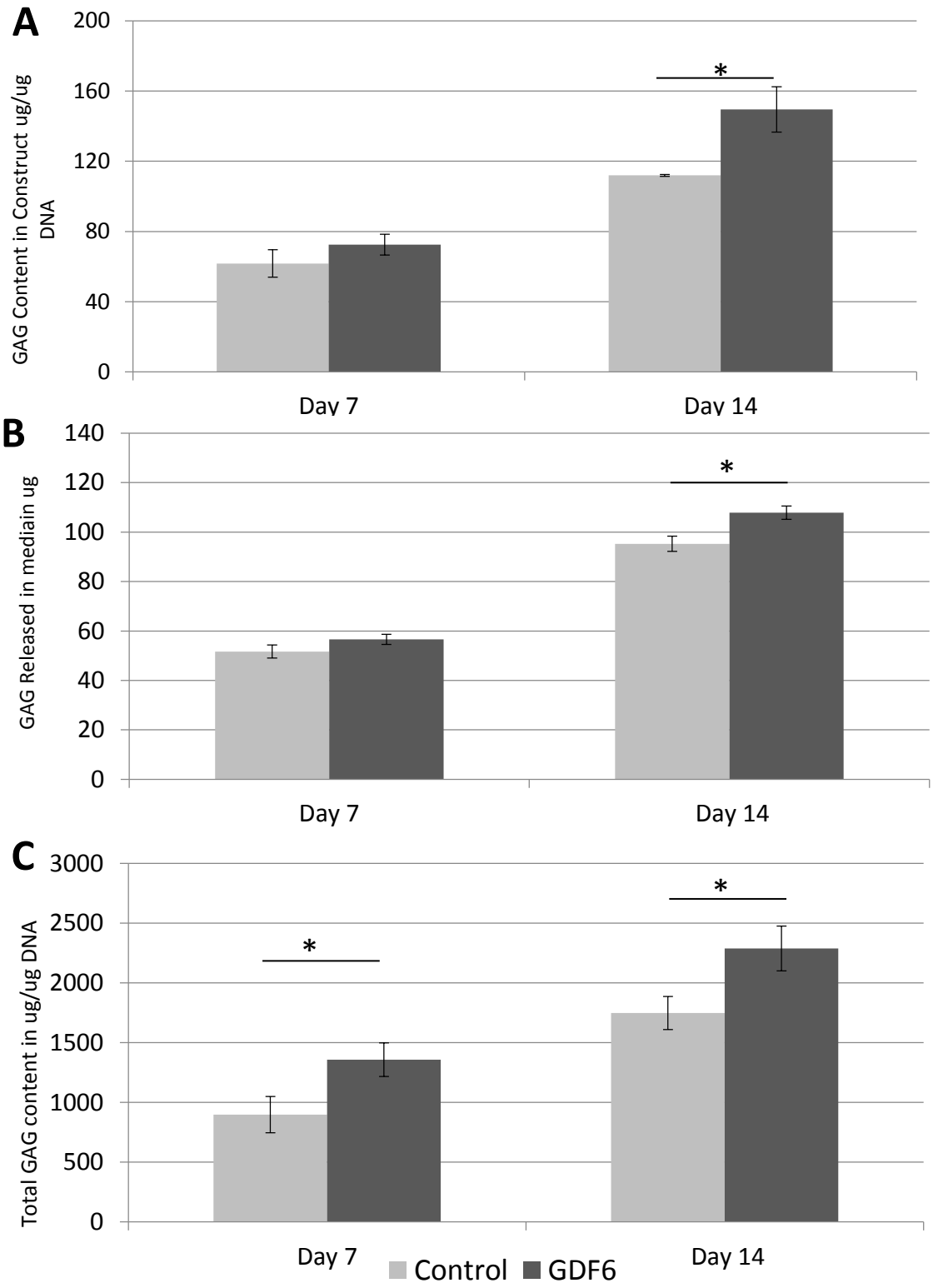

Figure 6.4 Quantification of sGAG in mature NP seeded constructs treated with and without GDF6 for 7 or 14 days. (A) sGAG retained within hydrogel constructs, normalised to DNA content within the construct. **(B)** DMMB quantification of sGAG released cumulatively into the media throughout the 21 day culture period. **(C)** Quantification of total sGAG content in the construct and media normalised to DNA content within the construct at day 21. $N = 4$, data represent mean ± SEM. $*P < 0.05$.

6.4.5 Treatment of NP cells with GDF6 and Exposure to IL-1 β

The second part of this study was undertaken to assess whether treatment of NP cells with GDF6 could protect the cells against the catabolic effects of IL-1β. Following a total of 21 days in culture expression was normalised to housekeeping genes and then to NP cells that had no exposure to GDF6 or IL-1β (group1).

6.4.5.1 Expression of ECM Genes

As shown in the previous chapter, culture of NP cells for 14 days with no growth factor followed by treatment with IL-1β for 7 days demonstrates a significant downregulation of all three ECM genes SOX9, COL2A1 and ACAN compared to no treatment in Figure 6.6 A,B,C, respectively.

When cells were pre-treated with GDF6 for 14 days and then GDF6 withdrawn for a further 7 days the expression of ACAN (Figure 6.5C) and COL2A1 (Figure 6.5 B) were significantly upregulated (7.39-fold and 3.87-fold, respectively) whilst SOX9 was upregulated (1.60-fold) but not to a significant extent compared to control. Pre-treatment of the cells with GDF6 for 14 days and exposure to IL-1β for 7 days resulted in a significant decrease for all three genes compared to pre-treatment and no IL-1β; however the expression levels did not differ to the control sample for COL2A1 and SOX9, whereas ACAN expression was significantly increased (3.11-fold). All three genes were significantly greater expressed than in cells that had not been treated with GDF6 and exposed to IL-1β.

Similarly cells that were exposed to GDF6 for the whole 21 day culture demonstrated significant increases in expression compared to the control sample. The cells that were exposed to GDF6 for 21 days and IL-1β for 7 days, demonstrated reduced expression compared to no IL-1β treatment, but were significantly increased compared to no treatment with GDF6. The results suggest that treatment with GDF6 protects the cells to some extent against the effect of IL-1 β.

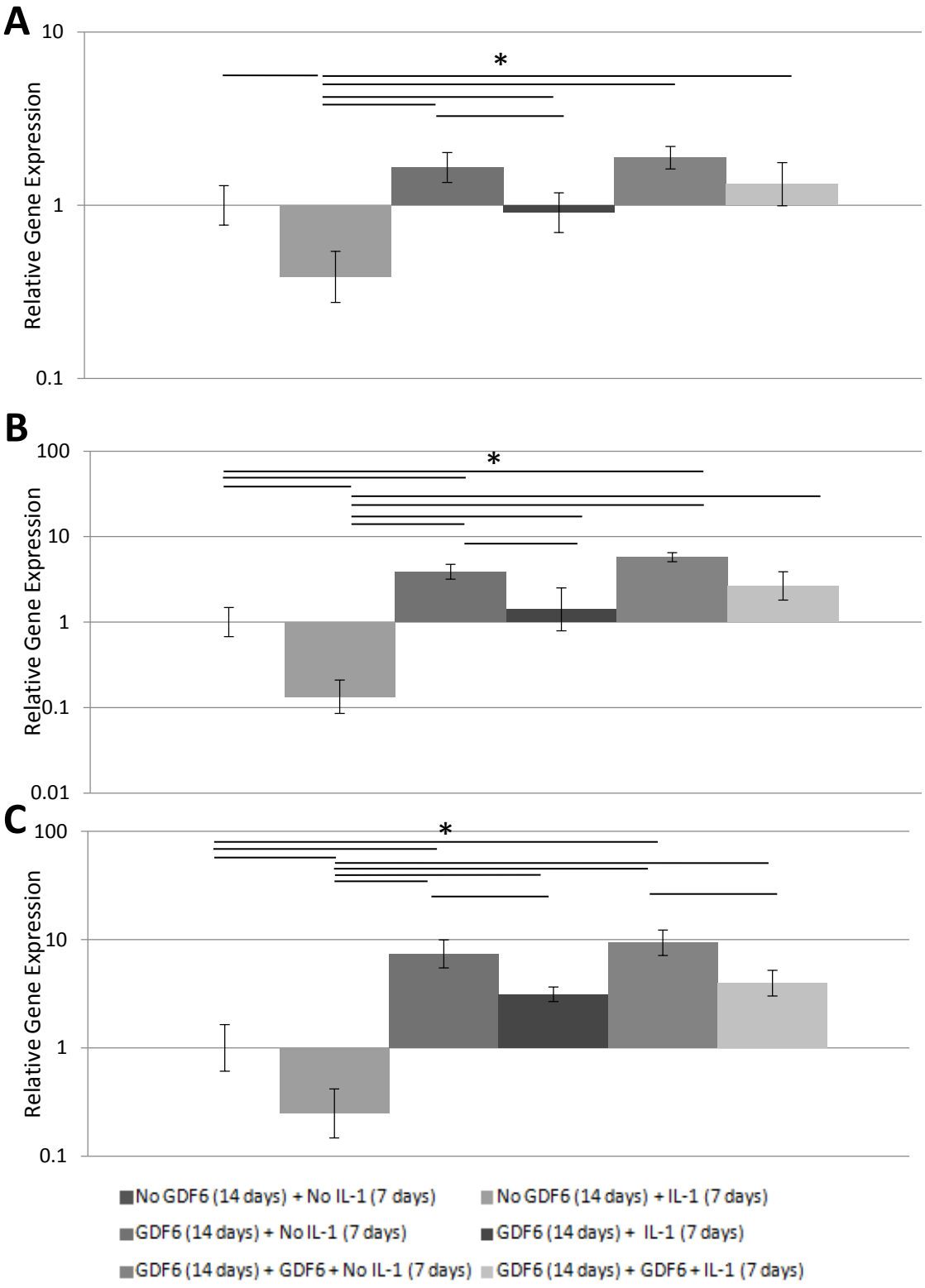

Figure 6.5 ECM Gene Expression in NP cells culture in the presence and absence of GDF6 and IL-1β. NP cells were encapsulated in type I collagen and divided into six experimental groups which were exposed to a total of 21 days culture and exposed to GDF6, IL-1β in varying combinations. qPCR was undertaken to assess **A.** SOX9 **B** COL2A1 **C** ACAN. Relative gene expression was normalised to housekeeping gene expression and then to NP cells not treated with GDF6 and IL-1β and plotted on a log scale $N = 4$; all data represent mean ± SEM. $*P < 0.05$.

6.4.5.2 Expression of Catabolic Genes

In the previous chapter it was demonstrated that NP cells cultured for 14 days with no growth factor and then exposed to IL1 β has a significantly increased expression of catabolic markers MMP3, MMP13 (Figure 6.6 A,B) and ADAMTS4 (Figure 6.7A).

However here, following either pre-treatment for 14 days with GDF6 or continual presence of GDF6 and IL-1β no significant differences compared with the control sample were observed.

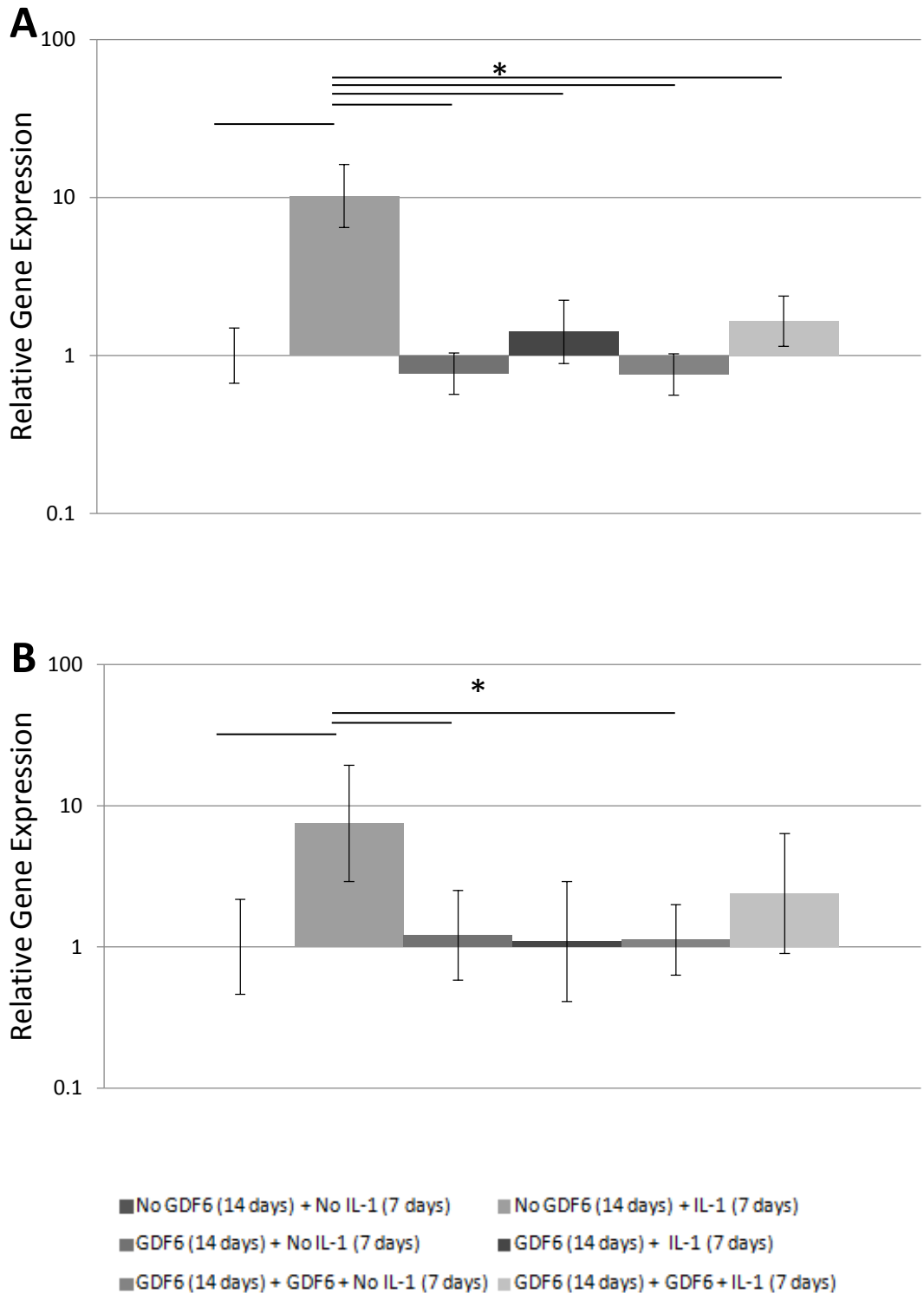

Figure 6.6 Catabolic Gene Expression in NP cells culture in the presence and absence of GDF6 and IL-1β. NP cells were encapsulated in type I collagen and divided into six experimental groups which were exposed to a total of 21 days culture and exposed to GDF6, IL-1β in varying combinations. qPCR was undertaken to assess **A.** MMP3 **B.** MMP13 Relative gene expression was normalised to housekeeping gene expression and then to NP cells not treated with GDF6 and IL-1β and plotted on a log scale. N = 4; all data represent mean ± SEM. *P < 0.05.

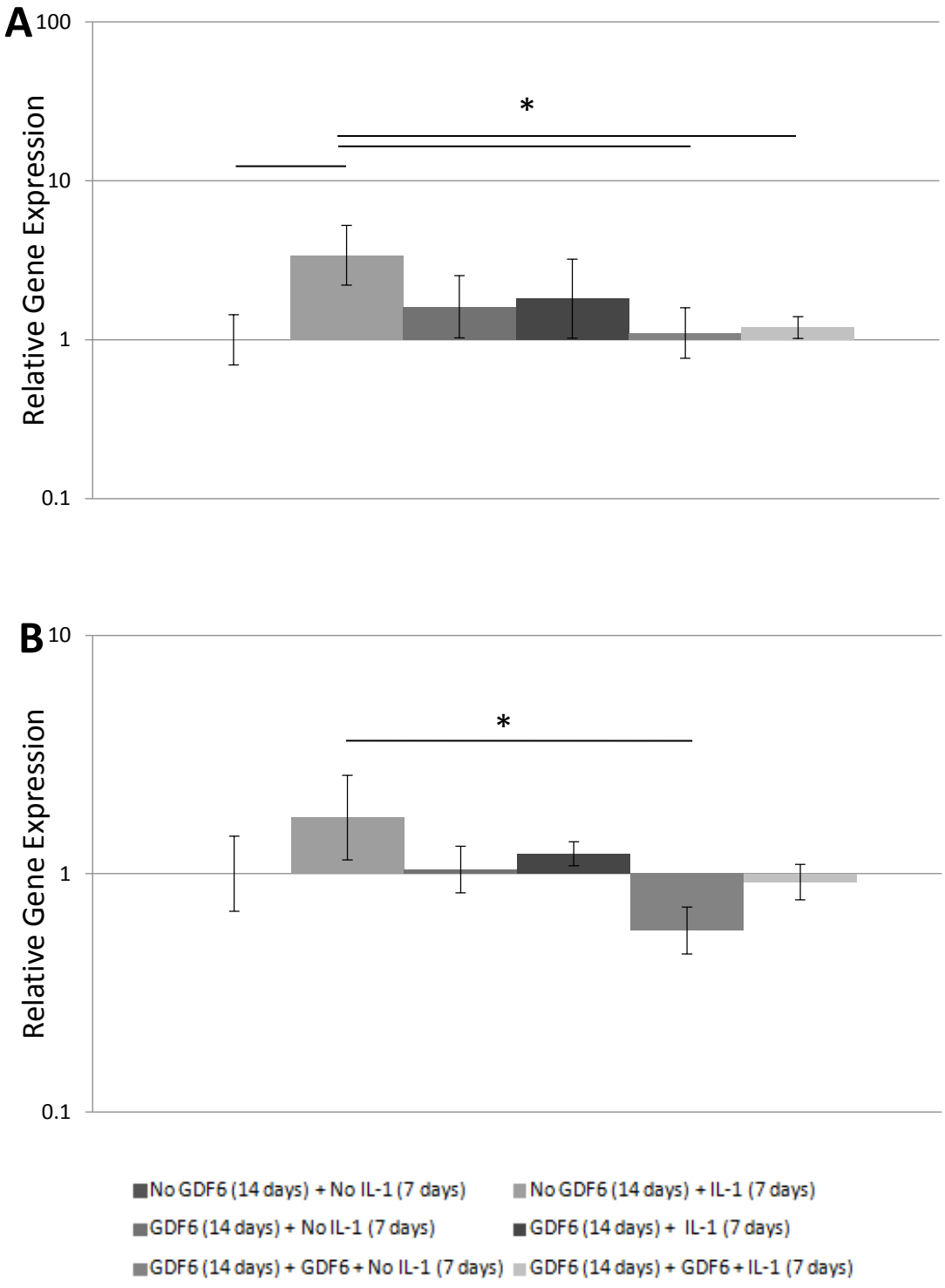

Figure 6.7 Catabolic Gene Expression in NP cells culture in the presence and absence of GDF6 and IL-1β. NP cells were encapsulated in type I collagen and divided into six experimental groups which were exposed to a total of 21 days culture and exposed to GDF6, IL-1β in varying combinations. qPCR was undertaken to assess **A.** ADAMTS4 **B** ADAMTS5. Relative gene expression was normalised to housekeeping gene expression and then to NP cells not treated with GDF6 and IL-1β and plotted on a log scale. N = 4; all data represent mean ± SEM. *P < 0.05.

6.4.5.3 Expression of Anti-catabolic Genes

Exposure of NP cells to IL-1β has been demonstrated to significantly reduce anti-catabolic gene expression of TIMP1 and TIMP2 (Figure 6.8 A, B).

With regard to TIMP1 expression (Figure 5.9A) pre-treatment of cells with GDF6 demonstrated no significant difference compared to the overall control, and pre-treatment followed by exposure to IL-1β also demonstrated no difference compared to the control, however both groups showed significantly greater expression than exposure to IL-1β alone. This was also seen in cells that were exposed to GDF6 for the 21 days of culture.

TIMP2 expression (Figure 6.8B) showed no differences compared to the control when pre-treated with GDF6 and cultured for 21 days with GDF6. When these cells were exposed to IL-1β both showed decreased expression levels but not to the same extent as no treatment with GDF6.

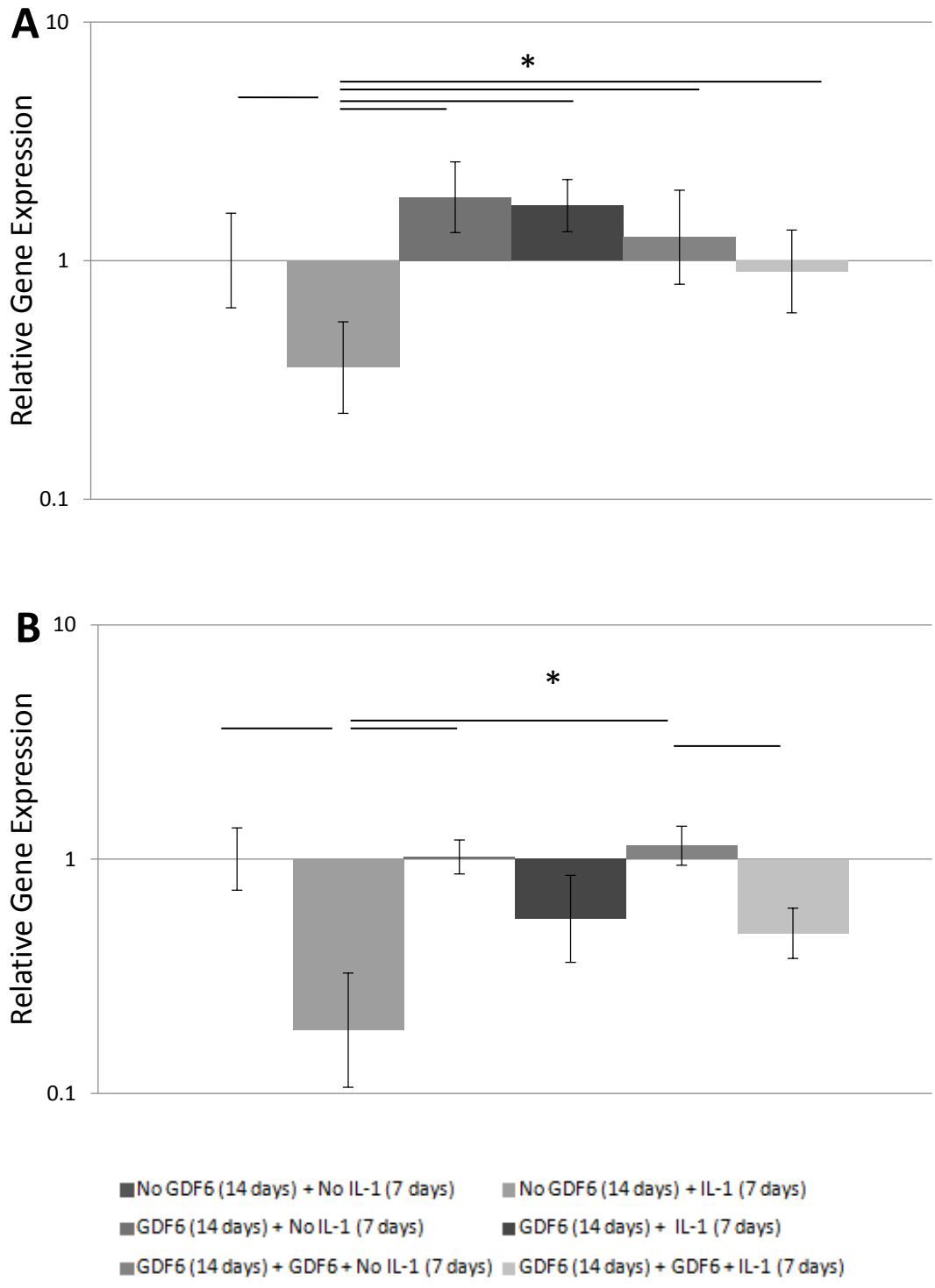

Figure 6.8 Anti-catabolic Gene Expression in NP cells culture in the presence and absence of GDF6 and IL-1β. NP cells were encapsulated in type I collagen and divided into six experimental groups which were exposed to a total of 21 days culture and exposed to GDF6, IL-1β in varying combinations. qPCR was undertaken to assess **A.** TIMP1 **B** TIMP2. Relative gene expression was normalised to housekeeping gene expression and then to NP cells not treated with GDF6 and IL-1β and plotted on a log scale N = 4; all data represent mean ± SEM. *P < 0.05.

6.4.5.4 Quantification of sGAG synthesis

Following 21 days of culture the sGAG content was assessed. When examining the sGAG content retained within the construct (Figure 6.9A) NP cells exposed to no growth factor or IL-1β demonstrated a content of 134.47 μg/μg DNA ±19.23 which was significantly reduced when NP cells were exposed to IL-1β 98.25 μg/μg DNA ± 6.67. NP cells that were pre-treated with GDF6 for 14 days and for the whole 21 day culture period demonstrated significantly increased sGAG levels compared to the controls (187.43 μg/μg DNA ± 17.63 and 191.92 μg/μg DNA ± 15.19, respectively). When the cells were exposed to IL-1β the content was decreased (146.17 μg/μg DNA ±24.09 and 146.88 μg/μg DNA ± 24.31, respectively), this showed no difference to the control, however the content for both groups was greater than cells not treated with GDF6 and exposed to IL-1β.

Likewise sGAG that was released into the media (Figure 6.9B) was at the greatest levels in cells that had been exposed to GDF6 for 14 and 21 days (201.31 μg/μg ±25.60 and 199.13 μg/μg ± 32.02). Whilst cells treated with GDF6 for 14 days and then were exposed to IL-1β showed significantly less sGAG than no IL-1β treatment (146.86 μg/μg ± 8.89) this was not different than the overall control (167.95 μg/μg ± 16.85).

When the sGAG totals were combined (Figure 6.9C) the control sample 2846.63 μg/μg DNA ± 255.98 had a greater content than samples treated with IL-1β 1764.19 μg/μg DNA ±328.65. However when cells were exposed to GDF6 for 14 and 21 days the total content was significantly increased (3476.34 μg/μg DNA ±256.73 and 3636.84 μg/μg DNA ±175.44, respectively). Also when the cells were exposed to GDF6 and then IL-1β the reduced sGAG was significantly less than with no GDF6 treatment (2904.78 μg/μg DNA ±295.23 and 2917.23 μg/μg DNA ±408.35).

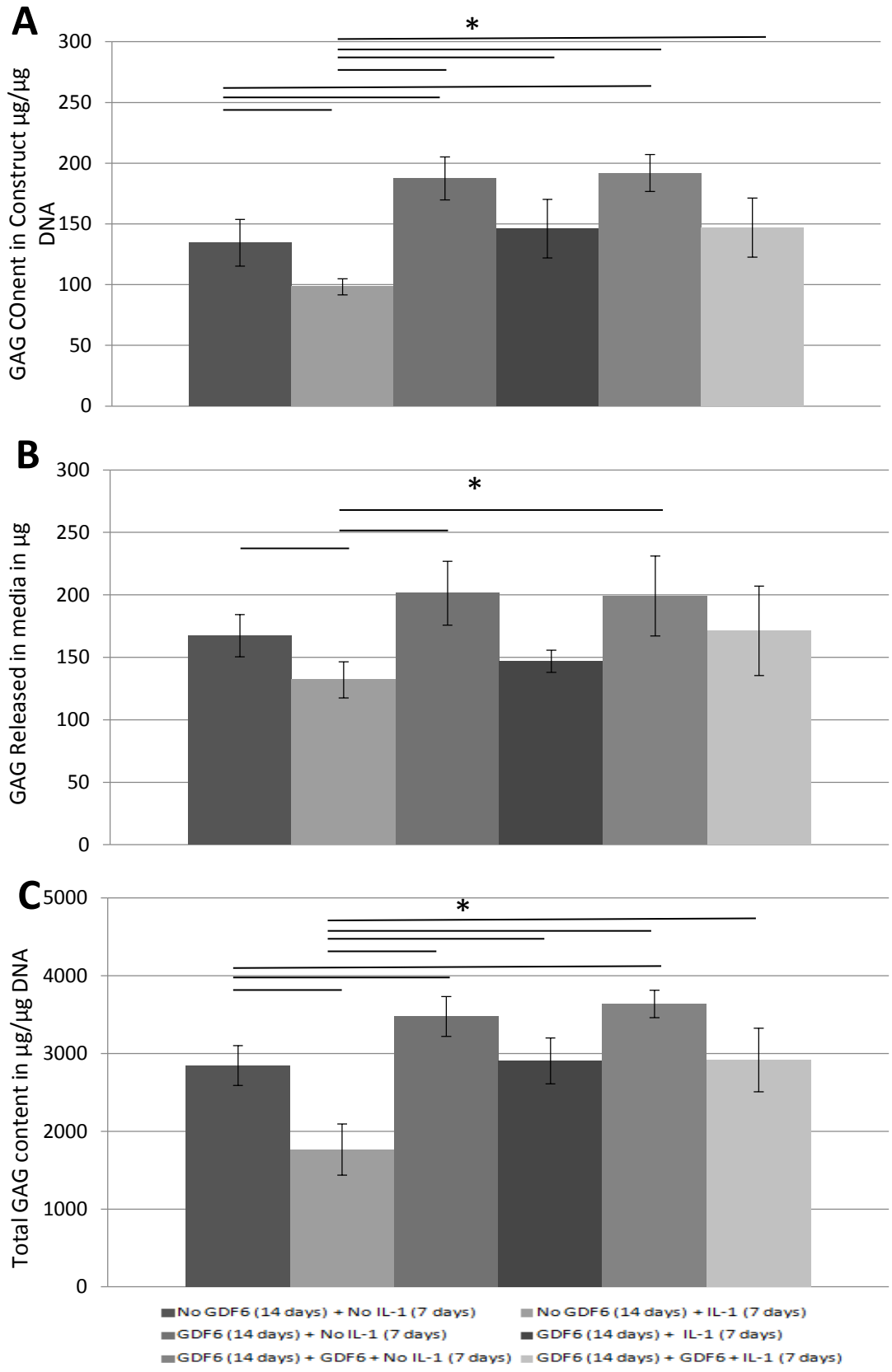

Figure 6.9 Quantification of sGAG in NP cell seeded constructs. A. Quantification of sGAG retained within hydrogel constructs, normalisedto DNA content within the construct. **B.** DMMB quantification of sGAG released cumulatively into the media throughout the culture period. **C.** Quantification of total sGAG content in the construct and media normalisedto DNA content within the construct at day 14. $N = 3$, data represent mean ± SEM. *$P < 0.05$.

6.4.5.5 Histological Assessment of sGAG

sGAG was localised to the constructs and histological assessment demonstrated homogenous distribution throughout, however NP cells that were not treated with IL-1β demonstrated less staining than the other samples (Figure 6.10).

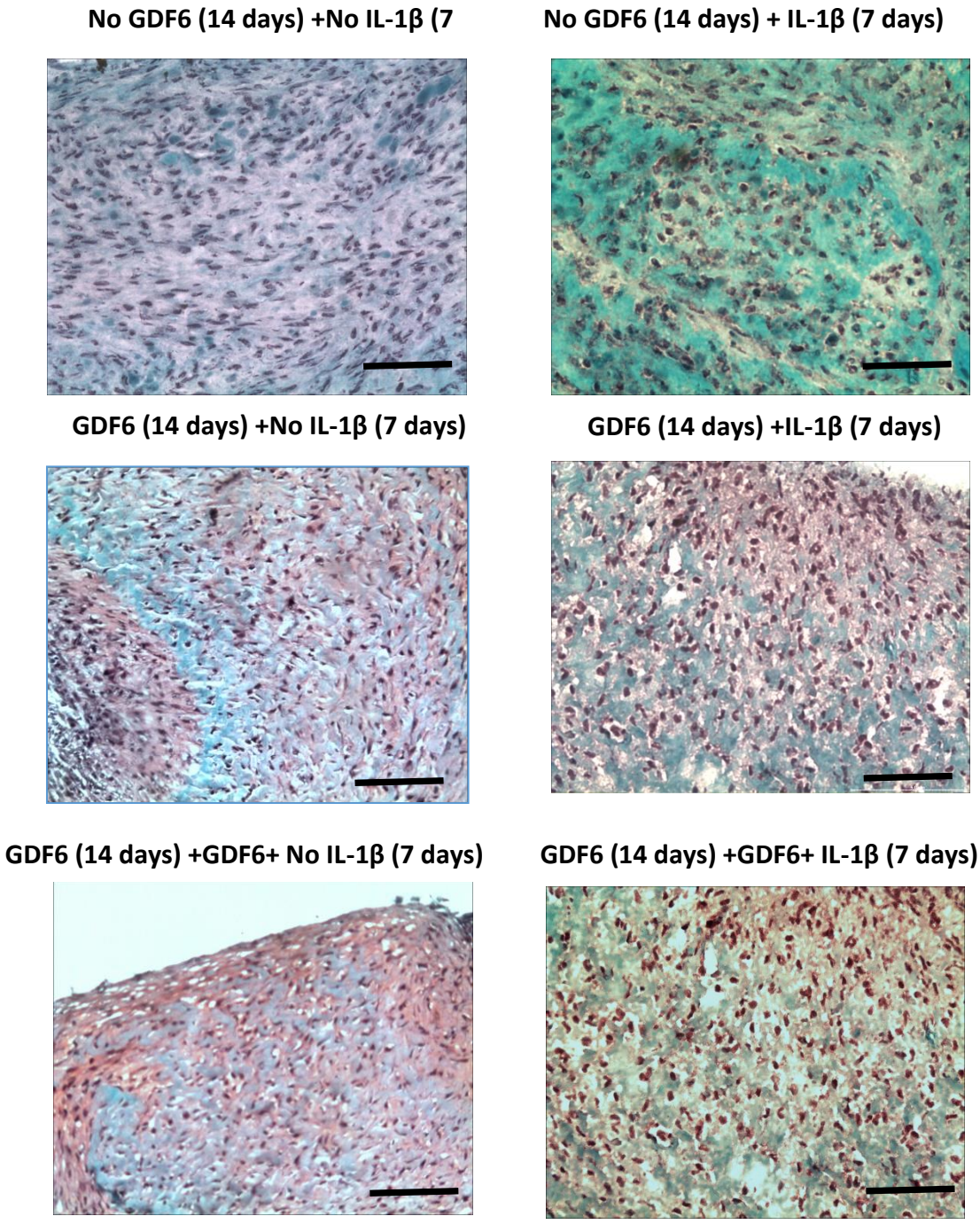

Figure 6.10 Histological localisation of sGAG of mature NP cells treated with or without IL-1β or GDF6. Safranin O staining of mature NP cells seeded constructs demonstrating deposition of sGAG. Scale bars, 50μm.

6.5 Discussion

With the advancement of IVD degeneration the native NP cells change and undergo pathological differences compared to healthy cells including clustering, senescence and a change in phenotype. Recent studies have focused on the use of GDF6 as a potential biological therapy for IVD regeneration. As discussed, GDF6 is important for skeletal growth, to promote correct vertebral segmentation and has been shown to be expressed by NP cells (Le Maitre et al., 2009c; Gulati et al., 2015). The ability to increase ECM in a degenerate ovine model (Wei et al., 2009) and to also increase ECM expression in *in vitro* experiments (Gulati et al., 2015) highlights the potential of the growth factor as a biological therapy for the treatment of IVD degeneration. Whilst the studies mentioned highlight the increase in ECM synthesis, there has been no focus on the phenotypic effect of GDF6 or the catabolic profile of the cells.

6.5.1 Restoration of NP Phenotype when Cultured with GDF6

Mature NP cells were cultured for 7 and 14 days in the presence of GDF6 and demonstrated a significant upregulation of ECM markers ACAN and COL2A1. With regard to COL2A1 expression this was increased with time in culture, which is consistent with a number of studies that have reported that GDF6can induce expression of COL2A1 in vitro in a range of cell types (Shen et al., 2009; Yeh et al., 2004; Nochi et al., 2004) and also in a degenerate disc model (Wei et al., 2009). Similarly an increase in ACAN expression has also previously been noted in fibroblasts (Bobacz et al., 2006), AF cells (Zhang et al., 2007) and NP cells (Zhang et al., 2006; Gulati et al., 2015). The results also demonstrated an increase in ACAN: COL2A1 at a gene expression level, suggesting that an appropriate matrix is being formed (Mwale et al., 2004). In addition NP cells supplemented with GDF6 demonstrated a significant increase in sGAG over both 7 and 14 days, this was also demonstrated the study by Gulati et al. (Gulati et al., 2015), however Gulati and colleagues use much greater concentrations of GDF6 (400ng/ml) in comparison to this study (100ng/ml). Therefore our data suggest that GDF6 can induce matrix formation at a lower concentration, which is beneficial for cost reasons. Taken together the results demonstrate that GDF6 has the ability to enhance matrix production of degenerate NP cells, which is important for the restoration of a functional matrix.

Whilst there is a body of data that suggests GDF6 can enhance matrix production, and prevent osteogenic differentiation (Shen et al., 2009) there are currently no studies that have examined the effect of GDF6 on the phenotypic profile. Therefore in this study we investigated the novel NP markers, KRT8, KRT18, KRT19, CAXII, FOXF1 and T. Interestingly with sustained time in culture and supplementation of GDF6 the expression levels of all genes were significantly upregulated. The reasons behind this are unclear, however it could be postulated that as GDF6 is significantly involved in the development of the disc, the supplementation with the growth factor may be driving toward a younger NP cell phenotype.

Additionally, in this study the catabolic profile of the cells was investigated. Again this is the first study that has assessed how supplementation with GDF6 affects a number of catabolic gens. As is well documented with increased age and degeneration the cells shift toward a more catabolic environment and demonstrate increased levels of MMPs and ADAMTSs (Roberts et al., 2000; Le Maitre et al., 2004a; Le Maitre et al., 2006a; Weiler et al., 2002; Pockert et al., 2009). Previous studies have shown that treatment of NP cells with TGFβ3, Dex and notochordal cell conditioned media (Abbott et al., 2012), could reduce expression of ADAMTS5 and MMP1, hence exhibiting an anti-catabolic profile. Whilst connective tissue growth factor (CTGF or CCN2), was shown to suppress MMP3 and ADAMTS5 when exposed to IL-β. In this study however following 14 days of culture there was no significant differences between any of the genes treated with or without GDF6. The limitation to this study is that these cells are degenerate and therefore the levels of catabolic genes are increased compared to normal cells.

6.5.2 Exposure to a Catabolic Environment

In chapter 4 results demonstrated that NP cells exposed to a catabolic environment decreases ECM and anti-catabolic genes and increases catabolic genes, in addition to a decreased production of sGAG. These results corroborate studies that have previously demonstrated that treatment with IL-1 is detrimental to the NP cells (Le Maitre et al., 2005). Hence the next objective to this study was to determine whether pre-treatment or sustained exposure to GDF6 would improve the ECM production and protect against the catabolic environment. When examining the ECM markers cells pre-treated or continually treated with GDF6 and exposed to IL-β resulted in

significantly greater gene expression than treatment of IL-1β alone. This suggests that NP cells supplemented with GDF6, and exposed to IL-1β can continue to produce a functional ECM, which is also demonstrated by the increase in sGAG and differential histological staining. A previous study has also demonstrated that NP cells cultured in NC cell secreted factors (Erwin et al., 2011), up-regulates anabolic activity and matrix production when exposed to IL-1β. Therefore is can be suggested that in a catabolic environment NP cells supplemented with GDF6 are anabolically active to greater levels than with no treatment with GDF6.

With regard to catabolic genes MMP3, MMP13 and ADAMTS4 there was a significant increase in expression when treated with IL-1β, as has previously been demonstrated (Le Maitre et al., 2005). Cells pre-treated with GDF6 and then exposed to IL-1β demonstrated a significant reduction in MMP3 gene expression, whilst cells that were pre-treated or continually supplemented with GDF6 showed a decrease in ADAMTS4 when in a catabolic environment. There was also reduction in MMP13 and ADAMTS5 but not to a significant extent. Hence suggesting that GDF6 is also protective against a catabolic environment demonstrated by the downregulation of genes compared to IL-1β treatment alone. As such, delivery of exogenous GDF6 could be a biological therapy for IVD regeneration due to the ability to still produce functional ECM in a catabolic environment, and also as it suppresses expression of catabolic genes.

6.5.3 Conclusions

This study has demonstrated that stimulation of NP cells with GDF6 restores a non-degenerate NP phenotype, as shown by the upregulation of ECM and novel NP marker genes and resulting in a PG-rich ECM. Additionally treatment with GDF6 and then exposure to a catabolic environment protects the cells against the effects of IL-1β, is still able to produce a PG-rich ECM and can suppress catabolic gene expression.

Chapter 7

Assessment of the efficacy of GDF6 as a biological therapy: Development of an ex vivo degenerate IVD model and preliminary assessment of a microparticle growth factor delivery system

7.1 Overview

The previous chapters of this thesis have focused on a number of *in vitro* studies assessing the effect of GDF6 on MSC discogenic differentiation and native cell biology as a prerequisite to the optimisation/development of a biological/cell based therapy for IVD regeneration. However, before any therapy can be translated to clinical practice, it must be tested in an appropriate model system to ensure its efficacy.

7.1.1 The use of Microparticles as a potential delivery system for growth factors

In chapter 5 it was shown that GDF6 has the ability to restore the normal phenotype of degenerate NP cells and that sustained treatment had a protective effect on the NP cells in an in vitro system. Exogenous delivery of GDF6 in the media, to restore the NP would not be feasible for an ex vivo model due to the large diffusion pathway, and as such an alternative direct method should be used. In addition, a method to ensure sustained release of GDF6 in the IVD combined with implanted AD-MSCs could lead to in situ differentiation which would eliminate the need to pre-differentiate cells prior to implantation. However at present the method of delivery would be a repetitive injection directly into the disc through the AF. As previously described in section 6.1.6 needle puncture into the disc can cause degeneration and therefore there is a need for an alternative system, which does not require repetitive injection. Control of delivery can be achieved by incorporating the growth factor into a biomaterial carrier system; this strategy may also prevent growth factor degradation as the biomaterial vehicle can provide protection from proteolytic enzymes at the target site. The Shakesheff group (Kirby et al., 2011; White et al., 2013) at the University of Nottingham have fabricated a poly (D,L-lactic -*co*-glycolic acid) (PLGA) / PLGA - poly(ethylene glycol) (PEG)- PLGA microparticle system that has demonstrated sustained release of a number of growth factors including BMP-2 (Kirby et al., 2011). Such a system would be ideal for a controllable and sustained delivery of GDF-6, the efficacy of which can be tested in an ex vivo IVD model system and could be used ultimately in translation to clinic.

7.2 Hypotheses

This study was designed to optimise a degenerate ex vivo IVD model for testing the efficacy of biological/stem cell based therapies In addition, collaborative studies with the University of Nottingham were undertaken to test the feasibility of using PLGA based microparticles containing GDF6 as a potential method for delivery of the growth factor.

For this work it was hypothesised that:

1) An experimentally induced degenerate disc would have different biomechanical properties than normal IVDs, the biomechanical properties of which could be restored through implantation of an exemplar hydrogel
2) GDF6 loaded PLGA microparticles would induce discogenic differentiation of AD-MSCs equivalent to as exogenous supplementation of GDF6.

7.3 Experimental Design

In this chapter the overall study was divided into a number of sections. The initial study focused on the development of a degenerate ex vivo model, followed by the assessment of the biomechanical properties. Finally preliminary experiments were undertaken to assess the potential of microparticles as a GF delivery system for IVD regeneration therapies.

7.4 Results

7.4.1 Development of ex vivo IVD Model

7.4.1.1 Enzymatic Induction of Disc Degeneration

The overall aim of enzymatic digestion is to reduce disc volume, induce instability in biomechanics and essentially create a void of tissue in order to mimic severe degenerative changes. In order to determine an appropriate protocol to induce degeneration in the NP, discs were injected with a range of enzyme concentrations based on previous work undertaken by Roberts and colleagues (Roberts et al., 2008).

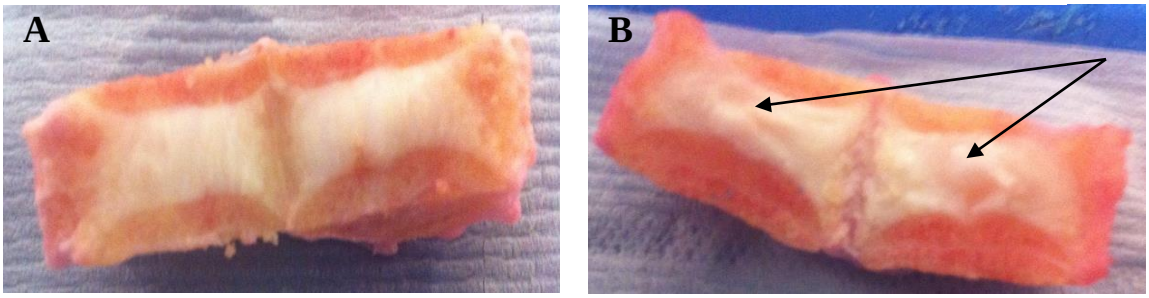

Figure 7.1 Images to demonstrate the macroscopic appearance of sagitally dissected bovine IVDs. Control disc (A) and a disc that had been injected with 35 mg/ml trypsin and incubated for 24 hours before the reaction was stopped with FCS (B).

The structural integrity of the control disc remained intact (Figure 7.1A); conversely the enzymatically digested disc contained a tissue void confined to the NP region as shown in Figure 7.1B. Macroscopic changes were visible at a trypsin concentration of 35 mg/ml only (Figure 7.1B; the discs digested with concentrations of 15 and 25 mg/ml trypsin concentrations showed no macroscopic /morphological changes compared to the control IVD.

7.4.1.2 Histological Assessment of Matrix Integrity

The discs were also assessed at a microscopic level and were stained with haematoxylin and eosin to determine the effects caused by the trypsin digestion (Figure 7.2). There was obvious loss of NP tissue with loss of cells together with the

formation of small fissures. The digested region was restricted solely to the NP region as staining on AF regions was normal.

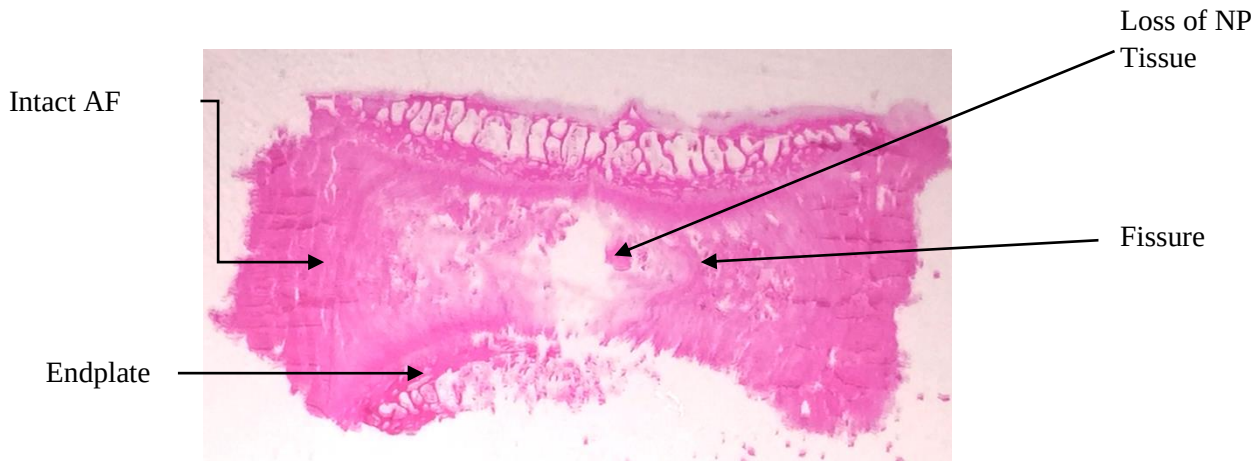

Figure 7.2 Haematoxylin and eosin staining of enzymatically digested bovine IVD. The disc was incubated with trypsin for 24 hours at 35 mg/ml prior to the reaction being stopped with an equal volume of FCS.

The results suggest that the use of trypsin at a concentration of 35 mg/ml was sufficient to induce adequate loss of matrix. Therefore to induce enzymatic degradation within an IVD in further experiments a concentration of 35 mg/ml trypsin was used.

7.4.2 Biomechanical Assessment

7.4.2.1 Optimisation of Compression Method

Initial compression experiments were undertaken to determine the optimum protocol to assess the biomechanical properties of a normal bovine IVD and to ascertain whether these changed following enzymatic degradation of tissue and if properties were restored following the injection of type I collagen hydrogel.

A recent publication from Chan and colleagues (Chan et al., 2011a), highlighted that for loading to be within a physiological zone this must be between a stress level of 0.2-0.8 MPa. These values were also adhered to in our own group's physiological loading system (Le Maitre et al., 2009). To establish the maximum load that could be

applied to the disc in order to achieve this physiological range, analysis of initial values were taken at 5kg intervals. Figure 7.3 shows that loads from 15–35 kg are within the 0.2-0.8 MPa range. Hence the optimal protocol was to expose the disc to a maximum load of 35 kg and the displacement value to reach this load was measured.

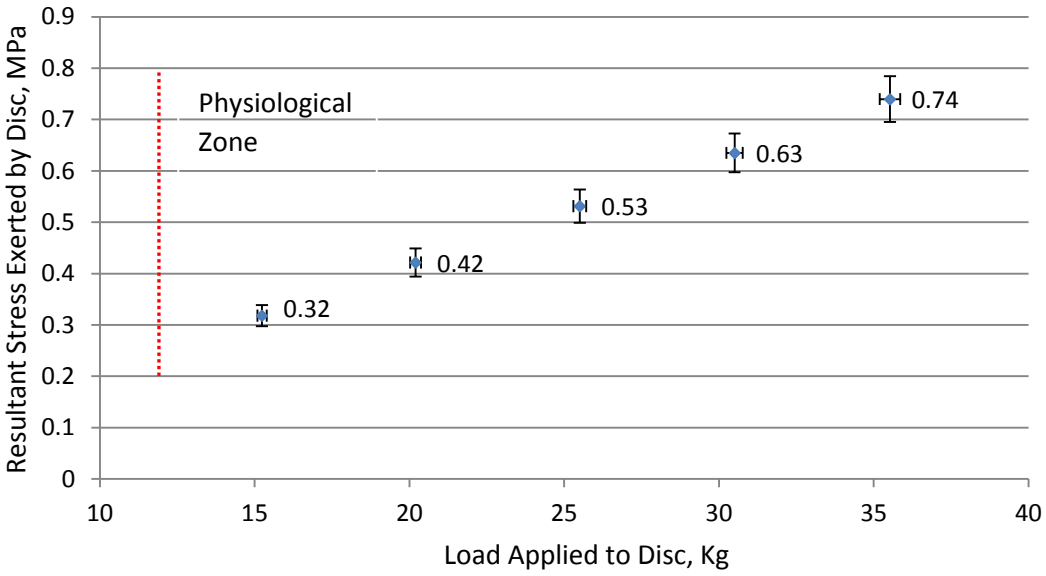

Figure 7.3 Resulting stress exerted by the disc at applied loads of 15, 20, 25, 30 and 35 kg. The discs were within the physiological range defined as 0.2-0.8 MPa, and the data demonstrated that values up to 35kg were within a physiological range. N=7 discs.

7.4.2.2 Biomechanical Characteristics of IVDs

Initially the biomechanical properties of control and enzymatically digested bovine IVDs were assessed by exposing the discs to a specific compression regime, which had been determined in preliminary experiments. The control discs were excised and incubated for 24 hours prior to application of load. Additionally an equal number of discs (n=10) were excised and injected with 35 mg/ml trypsin to induce degeneration before a 24 hour incubation period and compressive loading testing. When examining the combined results of both disc groups, there was a clear distinction between the two experimental conditions. The average displacement values for each experimental group were determined and statistically assed by a Mann-Whitney statistical analysis test (Figure 7.4). The results were found to be significantly different at all load points between experimental groups. The control discs had a

displacement range for all loads of 2.03 – 2.69 mm, whereas the induced degenerate discs had a displacement range from 2.98 -3.59mm. Therefore the experimentally induced degenerate discs had to be compressed an extra 0.9 mm in comparison to the control in order to exert the 35kg maximum load.

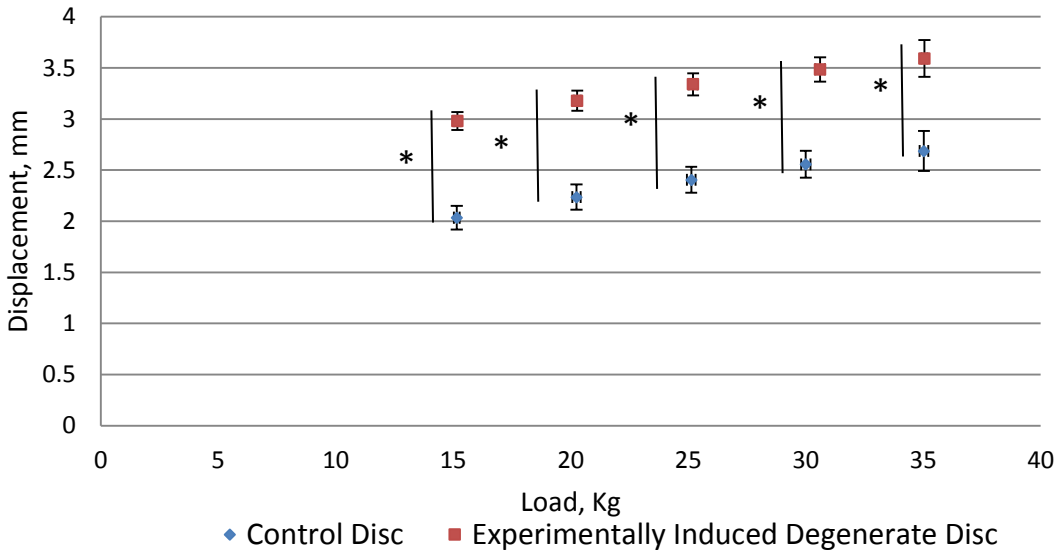

Figure 7.4 Average displacement values for control and experimentally induced degenerate discs. The graph shows average displacement values for all experimental discs at specific loads of 15,20,25,30 and 35 kg. At all loads the difference between experimental groups was significant (P, 0.05) as determined using Mann-Whitney statistical analysis.

To establish whether the discs had been exposed to loads within a physiological range the stress values were determined. The strain placed on the discs was also investigated to see whether this changed between the controls and experimentally induced degenerate discs.

The strain is the amount an object deforms when a force is applied; therefore this was calculated by the change in the thickness of the disc, in this case the displacement value divided by the original size of the disc. As all discs were of similar size the varying factor was the displacement value. Previous analysis had determined that the degenerate discs had a larger displacement value to exert the maximum load; hence the strain applied was also higher when compared to the control discs. Of the 20 discs, 19 remained within the physiological range of 0.2-0.8 MPa, with the majority of discs entering this range after a load of 15kg had been

reached. The average stress and strain values for each experimental group were determined at set loads of 15, 20, 25, 30 and 35kg and data assessed with the Mann-Whitney analysis test (Figure 7.5). The results were deemed to be significantly different at all load points between experimental groups.

The control discs had a stress range for all loads of 0.31–0.72 MPa while the induced degenerate discs had a stress range from 0.29 –0.67 MPa. This places the discs within a suitable physiological zone and also this aspect of the experiment is not significantly different between the discs. On the other hand the control discs had a strain range for all loads of 0.13–0.17, whereas in contrast the trypsinised degenerate discs had a strain range from 0.17-0.21. Therefore the trypsinised discs had been exerted to a significantly higher strain in comparison to the control as they had been compressed an extra 0.9mm in order to exert the 35kg maximum load.

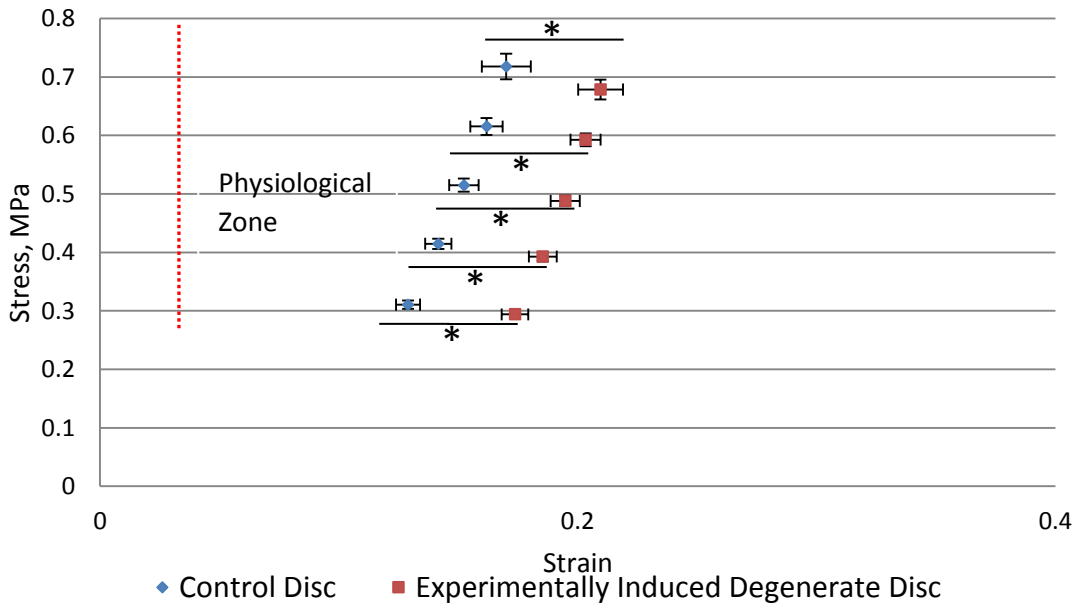

Figure 7.5 Average stress and strain values for control and experimentally induced degenerate discs. The graph shows average stress and strain values for all experimental discs at specific loads of 15,20,25,30 and 35 kg. At all loads the difference in strain between experimental groups is significant (P, 0.05) as determined using Mann-Whitney statistical analysis. All discs were within a physiological zone of 0.2-0.8MPa.

It was then postulated that injection of a biomaterial such as type I collagen hydrogel, which has been used throughout the previous chapters, would have the capacity to restore biomechanical properties. Hence initial experiments were undertaken to ensure that the hydrogel could be injected into the disc. Following digestion of the disc with 35 mg/ml trypsin, 200 µl of type I collagen hydrogel was injected into the disc. The disc was sagitally dissected in order to investigate whether the hydrogel had remained within the disc and to ascertain the distribution within the NP region. The black arrows displayed in Figure 7.6 specifically highlight traces of the hydrogel distributed throughout the NP. As the hydrogel appears in both halves of the disc this would suggest that the hydrogel spreads throughout the degraded NP tissue. The hydrogel also appeared in a hydrogel form rather than the liquid that was initially injected, which proves that the hydrogel is able to form in situ and can easily distribute to degraded areas.

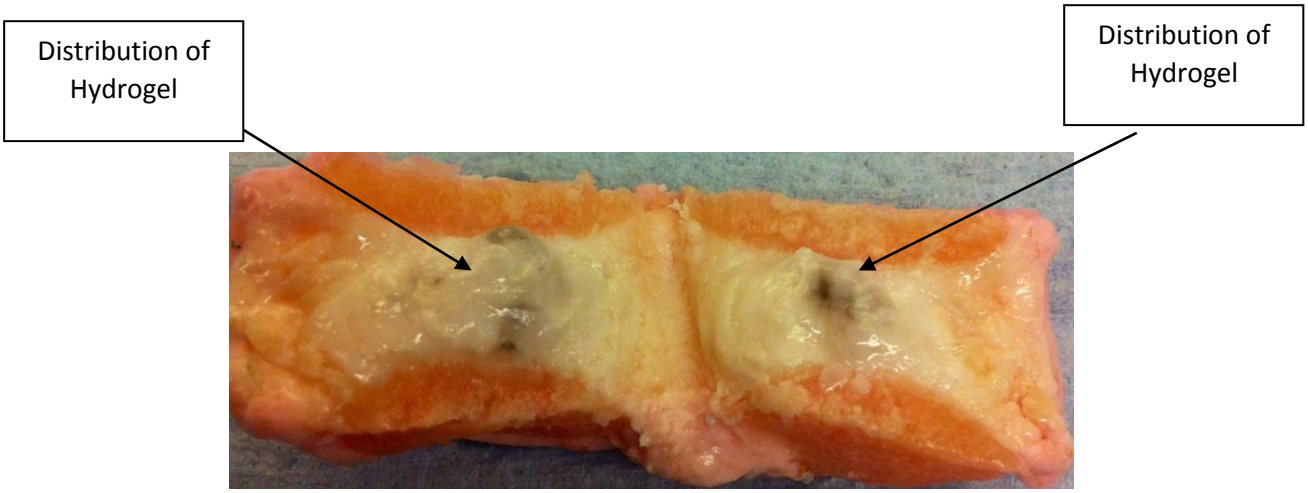

Figure 7.6 Injection of type I collagen into an experimentally induced degenerate IVD.A sagitally dissected IVD that had been enzymatically digested for 24 hours with 35 mg/ml trypsin. This was followed by the injection of type I collagen hydrogel stained with Indian ink and allowed to gel for 2 hours. The photograph illustrates where the hydrogel has been distributed.

Therefore, the next step was to investigate the biomechanical characteristics of discs that had been injected with type I collagen hydrogel. Whilst there was a significant difference between the experimentally induced degenerate and control IVDs there was no significant difference between the injected collagen group and the other

experimental groups. However the addition of the hydrogel did restore the biomechanical properties to some extent (Figure 7.7). The displacement range of the injected IVDs was 2.40-3.12mm.

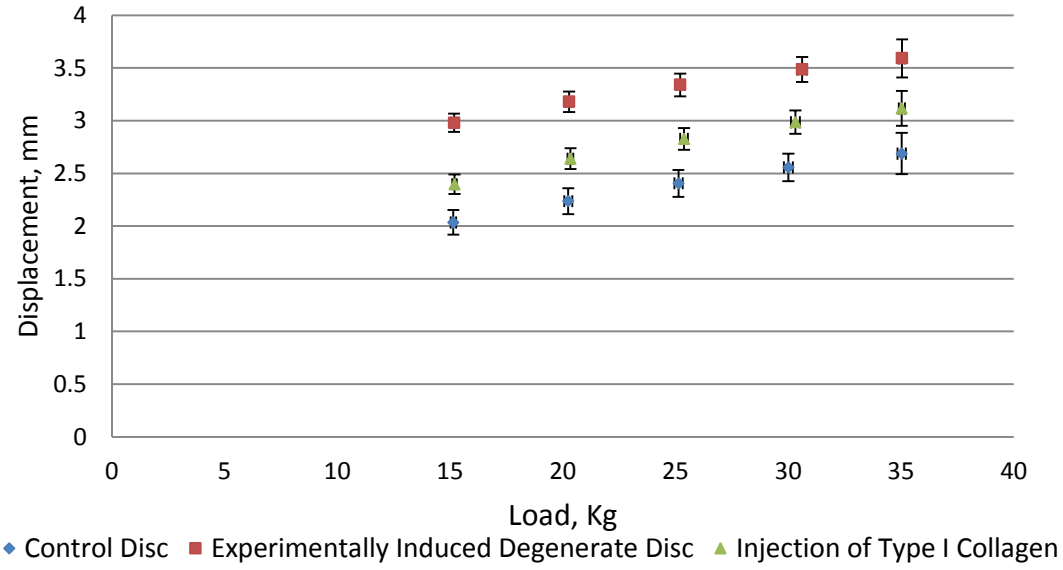

Figure 7.7 Average displacement values for three experimental groups. 10 bovine IVDs per experimental group were treated accordingly, then compressed at specific loads, 15, 20, 25, 30, 35 kg. N=10 per group, data represent mean +/- SE. *P<0.05.

The discs were also analysed to establish if the discs varied in the stress and strain values. In comparison to the control discs there was no significant differences seen in the stress or strain values. However in comparison to the degenerate samples there was a significant difference in strain values at 15, 20, 25 and 30kg, with the injected discs ranging from 0.13-0.17, which are identical to the control discs (Figure 7.8).

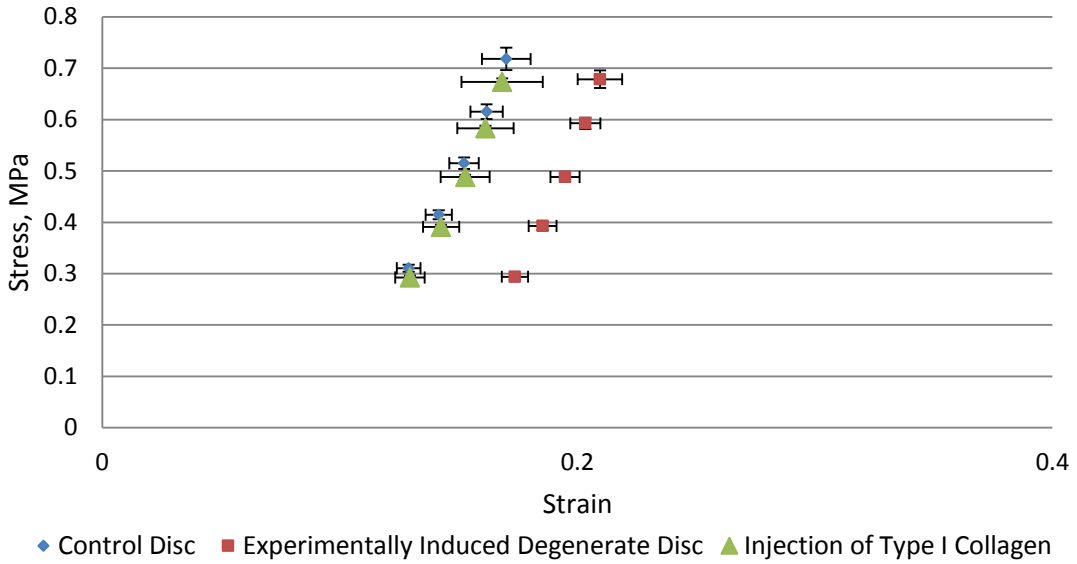

Figure 7.8 Average stress and strain values for all three groups The graph shows average stress and strain values for all discs at specific loads of 15,20,25,30 and 35 kg. At all loads the difference in strain between experimental groups is significant ($P < 0.05$) as determined using Mann-Whitney statistical analysis. All discs were within a physiological zone of 0.2-0.8 MPa.

The final analysis that was undertaken was to assess the Young's Modulus of the discs. This is a measurement of the stiffness of an elastic material and is determined using the linear portion of the stress – strain curve. The control discs had a Young's Modulus of 40.16 MPa, whereas the degenerate discs had a significantly lower modulus of 32.02 MPa. This proves that the non-degenerate control discs had a greater stiffness which means they are less likely to change shape when exposed to load. In contrast the enzymatically digested discs were more flexible due to the digestion of the NP tissue and more likely to change shape when load is applied as there is less resistance to counteract against the load. The discs which were injected which type I collagen hydrogel showed a Young's Modulus of 37.10 MPa, which is significantly different from the degenerate disc, but not the control disc. This suggests that the injection of type I collagen hydrogel can restore the stiffness of the disc to near normal levels (Figure 7.9).

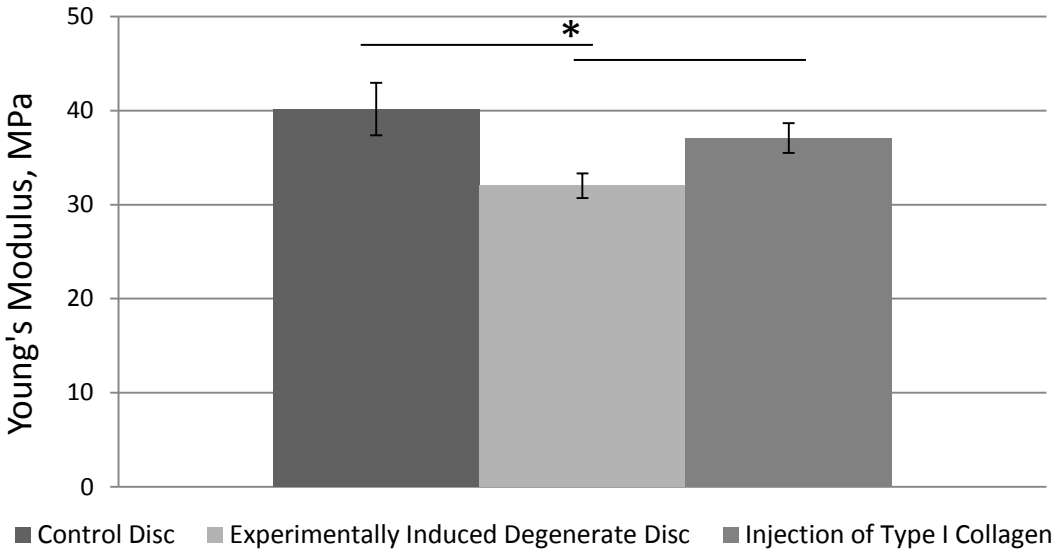

Figure 7.9 Average Young's Modulus values for experimental groups. 10 bovine IVDs per experimental group were treated as described. Then compressed at specific loads, 15, 20, 25, 30, 35 kg (equivalent to 0.2-0.8MPa). The Young's Modulus was then calculated. N=10 per group, data represent mean +/- SE. *P<0.05.

7.4.3 GDF6 Microparticles for Delivery to IVD

7.4.3.1 Smaller Microparticles Allow Formation of Hydrogel

To determine the appropriate size microparticle that would not disrupt the established cell seeded hydrogel, investigations were initially undertaken to examine the encapsulation of small (20-50 μm) or large (50-100 μm) microparticles. Following 7 days in culture, histological analysis demonstrated that compared to the control sample small microparticles disrupted the hydrogel to a lesser extent than large microparticles. This was shown across a range of microparticle loading weights (Figure 7.10 and Figure 7.11).

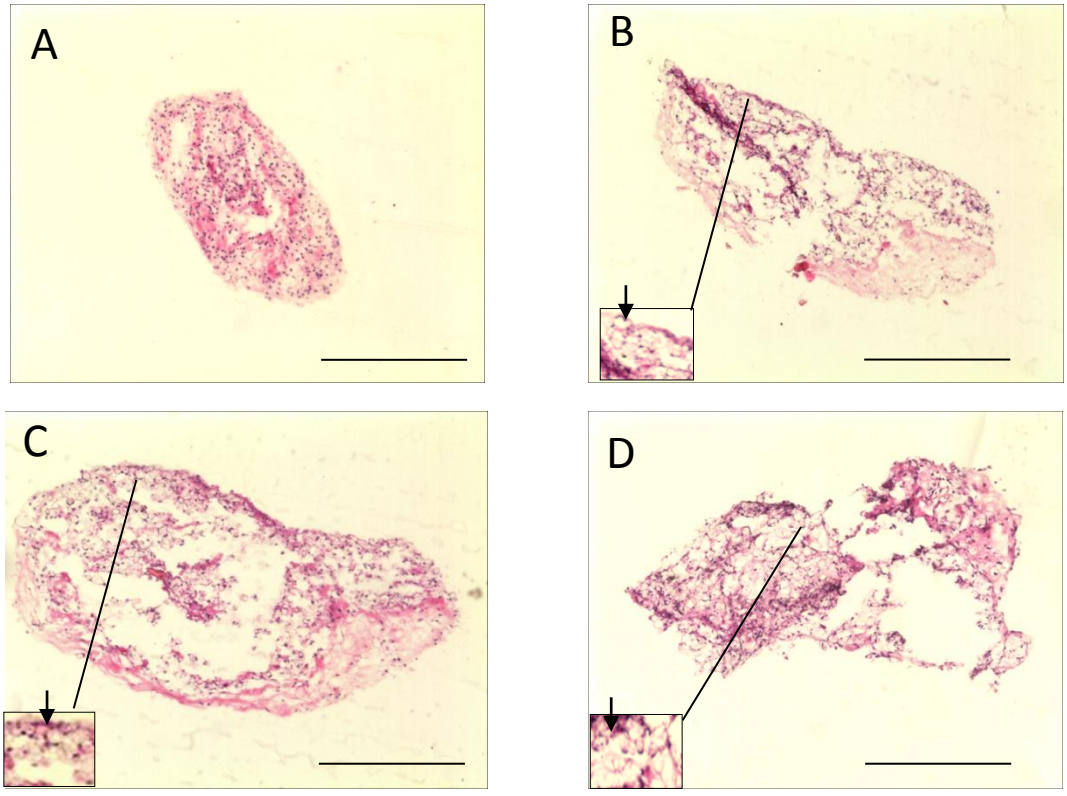

Figure 7.10 H and E stains of 20-50μm small microparticles loaded at different weights. A. Control, B. 1 mg, C. 2 mg D. 4mg encapsulated in AD-MSC seeded type I collagen hydrogels and cultured for 7 days and H and E stained to look at gross morphology. Scale bar 500 μm.

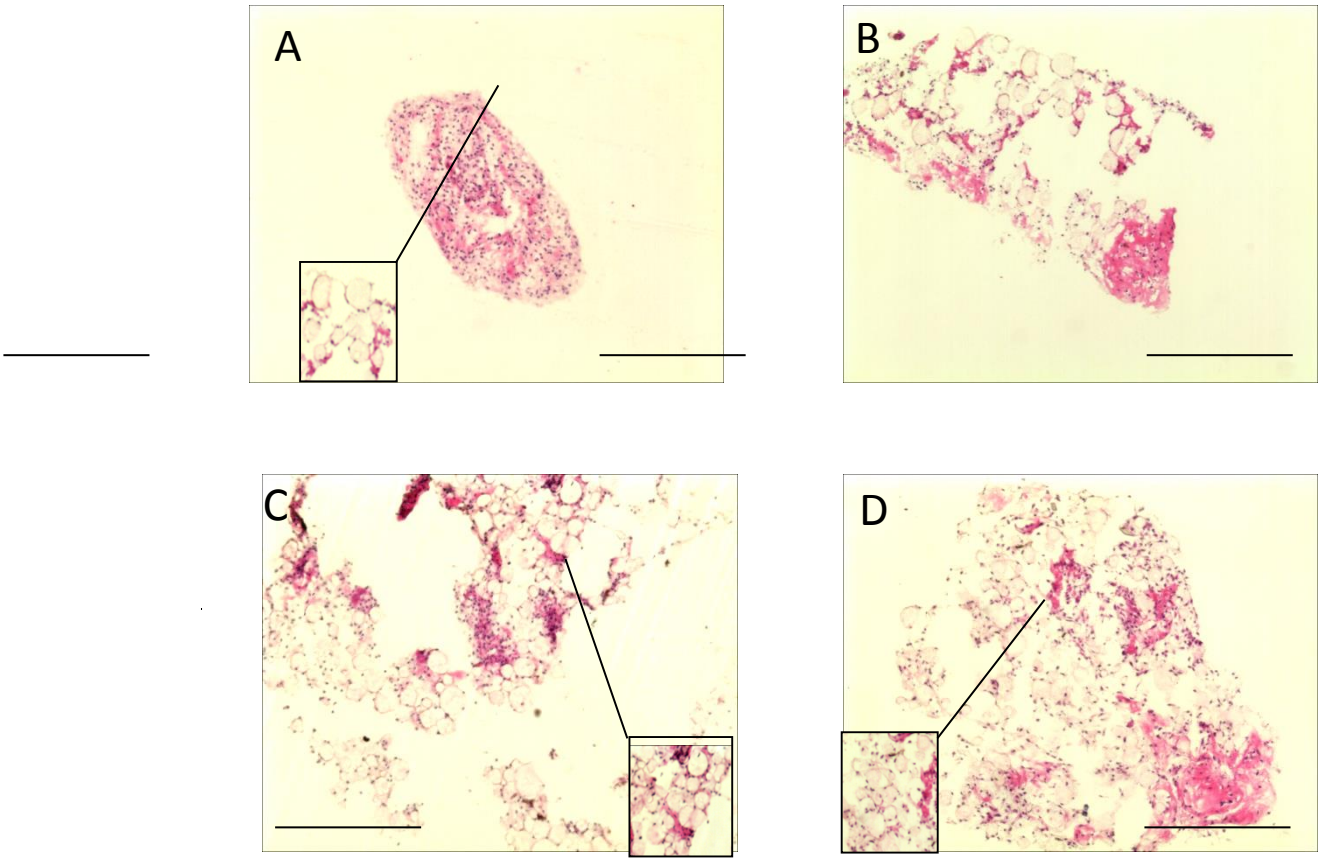

Figure 7.11 H and E stains of 50-100 μm large microparticles loaded at different weights. A. Control, B. 1 mg, C. 2 mg D. 4 mg encapsulated in AD-MSC seeded type I collagen hydrogels and cultured for 7 days and H and E stained to look at gross morphology. Scale bar 500μm.

The larger microparticles are clearly visible as demonstrated by Figure 7.11. The larger microparticles, as shown particularly in Figure 6.15C, disrupted the hydrogel extent large extent that gel integrity was not maintained and therefore not suitable for future experiments. As such the smaller (20-50 μm) microparticles were chosen for the remaining studies.

7.4.3.2 Protein Release Kinetics

After the fabrication of HSA and GDF6 small microparticles, protein release kinetics were assessed over a 14 day period. The results showed that there was an initial burst release of HSA, then a steady release of the protein over a 14 day period (Figure 7.12). In 1mg of microparticles there was cumulative release of 4.75 µg HSA.

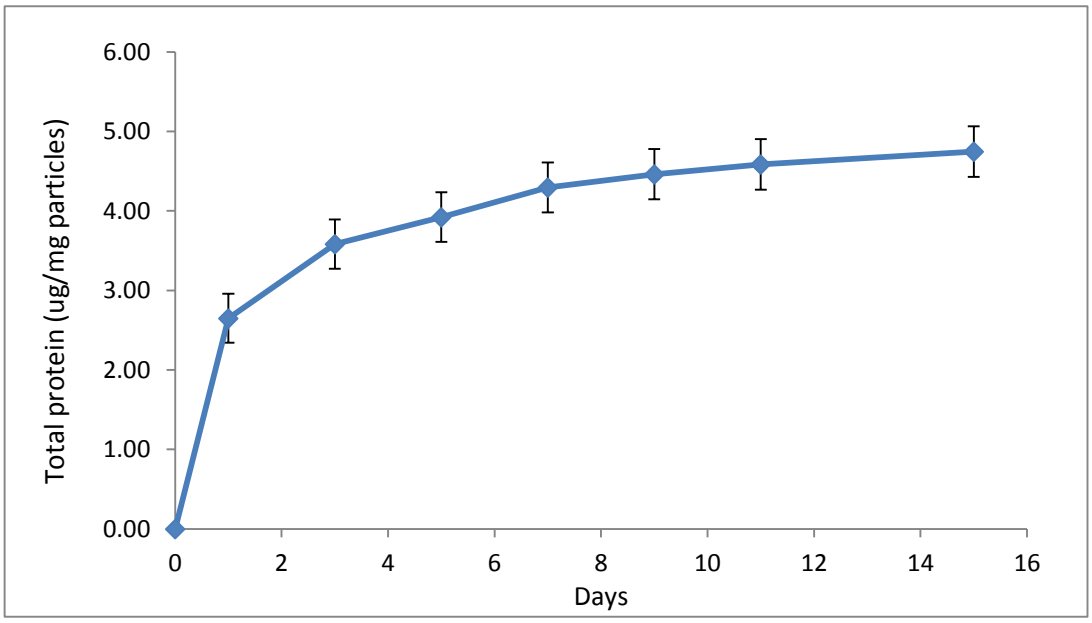

Figure 7.12 Release kinetics of HSA protein from HSA: GDF6 loaded microparticles over a 14 day time period. Microparticles (25 mg) were suspended in 1 ml of PBS and shaken; supernatant was collected every 2 days and replaced with fresh PBS. A BCA assay protein quantification kit was run to quantify HSA release. N=3, 25 mg of MPs in PBS.

7.4.3.3 Assessment of GDF6 Release

From the analysis of the HSA protein release it was estimated that over a 14 day period 0.567 µg of GDF6 would be released. Therefore assessment of GDF6 release was undertaken using a GDF6 ELISA kit The results obtained demonstrate that over a 14 day period there was a cumulative release of 0.620 µg GDF6 protein (Figure 7.13). Therefore in order to replicate the concentrations added exogenously 700 ng over 14 days in previous experiments a total of 1.13 mg should be added per hydrogel in order to achieve this.

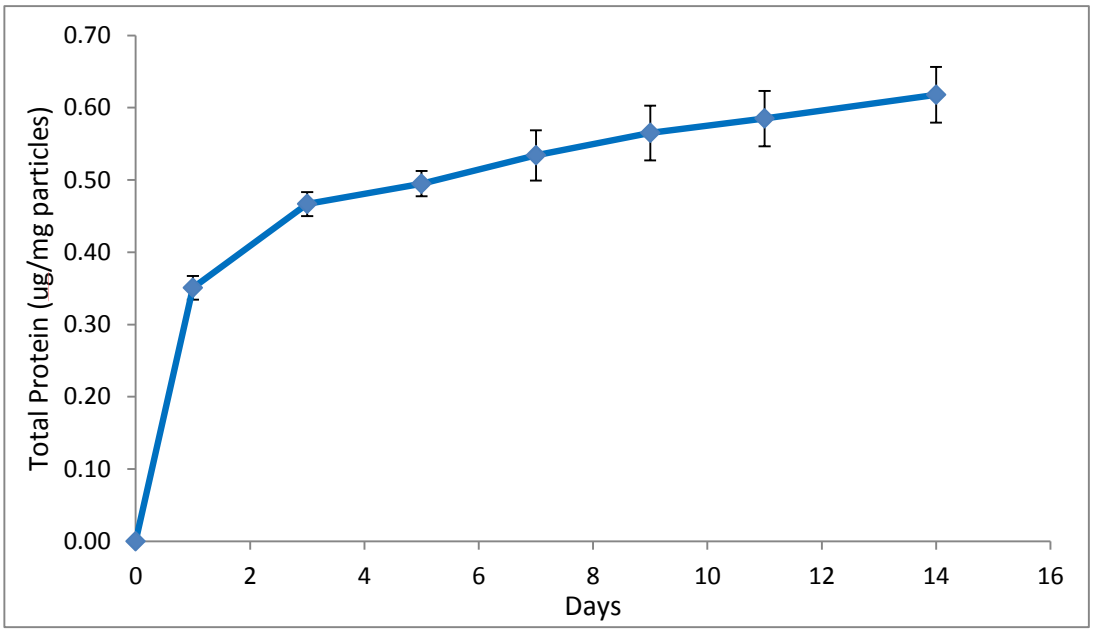

Figure 7.13 GDF6 ELISA of HSA: GDF6 loaded microparticles over a 14 day time period. Microparticles (25mg) were suspended in 1 ml of PBS and shaken; supernatant was collected every 2 days and replaced with fresh PBS. A GDF6 ELISA plate was run to quantify GDF6 release. N=3, 25 mg of MPs in PBS.

7.4.3.4 Discogenic Differentiation of AD-MSCs using Microparticles

Investigations were undertaken to assess whether the GDF6 loaded microparticles could induce equivalent discogenic differentiation as exogenous treatment over a specified culture period. The three experimental groups, control (no microparticles), HSA only microparticles, which were cultured in the presence of exogenous GDF6 and the GDF6 loaded microparticles, were encapsulated into AD-MSC seeded type I collagen hydrogels and discogenic differentiation assessed as described in section 7.3.5.5.

7.4.3.4.1ECM and Novel NP genes

Both ECM and novel NP markers were assessed using qPCR, there were no significant differences in levels of gene expression for any of the marker genes observed between any of the groups (Figure 7.14).

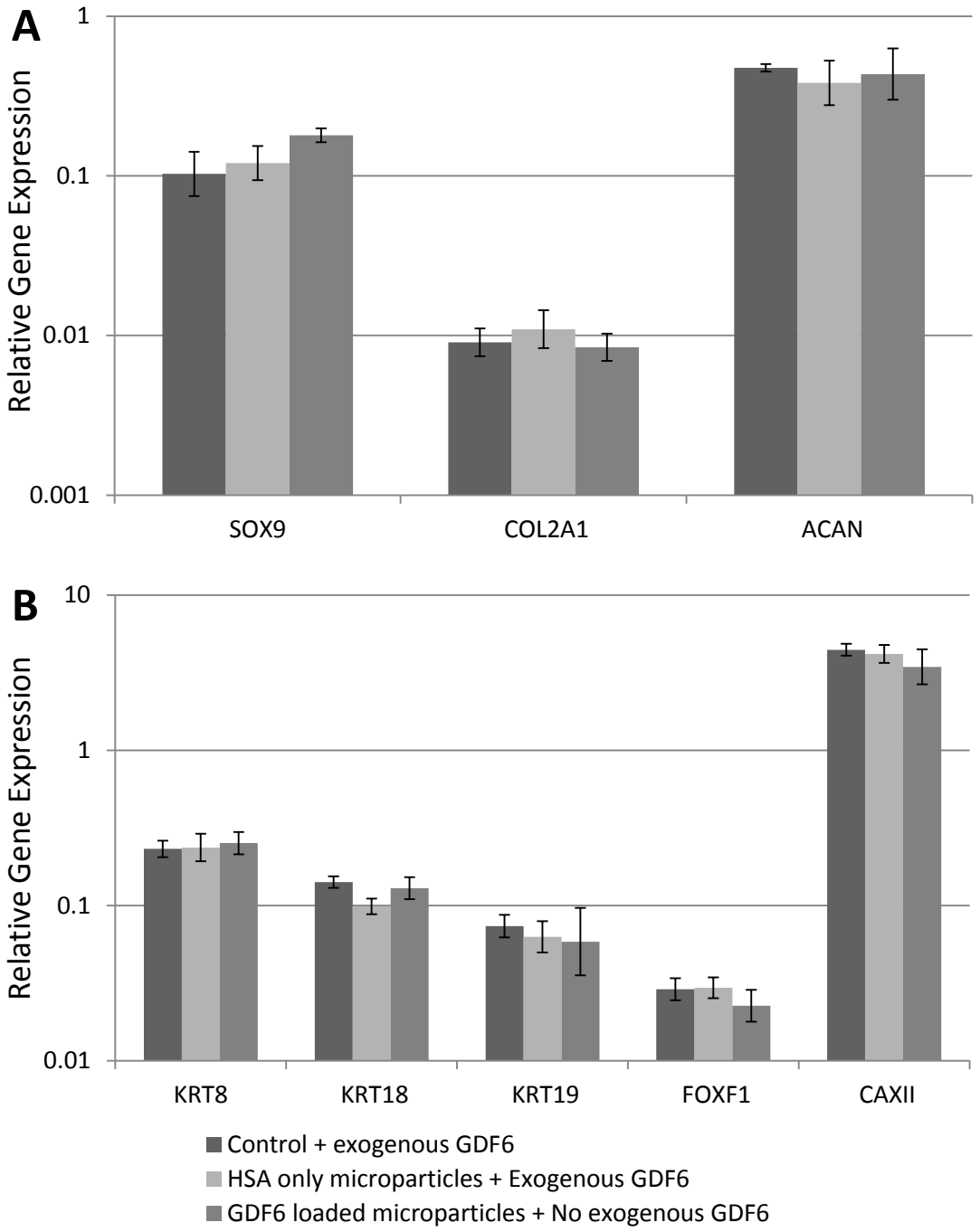

Figure 7.14 ECM and novel NP marker gene expression of control, HSA only and GDF6 loaded microparticles. AD-MSC seeded hydrogels were loaded with either no microparticles, HSA only or GDF6 loaded microparticles and cultured in respective media for 14 days. Q-PCR was undertaken to assess the **A**. ECM and **B.** novel NP gene profiles. +/- SE, N=2 patient samples, $p < 0.05$.

7.4.3.4.2 Assessment of GAG in Constructs

The quantification of sGAG was further divided into construct and media components and the combined total. AD-MSC seeded hydrogels loaded with the respective treatment demonstrated no significant differences in the sGAG/DNA content within the constructs (Figure 7.15A) across all treatment groups Control (255.3 μg/μg DNA ±21.0), HSA only microparticles (236.7 μg/μg DNA ±27.3) or GDF6 loaded microparticles (250.7 μg/μg DNA ±13.8).

Over the 14 day culture period media was collected every 48 hours and analysed for cumulative release of sGAG into the media (Figure 7.15B). As with the sGAG content within the construct there were no significant differences between all treatment groups control (111 μg ±12.3), HSA only (97.6 μg ±11.2) or GDF6 loaded microparticles (116.8 μg ±6.9).

The combination of sGAG/DNA for both construct and media (Figure 7.15C) demonstrated no significant differences across all treatment groups, control (3292.7 μg/μg DNA ±218.9), HSA only (3053.37 μg/μg DNA ±226.9) or GDF6 loaded microparticles (320 7 μg/μg DNA ±305.5).

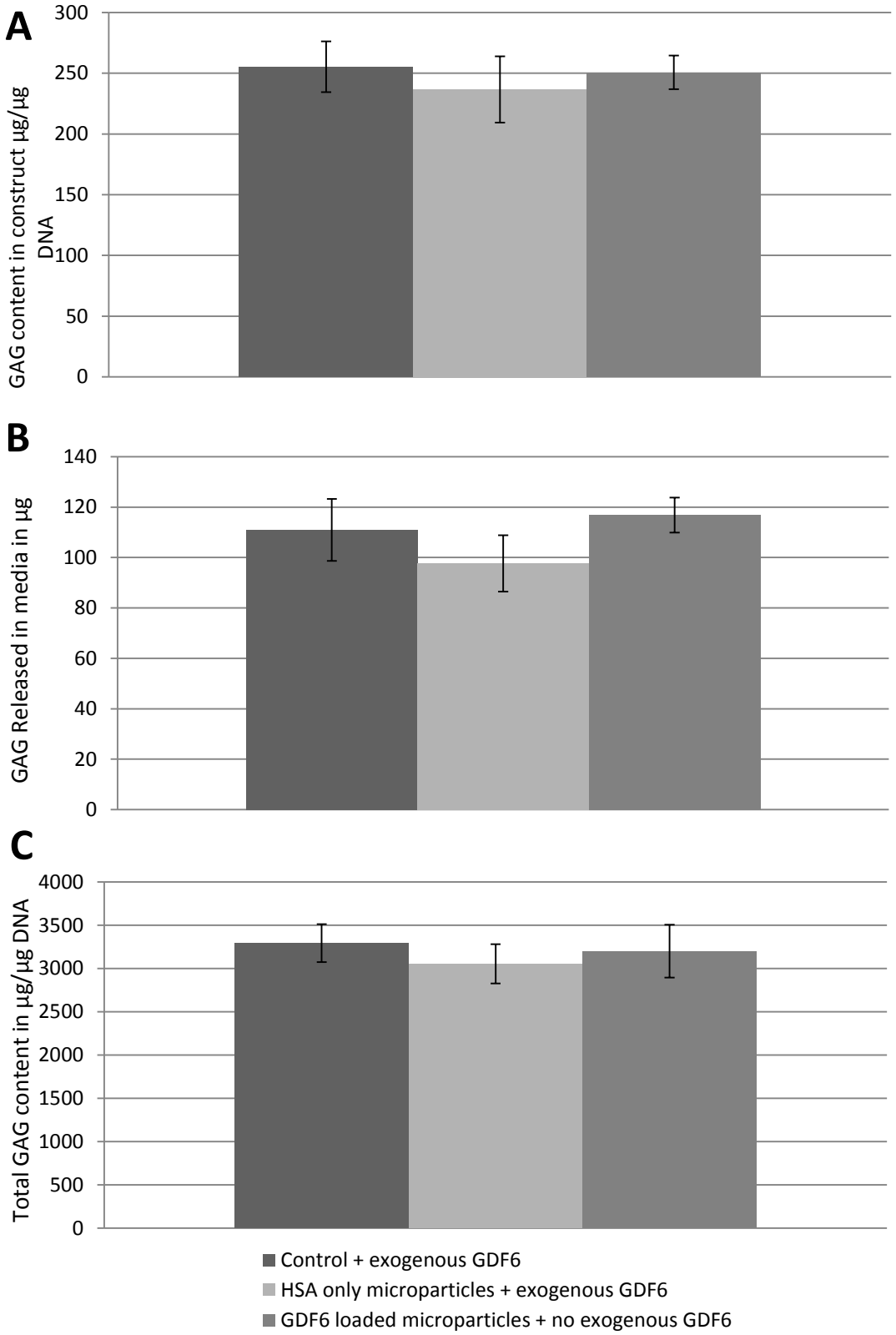

Figure 7.15 Quantification of sGAG in microparticle loaded constructs. (A) Quantification of sGAG retained within hydrogel constructs, normalisedto DNA content within the construct. **(B)** DMMB quantification of sGAG released cumulatively into the media throughout the culture period. **(C)** Quantification of total sGAG content in the construct and media normalisedto DNA content within the construct at day 14. $N = 2$, data represent mean ± SEM. $^{*}P < 0.05$.

7.4.3.4.3 Localisation of sGAG within constructs

All samples demonstrate homogenous distribution of sGAG staining throughout the construct (Figure 7.16). However, images B and C representing HSA only and GDF6 loaded microparticles respectively, are larger in size due to the incorporation of microparticles.

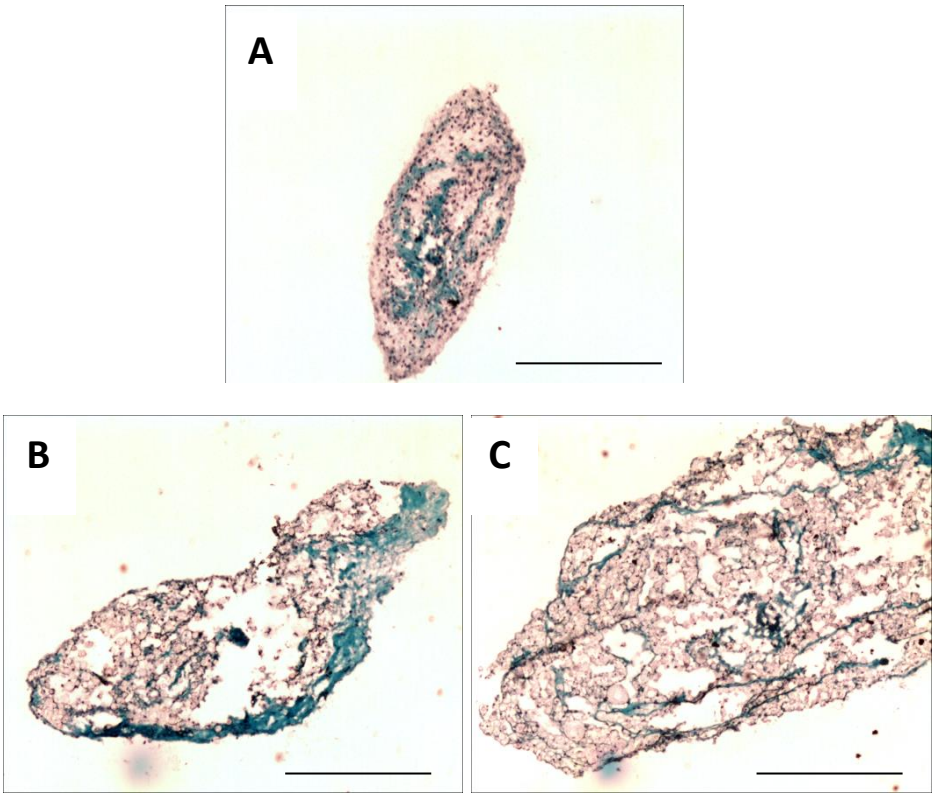

Figure 7.16 Safranin O staining of ADMSC-seeded collagen hydrogels and respective microparticle treatment. A. Control, B. HSA only C. GDF6 loaded. All samples demonstrate deposition of red sGAG throughout the constructs. Scale bar 500μm.

7.5 Discussion

In order for novel therapies targeting intervertebral disc regeneration to advance, they must be sufficiently and effectively examined in animal/preclinical models prior to any clinical translation. One particular model that permits an insight into a biologically native environment is an *ex vivo* animal model, which also allows superior control of systemic variables in comparison to an in vivo model. The overall objective of this study was to develop methods to test the efficacy of GDF6 as a potential therapeutic factor in disc regeneration strategies. As such the study was divided into a number of parts. Firstly was to validate an ex vivo model using enzymatic digestion in normal bovine IVDs. This was followed by the assessment of biomechanical properties of a normal, experimentally induced degenerate and discs that had been injected with a biomaterial. In addition, in collaboration with the University of Nottingham preliminary studies were undertaken to assess a protein loaded microparticle delivery system.

7.5.1 Ex vivo Model and Induction of Degeneration

When designing a degenerative model there are a number of crucial aspects that must be considered. One factor is the particular animal species that experimental discs are isolated from and the validity behind this choice. Bovine discs were utilised in this study because they are inexpensive, easily available from local abattoirs' and are a similar size to human lumbar discs. As a larger skeletally mature animal they also encompass several advantages over smaller animal models, such as the absence of notochordal cells. Similarly previous studies have determined that bovine discs are a similar size and have a similar matrix composition comparative to a human, providing a dependable model (Oshima et al., 1993).

Another consideration is to establish a distinguishable stage of degeneration that the model is intended to represent. For example a severely degenerative disc will be environmentally different from a disc in the early stages of degeneration which would possess more subtle changes. Therefore throughout this study we adopted a proof of principle concept and aimed to induce loss of tissue and matrix to mimic severe degeneration. Such a system could then be used to test the efficacy of a hydrogel in restoring disc structure and function; as such enzymatic digestion of the NP tissue was utilised to achieve this. The process of enzymatic degradation is a

procedure to selectively degrade ECM in order to reduce disc volume, induce instability in biomechanics and essentially create a void in the tissue in order to mimic severe degenerative changes. Whilst this method does not mimic the slow progressive nature of intervertebral disc degeneration, it accelerates degradative changes to present an adequate *ex vivo* model in which reparative treatments can be tested. Due to the high osmotic pressure within the normal intact disc injection of fluid/hydrogel is difficult. Thus another advantage of trypsinisation is that creating a void within the disc creates a space into which a hydrogel can be injected. There have been various enzymes utilised in a number of previous studies to induce degeneration including: chondroitinase ABC (Norcross et al., 2002; Imai et al., 2007b), collagenase (Barbir et al., 2009), elastinase (Barbir et al., 2009), papain (Roberts et al., 2008) and trypsin (Roberts et al., 2008; Jim et al., 2011). The enzyme that was selected for this study was trypsin as work undertaken by Roberts and colleagues (Roberts et al., 2008) using this enzyme had shown there was severe disruption to the NP. Trypsin has accurate cleavage specificity and degrades the majority of ECM proteins besides collagen fibrils. Another advantage of this enzyme is that the reaction can be inactivated using FCS so that effectively degradation can be controlled so that it does not spread into the AF tissue. After testing a range of enzyme concentrations 35 mg/ml was shown to be the most appropriate concentration as this resulted in loss of ECM , creating a void and fissure formation. With regard to other studies Roberts et al., utilised a concentration of 20mg/ml, whereas Mwale et al., (Mwale et al., 2014) use concentrations as low as 50μg/ml and 1.3mg/ml. However findings in both this study and Roberts et al (Roberts et al., 2008) demonstrated in sufficient ECM changes to cause a large tissue void at these low concentration levels.

It must also be considered that needle puncture has also been shown to cause degenerative changes in discs as several studies have demonstrated that. One particular study undertaken by Zhang and colleagues (Zhang et al., 2009a) using an in vivo rat model, demonstrated that injury with 18G and 21G over a 12 week period induced degenerative changes as shown by both histological and MR imaging analysis. However a study carried out by Korecki and colleagues (Korecki et al., 2008) using ex vivo bovine discs that had been punctured with a 25G and 14G needle over a 6 day culture period showed no change in proteoglycan, disc height or cell viability. The stab model in our particular study was for a time period of only 24 hours, which as demonstrated by Korecki and colleagues is unlikely to cause

morphological changes in the disc. However if the experiment was extended for a longer term the effect of the injection must be considered.

7.5.2 Biomechanical Assessment

Having established a model system the biomechanical properties of normal and experimentally induced degenerate discs were initially investigated. As there was no current protocol in place for this analysis, there were a number of parameters (including the speed of piston compressing the disc, distance the disc is displaced by and the size of disc) that needed to be assessed to ensure a reproducible method to investigate IVD biomechanics. Following a recent publication by Chan and Gantenbein-Ritter (Chan and Gantenbein-Ritter., 2012) which highlighted differences in size of discs from different regions, discs from a restricted region (discs 3-6) of the tail were used to ensure that discs were similar in size and structure. Initial biomechanical experiments were undertaken and a number of variables became apparent from these preliminary results. Firstly repetitive measures to the same disc were deemed to be detrimental to the disc. Hence it was decided that a larger number of discs n=10, would be used for each experimental group to combat variability and compressive measurements only taken once on each disc. Secondly the application of the load (initially 100kg) to the discs was too high and not in an appropriate physiological range as this equated to 1-2MPa of stress, thus damaging the disc. The initial method to compress the discs was to apply uni-axial compression to the disc for a set distance rather than to enforce a maximum load; hence the majority of discs were experiencing greater forces than acceptable. A recent publication by Chan and colleagues (Chan et al., 2011a) states the physiological stresses experienced by a human range and that have been demonstrated in culture models is between 0.3-0.8MPa. Further experiments taking initial measurements at every 5kg highlighted that to maintain an acceptable physiological zone the maximum load that could be applied was 35kg (0.35kN). The establishment of a feasible protocol determined that discs of a similar size and shape were to be used, the piston moved at 0.02mm/second and that the maximum load applied to the discs was 35kg to maintain a physiological environment.

The results showed that induction of degeneration altered biomechanical properties compared to normal discs. This suggests that because the control discs boast an intact NP, the disc cannot be compressed readily as the tissue provides resistance and hence this resistance allows the disc to reach the required loading value sooner.

Conversely discs that have been enzymatically digested do not have an intact NP tissue to resist the compressive force and will be compressed more readily. Therefore the lack of NP resistance means that the disc must be compressed a greater distance to attain the maximum load limit.

It was then demonstrated that injection of type I collagen hydrogel can restore the biomechanics of the IVD, as the discs showed no significantly difference than normal biomechanics. Other studies have demonstrated injection of different types of biomaterials including PVP/PVA hydrogels (Joshi et al., 2005a; Joshi et al 2005b) and pH responsive microgels (Saunders et al., 2007) could restore the biomechanical properties comparable to normal/untreated discs.

The establishment of a novel compression protocol allows the analysis of uni-axial compression which is one aspect of disc biomechanics. As a bipedal species the disc is constantly under compressive loads, although the amount of load varies during normal movement. This protocol applies a physiological range of loads under dynamic compression which is beneficial to the disc, rather than the application of a static load. Through the gradual application of load at a defined rate, this method allows the application of a high physiological load (35kg) without damaging the disc, as would happen with the rapid application of an equivalent load. The novelty of this methodology allows the disc to be analysed at any particular point between a low (0.2MPa) and high (0.8MPa) physiological range. This equates to different activities *in vivo* such as walking 0.53-0.65 MPa, sitting or standing 0.49-0.51 MPa or jogging 0.35-0.95 MPa (Wilke et al., 1999; Le Maitre et al., 2009b).

In conclusion, a severely degenerate *ex vivo* IVD model was established using enzymatic degradation of the NP tissue via trypsin. Biomechanical tests were applied to a range of IVDs, including normal, induced degenerate and injected with a biomaterial to assess the difference in characteristics. The degenerate discs differed significantly to properties displayed by normal discs. The creation of the model also presents itself as a platform to test other reparative therapies to assess their potential as a regenerative alternative and essentially allows novel methods to be thoroughly investigated prior to clinical trials/translation.

7.5.3 GDF6 Loaded Microparticles as a Delivery System to the IVD

As described the ex vivo model presents itself as a platform to investigate the injection of reparative therapies. Throughout this thesis work has focused on the use

of AD-MSCs, stimlauted with GDF6 and cultured in type 1 collagen hydrogel as a potential strategy. However for this to be tested in an ex vivo model the exogenous application of GDF6 is not feasible as it would have to be added to the media in large amounts which is costly and additionally the delivery is not controlled as it relies upon diffusion through the disc which. Hence microparticles offer a potential benefit for the controlled delivery of GDF6 to the disc. The microparticles used in this study were fabricated at the University of Nottingham and comprised of PLGA–PLGA/PEG/PLGA. PLGA is a biocompatible and biodegradable polymer (Anderson et al., 1997; Jain 2000) and is widely used in the field of biomaterials. Similarly, the double emulsion method used to encapsulate GDF6 protein can be described as a robust technique (Meng et al., 2003; Nihant et al., 1995; Schugens et al., 1994) and the formulation of 9:1 PLGA and PLGA-PEG-PLGA enables the sustained delivery of the protein (Giteau et al.,2008). This was effectively demonstrated by the sustained release of GDF6 over a 14 day period. Previous work has examined the continual application of GDF6 every 48 hours, which is not feasible in an ex vivo system or in a clinical setting. A therapeutic delivery system of GDF6 with the ability to sustain active doses of GDF6 is therefore a more effective method. The results show that sustained release over 14 days is sufficient to stimulate discogenic differentiation and is equivalent of exogenous GDF6.However in this preliminary study it is noted that 57.9% of the total protein released over 14 days is released within the first day, which could be described as a burst release. This may need to be examined after only 3 days of culture to determine whether the burst release of GDF6 shows significant differences to the standard application of GDF6. The majority of studies that have utilised these PLGA microparticles have investigated incorporation of the osteogenic growth factor BMP2.In a similar manner to this study Kirby et al., (Kirby et al., 2011) demonstrated that culture of MC3T3-E1 cells with BMP2 loaded microparticles over a 14 day period differentiated the cells to an osteogenic lineage. This shows that the microparticles have the ability to sustain delivery of different growth factors in different systems and induce differentiation of cells. In addition to this Rahman et al. (Rahman et al., 2012) observed an increase of 55% new bone volume in a mouse calvarial defect model, when BMP2 loaded microparticles were injected into the site. This data suggests that the delivery of the growth factor alone in a controlled system enhanced the formation of bone

production. With regard to the regeneration of the NP this would be something to consider in future work.

6.5.4 Conclusions

An ex vivo model of severe IVD degeneration was established which will provide a platform for the testing of reparative treatments. Importantly, it was shown that injection of a hydrogel could restore the biomechanical properties of the "experimentally induced "degenerate disc. Additionally, the feasibility of using GDF6 loaded microparticles was assessed and data shows that delivery of GF by MPS induced discogenic differentiation of AD-MSC seeded hydrogels equivalent to exogenous application. The preliminary data for the ex vivo model and delivery system is promising and hence needs to be developed in order to test the efficacy of future therapies.

Chapter 8

Conclusions and Future Work

8.1 General Discussion and Conclusions

IVD degeneration is a major cause of LBP (Cheung et al., 2009) and is a socioeconomic burden to western society (Maniadakis and Gray, 2000). The current treatments offered are conservative and do not target the underlying cause of disc degeneration. The pathology of disc degeneration is considered to be a cell driven process resulting in a number of characteristic alterations at both a morphological and molecular level. As current treatments have poor long-term efficacy there is an urgent need for a feasible alternative therapy that addresses the underlying cause of degeneration. In recent years numerous studies have aimed to identify an appropriate cell based therapy to repair and restore the IVD. There have been a number of cell types proposed as a potential choice for cell therapy including NP cells (Nishimura and Mochida, 1998; Nomura et al., 2001; Okuma et al., 2000; Watanabe et al., 2003), IVD progenitor cells (Henriksson et al., 2009; Risbud et al., 2007; Sakai et al., 2012) and Mesenchymal stem cells (Risbud et al., 2004; Richardson et al., 2006; Minogue et al., 2010b). If MSCs are to be used the most appropriate cell source, a growth factor to induce differentiation must be identified, together with an understanding on the effect of the IVD niche on such cells. Therefore, the studies in this thesis have focused on a number of *in vitro* experiments to test the efficacy of GDF6 as a potential biological therapy for the treatment of IVD degeneration.

Key outcomes:

1. In chapter three it was established that AD-MSCs supplemented with GDF6 resulted in a superior discogenic phenotype, in comparison to BM-MSCs and more commonly utilised growth factors TGF-β and GDF5. The resulting constructs were PG rich and expressed both novel and ECM markers. In addition it was recognised that assessment of the biomechanical properties is important, as NP is a gelatinous tissue, treatment with GDF6 produced a less stiff matrix than cells treated with TGF-β. Hence the study demonstrated AD-MSCs and GDF6 as a more suitable cell and growth factor choice to induce correct differentiation.

2. Chapter four demonstrated how microenvironmental factors of the IVD can influence discogenic differentiation. Hypoxia greatly enhanced ACAN

expression whilst, hypoxia and load significantly increased COL2A1. Although expression ECM and NP markers were increased, the ratio of ACAN: COL2A1 was not appropriate this resulted in constructs exposed to hypoxia and load having a stiffer ECM. This study also demonstrated the importance of analysing the mechanics of the constructs as both biochemical and biomechanical parameters must be appropriate to ensure success of a therapy.

3. Chapter five highlighted the differential response of aNPCs and mature NP cells in a catabolic environment. As aNPCs demonstrated no catabolic shift when treated with IL-1β it can be postulated that initial pre-differentiation of AD-MSCs with GDF6 can improve the potential of the cell therapy in vivo in the hostile IVD niche.

4. Chapter six demonstrated that GDF6 also enhanced the ECM production of degenerate NP cells and increased phenotypic marker expression. In addition as with aNPCs, pre-treatment of NP cells with GDF6 was protective against the detrimental effects of IL-1β.

5. In the final chapter preliminary studies developed and a severely degenerate ex vivo model to test the efficacy of potential therapies. Also the potential of utilising a microparticle delivery system was explored. The GDF6 microparticles fabricated in collaboration with The University of Nottingham, demonstrated the same discogenic potential as treatment with exogenous GDF6.

Taken together, GDF6 has demonstrated the potential to be utilised as a biological treatment to regenerate the IVD. The experiments undertaken have highlighted how the growth factor can enhance discogenic differentiation of AD-MSCs to a superior NP phenotype than alternative growth factors. This is clinically important as the appropriate choice of cell and growth factor is imperative to produce functional matrix and the ultimate success of a therapy. Interestingly, GDF6 has also demonstrated a protective quality against the detrimental effects of a catabolic

environment, in both AD-MSCs and NP cells. If an aNPC cell-based therapy is utilised then the aNPCs would be protected from the degenerate environment, but also GDF6 can exert its effects on native cells and help to restore their normal phenotype and enchance matrix production as demonstrated in chapter 5. At present, studies have mainly been undertaken in an *in vitro* system thus the development of a degenerate IVD model presents itself as a platform to test the efficacy of GDF6 and aNPCs as a potential therapy. In addition, the development of a controlled delivery system of GDF6 is extremely important for clinical translation as the microparticles are biocompatible, biodegradable and prevent the multiple applications of the growth factor. In the study by Wei and colleagues (Wei et al., 2009) direct injection of GDF6 into an in vivo degenerate ovine model enhanced the ECM, however multiple injections could also damage the disc (Korecki et al., 2008) hence controlled delivery is more clinically transferable.

A particular limitation to this study is the lack of protein and signalling analysis that would help to demonstrate the effects that GDF6 is having on the cells, and also why there are differences between cell types. Additionally, whilst the qPCR markers investigated were NP cell specific, such as COL2A1, the study could have examined other collagens such as COL1 or COLX to illustrate that the cells were definitely differentiated and have used this as a negative control.

8.2 Future Work

This study has demonstrated the potential of GDF6 as a biological therapy for IVD regeneration by numerous *in vitro* experiments. The results from these studies demonstrated GDF6 has a positive effect on both AD-MSCs and NP cells. However in order to develop this potential therapy further it is essential to assess the effects of GDF6, and aNPCs in an ex vivo model. The model developed in this study is a severely degenerate model, and essentially a proof of principle to demonstrate that a hydrogel could form in situ and restore altered biomechanical properties. A model that reflects the true pathological changes of disease (ie. driven by IL-1) would be beneficial to investigate the potential of GDF6 and the implantation of aNPCs. Once examined in an ex vivo model, a larger animal model would be important to assess how the cells respond in vivo.

Another important aspect is to identify whether there is a sub-population of AD-MSCs that are more responsive to GDF6 supplementation. Therefore experiments should be undertaken to identify if cells have more GDF6 receptors or different receptor profiles and isolate these cells using FACS. This isolated population of cells may be more responsive to GDF6 treatment and as such could respond in an even more appropriate manner when induced to an aNPC.

As demonstrated in chapter 4, aNPCs do not respond in the same manner as mature NP cells when exposed to IL-1. It was demonstrated that both cell types expressed IL-1R, however investigation further into the IL-1 signalling pathway and alternative pathways such as the toll like receptors (TLRs) should be elucidated to determine why there are differential responses and also what it is that is different in aNPCs, and to try to apply this to NP cells. In addition to this NP cells also treated with GDF6 proved to be protective against the catabolic environment. Hence further studies should investigate if and how the cells have changed, for example examining receptor profiles to see whether GDF6 alters the expression of specific IL-1 receptors. Also investigations to determine whether in fact GDF6 is protective, or whether there is just a greater shift toward anabolic activity, as shown by the upregulation of ACAN and COL2A1 would be interesting to determine the mechanisms that GDF6 inflicts the positive effect on NP cells.

Finally, a preliminary study showed that microparticles loaded with GDF6 could induce the equivalent discogenic differentiation as supplementation exogenously. Further experiments should also be undertaken to examine whether treatment of NP cells restores or enhances the normal phenotype, and if the GDF6 microparticles can be protective against a catabolic environment to the same extent as treatment with exogenous GDF6. Moving forward microparticles should also be investigated in the ex vivo model and observe how treatment with only microparticles encapsulated in type I collagen compares to microparticles and cells (aNPCs). It would also be interesting to see if the GDF6 microparticles could differentiate AD-MSCs to an aNPC in situ as this would eliminate the need to pre-differentiate cells in vitro for 14 days, which would enhance the clinical transferability of this potential therapy.

Chapter 9

References

ABBOTT, R. D., PURMESSUR, D., MONSEY, R. D. & IATRIDIS, J. C. 2012. Regenerative potential of TGFbeta3 + Dex and notochordal cell conditioned media on degenerated human intervertebral disc cells. *J Orthop Res,* 30**,** 482-8.

ADAMS, M. A., MCNALLY, D. S. & DOLAN, P. 1996. 'Stress' distributions inside intervertebral discs. The effects of age and degeneration. *J Bone Joint Surg Br,* 78**,** 965-72.

ADAMS, M. A. & ROUGHLEY, P. J. 2006. What is intervertebral disc degeneration, and what causes it? *Spine (Phila Pa 1976),* 31**,** 2151-61.

AKMAL, M., KESANI, A., ANAND, B., SINGH, A., WISEMAN, M. & GOODSHIP, A. 2004. Effect of nicotine on spinal disc cells: a cellular mechanism for disc degeneration. *Spine (Phila Pa 1976),* 29**,** 568-75.

AKYOL, S., ERASLAN, B. S., ETYEMEZ, H., TANRIVERDI, T. & HANCI, M. 2010. Catabolic cytokine expressions in patients with degenerative disc disease. *Turk Neurosurg,* 20**,** 492-9.

ALINI, M., EISENSTEIN, S. M., ITO, K., LITTLE, C., KETTLER, A. A., MASUDA, K., MELROSE, J., RALPHS, J., STOKES, I. & WILKE, H. J. 2008. Are animal models useful for studying human disc disorders/degeneration? *Eur Spine J,* 17**,** 2-19.

ALTAF, F. M., HERING, T. M., KAZMI, N. H., YOO, J. U. & JOHNSTONE, B. 2006. Ascorbate-enhanced chondrogenesis of ATDC5 cells. *Eur Cell Mater,* 12**,** 64-9; discussion 69-70.

AN, H. S. & MASUDA, K. 2006. Relevance of in vitro and in vivo models for intervertebral disc degeneration. *J Bone Joint Surg Am,* 88 Suppl 2**,** 88-94.

ANDERSSON, G. B. 1999. Epidemiological features of chronic low-back pain. *Lancet,* 354**,** 581-5.

ANDRADE, P., HOOGLAND, G., GARCIA, M. A., STEINBUSCH, H. W., DAEMEN, M. A. & VISSER-VANDEWALLE, V. 2013. Elevated IL-1beta and IL-6 levels in lumbar herniated discs in patients with sciatic pain. *Eur Spine J,* 22**,** 714-20.

ANNUNEN, S., PAASSILTA, P., LOHINIVA, J., PERALA, M., PIHLAJAMAA, T., KARPPINEN, J., TERVONEN, O., KROGER, H., LAHDE, S., VANHARANTA, H., RYHANEN, L., GORING, H. H., OTT, J., PROCKOP, D. J. & ALA-KOKKO, L. 1999. An allele of COL9A2 associated with intervertebral disc disease. *Science,* 285**,** 409-12.

ANTONIOU, J., GOUDSOUZIAN, N. M., HEATHFIELD, T. F., WINTERBOTTOM, N., STEFFEN, T., POOLE, A. R., AEBI, M. & ALINI, M. 1996. The human lumbar endplate. Evidence of changes in biosynthesis and denaturation of the extracellular matrix with growth, maturation, aging, and degeneration. *Spine (Phila Pa 1976),* 21**,** 1153-61.

ARIGA, K., YONENOBU, K., NAKASE, T., HOSONO, N., OKUDA, S., MENG, W., TAMURA, Y. & YOSHIKAWA, H. 2003. Mechanical stress-induced apoptosis of endplate chondrocytes in organ-cultured mouse intervertebral discs: an ex vivo study. *Spine (Phila Pa 1976),* 28**,** 1528-33.

ASAI-COAKWELL, M., FRENCH, C. R., YE, M., GARCHA, K., BIGOT, K., PERERA, A. G., STAEHLING-HAMPTON, K., MEMA, S. C., CHANDA, B., MUSHEGIAN, A., BAMFORTH, S., DOSCHAK, M. R., LI, G., DOBBS, M. B., GIAMPIETRO, P. F., BROOKS, B. P., VIJAYALAKSHMI, P., SAUVE, Y., ABITBOL, M., SUNDARESAN, P., VAN HEYNINGEN, V., POURQUIE, O., UNDERHILL, T. M., WASKIEWICZ, A. J. & LEHMANN, O. J. 2009. Incomplete penetrance and phenotypic variability characterize Gdf6-attributable oculo-skeletal phenotypes. *Hum Mol Genet,* 18**,** 1110-21.

BARBIR, A., MICHALEK, A. J., ABBOTT, R. D. & IATRIDIS, J. C. 2010. Effects of enzymatic digestion on compressive properties of rat intervertebral discs. *J Biomech,* 43**,** 1067-73.

BARTELS, E. M., FAIRBANK, J. C., WINLOVE, C. P. & URBAN, J. P. 1998. Oxygen and lactate concentrations measured in vivo in the intervertebral discs of patients with scoliosis and back pain. *Spine (Phila Pa 1976),* 23**,** 1-7; discussion 8.

BATTIE, M. C., HAYNOR, D. R., FISHER, L. D., GILL, K., GIBBONS, L. E. & VIDEMAN, T. 1995a. Similarities in degenerative findings on magnetic resonance images of the lumbar spines of identical twins. *J Bone Joint Surg Am,* 77**,** 1662-70.

BATTIE, M. C., VIDEMAN, T., GIBBONS, L. E., FISHER, L. D., MANNINEN, H. & GILL, K. 1995b. 1995 Volvo Award in clinical sciences. Determinants of lumbar disc degeneration. A study relating lifetime exposures and magnetic resonance imaging findings in identical twins. *Spine (Phila Pa 1976),* 20**,** 2601-12.

BATTIE, M. C., VIDEMAN, T., KAPRIO, J., GIBBONS, L. E., GILL, K., MANNINEN, H., SAARELA, J. & PELTONEN, L. 2009. The Twin Spine Study: contributions to a changing view of disc degeneration. *Spine J,* 9**,** 47-59.

BAUMGARTNER, L., ARNHOLD, S., BRIXIUS, K., ADDICKS, K. & BLOCH, W. 2010. Human mesenchymal stem cells: Influence of oxygen pressure on proliferation and chondrogenic differentiation in fibrin glue in vitro. *J Biomed Mater Res A,* 93**,** 930-40.

BERG, S., TROPP, H. T. & LEIVSETH, G. 2011. Disc height and motion patterns in the lumbar spine in patients operated with total disc replacement or fusion for discogenic back pain. Results from a randomized controlled trial. *Spine J,* 11**,** 991-8.

BERTOLO, A., MEHR, M., AEBLI, N., BAUR, M., FERGUSON, S. J. & STOYANOV, J. V. 2012. Influence of different commercial scaffolds on the in vitro differentiation of human mesenchymal stem cells to nucleus pulposus-like cells. *Eur Spine J,* 21 Suppl 6**,** S826-38.

BERTRAM, H., NERLICH, A., OMLOR, G., GEIGER, F., ZIMMERMANN, G. & FELLENBERG, J. 2009. Expression of TRAIL and the death receptors DR4 and DR5 correlates with progression of degeneration in human intervertebral disks. *Mod Pathol,* 22**,** 895-905.

BIBBY, S. R., JONES, D. A., RIPLEY, R. M. & URBAN, J. P. 2005. Metabolism of the intervertebral disc: effects of low levels of oxygen, glucose, and pH on rates of energy metabolism of bovine nucleus pulposus cells. *Spine (Phila Pa 1976),* 30**,** 487-96.

BIBBY, S. R. & URBAN, J. P. 2004. Effect of nutrient deprivation on the viability of intervertebral disc cells. *Eur Spine J,* 13**,** 695-701.

BIJKERK, C., HOUWING-DUISTERMAAT, J. J., VALKENBURG, H. A., MEULENBELT, I., HOFMAN, A., BREEDVELD, F. C., POLS, H. A., VAN DUIJN, C. M. & SLAGBOOM, P. E. 1999. Heritabilities of radiologic osteoarthritis in peripheral joints and of disc degeneration of the spine. *Arthritis Rheum,* 42**,** 1729-35.

BINCH, A. L., COLE, A. A., BREAKWELL, L. M., MICHAEL, A. L., CHIVERTON, N., CROSS, A. K. & LE MAITRE, C. L. 2014. Expression and regulation of neurotrophic and angiogenic factors during human intervertebral disc degeneration. *Arthritis Res Ther,* 16**,** 416.

BLANCO, J. F., GRACIANI, I. F., SANCHEZ-GUIJO, F. M., MUNTION, S., HERNANDEZ-CAMPO, P., SANTAMARIA, C., CARRANCIO, S., BARBADO, M. V., CRUZ, G., GUTIERREZ-COSIO, S., HERRERO, C., SAN MIGUEL, J. F., BRINON, J. G. & DEL CANIZO, M. C. 2010. Isolation and characterization of mesenchymal stromal cells from human degenerated nucleus pulposus: comparison with bone marrow mesenchymal stromal cells from the same subjects. *Spine (Phila Pa 1976),* 35**,** 2259-65.

BOBACZ, K., ULLRICH, R., AMOYO, L., ERLACHER, L., SMOLEN, J. S. & GRANINGER, W. B. 2006. Stimulatory effects of distinct members of the bone morphogenetic protein family on ligament fibroblasts. *Ann Rheum Dis,* 65**,** 169-77.

BOOS, N., DREIER, D., HILFIKER, E., SCHADE, V., KREIS, R., HORA, J., AEBI, M. & BOESCH, C. 1997. Tissue characterization of symptomatic and asymptomatic disc herniations by quantitative magnetic resonance imaging. *J Orthop Res,* 15**,** 141-9.

BOOS, N., WEISSBACH, S., ROHRBACH, H., WEILER, C., SPRATT, K. F. & NERLICH, A. G. 2002. Classification of age-related changes in lumbar intervertebral discs: 2002 Volvo Award in basic science. *Spine (Phila Pa 1976),* 27**,** 2631-44.

BORZI, R. M., MAZZETTI, I., CATTINI, L., UGUCCIONI, M., BAGGIOLINI, M. & FACCHINI, A. 2000. Human chondrocytes express functional chemokine receptors and release matrix-degrading enzymes in response to C-X-C and C-C chemokines. *Arthritis Rheum,* 43**,** 1734-41.

BOSCH, P., MUSGRAVE, D., GHIVIZZANI, S., LATTERMAN, C., DAY, C. S. & HUARD, J. 2000. The efficiency of muscle-derived cell-mediated bone formation. *Cell Transplant,* 9**,** 463-70.

BOUGAULT, C., PAUMIER, A., AUBERT-FOUCHER, E. & MALLEIN-GERIN, F. 2009. Investigating conversion of mechanical force into biochemical signaling in three-dimensional chondrocyte cultures. *Nat Protoc,* 4**,** 928-38.

BRISBY, H., PAPADIMITRIOU, N., BRANTSING, C., BERGH, P., LINDAHL, A. & BARRETO HENRIKSSON, H. 2013. The presence of local mesenchymal progenitor cells in human degenerated intervertebral discs and possibilities to influence these in vitro: a descriptive study in humans. *Stem Cells Dev,* 22**,** 804-14.

BROBERG, K. B. 1983. On the mechanical behaviour of intervertebral discs. *Spine (Phila Pa 1976),* 8**,** 151-65.

BRON, J. L., HELDER, M. N., MEISEL, H. J., VAN ROYEN, B. J. & SMIT, T. H. 2009. Repair, regenerative and supportive therapies of the annulus fibrosus: achievements and challenges. *Eur Spine J,* 18**,** 301-13.

BUCKLEY, C. T. & KELLY, D. J. 2012. Expansion in the presence of FGF-2 enhances the functional development of cartilaginous tissues engineered using infrapatellar fat pad derived MSCs. *J Mech Behav Biomed Mater,* 11**,** 102-11.

BUCKWALTER, J. A. 1995. Aging and degeneration of the human intervertebral disc. *Spine (Phila Pa 1976),* 20**,** 1307-14.

CALDERON, L., COLLIN, E., VELASCO-BAYON, D., MURPHY, M., O'HALLORAN, D. & PANDIT, A. 2010. Type II collagen-hyaluronan hydrogel--a step towards a scaffold for intervertebral disc tissue engineering. *Eur Cell Mater,* 20**,** 134-48.

CAMPISI, J. 1997. The biology of replicative senescence. *Eur J Cancer,* 33**,** 703-9.

CAPLAN, A. I. 1994. The mesengenic process. *Clin Plast Surg,* 21**,** 429-35.

CATTELL, M. A., ANDERSON, J. C. & HASLETON, P. S. 1996. Age-related changes in amounts and concentrations of collagen and elastin in normotensive human thoracic aorta. *Clin Chim Acta,* 245**,** 73-84.

CHAN, S. C., FERGUSON, S. J. & GANTENBEIN-RITTER, B. 2011a. The effects of dynamic loading on the intervertebral disc. *Eur Spine J,* 20**,** 1796-812.

CHAN, S. C., FERGUSON, S. J., WUERTZ, K. & GANTENBEIN-RITTER, B. 2011b. Biological response of the intervertebral disc to repetitive short-term cyclic torsion. *Spine (Phila Pa 1976),* 36**,** 2021-30.

CHAN, S. C. & GANTENBEIN-RITTER, B. 2012. Preparation of intact bovine tail intervertebral discs for organ culture. *J Vis Exp*.

CHAN, S. C., WALSER, J., KAPPELI, P., SHAMSOLLAHI, M. J., FERGUSON, S. J. & GANTENBEIN-RITTER, B. 2013. Region specific response of

intervertebral disc cells to complex dynamic loading: an organ culture study using a dynamic torsion-compression bioreactor. *PLoS One,* 8**,** e72489.

CHANDA, D., KUMAR, S. & PONNAZHAGAN, S. 2010. Therapeutic potential of adult bone marrow-derived mesenchymal stem cells in diseases of the skeleton. *J Cell Biochem,* 111**,** 249-57.

CHEN, Z. H., JIN, S. H., WANG, M. Y., JIN, X. L., LV, C., DENG, Y. F. & WANG, J. L. 2015. Enhanced NLRP3, caspase-1, and IL- 1beta levels in degenerate human intervertebral disc and their association with the grades of disc degeneration. *Anat Rec (Hoboken),* 298**,** 720-6.

CHEUNG, K. M., KARPPINEN, J., CHAN, D., HO, D. W., SONG, Y. Q., SHAM, P., CHEAH, K. S., LEONG, J. C. & LUK, K. D. 2009. Prevalence and pattern of lumbar magnetic resonance imaging changes in a population study of one thousand forty-three individuals. *Spine (Phila Pa 1976),* 34**,** 934-40.

CHIBA, K., MASUDA, K., ANDERSSON, G. B., MOMOHARA, S. & THONAR, E. J. 2007. Matrix replenishment by intervertebral disc cells after chemonucleolysis in vitro with chondroitinase ABC and chymopapain. *Spine J,* 7**,** 694-700.

CHICHE, J., ILC, K., LAFERRIERE, J., TROTTIER, E., DAYAN, F., MAZURE, N. M., BRAHIMI-HORN, M. C. & POUYSSEGUR, J. 2009. Hypoxia-inducible carbonic anhydrase IX and XII promote tumor cell growth by counteracting acidosis through the regulation of the intracellular pH. *Cancer Res,* 69**,** 358-68.

CHOI, K. S., COHN, M. J. & HARFE, B. D. 2008. Identification of nucleus pulposus precursor cells and notochordal remnants in the mouse: implications for disk degeneration and chordoma formation. *Dev Dyn,* 237**,** 3953-8.

CHOI, Y. S. 2009. Pathophysiology of degenerative disc disease. *Asian Spine J,* 3**,** 39-44.

CHOU, R., HUFFMAN, L. H., AMERICAN PAIN, S. & AMERICAN COLLEGE OF, P. 2007a. Nonpharmacologic therapies for acute and chronic low back pain: a review of the evidence for an American Pain Society/American College of Physicians clinical practice guideline. *Ann Intern Med,* 147**,** 492-504.

CHOU, R., QASEEM, A., SNOW, V., CASEY, D., CROSS, J. T., JR., SHEKELLE, P., OWENS, D. K., CLINICAL EFFICACY ASSESSMENT SUBCOMMITTEE OF THE AMERICAN COLLEGE OF, P., AMERICAN COLLEGE OF, P. & AMERICAN PAIN SOCIETY LOW BACK PAIN GUIDELINES, P. 2007b. Diagnosis and treatment of low back pain: a joint clinical practice guideline from the American College of Physicians and the American Pain Society. *Ann Intern Med,* 147**,** 478-91.

CICIONE, C., MUINOS-LOPEZ, E., HERMIDA-GOMEZ, T., FUENTES-BOQUETE, I., DIAZ-PRADO, S. & BLANCO, F. J. 2013. Effects of severe hypoxia on bone marrow mesenchymal stem cells differentiation potential. *Stem Cells Int,* 2013**,** 232896.

CLARKE, L. E., MCCONNELL, J. C., SHERRATT, M. J., DERBY, B., RICHARDSON, S. M. & HOYLAND, J. A. 2014. Growth differentiation factor 6 and transforming growth factor-beta differentially mediate mesenchymal stem cell differentiation, composition, and micromechanical properties of nucleus pulposus constructs. *Arthritis Res Ther,* 16**,** R67.

CLARKE, L. E., RICHARDSON, S. M. & HOYLAND, J. A. 2015. Harnessing the Potential of Mesenchymal Stem Cells for IVD Regeneration. *Curr Stem Cell Res Ther,* 10**,** 296-306.

CLOUET, J., GRIMANDI, G., POT-VAUCEL, M., MASSON, M., FELLAH, H. B., GUIGAND, L., CHEREL, Y., BORD, E., RANNOU, F., WEISS, P., GUICHEUX, J. & VINATIER, C. 2009. Identification of phenotypic discriminating markers for intervertebral disc cells and articular chondrocytes. *Rheumatology (Oxford),* 48**,** 1447-50.

COLLIN, E. C., GRAD, S., ZEUGOLIS, D. I., VINATIER, C. S., CLOUET, J. R., GUICHEUX, J. J., WEISS, P., ALINI, M. & PANDIT, A. S. 2011. An injectable vehicle for nucleus pulposus cell-based therapy. *Biomaterials,* 32**,** 2862-70.

COSTI, J. J., STOKES, I. A., GARDNER-MORSE, M. G. & IATRIDIS, J. C. 2008. Frequency-dependent behavior of the intervertebral disc in response to each of six degree of freedom dynamic loading: solid phase and fluid phase contributions. *Spine (Phila Pa 1976),* 33**,** 1731-8.

CREAN, J. K., ROBERTS, S., JAFFRAY, D. C., EISENSTEIN, S. M. & DUANCE, V. C. 1997. Matrix metalloproteinases in the human intervertebral disc: role in disc degeneration and scoliosis. *Spine (Phila Pa 1976),* 22**,** 2877-84.

CREVENSTEN, G., WALSH, A. J., ANANTHAKRISHNAN, D., PAGE, P., WAHBA, G. M., LOTZ, J. C. & BERVEN, S. 2004. Intervertebral disc cell therapy for regeneration: mesenchymal stem cell implantation in rat intervertebral discs. *Ann Biomed Eng,* 32**,** 430-4.

DAI, J., WANG, H., LIU, G., XU, Z., LI, F. & FANG, H. 2014. Dynamic compression and co-culture with nucleus pulposus cells promotes proliferation and differentiation of adipose-derived mesenchymal stem cells. *J Biomech,* 47**,** 966-72.

DE BARI, C., DELL'ACCIO, F., VANDENABEELE, F., VERMEESCH, J. R., RAYMACKERS, J. M. & LUYTEN, F. P. 2003. Skeletal muscle repair by adult human mesenchymal stem cells from synovial membrane. *J Cell Biol,* 160**,** 909-18.

DEYO, R. A. & BASS, J. E. 1989. Lifestyle and low-back pain. The influence of smoking and obesity. *Spine (Phila Pa 1976),* 14**,** 501-6.

DUDLI, S., HASCHTMANN, D. & FERGUSON, S. J. 2015. Persistent degenerative changes in the intervertebral disc after burst fracture in an in vitro model mimicking physiological post-traumatic conditions. *Eur Spine J,* 24**,** 1901-8.

ELFERING, A., SEMMER, N., BIRKHOFER, D., ZANETTI, M., HODLER, J. & BOOS, N. 2002. Risk factors for lumbar disc degeneration: a 5-year prospective MRI study in asymptomatic individuals. *Spine (Phila Pa 1976),* 27**,** 125-34.

ERNST, E. 1993. Smoking, a cause of back trouble? *Br J Rheumatol,* 32**,** 239-42.

ERWIN, W. M., ISLAM, D., INMAN, R. D., FEHLINGS, M. G. & TSUI, F. W. 2011. Notochordal cells protect nucleus pulposus cells from degradation and apoptosis: implications for the mechanisms of intervertebral disc degeneration. *Arthritis Res Ther,* 13**,** R215.

ESER, B., CORA, T., ESER, O., KALKAN, E., HAKTANIR, A., ERDOGAN, M. O. & SOLAK, M. 2010. Association of the polymorphisms of vitamin D receptor and aggrecan genes with degenerative disc disease. *Genet Test Mol Biomarkers,* 14**,** 313-7.

EYRE, D. R., MATSUI, Y. & WU, J. J. 2002. Collagen polymorphisms of the intervertebral disc. *Biochem Soc Trans,* 30**,** 844-8.

EYRE, D. R. & MUIR, H. 1976. Types I and II collagens in intervertebral disc. Interchanging radial distributions in annulus fibrosus. *Biochem J,* 157**,** 267-70.

FAN, H., ZHAO, G., LIU, L., LIU, F., GONG, W., LIU, X., YANG, L., WANG, J. & HOU, Y. 2012. Pre-treatment with IL-1beta enhances the efficacy of MSC transplantation in DSS-induced colitis. *Cell Mol Immunol,* 9**,** 473-81.

FELAND, J. B., MYRER, J. W., SCHULTHIES, S. S., FELLINGHAM, G. W. & MEASOM, G. W. 2001. The effect of duration of stretching of the hamstring muscle group for increasing range of motion in people aged 65 years or older. *Phys Ther,* 81**,** 1110-7.

FELKA, T., SCHAFER, R., SCHEWE, B., BENZ, K. & AICHER, W. K. 2009. Hypoxia reduces the inhibitory effect of IL-1beta on chondrogenic differentiation of FCS-free expanded MSC. *Osteoarthritis Cartilage,* 17**,** 1368-76.

FENG, G., JIN, X., HU, J., MA, H., GUPTE, M. J., LIU, H. & MA, P. X. 2011a. Effects of hypoxias and scaffold architecture on rabbit mesenchymal stem cell differentiation towards a nucleus pulposus-like phenotype. *Biomaterials,* 32**,** 8182-9.

FENG, G., ZHAO, X., LIU, H., ZHANG, H., CHEN, X., SHI, R., LIU, X., ZHAO, X., ZHANG, W. & WANG, B. 2011b. Transplantation of mesenchymal stem cells and nucleus pulposus cells in a degenerative disc model in rabbits: a comparison of 2 cell types as potential candidates for disc regeneration. *J Neurosurg Spine,* 14**,** 322-9.

FENG, H., DANFELTER, M., STROMQVIST, B. & HEINEGARD, D. 2006. Extracellular matrix in disc degeneration. *J Bone Joint Surg Am,* 88 Suppl 2**,** 25-9.

FIRTH, J. D., EBERT, B. L. & RATCLIFFE, P. J. 1995. Hypoxic regulation of lactate dehydrogenase A. Interaction between hypoxia-inducible factor 1 and cAMP response elements. *J Biol Chem,* 270**,** 21021-7.

FONTANA, G., THOMAS, D., COLLIN, E. & PANDIT, A. 2014. Microgel microenvironment primes adipose-derived stem cells towards an NP cells-like phenotype. *Adv Healthc Mater,* 3**,** 2012-22.

FREEMONT, A. J. 2009. The cellular pathobiology of the degenerate intervertebral disc and discogenic back pain. *Rheumatology (Oxford),* 48**,** 5-10.

FREEMONT, A. J., WATKINS, A., LE MAITRE, C., BAIRD, P., JEZIORSKA, M., KNIGHT, M. T., ROSS, E. R., O'BRIEN, J. P. & HOYLAND, J. A. 2002a. Nerve growth factor expression and innervation of the painful intervertebral disc. *J Pathol,* 197**,** 286-92.

FREEMONT, A. J., WATKINS, A., LE MAITRE, C., JEZIORSKA, M. & HOYLAND, J. A. 2002b. Current understanding of cellular and molecular events in intervertebral disc degeneration: implications for therapy. *J Pathol,* 196**,** 374-9.

FRIEDENSTEIN, A. J., PETRAKOVA, K. V., KUROLESOVA, A. I. & FROLOVA, G. P. 1968. Heterotopic of bone marrow. Analysis of precursor cells for osteogenic and hematopoietic tissues. *Transplantation,* 6**,** 230-47.

FROBIN, W., BRINCKMANN, P., KRAMER, M. & HARTWIG, E. 2001. Height of lumbar discs measured from radiographs compared with degeneration and height classified from MR images. *Eur Radiol,* 11**,** 263-9.

GANTENBEIN-RITTER, B., BENNEKER, L. M., ALINI, M. & GRAD, S. 2011. Differential response of human bone marrow stromal cells to either TGF-beta(1) or rhGDF-5. *Eur Spine J,* 20**,** 962-71.

GANTENBEIN, B., GRUNHAGEN, T., LEE, C. R., VAN DONKELAAR, C. C., ALINI, M. & ITO, K. 2006. An in vitro organ culturing system for intervertebral disc explants with vertebral endplates: a feasibility study with ovine caudal discs. *Spine (Phila Pa 1976),* 31**,** 2665-73.

GAO, Y., KOSTROMINOVA, T. Y., FAULKNER, J. A. & WINEMAN, A. S. 2008. Age-related changes in the mechanical properties of the epimysium in skeletal muscles of rats. *J Biomech,* 41**,** 465-9.

GAWRI, R., MWALE, F., OUELLET, J., ROUGHLEY, P. J., STEFFEN, T., ANTONIOU, J. & HAGLUND, L. 2011. Development of an organ culture system for long-term survival of the intact human intervertebral disc. *Spine (Phila Pa 1976),* 36**,** 1835-42.

GILLET, P. 2003. The fate of the adjacent motion segments after lumbar fusion. *J Spinal Disord Tech,* 16**,** 338-45.

GILSON, A., DREGER, M. & URBAN, J. P. 2010. Differential expression level of cytokeratin 8 in cells of the bovine nucleus pulposus complicates the search for specific intervertebral disc cell markers. *Arthritis Res Ther,* 12**,** R24.

GITEAU, A., VENIER-JULIENNE, M. C., AUBERT-POUESSEL, A. & BENOIT, J. P. 2008. How to achieve sustained and complete protein release from PLGA-based microparticles? *Int J Pharm,* 350**,** 14-26.

GOSSELIN, L. E., ADAMS, C., COTTER, T. A., MCCORMICK, R. J. & THOMAS, D. P. 1998. Effect of exercise training on passive stiffness in locomotor skeletal muscle: role of extracellular matrix. *J Appl Physiol (1985),* 85**,** 1011-6.

GRAHAM, H. K., AKHTAR, R., KRIDIOTIS, C., DERBY, B., KUNDU, T., TRAFFORD, A. W. & SHERRATT, M. J. 2011. Localised micro-mechanical stiffening in the ageing aorta. *Mech Ageing Dev,* 132**,** 459-67.

GRUBER, H. E., FISHER, E. C., JR., DESAI, B., STASKY, A. A., HOELSCHER, G. & HANLEY, E. N., JR. 1997. Human intervertebral disc cells from the annulus: three-dimensional culture in agarose or alginate and responsiveness to TGF-beta1. *Exp Cell Res,* 235**,** 13-21.

GRUBER, H. E. & HANLEY, E. N., JR. 1998. Analysis of aging and degeneration of the human intervertebral disc. Comparison of surgical specimens with normal controls. *Spine (Phila Pa 1976),* 23**,** 751-7.

GRUBER, H. E. & HANLEY, E. N., JR. 2000. Human disc cells in monolayer vs 3D culture: cell shape, division and matrix formation. *BMC Musculoskelet Disord,* 1**,** 1.

GRUBER, H. E., HOELSCHER, G. L., BETHEA, S. & HANLEY, E. N., JR. 2012. Interleukin 1-beta upregulates brain-derived neurotrophic factor, neurotrophin 3 and neuropilin 2 gene expression and NGF production in annulus cells. *Biotech Histochem,* 87**,** 506-11.

GRUBER, H. E., HOELSCHER, G. L., INGRAM, J. A., NORTON, H. J. & HANLEY, E. N., JR. 2013. Increased IL-17 expression in degenerated human discs and increased production in cultured annulus cells exposed to IL-1ss and TNF-alpha. *Biotech Histochem,* 88**,** 302-10.

GRUBER, H. E., HOELSCHER, G. L., LESLIE, K., INGRAM, J. A. & HANLEY, E. N., JR. 2006. Three-dimensional culture of human disc cells within agarose or a collagen sponge: assessment of proteoglycan production. *Biomaterials,* 27**,** 371-6.

GRUBER, H. E., INGRAM, J. A., NORTON, H. J. & HANLEY, E. N., JR. 2007. Senescence in cells of the aging and degenerating intervertebral disc: immunolocalization of senescence-associated beta-galactosidase in human and sand rat discs. *Spine (Phila Pa 1976),* 32**,** 321-7.

GRUNHAGEN, T., WILDE, G., SOUKANE, D. M., SHIRAZI-ADL, S. A. & URBAN, J. P. 2006. Nutrient supply and intervertebral disc metabolism. *J Bone Joint Surg Am,* 88 Suppl 2**,** 30-5.

GUGGISBERG, S., BENNEKER, L.M., KEEL, M.J. & GANTENBIEN, B. 2015. Mechanical loading promoted discogenic differentiation of human

mesenchymal stem cells incorporated in 3D-PEG scaffolds with rhGDF5 and RGD. *Int J Stem Cell ResTher,*2:1.

GUILLAUME, O., DALY, A., LENNON, K., GANSAU, J., BUCKLEY, S. F. & BUCKLEY, C. T. 2014. Shape-memory porous alginate scaffolds for regeneration of the annulus fibrosus: effect of TGF-beta3 supplementation and oxygen culture conditions. *Acta Biomater,* 10**,** 1985-95.

GULATI, T., CHUNG, S. A., WEI, A. Q. & DIWAN, A. D. 2015. Localization of bone morphogenetic protein 13 in human intervertebral disc and its molecular and functional effects in vitro in 3D culture. *J Orthop Res*.

GUPTA, M. S., COOPER, E. S. & NICOLL, S. B. 2011. Transforming growth factor-beta 3 stimulates cartilage matrix elaboration by human marrow-derived stromal cells encapsulated in photocrosslinked carboxymethylcellulose hydrogels: potential for nucleus pulposus replacement. *Tissue Eng Part A,* 17**,** 2903-10.

HAGLUND, L., MOIR, J., BECKMAN, L., MULLIGAN, K. R., JIM, B., OUELLET, J. A., ROUGHLEY, P. & STEFFEN, T. 2011. Development of a bioreactor for axially loaded intervertebral disc organ culture. *Tissue Eng Part C Methods,* 17**,** 1011-9.

HALLORAN, D. O., GRAD, S., STODDART, M., DOCKERY, P., ALINI, M. & PANDIT, A. S. 2008. An injectable cross-linked scaffold for nucleus pulposus regeneration. *Biomaterials,* 29**,** 438-47.

HASCHTMANN, D., STOYANOV, J. V., ETTINGER, L., NOLTE, L. P. & FERGUSON, S. J. 2006. Establishment of a novel intervertebral disc/endplate culture model: analysis of an ex vivo in vitro whole-organ rabbit culture system. *Spine (Phila Pa 1976),* 31**,** 2918-25.

HAYES, A. J. & RALPHS, J. R. 2011. The response of foetal annulus fibrosus cells to growth factors: modulation of matrix synthesis by TGF-beta1 and IGF-1. *Histochem Cell Biol,* 136**,** 163-75.

HENNIG, T., LORENZ, H., THIEL, A., GOETZKE, K., DICKHUT, A., GEIGER, F. & RICHTER, W. 2007. Reduced chondrogenic potential of adipose tissue derived stromal cells correlates with an altered TGFbeta receptor and BMP profile and is overcome by BMP-6. *J Cell Physiol,* 211**,** 682-91.

HENRIKSSON, H., THORNEMO, M., KARLSSON, C., HAGG, O., JUNEVIK, K., LINDAHL, A. & BRISBY, H. 2009. Identification of cell proliferation zones, progenitor cells and a potential stem cell niche in the intervertebral disc region: a study in four species. *Spine (Phila Pa 1976),* 34**,** 2278-87.

HENRIKSSON, H. B., SVALA, E., SKIOLDEBRAND, E., LINDAHL, A. & BRISBY, H. 2012. Support of concept that migrating progenitor cells from stem cell niches contribute to normal regeneration of the adult mammal intervertebral disc: a descriptive study in the New Zealand white rabbit. *Spine (Phila Pa 1976),* 37**,** 722-32.

HIYAMA, A., MOCHIDA, J., IWASHINA, T., OMI, H., WATANABE, T., SERIGANO, K., TAMURA, F. & SAKAI, D. 2008. Transplantation of mesenchymal stem cells in a canine disc degeneration model. *J Orthop Res,* 26**,** 589-600.

HOHAUS, C., GANEY, T. M., MINKUS, Y. & MEISEL, H. J. 2008. Cell transplantation in lumbar spine disc degeneration disease. *Eur Spine J,* 17 Suppl 4**,** 492-503.

HOLM, S., MAROUDAS, A., URBAN, J. P., SELSTAM, G. & NACHEMSON, A. 1981. Nutrition of the intervertebral disc: solute transport and metabolism. *Connect Tissue Res,* 8**,** 101-19.

HORMEL, S. E. & EYRE, D. R. 1991. Collagen in the ageing human intervertebral disc: an increase in covalently bound fluorophores and chromophores. *Biochim Biophys Acta,* 1078**,** 243-50.

HORNER, H. A. & URBAN, J. P. 2001. 2001 Volvo Award Winner in Basic Science Studies: Effect of nutrient supply on the viability of cells from the nucleus pulposus of the intervertebral disc. *Spine (Phila Pa 1976),* 26**,** 2543-9.

HOU, Q., CHAU, D. Y., PRATOOMSOOT, C., TIGHE, P. J., DUA, H. S., SHAKESHEFF, K. M. & ROSE, F. R. 2008. In situ gelling hydrogels incorporating microparticles as drug delivery carriers for regenerative medicine. *J Pharm Sci,* 97**,** 3972-80.

HOY, D., BAIN, C., WILLIAMS, G., MARCH, L., BROOKS, P., BLYTH, F., WOOLF, A., VOS, T. & BUCHBINDER, R. 2012. A systematic review of the global prevalence of low back pain. *Arthritis Rheum,* 64**,** 2028-37.

HSIEH, A. H. & LOTZ, J. C. 2003. Prolonged spinal loading induces matrix metalloproteinase-2 activation in intervertebral discs. *Spine (Phila Pa 1976),* 28**,** 1781-8.

HSU, Y. H., HSIEH, M. S., LIANG, Y. C., LI, C. Y., SHEU, M. T., CHOU, D. T., CHEN, T. F. & CHEN, C. H. 2004. Production of the chemokine eotaxin-1 in osteoarthritis and its role in cartilage degradation. *J Cell Biochem,* 93**,** 929-39.

HUANG, B., LIU, L. T., LI, C. Q., ZHUANG, Y., LUO, G., HU, S. Y. & ZHOU, Y. 2012. Study to determine the presence of progenitor cells in the degenerated human cartilage endplates. *Eur Spine J,* 21**,** 613-22.

HUANG, B., ZHUANG, Y., LI, C. Q., LIU, L. T. & ZHOU, Y. 2011. Regeneration of the intervertebral disc with nucleus pulposus cell-seeded collagen II/hyaluronan/chondroitin-6-sulfate tri-copolymer constructs in a rabbit disc degeneration model. *Spine (Phila Pa 1976),* 36**,** 2252-9.

HUANG, C. Y., HAGAR, K. L., FROST, L. E., SUN, Y. & CHEUNG, H. S. 2004. Effects of cyclic compressive loading on chondrogenesis of rabbit bone-marrow derived mesenchymal stem cells. *Stem Cells,* 22**,** 313-23.

HUSKINS, D.W. 2005. Tissue engineering: a live disc. *Nat Mater, 4,* 881-882.

HUNTER, C. J., MATYAS, J. R. & DUNCAN, N. A. 2003. The notochordal cell in the nucleus pulposus: a review in the context of tissue engineering. *Tissue Eng,* 9**,** 667-77.

HUNTER, C.J. 2005.The notochordal cell in the postnatal intervertebral disc. *Eur Cell Mater,* 10, 15.

HUNTER, C. J., MATYAS, J. R. & DUNCAN, N. A. 2004. The functional significance of cell clusters in the notochordal nucleus pulposus: survival and signaling in the canine intervertebral disc. *Spine (Phila Pa 1976),* 29**,** 1099-104.

IGARASHI, T., KIKUCHI, S., SHUBAYEV, V. & MYERS, R. R. 2000. 2000 Volvo Award winner in basic science studies: Exogenous tumor necrosis factor-alpha mimics nucleus pulposus-induced neuropathology. Molecular, histologic, and behavioral comparisons in rats. *Spine (Phila Pa 1976),* 25**,** 2975-80.

ILLIEN-JUNGER, S., GANTENBEIN-RITTER, B., GRAD, S., LEZUO, P., FERGUSON, S. J., ALINI, M. & ITO, K. 2010. The combined effects of limited nutrition and high-frequency loading on intervertebral discs with endplates. *Spine (Phila Pa 1976),* 35**,** 1744-52.

IMAI, Y., MIYAMOTO, K., AN, H. S., THONAR, E. J., ANDERSSON, G. B. & MASUDA, K. 2007a. Recombinant human osteogenic protein-1 upregulates proteoglycan metabolism of human anulus fibrosus and nucleus pulposus cells. *Spine (Phila Pa 1976),* 32**,** 1303-9; discussion 1310.

IMAI, Y., OKUMA, M., AN, H. S., NAKAGAWA, K., YAMADA, M., MUEHLEMAN, C., THONAR, E. & MASUDA, K. 2007b. Restoration of disc height loss by recombinant human osteogenic protein-1 injection into intervertebral discs undergoing degeneration induced by an intradiscal injection of chondroitinase ABC. *Spine (Phila Pa 1976),* 32**,** 1197-205.

INKINEN, R. I., LAMMI, M. J., LEHMONEN, S., PUUSTJARVI, K., KAAPA, E. & TAMMI, M. I. 1998. Relative increase of biglycan and decorin and altered chondroitin sulfate epitopes in the degenerating human intervertebral disc. *J Rheumatol,* 25**,** 506-14.

INOUE, H. 1981. Three-dimensional architecture of lumbar intervertebral discs. *Spine (Phila Pa 1976),* 6**,** 139-46.

IOZZO, R. V. & MURDOCH, A. D. 1996. Proteoglycans of the extracellular environment: clues from the gene and protein side offer novel perspectives in molecular diversity and function. *FASEB J,* 10**,** 598-614.

ISHII, Y., THOMAS, A. O., GUO, X. E., HUNG, C. T. & CHEN, F. H. 2006. Localization and distribution of cartilage oligomeric matrix protein in the rat intervertebral disc. *Spine (Phila Pa 1976),* 31**,** 1539-46.

IVANOV, S. V., KUZMIN, I., WEI, M. H., PACK, S., GEIL, L., JOHNSON, B. E., STANBRIDGE, E. J. & LERMAN, M. I. 1998. Down-regulation of transmembrane carbonic anhydrases in renal cell carcinoma cell lines by wild-type von Hippel-Lindau transgenes. *Proc Natl Acad Sci U S A,* 95**,** 12596-601.

JAIN, R. A. 2000. The manufacturing techniques of various drug loaded biodegradable poly(lactide-co-glycolide) (PLGA) devices. *Biomaterials,* 21**,** 2475-90.

JEONG, J. H., JIN, E. S., MIN, J. K., JEON, S. R., PARK, C. S., KIM, H. S. & CHOI, K. H. 2009. Human mesenchymal stem cells implantation into the degenerated coccygeal disc of the rat. *Cytotechnology,* 59**,** 55-64.

JIM, B., STEFFEN, T., MOIR, J., ROUGHLEY, P. & HAGLUND, L. 2011. Development of an intact intervertebral disc organ culture system in which degeneration can be induced as a prelude to studying repair potential. *Eur Spine J,* 20**,** 1244-54.

JIM, J. J., NOPONEN-HIETALA, N., CHEUNG, K. M., OTT, J., KARPPINEN, J., SAHRARAVAND, A., LUK, K. D., YIP, S. P., SHAM, P. C., SONG, Y. Q., LEONG, J. C., CHEAH, K. S., ALA-KOKKO, L. & CHAN, D. 2005. The TRP2 allele of COL9A2 is an age-dependent risk factor for the development and severity of intervertebral disc degeneration. *Spine (Phila Pa 1976),* 30**,** 2735-42.

JIMBO, K., PARK, J. S., YOKOSUKA, K., SATO, K. & NAGATA, K. 2005. Positive feedback loop of interleukin-1beta upregulating production of inflammatory mediators in human intervertebral disc cells in vitro. *J Neurosurg Spine,* 2**,** 589-95.

JOHNSON, W. E., CATERSON, B., EISENSTEIN, S. M., HYNDS, D. L., SNOW, D. M. & ROBERTS, S. 2002. Human intervertebral disc aggrecan inhibits nerve growth in vitro. *Arthritis Rheum,* 46**,** 2658-64.

JOHNSON, W. E., CATERSON, B., EISENSTEIN, S. M. & ROBERTS, S. 2005. Human intervertebral disc aggrecan inhibits endothelial cell adhesion and cell migration in vitro. *Spine (Phila Pa 1976),* 30**,** 1139-47.

JOHNSON, W. E., EISENSTEIN, S. M. & ROBERTS, S. 2001. Cell cluster formation in degenerate lumbar intervertebral discs is associated with increased disc cell proliferation. *Connect Tissue Res,* 42**,** 197-207.

JOSHI, A., MEHTA, S., VRESILOVIC, E., KARDUNA, A. & MARCOLONGO, M. 2005. Nucleus implant parameters significantly change the compressive stiffness of the human lumbar intervertebral disc. *J Biomech Eng,* 127**,** 536-40.

JUNG, D. I., HA, J., KANG, B. T., KIM, J. W., QUAN, F. S., LEE, J. H., WOO, E. J. & PARK, H. M. 2009. A comparison of autologous and allogenic bone marrow-derived mesenchymal stem cell transplantation in canine spinal cord injury. *J Neurol Sci,* 285**,** 67-77.

JUNGER, S., GANTENBEIN-RITTER, B., LEZUO, P., ALINI, M., FERGUSON, S. J. & ITO, K. 2009. Effect of limited nutrition on in situ intervertebral disc cells under simulated-physiological loading. *Spine (Phila Pa 1976),* 34**,** 1264-71.

JUNIPER, M., LE, T. K. & MLADSI, D. 2009. The epidemiology, economic burden, and pharmacological treatment of chronic low back pain in France, Germany, Italy, Spain and the UK: a literature-based review. *Expert Opin Pharmacother,* 10**,** 2581-92.

KARSENTY, G. & WAGNER, E. F. 2002. Reaching a genetic and molecular understanding of skeletal development. *Dev Cell,* 2**,** 389-406.

KASHIWAGI, M., TORTORELLA, M., NAGASE, H. & BREW, K. 2001. TIMP-3 is a potent inhibitor of aggrecanase 1 (ADAM-TS4) and aggrecanase 2 (ADAM-TS5). *J Biol Chem,* 276**,** 12501-4.

KAWAGUCHI, Y., OSADA, R., KANAMORI, M., ISHIHARA, H., OHMORI, K., MATSUI, H. & KIMURA, T. 1999. Association between an aggrecan gene polymorphism and lumbar disc degeneration. *Spine (Phila Pa 1976),* 24**,** 2456-60.

KEPLER, C. K., PONNAPPAN, R. K., TANNOURY, C. A., RISBUD, M. V. & ANDERSON, D. G. 2013. The molecular basis of intervertebral disc degeneration. *Spine J,* 13**,** 318-30.

KIM, J. H., CHOI, H., SUH, M. J., SHIN, J. H., HWANG, M. H. & LEE, H. M. 2013. Effect of biphasic electrical current stimulation on IL-1beta-stimulated annulus fibrosus cells using in vitro microcurrent generating chamber system. *Spine (Phila Pa 1976),* 38**,** E1368-76.

KIM, K. W., KIM, Y. S., HA, K. Y., WOO, Y. K., PARK, J. B., PARK, W. S. & AN, H. S. 2005. An autocrine or paracrine Fas-mediated counterattack: a potential mechanism for apoptosis of notochordal cells in intact rat nucleus pulposus. *Spine (Phila Pa 1976),* 30**,** 1247-51.

KIRBY, G.T.S., WHITE, L.J., RAHMAN, C.V., COX, H.C., QUTACHI, O., ROSE, F.R.A.J., HUTMACHER, D.W., SHAKESHEFF, K.M. & WOODRUFF, M.A. 2011.PLGA-Based microparticles for the sustained release of BMP-2. *Polymers,* 3, 571-586.

KLAWITTER, M., HAKOZAKI, M., KOBAYASHI, H., KRUPKOVA, O., QUERO, L., OSPELT, C., GAY, S., HAUSMANN, O., LIEBSCHER, T., MEIER, U., SEKIGUCHI, M., KONNO, S., BOOS, N., FERGUSON, S. J. & WUERTZ, K. 2014. Expression and regulation of toll-like receptors (TLRs) in human intervertebral disc cells. *Eur Spine J,* 23**,** 1878-91.

KOLF, C. M., CHO, E. & TUAN, R. S. 2007. Mesenchymal stromal cells. Biology of adult mesenchymal stem cells: regulation of niche, self-renewal and differentiation. *Arthritis Res Ther,* 9**,** 204.

KORECKI, C. L., COSTI, J. J. & IATRIDIS, J. C. 2008. Needle puncture injury affects intervertebral disc mechanics and biology in an organ culture model. *Spine (Phila Pa 1976),* 33**,** 235-41.

KORECKI, C. L., MACLEAN, J. J. & IATRIDIS, J. C. 2007. Characterization of an in vitro intervertebral disc organ culture system. *Eur Spine J,* 16**,** 1029-37.

KOSHY, P. J., LUNDY, C. J., ROWAN, A. D., PORTER, S., EDWARDS, D. R., HOGAN, A., CLARK, I. M. & CAWSTON, T. E. 2002. The modulation of matrix metalloproteinase and ADAM gene expression in human chondrocytes by interleukin-1 and oncostatin M: a time-course study using real-time quantitative reverse transcription-polymerase chain reaction. *Arthritis Rheum,* 46**,** 961-7.

KRAGSTRUP, T. W., KJAER, M. & MACKEY, A. L. 2011. Structural, biochemical, cellular, and functional changes in skeletal muscle extracellular matrix with aging. *Scand J Med Sci Sports,* 21**,** 749-57.

KREBS, S., FISCHALECK, M. & BLUM, H. 2009. A simple and loss-free method to remove TRIzol contaminations from minute RNA samples. *Anal Biochem,* 387**,** 136-8.

KUH, S. U., ZHU, Y., LI, J., TSAI, K. J., FEI, Q., HUTTON, W. C. & YOON, S. T. 2008. The AdLMP-1 transfection in two different cells; AF cells, chondrocytes as potential cell therapy candidates for disc degeneration. *Acta Neurochir (Wien),* 150**,** 803-10.

KUMAR, A., VARGHESE, M., MOHAN, D., MAHAJAN, P., GULATI, P. & KALE, S. 1999. Effect of whole-body vibration on the low back. A study of tractor-driving farmers in north India. *Spine (Phila Pa 1976),* 24**,** 2506-15.

LAI-FOOK, S. J. & HYATT, R. E. 2000. Effects of age on elastic moduli of human lungs. *J Appl Physiol (1985),* 89**,** 163-8.

LAZEBNIK, M., SINGH, M., GLATT, P., FRIIS, L. A., BERKLAND, C. J. & DETAMORE, M. S. 2011. Biomimetic method for combining the nucleus pulposus and annulus fibrosus for intervertebral disc tissue engineering. *J Tissue Eng Regen Med,* 5**,** e179-87.

LE MAITRE, C. L., BAIRD, P., FREEMONT, A. J. & HOYLAND, J. A. 2009a. An in vitro study investigating the survival and phenotype of mesenchymal stem cells following injection into nucleus pulposus tissue. *Arthritis Res Ther,* 11**,** R20.

LE MAITRE, C. L., FOTHERINGHAM, A. P., FREEMONT, A. J. & HOYLAND, J. A. 2009b. Development of an in vitro model to test the efficacy of novel therapies for IVD degeneration. *J Tissue Eng Regen Med,* 3**,** 461-9.

LE MAITRE, C. L., FREEMONT, A. J. & HOYLAND, J. A. 2004a. Localization of degradative enzymes and their inhibitors in the degenerate human intervertebral disc. *J Pathol,* 204**,** 47-54.

LE MAITRE, C. L., FREEMONT, A. J. & HOYLAND, J. A. 2005. The role of interleukin-1 in the pathogenesis of human intervertebral disc degeneration. *Arthritis Res Ther,* 7**,** R732-45.

LE MAITRE, C. L., FREEMONT, A. J. & HOYLAND, J. A. 2006a. Human disc degeneration is associated with increased MMP 7 expression. *Biotech Histochem,* 81**,** 125-31.

LE MAITRE, C. L., FREEMONT, A. J. & HOYLAND, J. A. 2006b. A preliminary in vitro study into the use of IL-1Ra gene therapy for the inhibition of intervertebral disc degeneration. *Int J Exp Pathol,* 87**,** 17-28.

LE MAITRE, C. L., FREEMONT, A. J. & HOYLAND, J. A. 2007a. Accelerated cellular senescence in degenerate intervertebral discs: a possible role in the pathogenesis of intervertebral disc degeneration. *Arthritis Res Ther,* 9**,** R45.

LE MAITRE, C. L., FREEMONT, A. J. & HOYLAND, J. A. 2009c. Expression of cartilage-derived morphogenetic protein in human intervertebral discs and its effect on matrix synthesis in degenerate human nucleus pulposus cells. *Arthritis Res Ther,* 11**,** R137.

LE MAITRE, C. L., HOYLAND, J. A. & FREEMONT, A. J. 2004b. Studies of human intervertebral disc cell function in a constrained in vitro tissue culture system. *Spine (Phila Pa 1976),* 29**,** 1187-95.

LE MAITRE, C. L., HOYLAND, J. A. & FREEMONT, A. J. 2007b. Catabolic cytokine expression in degenerate and herniated human intervertebral discs: IL-1beta and TNFalpha expression profile. *Arthritis Res Ther,* 9**,** R77.

LE MAITRE, C. L., HOYLAND, J. A. & FREEMONT, A. J. 2007c. Interleukin-1 receptor antagonist delivered directly and by gene therapy inhibits matrix degradation in the intact degenerate human intervertebral disc: an in situ zymographic and gene therapy study. *Arthritis Res Ther,* 9**,** R83.

LE MAITRE, C. L., POCKERT, A., BUTTLE, D. J., FREEMONT, A. J. & HOYLAND, J. A. 2007d. Matrix synthesis and degradation in human intervertebral disc degeneration. *Biochem Soc Trans,* 35**,** 652-5.

LEE, C. K. 1988. Accelerated degeneration of the segment adjacent to a lumbar fusion. *Spine (Phila Pa 1976),* 13**,** 375-7.

LEE, C. R., IATRIDIS, J. C., POVEDA, L. & ALINI, M. 2006. In vitro organ culture of the bovine intervertebral disc: effects of vertebral endplate and potential for mechanobiology studies. *Spine (Phila Pa 1976),* 31**,** 515-22.

LEE, C. R., SAKAI, D., NAKAI, T., TOYAMA, K., MOCHIDA, J., ALINI, M. & GRAD, S. 2007. A phenotypic comparison of intervertebral disc and articular cartilage cells in the rat. *Eur Spine J,* 16**,** 2174-85.

LEE, J. M., SONG, J. Y., BAEK, M., JUNG, H. Y., KANG, H., HAN, I. B., KWON, Y. D. & SHIN, D. E. 2011. Interleukin-1beta induces angiogenesis and innervation in human intervertebral disc degeneration. *J Orthop Res,* 29**,** 265-9.

LI, H., TAO, Y., LIANG, C., HAN, B., LI, F., CHEN, G. & CHEN, Q. 2013. Influence of hypoxia in the intervertebral disc on the biological behaviors of rat adipose- and nucleus pulposus-derived mesenchymal stem cells. *Cells Tissues Organs,* 198**,** 266-77.

LI, X., LEO, B. M., BECK, G., BALIAN, G. & ANDERSON, G. D. 2004. Collagen and proteoglycan abnormalities in the GDF-5-deficient mice and molecular changes when treating disk cells with recombinant growth factor. *Spine (Phila Pa 1976),* 29**,** 2229-34.

LI, Y. Y., DIAO, H. J., CHIK, T. K., CHOW, C. T., AN, X. M., LEUNG, V., CHEUNG, K. M. & CHAN, B. P. 2014. Delivering mesenchymal stem cells in collagen microsphere carriers to rabbit degenerative disc: reduced risk of osteophyte formation. *Tissue Eng Part A,* 20**,** 1379-91.

LIANG, C. Z., LI, H., TAO, Y. Q., ZHOU, X. P., YANG, Z. R., LI, F. C. & CHEN, Q. X. 2012. The relationship between low pH in intervertebral discs and low back pain: a systematic review. *Arch Med Sci,* 8**,** 952-6.

LIEBSCHER, T., HAEFELI, M., WUERTZ, K., NERLICH, A. G. & BOOS, N. 2011. Age-related variation in cell density of human lumbar intervertebral disc. *Spine (Phila Pa 1976),* 36**,** 153-9.

LIU, L. T., HUANG, B., LI, C. Q., ZHUANG, Y., WANG, J. & ZHOU, Y. 2011. Characteristics of stem cells derived from the degenerated human intervertebral disc cartilage endplate. *PLoS One,* 6**,** e26285.

LIU, X. W., KANG, J., FAN, X. D. & SUN, L. F. 2013. Expression and significance of VEGF and p53 in rat degenerated intervertebral disc tissues. *Asian Pac J Trop Med,* 6**,** 404-6.

LIVAK, K. J. & SCHMITTGEN, T. D. 2001. Analysis of relative gene expression data using real-time quantitative PCR and the 2(-Delta Delta C(T)) Method. *Methods,* 25**,** 402-8.

LONGOBARDI, L., O'REAR, L., AAKULA, S., JOHNSTONE, B., SHIMER, K., CHYTIL, A., HORTON, W. A., MOSES, H. L. & SPAGNOLI, A. 2006. Effect of IGF-I in the chondrogenesis of bone marrow mesenchymal stem cells in the presence or absence of TGF-beta signaling. *J Bone Miner Res,* 21**,** 626-36.

LOTZ, J. C. 2004. Animal models of intervertebral disc degeneration: lessons learned. *Spine (Phila Pa 1976),* 29**,** 2742-50.

LOUMAN-GARDINER, K. M., COOMBE, D. & HUNTER, C. J. 2011. Computation models simulating notochordal cell extinction during early ageing of an intervertebral disc. *Comput Methods Biomech Biomed Engin,* 14**,** 1071-7.

LUDWINSKI, F. E., GNANALINGHAM, K., RICHARDSON, S. M. & HOYLAND, J. A. 2013. Understanding the native nucleus pulposus cell phenotype has important implications for intervertebral disc regeneration strategies. *Regen Med,* 8**,** 75-87.

MACLEAN, J. J., LEE, C. R., ALINI, M. & IATRIDIS, J. C. 2004. Anabolic and catabolic mRNA levels of the intervertebral disc vary with the magnitude and frequency of in vivo dynamic compression. *J Orthop Res,* 22**,** 1193-200.

MAERZ, T., HERKOWITZ, H. & BAKER, K. 2013. Molecular and genetic advances in the regeneration of the intervertebral disc. *Surg Neurol Int,* 4**,** S94-S105.

MAIDHOF, R., ALIPUI, D. O., RAFIUDDIN, A., LEVINE, M., GRANDE, D. A. & CHAHINE, N. O. 2012. Emerging trends in biological therapy for intervertebral disc degeneration. *Discov Med,* 14**,** 401-11.

MALDA, J., VAN BLITTERSWIJK, C. A., GROJEC, M., MARTENS, D. E., TRAMPER, J. & RIESLE, J. 2003. Expansion of bovine chondrocytes on microcarriers enhances redifferentiation. *Tissue Eng,* 9**,** 939-48.

MANIADAKIS, N. & GRAY, A. 2000. The economic burden of back pain in the UK. *Pain,* 84**,** 95-103.

MARCHAND, F. & AHMED, A. M. 1990. Investigation of the laminate structure of lumbar disc anulus fibrosus. *Spine (Phila Pa 1976),* 15**,** 402-10.

MARKWAY, B. D., TAN, G. K., BROOKE, G., HUDSON, J. E., COOPER-WHITE, J. J. & DORAN, M. R. 2010. Enhanced chondrogenic differentiation of human bone marrow-derived mesenchymal stem cells in low oxygen environment micropellet cultures. *Cell Transplant,* 19**,** 29-42.

MAROUDAS, A., STOCKWELL, R. A., NACHEMSON, A. & URBAN, J. 1975. Factors involved in the nutrition of the human lumbar intervertebral disc: cellularity and diffusion of glucose in vitro. *J Anat,* 120**,** 113-30.

MARTIN, B. I., DEYO, R. A., MIRZA, S. K., TURNER, J. A., COMSTOCK, B. A., HOLLINGWORTH, W. & SULLIVAN, S. D. 2008. Expenditures and health status among adults with back and neck problems. *JAMA,* 299**,** 656-64.

MASHAYEKHI, F., SHAFIEE, G., KAZEMI, M. & DOLATI, P. 2010. Lumbar disk degeneration disease and aggrecan gene polymorphism in northern Iran. *Biochem Genet,* 48**,** 684-9.

MASUDA, K., TAKEGAMI, K., AN, H., KUMANO, F., CHIBA, K., ANDERSSON, G. B., SCHMID, T. & THONAR, E. 2003. Recombinant osteogenic protein-1 upregulates extracellular matrix metabolism by rabbit annulus fibrosus and nucleus pulposus cells cultured in alginate beads. *J Orthop Res,* 21**,** 922-30.

MATSUI, H., KANAMORI, M., ISHIHARA, H., YUDOH, K., NARUSE, Y. & TSUJI, H. 1998. Familial predisposition for lumbar degenerative disc disease. A case-control study. *Spine (Phila Pa 1976),* 23**,** 1029-34.

MATSUMOTO, T., KAWAKAMI, M., KURIBAYASHI, K., TAKENAKA, T. & TAMAKI, T. 1999. Cyclic mechanical stretch stress increases the growth rate and collagen synthesis of nucleus pulposus cells in vitro. *Spine (Phila Pa 1976),* 24**,** 315-9.

MCCANN, M. R., TAMPLIN, O. J., ROSSANT, J. & SEGUIN, C. A. 2012. Tracing notochord-derived cells using a Noto-cre mouse: implications for intervertebral disc development. *Dis Model Mech,* 5**,** 73-82.

MEISEL, H. J., SIODLA, V., GANEY, T., MINKUS, Y., HUTTON, W. C. & ALASEVIC, O. J. 2007. Clinical experience in cell-based therapeutics: disc chondrocyte transplantation A treatment for degenerated or damaged intervertebral disc. *Biomol Eng,* 24**,** 5-21.

MELROSE, J., SMITH, S. M., APPLEYARD, R. C. & LITTLE, C. B. 2008. Aggrecan, versican and type VI collagen are components of annular translamellar crossbridges in the intervertebral disc. *Eur Spine J,* 17**,** 314-24.

MENG, F. T., MA, G. H., QIU, W. & SU, Z. G. 2003. W/O/W double emulsion technique using ethyl acetate as organic solvent: effects of its diffusion rate on the characteristics of microparticles. *J Control Release,* 91**,** 407-16.

MEYER, K. C., ROSENTHAL, N. S., SOERGEL, P. & PETERSON, K. 1998. Neutrophils and low-grade inflammation in the seemingly normal aging human lung. *Mech Ageing Dev,* 104**,** 169-81.

MILLER, V. M., CLOUSE, W. D., TONNESSEN, B. H., BOSTON, U. S., SEVERSON, S. R., BONDE, S., RUD, K. S. & HURT, R. D. 2000. Time and dose effect of transdermal nicotine on endothelial function. *Am J Physiol Heart Circ Physiol,* 279**,** H1913-21.

MILLWARD-SADLER, S. J., COSTELLO, P. W., FREEMONT, A. J. & HOYLAND, J. A. 2009. Regulation of catabolic gene expression in normal and degenerate human intervertebral disc cells: implications for the pathogenesis of intervertebral disc degeneration. *Arthritis Res Ther,* 11**,** R65.

MINOGUE, B. M., RICHARDSON, S. M., ZEEF, L. A., FREEMONT, A. J. & HOYLAND, J. A. 2010a. Characterization of the human nucleus pulposus cell phenotype and evaluation of novel marker gene expression to define adult stem cell differentiation. *Arthritis Rheum,* 62**,** 3695-705.

MINOGUE, B. M., RICHARDSON, S. M., ZEEF, L. A., FREEMONT, A. J. & HOYLAND, J. A. 2010b. Transcriptional profiling of bovine intervertebral disc cells: implications for identification of normal and degenerate human intervertebral disc cell phenotypes. *Arthritis Res Ther,* 12**,** R22.

MIYAMOTO, K., MASUDA, K., KIM, J. G., INOUE, N., AKEDA, K., ANDERSSON, G. B. & AN, H. S. 2006. Intradiscal injections of osteogenic protein-1 restore the viscoelastic properties of degenerated intervertebral discs. *Spine J,* 6**,** 692-703.

MIYAZAKI, T., KOBAYASHI, S., TAKENO, K., MEIR, A., URBAN, J. & BABA, H. 2009. A phenotypic comparison of proteoglycan production of intervertebral disc cells isolated from rats, rabbits, and bovine tails; which animal model is most suitable to study tissue engineering and biological repair of human disc disorders? *Tissue Eng Part A,* 15**,** 3835-46.

MOON, H. J., YURUBE, T., LOZITO, T. P., POHL, P., HARTMAN, R. A., SOWA, G. A., KANG, J. D. & VO, N. V. 2014. Effects of secreted factors in culture medium of annulus fibrosus cells on microvascular endothelial cells: elucidating the possible pathomechanisms of matrix degradation and nerve in-growth in disc degeneration. *Osteoarthritis Cartilage,* 22**,** 344-54.

MOSS, I. L., GORDON, L., WOODHOUSE, K. A., WHYNE, C. M. & YEE, A. J. 2011. A novel thiol-modified hyaluronan and elastin-like polypetide composite material for tissue engineering of the nucleus pulposus of the intervertebral disc. *Spine (Phila Pa 1976),* 36**,** 1022-9.

MWALE, F., CIOBANU, I., GIANNITSIOS, D., ROUGHLEY, P., STEFFEN, T. & ANTONIOU, J. 2011. Effect of oxygen levels on proteoglycan synthesis by intervertebral disc cells. *Spine (Phila Pa 1976),* 36**,** E131-8.

MWALE, F., ROUGHLEY, P. & ANTONIOU, J. 2004. Distinction between the extracellular matrix of the nucleus pulposus and hyaline cartilage: a requisite for tissue engineering of intervertebral disc. *Eur Cell Mater,* 8**,** 58-63; discussion 63-4.

MWALE, F., WANG, H. T., ROUGHLEY, P., ANTONIOU, J. & HAGLUND, L. 2014. Link N and mesenchymal stem cells can induce regeneration of the early degenerate intervertebral disc. *Tissue Eng Part A,* 20**,** 2942-9.

NAQVI, S. M. & BUCKLEY, C. T. 2015. Differential response of encapsulated nucleus pulposus and bone marrow stem cells in isolation and coculture in alginate and chitosan hydrogels. *Tissue Eng Part A,* 21**,** 288-99.

NERLICH, A. G., SCHLEICHER, E. D. & BOOS, N. 1997. 1997 Volvo Award winner in basic science studies. Immunohistologic markers for age-related changes of human lumbar intervertebral discs. *Spine (Phila Pa 1976),* 22**,** 2781-95.

NESTI, L. J., LI, W. J., SHANTI, R. M., JIANG, Y. J., JACKSON, W., FREEDMAN, B. A., KUKLO, T. R., GIULIANI, J. R. & TUAN, R. S. 2008. Intervertebral disc tissue engineering using a novel hyaluronic acid-nanofibrous scaffold (HANFS) amalgam. *Tissue Eng Part A,* 14**,** 1527-37.

NIHANT, N., SCHUGENS, C., GRANDFILS, C., JEROME, R. & TEYSSIE, P. 1994. Polylactide microparticles prepared by double emulsion/evaporation technique. I. Effect of primary emulsion stability. *Pharm Res,* 11**,** 1479-84.

NISHIDA, K., KANG, J. D., GILBERTSON, L. G., MOON, S. H., SUH, J. K., VOGT, M. T., ROBBINS, P. D. & EVANS, C. H. 1999. Modulation of the biologic activity of the rabbit intervertebral disc by gene therapy: an in vivo study of adenovirus-mediated transfer of the human transforming growth factor beta 1 encoding gene. *Spine (Phila Pa 1976),* 24**,** 2419-25.

NISHIMURA, K. & MOCHIDA, J. 1998. Percutaneous reinsertion of the nucleus pulposus. An experimental study. *Spine (Phila Pa 1976),* 23**,** 1531-8; discussion 1539.

NOCHI, H., SUNG, J. H., LOU, J., ADKISSON, H. D., MALONEY, W. J. & HRUSKA, K. A. 2004. Adenovirus mediated BMP-13 gene transfer induces chondrogenic differentiation of murine mesenchymal progenitor cells. *J Bone Miner Res,* 19**,** 111-22.

NOMURA, T., MOCHIDA, J., OKUMA, M., NISHIMURA, K. & SAKABE, K. 2001. Nucleus pulposus allograft retards intervertebral disc degeneration. *Clin Orthop Relat Res***,** 94-101.

NORCROSS, J. P., LESTER, G. E., WEINHOLD, P. & DAHNERS, L. E. 2003. An in vivo model of degenerative disc disease. *J Orthop Res,* 21**,** 183-8.

O'CONNELL, G. D., GUERIN, H. L. & ELLIOTT, D. M. 2009. Theoretical and uniaxial experimental evaluation of human annulus fibrosus degeneration. *J Biomech Eng,* 131**,** 111007.

OGAWA, R., MIZUNO, S., MURPHY, G. F. & ORGILL, D. P. 2009. The effect of hydrostatic pressure on three-dimensional chondroinduction of human adipose-derived stem cells. *Tissue Eng Part A,* 15**,** 2937-45.

OKUMA, M., MOCHIDA, J., NISHIMURA, K., SAKABE, K. & SEIKI, K. 2000. Reinsertion of stimulated nucleus pulposus cells retards intervertebral disc degeneration: an in vitro and in vivo experimental study. *J Orthop Res,* 18**,** 988-97.

OLDERSHAW, R. A., BAXTER, M. A., LOWE, E. T., BATES, N., GRADY, L. M., SONCIN, F., BRISON, D. R., HARDINGHAM, T. E. & KIMBER, S. J. 2010. Directed differentiation of human embryonic stem cells toward chondrocytes. *Nat Biotechnol,* 28**,** 1187-94.

OROZCO, L., SOLER, R., MORERA, C., ALBERCA, M., SANCHEZ, A. & GARCIA-SANCHO, J. 2011. Intervertebral disc repair by autologous mesenchymal bone marrow cells: a pilot study. *Transplantation,* 92**,** 822-8.

ORRENIUS, S., GOGVADZE, V. & ZHIVOTOVSKY, B. 2015. Calcium and mitochondria in the regulation of cell death. *Biochem Biophys Res Commun,* 460**,** 72-81.

OSADA, R., OHSHIMA, H., ISHIHARA, H., YUDOH, K., SAKAI, K., MATSUI, H. & TSUJI, H. 1996. Autocrine/paracrine mechanism of insulin-like growth factor-1 secretion, and the effect of insulin-like growth factor-1 on proteoglycan synthesis in bovine intervertebral discs. *J Orthop Res,* 14**,** 690-9.

OSHIMA, H., ISHIHARA, H., URBAN, J. P. & TSUJI, H. 1993. The use of coccygeal discs to study intervertebral disc metabolism. *J Orthop Res,* 11**,** 332-8.

OZASA, Y., GINGERY, A., THORESON, A. R., AN, K. N., ZHAO, C. & AMADIO, P. C. 2014. A comparative study of the effects of growth and differentiation factor 5 on muscle-derived stem cells and bone marrow stromal cells in an in vitro tendon healing model. *J Hand Surg Am,* 39**,** 1706-13.

PAPAGEORGIOU, A. C., CROFT, P. R., FERRY, S., JAYSON, M. I. & SILMAN, A. J. 1995. Estimating the prevalence of low back pain in the general population. Evidence from the South Manchester Back Pain Survey. *Spine (Phila Pa 1976),* 20**,** 1889-94.

PATTAPPA, G., LI, Z., PEROGLIO, M., WISMER, N., ALINI, M. & GRAD, S. 2012. Diversity of intervertebral disc cells: phenotype and function. *J Anat,* 221**,** 480-96.

PAUL, C. P., SCHOORL, T., ZUIDERBAAN, H. A., ZANDIEH DOULABI, B., VAN DER VEEN, A. J., VAN DE VEN, P. M., SMIT, T. H., VAN ROYEN, B. J., HELDER, M. N. & MULLENDER, M. G. 2013. Dynamic and static overloading induce early degenerative processes in caprine lumbar intervertebral discs. *PLoS One,* 8**,** e62411.

PAUL, C. P., ZUIDERBAAN, H. A., ZANDIEH DOULABI, B., VAN DER VEEN, A. J., VAN DE VEN, P. M., SMIT, T. H., HELDER, M. N., VAN ROYEN, B. J. & MULLENDER, M. G. 2012. Simulated-physiological loading conditions preserve biological and mechanical properties of caprine lumbar intervertebral discs in ex vivo culture. *PLoS One,* 7**,** e33147.

PAUL, R., HAYDON, R. C., CHENG, H., ISHIKAWA, A., NENADOVICH, N., JIANG, W., ZHOU, L., BREYER, B., FENG, T., GUPTA, P., HE, T. C. & PHILLIPS, F. M. 2003. Potential use of Sox9 gene therapy for intervertebral degenerative disc disease. *Spine (Phila Pa 1976),* 28**,** 755-63.

PEREIRA, C. L., GONCALVES, R. M., PEROGLIO, M., PATTAPPA, G., D'ESTE, M., EGLIN, D., BARBOSA, M. A., ALINI, M. & GRAD, S. 2014. The effect of hyaluronan-based delivery of stromal cell-derived factor-1 on the recruitment of MSCs in degenerating intervertebral discs. *Biomaterials,* 35**,** 8144-53.

PEREIRA, D. R., SILVA-CORREIA, J., OLIVEIRA, J. M. & REIS, R. L. 2013. Hydrogels in acellular and cellular strategies for intervertebral disc regeneration. *J Tissue Eng Regen Med,* 7**,** 85-98.

PEROGLIO, M., EGLIN, D., BENNEKER, L. M., ALINI, M. & GRAD, S. 2013. Thermoreversible hyaluronan-based hydrogel supports in vitro and ex vivo disc-like differentiation of human mesenchymal stem cells. *Spine J,* 13**,** 1627-39.

PEROGLIO, M., GRAD, S., MORTISEN, D., SPRECHER, C. M., ILLIEN-JUNGER, S., ALINI, M. & EGLIN, D. 2012. Injectable thermoreversible hyaluronan-based hydrogels for nucleus pulposus cell encapsulation. *Eur Spine J,* 21 Suppl 6**,** S839-49.

PHILLIPS, K. L., CHIVERTON, N., MICHAEL, A. L., COLE, A. A., BREAKWELL, L. M., HADDOCK, G., BUNNING, R. A., CROSS, A. K. & LE MAITRE, C. L. 2013. The cytokine and chemokine expression profile of nucleus pulposus cells: implications for degeneration and regeneration of the intervertebral disc. *Arthritis Res Ther,* 15**,** R213.

PHILLIPS, K. L., CULLEN, K., CHIVERTON, N., MICHAEL, A. L., COLE, A. A., BREAKWELL, L. M., HADDOCK, G., BUNNING, R. A., CROSS, A. K. & LE MAITRE, C. L. 2015. Potential roles of cytokines and chemokines in human intervertebral disc degeneration: interleukin-1 is a master regulator of catabolic processes. *Osteoarthritis Cartilage,* 23**,** 1165-77.

PITTENGER, M. F., MACKAY, A. M., BECK, S. C., JAISWAL, R. K., DOUGLAS, R., MOSCA, J. D., MOORMAN, M. A., SIMONETTI, D. W., CRAIG, S. & MARSHAK, D. R. 1999. Multilineage potential of adult human mesenchymal stem cells. *Science,* 284**,** 143-7.

PLUIJM, S. M., VAN ESSEN, H. W., BRAVENBOER, N., UITTERLINDEN, A. G., SMIT, J. H., POLS, H. A. & LIPS, P. 2004. Collagen type I alpha1 Sp1 polymorphism, osteoporosis, and intervertebral disc degeneration in older men and women. *Ann Rheum Dis,* 63**,** 71-7.

POCKERT, A. J., RICHARDSON, S. M., LE MAITRE, C. L., LYON, M., DEAKIN, J. A., BUTTLE, D. J., FREEMONT, A. J. & HOYLAND, J. A. 2009. Modified expression of the ADAMTS enzymes and tissue inhibitor of metalloproteinases 3 during human intervertebral disc degeneration. *Arthritis Rheum,* 60**,** 482-91.

PONNAPPAN, R. K., MARKOVA, D. Z., ANTONIO, P. J., MURRAY, H. B., VACCARO, A. R., SHAPIRO, I. M., ANDERSON, D. G., ALBERT, T. J. & RISBUD, M. V. 2011. An organ culture system to model early degenerative changes of the intervertebral disc. *Arthritis Res Ther,* 13**,** R171.

PORTER, S., CLARK, I. M., KEVORKIAN, L. & EDWARDS, D. R. 2005. The ADAMTS metalloproteinases. *Biochem J,* 386**,** 15-27.

POSTACCHINI, F., LAMI, R. & PUGLIESE, O. 1988. Familial predisposition to discogenic low-back pain. An epidemiologic and immunogenetic study. *Spine (Phila Pa 1976),* 13**,** 1403-6.

POWER, K. A., GRAD, S., RUTGES, J. P., CREEMERS, L. B., VAN RIJEN, M. H., O'GAORA, P., WALL, J. G., ALINI, M., PANDIT, A. & GALLAGHER, W. M. 2011. Identification of cell surface-specific markers to target human nucleus pulposus cells: expression of carbonic anhydrase XII varies with age and degeneration. *Arthritis Rheum,* 63**,** 3876-86.

PURMESSUR, D., FREEMONT, A. J. & HOYLAND, J. A. 2008. Expression and regulation of neurotrophins in the nondegenerate and degenerate human intervertebral disc. *Arthritis Res Ther,* 10**,** R99.

PURMESSUR, D., WALTER, B. A., ROUGHLEY, P. J., LAUDIER, D. M., HECHT, A. C. & IATRIDIS, J. 2013. A role for TNFalpha in intervertebral disc degeneration: a non-recoverable catabolic shift. *Biochem Biophys Res Commun,* 433**,** 151-6.

RAHMAN, C. V., BEN-DAVID, D., DHILLON, A., KUHN, G., GOULD, T. W., MULLER, R., ROSE, F. R., SHAKESHEFF, K. M. & LIVNE, E. 2014. Controlled release of BMP-2 from a sintered polymer scaffold enhances bone repair in a mouse calvarial defect model. *J Tissue Eng Regen Med,* 8**,** 59-66.

RAJ, P. P. 2008. Intervertebral disc: anatomy-physiology-pathophysiology-treatment. *Pain Pract,* 8**,** 18-44.

RATNER, B. D. & BRYANT, S. J. 2004. Biomaterials: where we have been and where we are going. *Annu Rev Biomed Eng,* 6**,** 41-75.

RATSEP, T., MINAJEVA, A. & ASSER, T. 2013. Relationship between neovascularization and degenerative changes in herniated lumbar intervertebral discs. *Eur Spine J,* 22**,** 2474-80.

RICHARDSON, S. M., CURRAN, J. M., CHEN, R., VAUGHAN-THOMAS, A., HUNT, J. A., FREEMONT, A. J. & HOYLAND, J. A. 2006a. The differentiation of bone marrow mesenchymal stem cells into chondrocyte-like cells on poly-L-lactic acid (PLLA) scaffolds. *Biomaterials,* 27**,** 4069-78.

RICHARDSON, S. M. & HOYLAND, J. A. 2008a. Stem cell regeneration of degenerated intervertebral discs: current status. *Curr Pain Headache Rep,* 12**,** 83-8.

RICHARDSON, S. M., HUGHES, N., HUNT, J. A., FREEMONT, A. J. & HOYLAND, J. A. 2008b. Human mesenchymal stem cell differentiation to NP-like cells in chitosan-glycerophosphate hydrogels. *Biomaterials,* 29**,** 85-93.

RICHARDSON, S. M., WALKER, R. V., PARKER, S., RHODES, N. P., HUNT, J. A., FREEMONT, A. J. & HOYLAND, J. A. 2006b. Intervertebral disc cell-mediated mesenchymal stem cell differentiation. *Stem Cells,* 24**,** 707-16.

RISBUD, M. V., ALBERT, T. J., GUTTAPALLI, A., VRESILOVIC, E. J., HILLIBRAND, A. S., VACCARO, A. R. & SHAPIRO, I. M. 2004. Differentiation of mesenchymal stem cells towards a nucleus pulposus-like phenotype in vitro: implications for cell-based transplantation therapy. *Spine (Phila Pa 1976),* 29**,** 2627-32.

RISBUD, M. V., GUTTAPALLI, A., STOKES, D. G., HAWKINS, D., DANIELSON, K. G., SCHAER, T. P., ALBERT, T. J. & SHAPIRO, I. M. 2006. Nucleus pulposus cells express HIF-1 alpha under normoxic culture conditions: a metabolic adaptation to the intervertebral disc microenvironment. *J Cell Biochem,* 98**,** 152-9.

RISBUD, M. V., GUTTAPALLI, A., TSAI, T. T., LEE, J. Y., DANIELSON, K. G., VACCARO, A. R., ALBERT, T. J., GAZIT, Z., GAZIT, D. & SHAPIRO, I. M. 2007. Evidence for skeletal progenitor cells in the degenerate human intervertebral disc. *Spine (Phila Pa 1976),* 32**,** 2537-44.

RISBUD, M. V., IZZO, M. W., ADAMS, C. S., ARNOLD, W. W., HILLIBRAND, A. S., VRESILOVIC, E. J., VACCARO, A. R., ALBERT, T. J. & SHAPIRO, I. M. 2003. An organ culture system for the study of the nucleus pulposus: description of the system and evaluation of the cells. *Spine (Phila Pa 1976),* 28**,** 2652-8; discussion 2658-9.

RISBUD, M. V., SCHOEPFLIN, Z. R., MWALE, F., KANDEL, R. A., GRAD, S., IATRIDIS, J. C., SAKAI, D. & HOYLAND, J. A. 2015. Defining the

phenotype of young healthy nucleus pulposus cells: recommendations of the Spine Research Interest Group at the 2014 annual ORS meeting. *J Orthop Res,* 33**,** 283-93.

ROBERTS, S., AYAD, S. & MENAGE, P. J. 1991. Immunolocalisation of type VI collagen in the intervertebral disc. *Ann Rheum Dis,* 50**,** 787-91.

ROBERTS, S., CATERSON, B., MENAGE, J., EVANS, E. H., JAFFRAY, D. C. & EISENSTEIN, S. M. 2000. Matrix metalloproteinases and aggrecanase: their role in disorders of the human intervertebral disc. *Spine (Phila Pa 1976),* 25**,** 3005-13.

ROBERTS, S., EVANS, H., TRIVEDI, J. & MENAGE, J. 2006. Histology and pathology of the human intervertebral disc. *J Bone Joint Surg Am,* 88 Suppl 2**,** 10-4.

ROBERTS, S., MENAGE, J., SIVAN, S. & URBAN, J. P. 2008. Bovine explant model of degeneration of the intervertebral disc. *BMC Musculoskelet Disord,* 9**,** 24.

ROBERTS, S., MENAGE, J. & URBAN, J. P. 1989. Biochemical and structural properties of the cartilage end-plate and its relation to the intervertebral disc. *Spine (Phila Pa 1976),* 14**,** 166-74.

ROBERTS, S., URBAN, J. P., EVANS, H. & EISENSTEIN, S. M. 1996. Transport properties of the human cartilage endplate in relation to its composition and calcification. *Spine (Phila Pa 1976),* 21**,** 415-20.

ROUGHLEY, P. J. 2004. Biology of intervertebral disc aging and degeneration: involvement of the extracellular matrix. *Spine (Phila Pa 1976),* 29**,** 2691-9.

RUTGES, J., CREEMERS, L. B., DHERT, W., MILZ, S., SAKAI, D., MOCHIDA, J., ALINI, M. & GRAD, S. 2010. Variations in gene and protein expression in human nucleus pulposus in comparison with annulus fibrosus and cartilage cells: potential associations with aging and degeneration. *Osteoarthritis Cartilage,* 18**,** 416-23.

SAKAI, D., MOCHIDA, J., IWASHINA, T., WATANABE, T., NAKAI, T., ANDO, K. & HOTTA, T. 2005. Differentiation of mesenchymal stem cells transplanted to a rabbit degenerative disc model: potential and limitations for stem cell therapy in disc regeneration. *Spine (Phila Pa 1976),* 30**,** 2379-87.

SAKAI, D., MOCHIDA, J., IWASHINA, T., WATANABE, T., SUYAMA, K., ANDO, K. & HOTTA, T. 2006. Atelocollagen for culture of human nucleus pulposus cells forming nucleus pulposus-like tissue in vitro: influence on the proliferation and proteoglycan production of HNPSV-1 cells. *Biomaterials,* 27**,** 346-53.

SAKAI, D., NAKAMURA, Y., NAKAI, T., MISHIMA, T., KATO, S., GRAD, S., ALINI, M., RISBUD, M. V., CHAN, D., CHEAH, K. S., YAMAMURA, K., MASUDA, K., OKANO, H., ANDO, K. & MOCHIDA, J. 2012. Exhaustion of nucleus pulposus progenitor cells with ageing and degeneration of the intervertebral disc. *Nat Commun,* 3**,** 1264.

SAMARTZIS, D., KARPPINEN, J., MOK, F., FONG, D. Y., LUK, K. D. & CHEUNG, K. M. 2011. A population-based study of juvenile disc degeneration and its association with overweight and obesity, low back pain, and diminished functional status. *J Bone Joint Surg Am,* 93**,** 662-70.

SAUNDERS, J. M., TONG, T., LE MAITRE, C.L., FREEMONT, T.J. & SAUNDERS, B.R. 2007. A study of pH-responsive microgel dispersions:from fluid-to-gel transitions to mechanical property restoration for load-bearing tissue.*Soft Matter*, 3, 486-494.

SCOTT, J. E., BOSWORTH, T. R., CRIBB, A. M. & TAYLOR, J. R. 1994. The chemical morphology of age-related changes in human intervertebral disc glycosaminoglycans from cervical, thoracic and lumbar nucleus pulposus and annulus fibrosus. *J Anat,* 184 (Pt 1)**,** 73-82.

SEE, E. Y., TOH, S. L. & GOH, J. C. 2012. Simulated intervertebral disc-like assembly using bone marrow-derived mesenchymal stem cell sheets and silk scaffolds for annulus fibrosus regeneration. *J Tissue Eng Regen Med,* 6**,** 528-35.

SEKIYA, I., VUORISTO, J. T., LARSON, B. L. & PROCKOP, D. J. 2002. In vitro cartilage formation by human adult stem cells from bone marrow stroma defines the sequence of cellular and molecular events during chondrogenesis. *Proc Natl Acad Sci U S A,* 99**,** 4397-402.

SETTLE, S. H., JR., ROUNTREE, R. B., SINHA, A., THACKER, A., HIGGINS, K. & KINGSLEY, D. M. 2003. Multiple joint and skeletal patterning defects caused by single and double mutations in the mouse Gdf6 and Gdf5 genes. *Dev Biol,* 254**,** 116-30.

SHEN, B., BHARGAV, D., WEI, A., WILLIAMS, L. A., TAO, H., MA, D. D. & DIWAN, A. D. 2009. BMP-13 emerges as a potential inhibitor of bone formation. *Int J Biol Sci,* 5**,** 192-200.

SHIVE, M. S. & ANDERSON, J. M. 1997. Biodegradation and biocompatibility of PLA and PLGA microspheres. *Adv Drug Deliv Rev,* 28**,** 5-24.

SHOWALTER, B. L., BECKSTEIN, J. C., MARTIN, J. T., BEATTIE, E. E., ESPINOZA ORIAS, A. A., SCHAER, T. P., VRESILOVIC, E. J. & ELLIOTT, D. M. 2012. Comparison of animal discs used in disc research to human lumbar disc: torsion mechanics and collagen content. *Spine (Phila Pa 1976),* 37**,** E900-7.

SILVA-CORREIA, J., OLIVEIRA, J. M., CARIDADE, S. G., OLIVEIRA, J. T., SOUSA, R. A., MANO, J. F. & REIS, R. L. 2011. Gellan gum-based hydrogels for intervertebral disc tissue-engineering applications. *J Tissue Eng Regen Med,* 5**,** e97-107.

SINGH, K., MASUDA, K., THONAR, E. J., AN, H. S. & CS-SZABO, G. 2009. Age-related changes in the extracellular matrix of nucleus pulposus and anulus fibrosus of human intervertebral disc. *Spine (Phila Pa 1976),* 34**,** 10-6.

SITTE, I., KATHREIN, A., PFALLER, K., PEDROSS, F. & ROBERTS, S. 2009. Intervertebral disc cell death in the porcine and human injured cervical spine after trauma: a histological and ultrastructural study. *Spine (Phila Pa 1976),* 34**,** 131-40.

SIVAN, S. S., HAYES, A. J., WACHTEL, E., CATERSON, B., MERKHER, Y., MAROUDAS, A., BROWN, S. & ROBERTS, S. 2014. Biochemical composition and turnover of the extracellular matrix of the normal and degenerate intervertebral disc. *Eur Spine J,* 23 Suppl 3**,** S344-53.

SIVE, J. I., BAIRD, P., JEZIORSK, M., WATKINS, A., HOYLAND, J. A. & FREEMONT, A. J. 2002. Expression of chondrocyte markers by cells of normal and degenerate intervertebral discs. *Mol Pathol,* 55**,** 91-7.

SLADE, S. C. & KEATING, J. L. 2007. Unloaded movement facilitation exercise compared to no exercise or alternative therapy on outcomes for people with nonspecific chronic low back pain: a systematic review. *J Manipulative Physiol Ther,* 30**,** 301-11.

SMITH, L. J., GORTH, D. J., SHOWALTER, B. L., CHIARO, J. A., BEATTIE, E. E., ELLIOTT, D. M., MAUCK, R. L., CHEN, W. & MALHOTRA, N. R. 2014. In vitro characterization of a stem-cell-seeded triple-interpenetrating-network hydrogel for functional regeneration of the nucleus pulposus. *Tissue Eng Part A,* 20**,** 1841-9.

SMITH, L. J., NERURKAR, N. L., CHOI, K. S., HARFE, B. D. & ELLIOTT, D. M. 2011. Degeneration and regeneration of the intervertebral disc: lessons from development. *Dis Model Mech,* 4**,** 31-41.

SOLOVIEVA, S., NOPONEN, N., MANNIKKO, M., LEINO-ARJAS, P., LUOMA, K., RAININKO, R., ALA-KOKKO, L. & RIIHIMAKI, H. 2007. Association between the aggrecan gene variable number of tandem repeats polymorphism and intervertebral disc degeneration. *Spine (Phila Pa 1976),* 32**,** 1700-5.

SOUKANE, D. M., SHIRAZI-ADL, A. & URBAN, J. P. 2007. Computation of coupled diffusion of oxygen, glucose and lactic acid in an intervertebral disc. *J Biomech,* 40**,** 2645-54.

STECK, E., BERTRAM, H., ABEL, R., CHEN, B., WINTER, A. & RICHTER, W. 2005. Induction of intervertebral disc-like cells from adult mesenchymal stem cells. *Stem Cells,* 23**,** 403-11.

STEWART, W. F., RICCI, J. A., CHEE, E., MORGANSTEIN, D. & LIPTON, R. 2003. Lost productive time and cost due to common pain conditions in the US workforce. *JAMA,* 290**,** 2443-54.

STOCKWELL, R. A. 1971. The interrelationship of cell density and cartilage thickness in mammalian articular cartilage. *J Anat,* 109**,** 411-21.

STOKES, I. A. & IATRIDIS, J. C. 2004. Mechanical conditions that accelerate intervertebral disc degeneration: overload versus immobilization. *Spine (Phila Pa 1976),* 29**,** 2724-32.

STOYANOV, J. V., GANTENBEIN-RITTER, B., BERTOLO, A., AEBLI, N., BAUR, M., ALINI, M. & GRAD, S. 2011. Role of hypoxia and growth and differentiation factor-5 on differentiation of human mesenchymal stem cells towards intervertebral nucleus pulposus-like cells. *Eur Cell Mater,* 21**,** 533-47.

STUDER, R. K., VO, N., SOWA, G., ONDECK, C. & KANG, J. 2011. Human nucleus pulposus cells react to IL-6: independent actions and amplification of response to IL-1 and TNF-alpha. *Spine (Phila Pa 1976),* 36**,** 593-9.

SUPURAN, C. T. 2008. Carbonic anhydrases: novel therapeutic applications for inhibitors and activators. *Nat Rev Drug Discov,* 7**,** 168-81.

TAKAHASHI, M., HARO, H., WAKABAYASHI, Y., KAWA-UCHI, T., KOMORI, H. & SHINOMIYA, K. 2001. The association of degeneration of the intervertebral disc with 5a/6a polymorphism in the promoter of the human matrix metalloproteinase-3 gene. *J Bone Joint Surg Br,* 83**,** 491-5.

TAKATALO, J., KARPPINEN, J., NIINIMAKI, J., TAIMELA, S., NAYHA, S., MUTANEN, P., SEQUEIROS, R. B., KYLLONEN, E. & TERVONEN, O. 2011. Does lumbar disc degeneration on magnetic resonance imaging associate with low back symptom severity in young Finnish adults? *Spine (Phila Pa 1976),* 36**,** 2180-9.

TASSABEHJI, M., FANG, Z. M., HILTON, E. N., MCGAUGHRAN, J., ZHAO, Z., DE BOCK, C. E., HOWARD, E., MALASS, M., DONNAI, D., DIWAN, A., MANSON, F. D., MURRELL, D. & CLARKE, R. A. 2008. Mutations in GDF6 are associated with vertebral segmentation defects in Klippel-Feil syndrome. *Hum Mutat,* 29**,** 1017-27.

THE COSTS OF ACCIDENTS AT WORK, HS(G) 96 2ND EDITION, HMSO 1997

THOMPSON, J. P., OEGEMA, T. R., JR. & BRADFORD, D. S. 1991. Stimulation of mature canine intervertebral disc by growth factors. *Spine (Phila Pa 1976),* 16**,** 253-60.

TILKERIDIS, C., BEI, T., GARANTZIOTIS, S. & STRATAKIS, C. A. 2005. Association of a COL1A1 polymorphism with lumbar disc disease in young military recruits. *J Med Genet,* 42**,** e44.

TIM YOON, S., SU KIM, K., LI, J., SOO PARK, J., AKAMARU, T., ELMER, W. A. & HUTTON, W. C. 2003. The effect of bone morphogenetic protein-2 on rat intervertebral disc cells in vitro. *Spine (Phila Pa 1976),* 28**,** 1773-80.

TRAN, C. M., SCHOEPFLIN, Z. R., MARKOVA, D. Z., KEPLER, C. K., ANDERSON, D. G., SHAPIRO, I. M. & RISBUD, M. V. 2014. CCN2 suppresses catabolic effects of interleukin-1beta through alpha5beta1 and alphaVbeta3 integrins in nucleus pulposus cells: implications in intervertebral disc degeneration. *J Biol Chem,* 289**,** 7374-87.

TROUT, J. J., BUCKWALTER, J. A. & MOORE, K. C. 1982. Ultrastructure of the human intervertebral disc: II. Cells of the nucleus pulposus. *Anat Rec,* 204**,** 307-14.

TRUONG, V. X., ABLETT, M. P., RICHARDSON, S. M., HOYLAND, J. A. & DOVE, A. P. 2015. Simultaneous orthogonal dual-click approach to tough, in-situ-forming hydrogels for cell encapsulation. *J Am Chem Soc,* 137**,** 1618-22.

TURNER, C. H., RHO, J., TAKANO, Y., TSUI, T. Y. & PHARR, G. M. 1999. The elastic properties of trabecular and cortical bone tissues are similar: results from two microscopic measurement techniques. *J Biomech,* 32**,** 437-41.

URBAN, J. P. 2002. The role of the physicochemical environment in determining disc cell behaviour. *Biochem Soc Trans,* 30**,** 858-64.

URBAN, J. P. & ROBERTS, S. 2003. Degeneration of the intervertebral disc. *Arthritis Res Ther,* 5**,** 120-30.

VERGROESEN, P. P., VAN DER VEEN, A. J., VAN ROYEN, B. J., KINGMA, I. & SMIT, T. H. 2014. Intradiscal pressure depends on recent loading and correlates with disc height and compressive stiffness. *Eur Spine J,* 23**,** 2359-68.

VIDEMAN, T., NURMINEN, M. & TROUP, J. D. 1990. 1990 Volvo Award in clinical sciences. Lumbar spinal pathology in cadaveric material in relation to history of back pain, occupation, and physical loading. *Spine (Phila Pa 1976),* 15**,** 728-40.

VIDEMAN, T., SAARELA, J., KAPRIO, J., NAKKI, A., LEVALAHTI, E., GILL, K., PELTONEN, L. & BATTIE, M. C. 2009. Associations of 25 structural, degradative, and inflammatory candidate genes with lumbar disc desiccation, bulging, and height narrowing. *Arthritis Rheum,* 60**,** 470-81.

VO, N. V., HARTMAN, R. A., YURUBE, T., JACOBS, L. J., SOWA, G. A. & KANG, J. D. 2013. Expression and regulation of metalloproteinases and their inhibitors in intervertebral disc aging and degeneration. *Spine J,* 13**,** 331-41.

WALLACH, C. J., SOBAJIMA, S., WATANABE, Y., KIM, J. S., GEORGESCU, H. I., ROBBINS, P., GILBERTSON, L. G. & KANG, J. D. 2003. Gene transfer of the catabolic inhibitor TIMP-1 increases measured proteoglycans in cells from degenerated human intervertebral discs. *Spine (Phila Pa 1976),* 28**,** 2331-7.

WALSH, A. J., BRADFORD, D. S. & LOTZ, J. C. 2004. In vivo growth factor treatment of degenerated intervertebral discs. *Spine (Phila Pa 1976),* 29**,** 156-63.

WALSH, A. J. & LOTZ, J. C. 2004. Biological response of the intervertebral disc to dynamic loading. *J Biomech,* 37**,** 329-37.

WALTER, B. A., KORECKI, C. L., PURMESSUR, D., ROUGHLEY, P. J., MICHALEK, A. J. & IATRIDIS, J. C. 2011. Complex loading affects

intervertebral disc mechanics and biology. *Osteoarthritis Cartilage,* 19**,** 1011-8.

WANG, G. L., JIANG, B. H., RUE, E. A. & SEMENZA, G. L. 1995. Hypoxia-inducible factor 1 is a basic-helix-loop-helix-PAS heterodimer regulated by cellular O2 tension. *Proc Natl Acad Sci U S A,* 92**,** 5510-4.

WANG, J., MARKOVA, D., ANDERSON, D. G., ZHENG, Z., SHAPIRO, I. M. & RISBUD, M. V. 2011. TNF-alpha and IL-1beta promote a disintegrin-like and metalloprotease with thrombospondin type I motif-5-mediated aggrecan degradation through syndecan-4 in intervertebral disc. *J Biol Chem,* 286**,** 39738-49.

WASH, E. 2012 Washington Center for Pain Management Begins Enrollment in United States Stem Cell Therapy Study in Subjects With Chronic Back Pain. (PRNewswire)

WATANABE, K., MOCHIDA, J., NOMURA, T., OKUMA, M., SAKABE, K. & SEIKI, K. 2003. Effect of reinsertion of activated nucleus pulposus on disc degeneration: an experimental study on various types of collagen in degenerative discs. *Connect Tissue Res,* 44**,** 104-8.

WEI, A., SHEN, B., WILLIAMS, L. A., BHARGAV, D., GULATI, T., FANG, Z., PATHMANANDAVEL, S. & DIWAN, A. D. 2015. Expression of growth differentiation factor 6 in the human developing fetal spine retreats from vertebral ossifying regions and is restricted to cartilaginous tissues. *J Orthop Res*.

WEI, A., WILLIAMS, L. A., BHARGAV, D., SHEN, B., KISHEN, T., DUFFY, N. & DIWAN, A. D. 2009. BMP13 prevents the effects of annular injury in an ovine model. *Int J Biol Sci,* 5**,** 388-96.

WEI, Y., ZHI-HONG, W., GUI-XING, Q., BIN, Y., JUN, C. & YI-PENG, W. 2013. Extracellular signal-regulated kinase inhibition modulates rat annulus fibrosus cell response to interleukin-1. *Spine (Phila Pa 1976),* 38**,** E1075-81.

WEILER, C., LOPEZ-RAMOS, M., MAYER, H. M., KORGE, A., SIEPE, C. J., WUERTZ, K., WEILER, V., BOOS, N. & NERLICH, A. G. 2011. Histological analysis of surgical lumbar intervertebral disc tissue provides evidence for an association between disc degeneration and increased body mass index. *BMC Res Notes,* 4**,** 497.

WEILER, C., NERLICH, A. G., SCHAAF, R., BACHMEIER, B. E., WUERTZ, K. & BOOS, N. 2010. Immunohistochemical identification of notochordal markers in cells in the aging human lumbar intervertebral disc. *Eur Spine J,* 19**,** 1761-70.

WEILER, C., NERLICH, A. G., ZIPPERER, J., BACHMEIER, B. E. & BOOS, N. 2002. 2002 SSE Award Competition in Basic Science: expression of major matrix metalloproteinases is associated with intervertebral disc degradation and resorption. *Eur Spine J,* 11**,** 308-20.

WHITE, L. J., KIRBY, G. T., COX, H. C., QODRATNAMA, R., QUTACHI, O., ROSE, F. R. & SHAKESHEFF, K. M. 2013. Accelerating protein release from microparticles for regenerative medicine applications. *Mater Sci Eng C Mater Biol Appl,* 33**,** 2578-83.

WIBERG, C., HEINEGARD, D., WENGLEN, C., TIMPL, R. & MORGELIN, M. 2002. Biglycan organizes collagen VI into hexagonal-like networks resembling tissue structures. *J Biol Chem,* 277**,** 49120-6.

WILKE, H. J., NEEF, P., CAIMI, M., HOOGLAND, T. & CLAES, L. E. 1999. New in vivo measurements of pressures in the intervertebral disc in daily life. *Spine (Phila Pa 1976),* 24**,** 755-62.

WU, Y. J., LA PIERRE, D. P., WU, J., YEE, A. J. & YANG, B. B. 2005. The interaction of versican with its binding partners. *Cell Res,* 15**,** 483-94.

WUERTZ, K., GODBURN, K. & IATRIDIS, J. C. 2009. MSC response to pH levels found in degenerating intervertebral discs. *Biochem Biophys Res Commun,* 379**,** 824-9.

WUERTZ, K., GODBURN, K., NEIDLINGER-WILKE, C., URBAN, J. & IATRIDIS, J. C. 2008. Behavior of mesenchymal stem cells in the chemical microenvironment of the intervertebral disc. *Spine (Phila Pa 1976),* 33**,** 1843-9.

Gallery 4Share avalible at (www.gallery4share.com/v/vertebral-column-unlabelled-lateral-view) [Accessed 7.1.2016]

Eurospine available at (www.eurospine.org/motion-preservation.htm) [Accessed 7.1.2016]

Biomedical Central website avaible at (www.biomedcentral.com) [Accessed 10.01.2016]

WYKOFF, C. C., BEASLEY, N. J., WATSON, P. H., TURNER, K. J., PASTOREK, J., SIBTAIN, A., WILSON, G. D., TURLEY, H., TALKS, K. L., MAXWELL, P. H., PUGH, C. W., RATCLIFFE, P. J. & HARRIS, A. L. 2000. Hypoxia-inducible expression of tumor-associated carbonic anhydrases. *Cancer Res,* 60**,** 7075-83.

YANG, C. L., RUI, H., MOSLER, S., NOTBOHM, H., SAWARYN, A. & MULLER, P. K. 1993. Collagen II from articular cartilage and annulus fibrosus. Structural and functional implication of tissue specific posttranslational modifications of collagen molecules. *Eur J Biochem,* 213**,** 1297-302.

YANG, D., WANG, D., SHIMER, A., SHEN, F. H., LI, X. & YANG, X. 2014. Glutathione protects human nucleus pulposus cells from cell apoptosis and inhibition of matrix synthesis. *Connect Tissue Res,* 55**,** 132-9.

YANG, S. D., YANG, D. L., SUN, Y. P., WANG, B. L., MA, L., FENG, S. Q. & DING, W. Y. 2015. 17beta-estradiol protects against apoptosis induced by

interleukin-1beta in rat nucleus pulposus cells by down-regulating MMP-3 and MMP-13. *Apoptosis,* 20**,** 348-57.

YEH, L. C., TSAI, A. D., ZAVALA, M. C. & LEE, J. C. 2004. Cartilage-derived morphogenetic proteins enhance the osteogenic protein-1-induced osteoblastic cell differentiation of C2C12 cells. *J Cell Physiol,* 201**,** 401-8.

YU, D. A., HAN, J. & KIM, B. S. 2012. Stimulation of chondrogenic differentiation of mesenchymal stem cells. *Int J Stem Cells,* 5**,** 16-22.

ZENTNER, G. M., RATHI, R., SHIH, C., MCREA, J. C., SEO, M. H., OH, H., RHEE, B. G., MESTECKY, J., MOLDOVEANU, Z., MORGAN, M. & WEITMAN, S. 2001. Biodegradable block copolymers for delivery of proteins and water-insoluble drugs. *J Control Release,* 72**,** 203-15.

ZHANG, C. C., ZHOU, J. S., HU, J. G., WANG, X., ZHOU, X. S., SUN, B. A., SHAO, C. & LIN, Q. 2013. Effects of IGF-1 on IL-1beta-induced apoptosis in rabbit nucleus pulposus cells in vitro. *Mol Med Rep,* 7**,** 441-4.

ZHANG, H., LA MARCA, F., HOLLISTER, S. J., GOLDSTEIN, S. A. & LIN, C. Y. 2009a. Developing consistently reproducible intervertebral disc degeneration at rat caudal spine by using needle puncture. *J Neurosurg Spine,* 10**,** 522-30.

ZHANG, Y., AN, H. S., TANNOURY, C., THONAR, E. J., FREEDMAN, M. K. & ANDERSON, D. G. 2008. Biological treatment for degenerative disc disease: implications for the field of physical medicine and rehabilitation. *Am J Phys Med Rehabil,* 87**,** 694-702.

ZHANG, Y., AN, H. S., THONAR, E. J., CHUBINSKAYA, S., HE, T. C. & PHILLIPS, F. M. 2006. Comparative effects of bone morphogenetic proteins and sox9 overexpression on extracellular matrix metabolism of bovine nucleus pulposus cells. *Spine (Phila Pa 1976),* 31**,** 2173-9.

ZHANG, Y., ANDERSON, D. G., PHILLIPS, F. M., THONAR, E. J., HE, T. C., PIETRYLA, D. & AN, H. S. 2007. Comparative effects of bone morphogenetic proteins and Sox9 overexpression on matrix accumulation by bovine anulus fibrosus cells: implications for anular repair. *Spine (Phila Pa 1976),* 32**,** 2515-20.

ZHANG, Y., CHEE, A., THONAR, E. J. & AN, H. S. 2011a. Intervertebral disk repair by protein, gene, or cell injection: a framework for rehabilitation-focused biologics in the spine. *PM R,* 3**,** S88-94.

ZHANG, Y., DRAPEAU, S., AN, H. S., MARKOVA, D., LENART, B. A. & ANDERSON, D. G. 2011b. Histological features of the degenerating intervertebral disc in a goat disc-injury model. *Spine (Phila Pa 1976),* 36**,** 1519-27.

ZHANG, Y. G., SUN, Z. M., LIU, J. T., WANG, S. J., REN, F. L. & GUO, X. 2009b. Features of intervertebral disc degeneration in rat's aging process. *J Zhejiang Univ Sci B,* 10**,** 522-7.

ZHANG, Z., LI, F., TIAN, H., GUAN, K., ZHAO, G., SHAN, J. & REN, D. 2014. Differentiation of adipose-derived stem cells toward nucleus pulposus-like cells induced by hypoxia and a three-dimensional chitosan-alginate gel scaffold in vitro. *Chin Med J (Engl),* 127**,** 314-21.

ZHAO, C. Q., WANG, L. M., JIANG, L. S. & DAI, L. Y. 2007. The cell biology of intervertebral disc aging and degeneration. *Ageing Res Rev,* 6**,** 247-61.

ZHAO, X., AKHTAR, R., NIJENHUIS, N., WILKINSON, S. J., MURPHY, L., BALLESTREM, C., SHERRATT, M. J., WATSON, R. E. & DERBY, B. 2012. Multi-layer phase analysis: quantifying the elastic properties of soft tissues and live cells with ultra-high-frequency scanning acoustic microscopy. *IEEE Trans Ultrason Ferroelectr Freq Control,* 59**,** 610-20.

ZUK, P. A., ZHU, M., MIZUNO, H., HUANG, J., FUTRELL, J. W., KATZ, A. J., BENHAIM, P., LORENZ, H. P. & HEDRICK, M. H. 2001. Multilineage cells from human adipose tissue: implications for cell-based therapies. *Tissue Eng,* 7**,** 211-28.

ZVAIFLER, N. J., MARINOVA-MUTAFCHIEVA, L., ADAMS, G., EDWARDS, C. J., MOSS, J., BURGER, J. A. & MAINI, R. N. 2000. Mesenchymal precursor cells in the blood of normal individuals. *Arthritis Res,* 2**,** 477-88.

Appendix 1

Amplicon Sequences utilised in this study

Primer BLAST Search

Primers listed in Table 2.3 were run through primer BLAST (http://www.ncbi.nlm.nih.gov/tools/primer-blast/index.cgi?LINK_LOC=BlastHome [last accessed 4 February 2016]) to confirm and cross check that the primers were appropriate for each particular gene. In addition, probe sequences were also run through a BLAST search using http://blast.ncbi.nlm.nih.gov/Blast.cgi?PROGRAM=blastn&PAGE_TYPE=BlastSearch&LINK_LOC=blasthome. The results are detailed below:

MRPL19

Primers

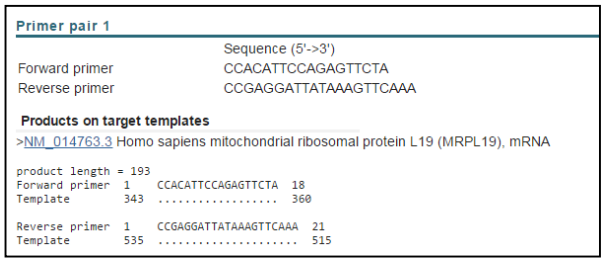

Probe

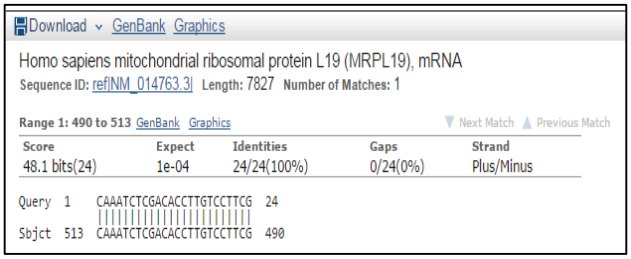

GAPDH

Primers

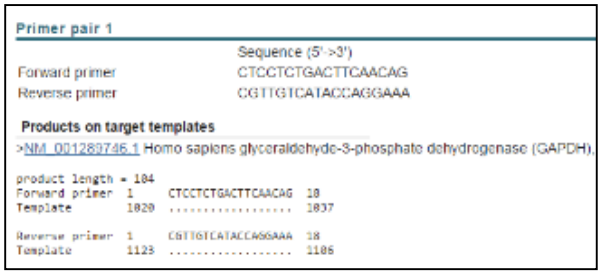

Probe

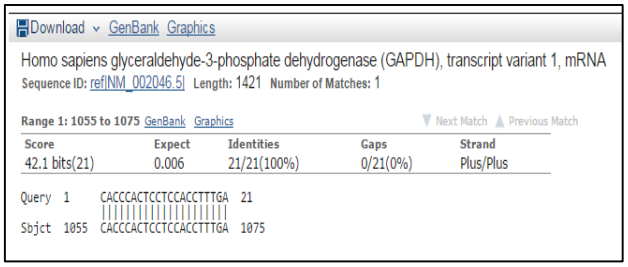

EIF2B1

Primers

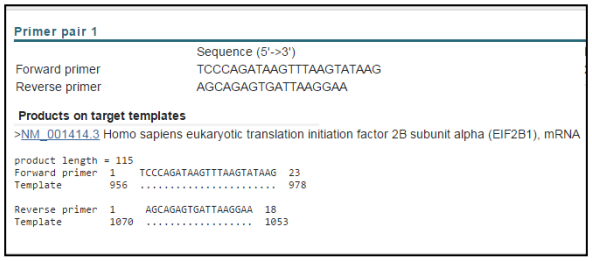

Probe

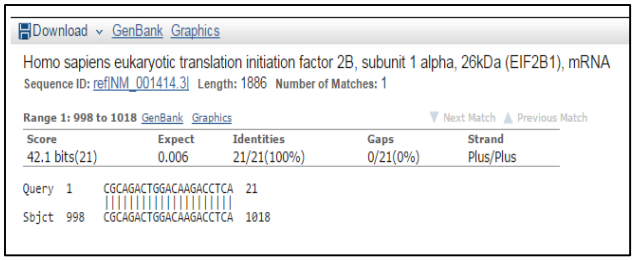

SOX9

Primers

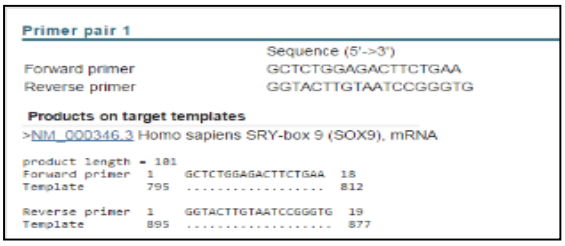

Primer pair 1

	Sequence (5'->3')
Forward primer	GCTCTGGAGACTTCTGAA
Reverse primer	GGTACTTGTAATCCGGGTG

Products on target templates

>NM_000346.3 Homo sapiens SRY-box 9 (SOX9), mRNA

```
product length = 181
Forward primer  1    GCTCTGGAGACTTCTGAA  18
Template        795  ..................  812

Reverse primer  1    GGTACTTGTAATCCGGGTG  19
Template        895  ..................  877
```

Probe

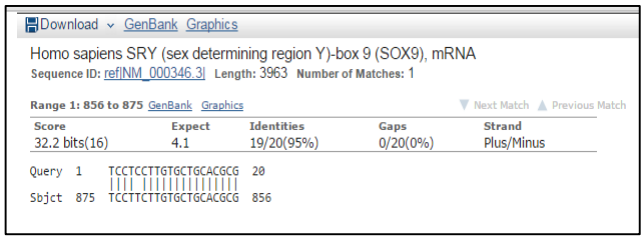

Download GenBank Graphics

Homo sapiens SRY (sex determining region Y)-box 9 (SOX9), mRNA

Sequence ID: ref|NM_000346.3| Length: 3963 Number of Matches: 1

Range 1: 856 to 875 GenBank Graphics Next Match Previous Match

Score	Expect	Identities	Gaps	Strand
32.2 bits(16)	4.1	19/20(95%)	0/20(0%)	Plus/Minus

```
Query  1    TCCTCCTTGTGCTGCACGCG  20
            |||| ||||||||||||||||
Sbjct  875  TCCTTCTTGTGCTGCACGCG  856
```

ACAN

Primers

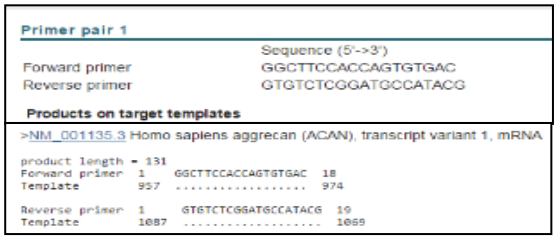

Primer pair 1

	Sequence (5'->3')
Forward primer	GGCTTCCACCAGTGTGAC
Reverse primer	GTGTCTCGGATGCCATACG

Products on target templates

>NM_001135.3 Homo sapiens aggrecan (ACAN), transcript variant 1, mRNA

```
product length = 131
Forward primer  1    GGCTTCCACCAGTGTGAC  18
Template        957  ..................  974

Reverse primer  1    GTGTCTCGGATGCCATACG  19
Template        1087 ..................  1069
```

Probe

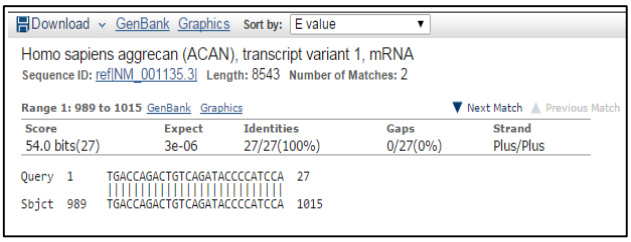

Download GenBank Graphics Sort by: E value

Homo sapiens aggrecan (ACAN), transcript variant 1, mRNA

Sequence ID: ref|NM_001135.3| Length: 8543 Number of Matches: 2

Range 1: 989 to 1015 GenBank Graphics Next Match Previous Match

Score	Expect	Identities	Gaps	Strand
54.0 bits(27)	3e-06	27/27(100%)	0/27(0%)	Plus/Plus

```
Query  1    TGACCAGACTGTCAGATACCCCATCCA  27
            ||||||||||||||||||||||||||
Sbjct  989  TGACCAGACTGTCAGATACCCCATCCA  1015
```

COL2A1

Primers

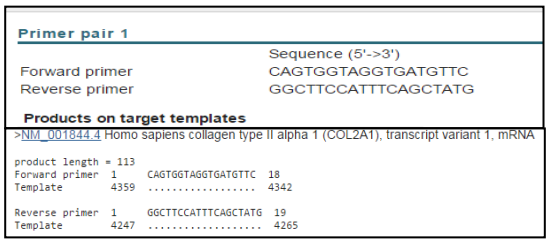

Primer pair 1

	Sequence (5'->3')
Forward primer	CAGTGGTAGGTGATGTTC
Reverse primer	GGCTTCCATTTCAGCTATG

Products on target templates

>NM_001844.4 Homo sapiens collagen type II alpha 1 (COL2A1), transcript variant 1, mRNA

```
product length = 113
Forward primer  1     CAGTGGTAGGTGATGTTC  18
Template        4359  ..................  4342

Reverse primer  1     GGCTTCCATTTCAGCTATG  19
Template        4247  ..................  4265
```

Probe

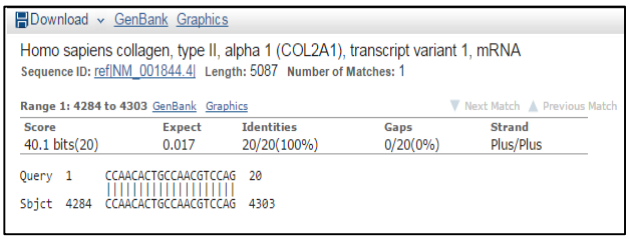

Download GenBank Graphics

Homo sapiens collagen, type II, alpha 1 (COL2A1), transcript variant 1, mRNA

Sequence ID: ref|NM_001844.4| Length: 5087 Number of Matches: 1

Range 1: 4284 to 4303 GenBank Graphics Next Match Previous Match

Score	Expect	Identities	Gaps	Strand
40.1 bits(20)	0.017	20/20(100%)	0/20(0%)	Plus/Plus

```
Query  1    CCAACACTGCCAACGTCCAG  20
            ||||||||||||||||||||
Sbjct  4284 CCAACACTGCCAACGTCCAG  4303
```

KRT8

Primers

Primer pair 1

	Sequence (5'->3')
Forward primer	TGACCGACGAGATCAACTTCC
Reverse primer	TGGACAGCACCACAGATGTGT

Products on target templates

>NM_001256282.1 Homo sapiens keratin 8, type II (KRT8), transcript variant 1, mRNA

```
product length = 93
Forward primer  1    TGACCGACGAGATCAACTTCC  21
Template        754  ....................  774

Reverse primer  1    TGGACAGCACCACAGATGTGT  21
Template        846  ....................  826
```

Probe

Download GenBank Graphics

Homo sapiens keratin 8, type II (KRT8), transcript variant 1, mRNA

Sequence ID: refNM_001256282.1 Length: 1807 Number of Matches: 1

Range 1: 780 to 800 GenBank Graphics Next Match Previous Match

Score	Expect	Identities	Gaps	Strand
42.1 bits(21)	0.006	21/21(100%)	0/21(0%)	Plus/Plus

```
Query  1    CAGCTATATGAAGAGGAGATC  21
            |||||||||||||||||||||
Sbjct  780  CAGCTATATGAAGAGGAGATC  800
```

KRT18

Primers

Primer pair 1

	Sequence (5'->3')
Forward primer	GCGAGGACTTTAATCTTGGTGATG
Reverse primer	TGGTCTTTTGGATGGTTTGCA

Products on target templates

>NM_000224.2 Homo sapiens keratin 18, type I (KRT18), transcript variant 1, mRNA

```
product length = 66
Forward primer  1     GCGAGGACTTTAATCTTGGTGATG  24
Template        1275  .......................  1298

Reverse primer  1     TGGTCTTTTGGATGGTTTGCA  21
Template        1340  ....................  1320
```

Probe

Download GenBank Graphics

Homo sapiens keratin 18, type I (KRT18), transcript variant 1, mRNA

Sequence ID: refNM_000224.2 Length: 1485 Number of Matches: 1

Range 1: 1309 to 1325 GenBank Graphics Next Match Previous Match

Score	Expect	Identities	Gaps	Strand
34.2 bits(17)	0.68	17/17(100%)	0/17(0%)	Plus/Plus

```
Query  1     CAGCAACTCCATGCAAA  17
             |||||||||||||||||
Sbjct  1309  CAGCAACTCCATGCAAA  1325
```

KRT19

Primers

Primer pair 1

	Sequence (5'->3')
Forward primer	GGTCATGGCCGAGCAGAA
Reverse primer	TTCAGTCCGGCTGGTGAAC

Products on target templates

>NM_002276.4 Homo sapiens keratin 19, type I (KRT19), mRNA

```
product length = 58
Forward primer  1    GGTCATGGCCGAGCAGAA  18
Template        913  ..................  930

Reverse primer  1    TTCAGTCCGGCTGGTGAAC  19
Template        970  ..................  952
```

Probe

Download GenBank Graphics

Homo sapiens keratin 19, type I (KRT19), mRNA

Sequence ID: refNM_002276.4 Length: 1490 Number of Matches: 1

Range 1: 932 to 947 GenBank Graphics Next Match Previous Match

Score	Expect	Identities	Gaps	Strand
32.2 bits(16)	2.7	16/16(100%)	0/16(0%)	Plus/Plus

```
Query  1    CGGAAGGATGCTGAAG  16
            ||||||||||||||||
Sbjct  932  CGGAAGGATGCTGAAG  947
```

FOXF1

Primers

Primer pair 1

	Sequence (5'->3')
Forward primer	CCGTATCTGCACCAGAAC
Reverse primer	TGGCGTTGAAAGAGAAGA

Products on target templates

>NM_001451.2 Homo sapiens forkhead box F1 (FOXF1), mRNA

```
product length = 118
Forward primer  1     CCGTATCTGCACCAGAAC  18
Template        977   ..................  994

Reverse primer  1     TGGCGTTGAAAGAGAAGA  18
Template        1094  ..................  1077
```

Probe

Download GenBank Graphics

Homo sapiens forkhead box F1 (FOXF1), mRNA

Sequence ID: refNM_001451.2 Length: 2579 Number of Matches: 1

Range 1: 1011 to 1030 GenBank Graphics Next Match Previous Match

Score	Expect	Identities	Gaps	Strand
40.1 bits(20)	0.017	20/20(100%)	0/20(0%)	Plus/Plus

```
Query  1     CCGAGCTGCAAGGCATCCCG  20
             ||||||||||||||||||||
Sbjct  1011  CCGAGCTGCAAGGCATCCCG  1030
```

CAXII

Primers

Primer pair 1

	Sequence (5'->3')
Forward primer	CCAGCAACAAGTCAGAAG
Reverse primer	TCCTGGCCTTTGTACTTTA

Products on target templates

>NM_001218.4 Homo sapiens carbonic anhydrase XII (CA12), transcript variant 1, mRNA

```
product length = 118
Forward primer  1    CCAGCAACAAGTCAGAAG  18
Template        869  ..................  886

Reverse primer  1    TCCTGGCCTTTGTACTTTA  19
Template        986  ...................  968
```

Probe

Download GenBank Graphics

Homo sapiens carbonic anhydrase XII (CA12), transcript variant 1, mRNA

Sequence ID: ref|NM_001218.4| Length: 4209 Number of Matches: 1

Range 1: 890 to 909 GenBank Graphics Next Match Previous Match

Score	Expect	Identities	Gaps	Strand
40.1 bits(20)	0.017	20/20(100%)	0/20(0%)	Plus/Plus

```
Query  1    TCGCTGTCCTGGCTGTTCTC  20
            ||||||||||||||||||||
Sbjct  890  TCGCTGTCCTGGCTGTTCTC  909
```

T

Primers

Primer pair 1

	Sequence (5'->3')	Length
Forward primer	TTCTCCAACCTATTCTGACAACTCA	25
Reverse primer	ATTCCAAGGCTGGACCAATTG	21

Products on target templates

>NM_003181.3 Homo sapiens T brachyury transcription factor (T), transcript variant 1, mRNA

```
product length = 78
Forward primer  1     TTCTCCAACCTATTCTGACAACTCA  25
Template        1416  .........................  1440

Reverse primer  1     ATTCCAAGGCTGGACCAATTG  21
Template        1493  ....................  1473
```

Probe

Download GenBank Graphics

Homo sapiens T, brachyury homolog (mouse) (T), transcript variant 1, mRNA

Sequence ID: ref|NM_003181.3| Length: 2500 Number of Matches: 1

Range 1: 1449 to 1466 GenBank Graphics Next Match Previous Match

Score	Expect	Identities	Gaps	Strand
36.2 bits(18)	0.17	18/18(100%)	0/18(0%)	Plus/Plus

```
Query  1     TTTATCCATGCTGCAATC  18
             ||||||||||||||||||
Sbjct  1449  TTTATCCATGCTGCAATC  1466
```

MMP3

Primers

Primer pair 1

	Sequence (5'->3')
Forward primer	GTGGAGTTCCTGATGTTG
Reverse primer	GCATCTTTTGGCAAATCTG

Products on target templates

>NM_002422.4 Homo sapiens matrix metallopeptidase 3 (MMP3), mRNA

```
product length = 112
Forward primer  1    GTGGAGTTCCTGATGTTG  18
Template        418  ..................  435

Reverse primer  1    GCATCTTTTGGCAAATCTG  19
Template        529  ...................  511
```

Probe

Download GenBank Graphics

Homo sapiens matrix metallopeptidase 3 (stromelysin 1, progelatinase) (MMP3), mRNA

Sequence ID: ref|NM_002422.3| Length: 1828 Number of Matches: 1

Range 1: 403 to 426 GenBank Graphics Next Match Previous Match

Score	Expect	Identities	Gaps	Strand
48.1 bits(24)	1e-04	24/24(100%)	0/24(0%)	Plus/Minus

```
Query  1    AATTCACAATCCTGTATGTAAGGT  24
            ||||||||||||||||||||||||
Sbjct  426  AATTCACAATCCTGTATGTAAGGT  403
```

MMP13

Primers

Primer pair 1

	Sequence (5'->3')
Forward primer	CCCCAGGCATCACCATTCAAG
Reverse primer	GACAAATCATCTTCATCACCACCAC

Products on target templates

>NM_002427.3 Homo sapiens matrix metallopeptidase 13 (MMP13), mRNA

```
product length = 116
Forward primer  1  CCCCAGGCATCACCATTCAAG  21
Template        9  .....................  29

Reverse primer  1    GACAAATCATCTTCATCACCACCAC  25
Template        124  .........................  100
```

Probe

Download GenBank Graphics

Homo sapiens matrix metallopeptidase 13 (collagenase 3) (MMP13), mRNA

Sequence ID: ref|NM_002427.3| Length: 2735 Number of Matches: 1

Range 1: 49 to 66 GenBank Graphics Next Match Previous Match

Score	Expect	Identities	Gaps	Strand
36.2 bits(18)	0.17	18/18(100%)	0/18(0%)	Plus/Plus

```
Query  1   CTGCCTTCCTCTTCTTGA  18
           ||||||||||||||||||
Sbjct  49  CTGCCTTCCTCTTCTTGA  66
```

ADAMTS4

Primers

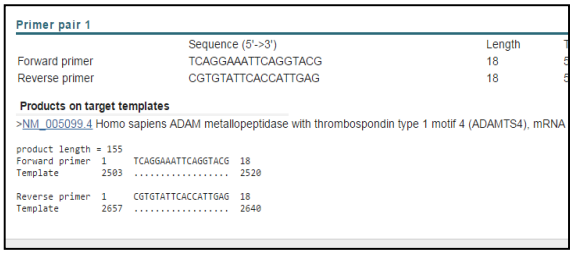

Primer pair 1

	Sequence (5'->3')	Length
Forward primer	TCAGGAAATTCAGGTACG	18
Reverse primer	CGTGTATTCACCATTGAG	18

Products on target templates

>NM_005099.4 Homo sapiens ADAM metallopeptidase with thrombospondin type 1 motif 4 (ADAMTS4), mRNA

```
product length = 155
Forward primer  1     TCAGGAAATTCAGGTACG  18
Template        2503  ..................  2520

Reverse primer  1     CGTGTATTCACCATTGAG  18
Template        2657  ..................  2640
```

Probe

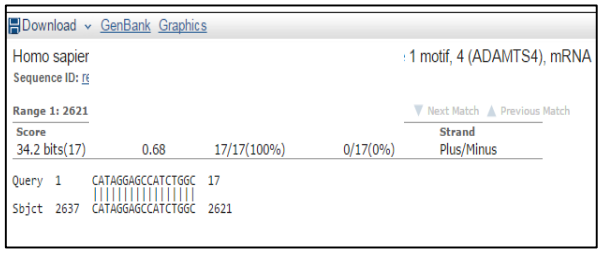

Download GenBank Graphics

Homo sapier : 1 motif, 4 (ADAMTS4), mRNA

Sequence ID: re

Range 1: 2621 Next Match Previous Match

Score				Strand
34.2 bits(17)	0.68	17/17(100%)	0/17(0%)	Plus/Minus

```
Query  1     CATAGGAGCCATCTGGC  17
             |||||||||||||||||
Sbjct  2637  CATAGGAGCCATCTGGC  2621
```

ADAMTS5

Primers

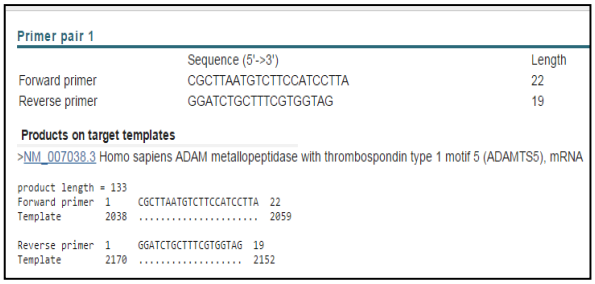

Primer pair 1

	Sequence (5'->3')	Length
Forward primer	CGCTTAATGTCTTCCATCCTTA	22
Reverse primer	GGATCTGCTTTCGTGGTAG	19

Products on target templates

>NM_007038.3 Homo sapiens ADAM metallopeptidase with thrombospondin type 1 motif 5 (ADAMTS5), mRNA

```
product length = 133
Forward primer  1     CGCTTAATGTCTTCCATCCTTA  22
Template        2038  ......................  2059

Reverse primer  1     GGATCTGCTTTCGTGGTAG  19
Template        2170  ...................  2152
```

Probe

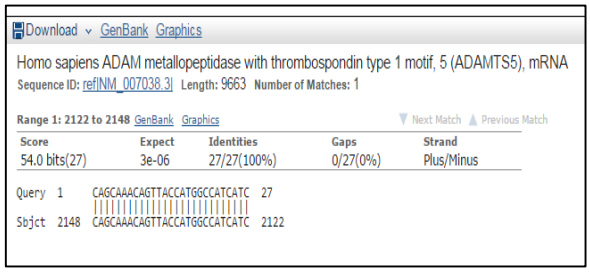

Download GenBank Graphics

Homo sapiens ADAM metallopeptidase with thrombospondin type 1 motif, 5 (ADAMTS5), mRNA

Sequence ID: refNM_007038.3| Length: 9663 Number of Matches: 1

Range 1: 2122 to 2148 GenBank Graphics Next Match Previous Match

Score	Expect	Identities	Gaps	Strand
54.0 bits(27)	3e-06	27/27(100%)	0/27(0%)	Plus/Minus

```
Query  1     CAGCAAACAGTTACCATGGCCATCATC  27
             |||||||||||||||||||||||||||
Sbjct  2148  CAGCAAACAGTTACCATGGCCATCATC  2122
```

TIMP1

Primers

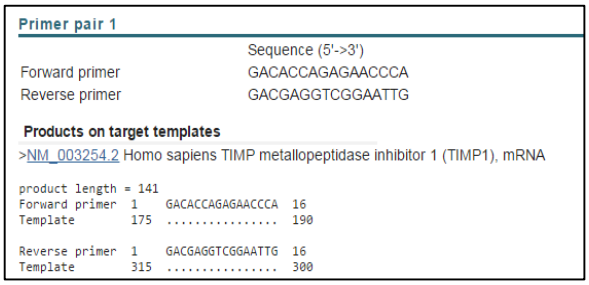

Primer pair 1

	Sequence (5'->3')
Forward primer	GACACCAGAGAACCCA
Reverse primer	GACGAGGTCGGAATTG

Products on target templates

>NM_003254.2 Homo sapiens TIMP metallopeptidase inhibitor 1 (TIMP1), mRNA

```
product length = 141
Forward primer  1    GACACCAGAGAACCCA  16
Template        175  ................  190

Reverse primer  1    GACGAGGTCGGAATTG  16
Template        315  ................  300
```

Probe

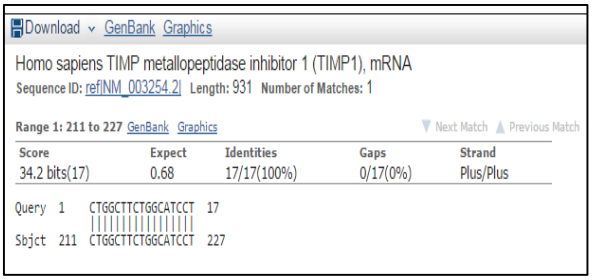

Download GenBank Graphics

Homo sapiens TIMP metallopeptidase inhibitor 1 (TIMP1), mRNA

Sequence ID: refNM_003254.2| Length: 931 Number of Matches: 1

Range 1: 211 to 227 GenBank Graphics Next Match Previous Match

Score	Expect	Identities	Gaps	Strand
34.2 bits(17)	0.68	17/17(100%)	0/17(0%)	Plus/Plus

```
Query  1    CTGGCTTCTGGCATCCT  17
            |||||||||||||||||
Sbjct  211  CTGGCTTCTGGCATCCT  227
```

TIMP2

Primers

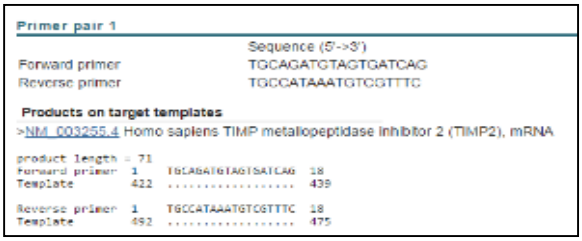

Primer pair 1

	Sequence (5'->3')
Forward primer	TGCAGATGTAGTGATCAG
Reverse primer	TGCCATAAATGTCGTTTC

Products on target templates

>NM_003255.4 Homo sapiens TIMP metallopeptidase inhibitor 2 (TIMP2), mRNA

```
product length = 71
Forward primer  1    TGCAGATGTAGTGATCAG  18
Template        422  ..................  439

Reverse primer  1    TGCCATAAATGTCGTTTC  18
Template        492  ..................  475
```

Probe

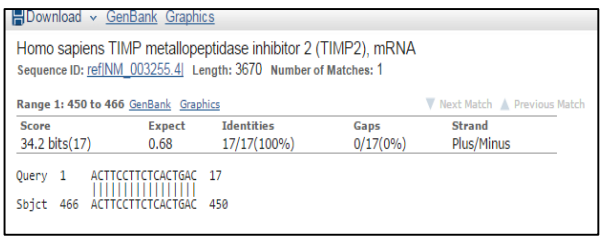

Download GenBank Graphics

Homo sapiens TIMP metallopeptidase inhibitor 2 (TIMP2), mRNA

Sequence ID: refNM_003255.4| Length: 3670 Number of Matches: 1

Range 1: 450 to 466 GenBank Graphics Next Match Previous Match

Score	Expect	Identities	Gaps	Strand
34.2 bits(17)	0.68	17/17(100%)	0/17(0%)	Plus/Minus

```
Query  1    ACTTCCTTCTCACTGAC  17
            |||||||||||||||||
Sbjct  466  ACTTCCTTCTCACTGAC  450
```

Amplicon Sequences

Sequencing was performed in both 5' and 3' directions using individual primers from the qPCR. Seq files were read using http://simgene.com/ReadSeq and the sequences opened. The sequences were then BLAST searched in the human genome and transcript database using http://blast.ncbi.nlm.nih.gov/Blast.cgi?PROGRAM=blastn&PAGE_TYPE=BlastSearch&LINK_LOC=blasthome. The accession number and homology were noted and are shown in Table 1.

Table 1. Amplicon sequences for Novel NP markers

Gene Name	5' Sequence	3' Sequence	Accession Number	Percentage Homology to Reference
Mitochondrial Ribosomal Protein L19	GTNCTANGCTGACCCATATGCCAGTGGAAAATCAGCC AGTTTCTGGGATTTGCATTCAGAGATCAGGAAGAGAC TTGGAGCTACTTTCATCCTTAGGAATGTTATCGAAGGA CAAGGTGCGAGATTTGCTTTGAACTTTATAATCCTCGG A	CTTCGATACATTCCTAAGGATGAAGTAGCTCCAAG TCCTCTTCCTGATCTCTGAATGCAATCCCCAGAAAC TGGCTGATTTTTCCACTGGCATATGGGTAGCTGTA GTAACACGAAGAAACTTCCAACATAGAACTCTGA ATGTGGA	NM014763.3	5' = 99% 3' = 99%
SRY (sex determining region Y)-box 9 (SOX9)	CTTCGTGNGGAGGCGGAGCGGCT GCGCGTGCAGCACAAGAAGGACCACCCGGATTACAA GTACNNGCCNN	GNNCGCGCGNGCTCG CCTCCTCCACGAAGGGCCGCTTCTCGCTCTCGTTC AGAAG TCTCCAGAGCANNCNN	NM000346.3	5' = 97% 3' = 98%
Collagen type II alpha 1 (COL2A1), transcript variant 1	CACCTGCCACGTCCAGATGACCTTCCTACGCCTGCTGT CCACGGAAGGCTCCCAGAACATCACCTACCATNNNN	AGGCGTAGGAGGTCA TCTGGACGTTGGCAGTGTTG GGAGCCAGATTGTCATCTCC ATAGCTGAAATGGAAGCNN	NM001844.4	5' = 99% 3' = 99%
Aggrecan (ACAN), transcript variant 1	TNTCNGATACCCCATCCACACTCCCCGGGAAGGCTGC TATGGAGACAAGGATGAGTTTCCTGGTGTGAGGACGT ATGGCATCCGAGACAC	TGTCTCATAGCAGCCTTCCCGGGGAGTGTGGATG GGGTATCTGACAGTCTGGTCAGCCAGCCAGCCGG CGTCACACTGGTGGAAGCCA	NM001135.3	5' = 100% 3' = 99%
Keratin 8, type II (KRT8), transcript variant 1	AGAGCTGGAGTCTCGCCTGGAGGGCTGACCGACGAG ATCAACTTCCTCAGGA	GCGAGATCAGCTCTACCTTGTTCATGTAAGCTTCA TCCACATCCTTCTTGATGAGGA	NM001256282.1	5' = 98% 3' = 97%

Keratin 18, type II (KRT18), transcript variant 1	CNACCGCCGCCTGCTGGAGATGGC GAGGACTTTAATCTTGGTGATGCACT	CNGGCGGCGGTAGGTGGCGATCTCAGCCTCCAGC TTGACCTTGATGTTCAGCAGA	NM000224.2	5’ = 98% 3’ = 100%
Keratin 19, type I (KRT19)	GNNNGGTCAGTGTGGAGGTGGATTCCGCTCCGGGCA CCGATCTCGCCAAGATCCTGAGTGACANNN	CACCTCACACTGACCTGGCCTCCACTTGGCCCCTC AGCGTACTGATTTCCTCCTCATGGA	NM002276.4	5’ = 100% 3’ = 98%
Forkhead box F1 (FOXF1)	CTGCAGGCATCCCGCGGTATCACTCGCAGTCGCCCAG CATGTGTGACCGAAAGGAGTTTGTCTTCTCTTTCAACG CCAA	TGCTGGGCGACTGCGAGTGATACCGCGGGATGCC TTGCAGCTCGGCTGGGGCGTTGTGGCTGTTCTGG TGCAGATACGGA	NM001451.2	5’ = 99% 3’ = 100%
Carbonic anhydrase CAXII (CA12)	CTATTGAGATGGGCTCCTTCATCCGTCCTATGACAAGA TCTTCAGTCACCTTCAACATGTAAAGTACAAAGGCCAG GAAGN	GACTTGTCTAGGACGGATTGAGGAGCCCATCTCA ATGAGAACAGCCAGGACAGCGAGGCCTTCTGACT TGTTGCTGGA	NM001218.4	5’ = 99% 3’ = 97%

Appendix 2

Clarke, L.E., McConnell, J.C., Sherratt, M.J., Derby, B., Richardson, S.M. and Hoyland, J.A. Growth differentiation factor 6 and transforming growth factor-beta differentially mediate mesenchymal stem cell differentiation, composition, and micromechanical properties of nucleus pulposus constructs. Arthritis Res Ther, 2014. **16**:R67.

Clarke et al. Arthritis Research & Therapy 2014, 16:R67
http://arthritis-research.com/content/16/2/R67

arthritis research&therapy

RESEARCH ARTICLE Open Access

Growth differentiation factor 6 and transforming growth factor-beta differentially mediate mesenchymal stem cell differentiation, composition, and micromechanical properties of nucleus pulposus constructs

Louise E Clarke[1], James C McConnell[1,2], Michael J Sherratt[1], Brian Derby[3], Stephen M Richardson[1] and Judith A Hoyland[1,4*]

Abstract

Introduction: Currently, there is huge research focus on the development of novel cell-based regeneration and tissue-engineering therapies for the treatment of intervertebral disc degeneration and the associated back pain. Both bone marrow-derived (BM) mesenchymal stem cells (MSCs) and adipose-derived MSCs (AD-MSCs) are proposed as suitable cells for such therapies. However, currently no consensus exists as to the optimum growth factor needed to drive differentiation to a nucleus pulposus (NP)-like phenotype. The aim of this study was to investigate the effect of growth differentiation factor-6 (GDF6), compared with other transforming growth factor (TGF) superfamily members, on discogenic differentiation of MSCs, the matrix composition, and micromechanics of engineered NP tissue constructs.

Methods: Patient-matched human AD-MSCs and BM-MSCs were seeded into type I collagen hydrogels and cultured in differentiating media supplemented with TGF-β3, GDF5, or GDF6. After 14 days, quantitative polymerase chain reaction analysis of chondrogenic and novel NP marker genes and sulfated glycosaminoglycan (sGAG) content of the construct and media components were measured. Additionally, construct micromechanics were analyzed by using scanning acoustic microscopy (SAM).

Results: GDF6 stimulation of BM-MSCs and AD-MSCs resulted in a significant increase in expression of novel NP marker genes, a higher aggrecan-to-type II collagen gene expression ratio, and higher sGAG production compared with TGF-β or GDF5 stimulation. These effects were greater in AD-MSCs than in BM-MSCs. Furthermore, the acoustic-wave speed measured by using SAM, and therefore tissue stiffness, was lowest in GDF6-stiumlated AD-MSC constructs.

Conclusions: The data suggest that GDF6 stimulation of AD-MSCs induces differentiation to an NP-like phenotype and results in a more proteoglycan-rich matrix. Micromechanical analysis shows that the GDF6-treated AD-MSCs have a less-stiff matrix composition, suggesting that the growth factor is inducing a matrix that is more akin to the native NP-like tissue. Thus, this cell and growth-factor combination may be the ideal choice for cell-based intervertebral disc (IVD)-regeneration therapies.

* Correspondence: judith.a.hoyland@manchester.ac.uk
[1]Centre for Tissue Injury and Repair, Institute of Inflammation and Repair, Faculty of Medical and Human Sciences, The University of Manchester, Oxford Road, Manchester M13 9PT, UK
[4]NIHR Manchester Musculoskeletal Biomedical Research Unit, Central Manchester University Hospitals NHS Foundation Trust, Manchester Academic Health Science Centre, Nowgen Building, 29 Grafton Street, Manchester M13 9WU, UK
Full list of author information is available at the end of the article

Introduction

Low back pain (LBP), is an increasing socioeconomic burden in today's society. Current therapies involve conservative symptomatic pain relief or end-stage surgical treatments. However, these therapies are relatively unsuccessful in the long term and do not address the underlying pathogenesis of LBP, such as IVD degeneration, which correlates with LBP in 40% of cases [1].

Degenerative changes occur predominantly in the highly hydrated central nucleus pulposus (NP) which is composed of the proteoglycan, aggrecan, and type II collagen. With degeneration, degradation of the extracellular matrix (ECM) occurs, with substantial loss of aggrecan [2]. These changes result in dehydration of the ECM, thereby influencing tissue stiffness and strength, which leads to a reduction in the structural integrity of the disc, ultimately compromising its function [3]. Given the poor long-term efficacy of current clinical interventions, research is now focused on cell-based tissue-engineering strategies. Such strategies aim to target the underlying pathogenesis by replacing the cell population and thereby restoring a functional IVD matrix. Of these approaches, minimally invasive implantation of mesenchymal stem cell (MSC)-seeded hydrogels offers the most promise.

Both bone marrow- and adipose-derived MSCs (BM-MSCs and AD-MSCs, respectively) are able to differentiate into NP-like cells [4-6]. Native adult NP cells are conventionally described as being "chondrocyte-like" and characterized through their rounded morphology and expression of classic chondrogenic markers, including *SOX-9*, type II collagen, and aggrecan [7]. However, the composition of the NP and articular cartilage ECM is significantly different, with NP tissue having a substantially more-proteoglycan-rich ECM than has cartilage [8]. Thus, if MSCs are to be used for IVD regeneration, it is essential to identify accurately the differentiated cell phenotype and to ensure appropriate ECM synthesis.

Our discovery of novel human NP cell markers (*CAXII*, *FOXF1*, *KRT 8*, *18*, *19*) [9] has allowed a clear distinction to be made between the chondrocyte and NP cell phenotype. We previously demonstrated that these markers can be used to identify accurately both BM-MSC and AD-MSC differentiation toward NP-like cells [6]. This work used culture in a three-dimensional (3D) environment with media containing TGF-β, a growth factor more commonly used to induce chondrogenesis, and focused on gene and protein marker expression by differentiated cells. However, although such studies demonstrate that MSCs can be induced to adopt an NP-like phenotype and hence synthesize an ECM matrix that, in biochemical terms, is compositionally similar to native NP tissue, they provide no information on the structural and biomechanical properties of the synthesized matrix. Importantly, the mechanical behavior of ECM-rich tissues is determined not only by the identity of the molecular components but also by their posttranslational modification and assembly into structurally malleable macromolecular aggregates [10-12]. Therefore, although TGF-β has been commonly used by several groups to induce NP-like differentiation, the effects of alternative growth factors should be characterized with regard to cell phenotype, protein synthesis, and crucially local stiffness to optimize the biochemical and biomechanical characteristics of the resultant construct.

Growth differentiation factor 5 (GDF5/BMP-14/CDMP-1) and growth differentiation factor 6 (GDF6/BMP-13/CDMP-2) are members of the TGF superfamily and are associated with skeletal development [13-15]. We previously demonstrated that they are expressed by human NP cells and that GDF5 increases type II collagen and aggrecan gene expression by degenerate human NP cells *in vitro* [16]. GDF5 has also recently been shown to improve differentiation of BM-MSCs to an NP-like phenotype (that is, discogenic differentiation) compared with TGF-β1, as shown by the enhanced expression of the novel markers *CAXII*, *KRT19*, and *FOXF1* [17-19]. However, whereas differentiation to NP-like cells was achieved, GDF5 did not produce a more-proteoglycan (PG)-rich ECM than did TGF-β1. As such, and given that GDF5 has also been shown to induce chondrogenic differentiation [20], this may not be the optimal growth factor for directing MSC differentiation to an NP-like cell capable of synthesizing an ECM with appropriate biochemical and biomechanical characteristics.

GDF6 has been shown to play an important role in spinal column development, implying that it may have a pivotal role in IVD development and homeostasis [21]. Furthermore, research has shown that injection of GDF6 prevents IVD degeneration in an experimentally induced ovine model [22]. Taken together, this suggests that GDF6 may be an appropriate growth factor to drive MSC differentiation toward an NP-like cell and hence to produce a PG-rich ECM more akin to native IVD tissue than that produced by TGF-β- or GDF5-stimulated MSCs.

Thus, we hypothesized that the choice of exogenous growth factor and MSC source would influence cell differentiation, ECM composition, and mechanical stiffness of engineered NP tissue constructs. Differentiation of both BM-MSCs and AD-MSCs after stimulation with TGF-β, GDF5, and GDF6 was assessed by expression of classic and novel NP marker genes and PG production. Additionally, by using scanning acoustic microscopy, the effect of exogenous growth factors on micromechanical stiffness of tissue constructs was assessed, with acoustic wave speed serving as a surrogate measure of tissue stiffness [23,24].

Methods

Mesenchymal stem cell culture

Human patient-matched AD-MSCs and BM-MSCs were isolated from subcutaneous fat and bone marrow removed

from the proximal femur during hip-replacement surgery after approval from the North West Research Ethics Committee and fully informed written consent of patients ($n = 7$; average age, 47 years (age range, 22 to 78 years); four women, three men). BM-MSCs were isolated and expanded in α-MEM with 20% fetal calf serum (hereafter termed standard media), as previously described [25]. After 5 days, nonadherent cells were discarded, and adherent cells were cultured to confluence.

To isolate AD-MSCs, adipose tissue was digested in collagenase solution (30 mg collagenase type I in Hanks Balanced Salt Solution (HBSS) and 20 m*M* calcium chloride) for 2 hours at 37°C. The solution was filtered, neutralized with standard media, and centrifuged for 5 minutes. Supernatant was aspirated, and cells cultured to confluence in standard media, with nonadherent cells discarded after 5 days.

The CD profile of BM-MSCs and AD-MSCs was analyzed by using flow cytometry and multipotentiality assessed along the three mesenchymal lineages by using standard methods (data not shown). Cells at passage 3 were used for subsequent experiments.

Encapsulation of MSCs in type I collagen hydrogels

Collagen gels were established by combining 3 mg/ml atelosoluble type I collagen (Devro, Edinburgh, Scotland) (pH 2), neutralization buffer (0.2 *M* sodium phosphate, 1.3 *M* sodium chloride, pH 11.2) and αMEM at an 8:1:1 ratio, respectively. MSCs were suspended in the collagen solution at room temperature to a final cell density of 4×10^6/ml and 100 μl gels formed in 0.4-μm high-density cell-culture inserts (BD Biosciences, San Jose, CA, USA). Gels were cultured for 24 hours in standard media, and media were subsequently replaced with a differentiating medium, as defined later, either with or without growth factor.

MSC pellet cultures

MSCs were dispensed into a 15-ml Falcon tube at a density of 250,000 cells in 2 ml of standard media. Subsequently cells were centrifuged, incubated at 37°C for 24 hours, and media replaced with a differentiating media either with or without the respective growth factor.

Differentiation of MSCs with TGF-β3, GDF5, and GDF6

MSCs were encapsulated in type I collagen gels and cultured in differentiating media consisting of high-glucose DMEM, 1% FCS, insulin-transferrin-selenium (ITS-X) (Gibco, Grand Island, NY, USA), 100 μ*M* ascorbic acid-2-phosphate, 1.25 mg/ml bovine serum albumin (BSA), 10^{-7} *M* dexamethasone, 5.4 μg/ml linoleic acid, 40 μg/ml L-proline, and 100 U/ml penicillin, 100 μg/ml streptomycin, and 2.5 μg/ml amphotericin B. To assess optimal growth-factor concentration, media were further supplemented with either no growth factor (control), TGF-β3 (Invitrogen) at concentrations of 1, 10, 100 ng/ml, GDF5 (PeproTech, Rocky Hill, NJ, United States) at concentrations of 10, 100, or 1,000 ng/ml, or GDF6 (PeproTech) at concentrations of 10, 100, or 1,000 ng/ml for 14 days. Concentration ranges were chosen to encompass manufacturers' recommendations and previously published concentrations [18,26,27].

After this assessment, cells were encapsulated in type I collagen gels or pellets and cultured in differentiating media supplemented with either no growth factor or optimal concentrations of growth factor for 14 days. Media were changed every 48 hours and retained for subsequent analysis of sulfated glycosaminoglycan (sGAG) content.

Assessment of NP marker gene expression with quantitative real-time PCR

After 14 days, cell-seeded collagen hydrogels and pellets were disrupted with Molecular Grinding Resin in TRIzol (Geno Technology Inc., St. Louis, MO, USA), and RNA was extracted according to the manufacturer's recommendations. cDNA was generated by using a high-capacity cDNA reverse-transcription kit (Life Technologies) and diluted to 5 ng/μl. Gene expression was analyzed with quantitative real-time PCR by using an Applied Biosystems StepOne Plus Real Time PCR system. Reactions were prepared in triplicate by using LuminoCt qPCR readymix reagents (Sigma-Aldrich, Irvine, UK) to a total volume of 10 μl, containing 10 ng cDNA, 900 n*M* each primer, and 250 n*M* probe. Data were analyzed according to the $2^{-\Delta\Delta}$ Ct method, with expression normalized to the average of two prevalidated housekeeping genes (*EIF2B1* and *MRPL19*) and to the control sample [28].

Assessment of PG sGAG content

sGAG production was assessed in triplicate by using a dimethylmethylene blue (DMMB) assay, as previously described [29,30], and quantified against a chondroitin sulfate C (shark cartilage, Sigma) standard curve. Media collected at each media change were also used to analyze the PG content released into media on a cumulative basis.

Total DNA content was measured by using a Quant-iT PicoGreen assay (Life Technologies) with a lambda DNA standard curve, according to manufacturer's instructions. sGAG values in gels/pellets were normalized to dsDNA content.

Histologic characterization of ECM deposition

Collagen constructs were embedded in OCT; snap-frozen in liquid nitrogen, and cryosectioned to a nominal thickness of 5 μm. Safranin-O/Fast Green staining was performed to localize sGAG according to standard protocols. Picrosirius red staining and polarized light microscopy were used to assess fibrillar collagen content, as previously described [31]. Fibrillar collagen content was assessed by

imaging the same area under bright-field and cross-polarized light microscopy. Total tissue area was compared with birefringent fibrillar collagen area, and percentage fibrillar collagen content calculated (these calculations were based on overall intensity of staining and did not distinguish between color of staining, which subjectively shows fibril diameter) [31]. Three areas were assessed per section, from each of three sections per cell type and growth-factor treatment.

Micromechanical characterization by scanning acoustic microscopy

The SAM imaging technique has been described in detail previously [11,24,32]. Imaging of hydrated cryosections was performed by using a KSI 2000 microscope (PVA TePla Analytical Systems GmbH; Herborn, Germany) with bespoke data acquisition and control systems. SAM data were collected in triplicate by using the Multi-Layer Phase Analysis (MLPA) method [24] with a scan size of 200 μm and a frequency of 770 MHz to produce an acoustic wave speed map.

Statistical analysis

The nonparametric Mann–Whitney *U* test was applied to determine significance to compare gene expression, sGAG, and DNA. Values are reported as mean ± SEM. Analysis of SAM data was conducted by using SPSS 20 (SPSS, Chicago, IL, USA). Q-q plots were used to test for normality, and one-way ANOVAs were used to compare means. For all analyses, a value of $P < 0.05$ was considered statistically significant.

Results

Optimal growth factor concentration

When compared with no growth factor controls, both BM-MSCs (Figure 1A) and AD-MSCs (Figure 1B) demonstrated dose-dependent responses to all growth factors. Both *COL2A1* and *ACAN* gene expressions were significantly upregulated with all growth factors, whereas novel maker gene expression was significantly upregulated after GDF6 stimulation, in particular in AD-MSCs. Overall, the optimal expression profiles were identified at 10 ng/ml TGF-β and 100 ng/ml of GDF5 and GDF6.

Conventional NP marker expression in type I collagen hydrogels

Culture of BM-MSCs in the presence of all growth factors (Figure 2A) resulted in a significant upregulation of *SOX9* and *ACAN* compared with the control, with the largest upregulation of *ACAN* (13-fold) being identified in the GDF6-stimulated cohort. Conversely, culture with TGF-β demonstrated the greatest increase in expression of *COL2A1* (66-fold compared with control) compared with treatment with either GDF5 (1.5-fold) or GDF6 (2.5-fold). Culture of AD-MSCs in the presence of all growth factors (Figure 2B) resulted in a significant increase in *ACAN* expression compared with control, with GDF6 again causing a significantly greater increase (20-fold) than other growth-factor treatments. As with BM-MSCs, TGF-β treatment of AD-MSCs resulted in the largest upregulation of *COL2A1* (34-fold) gene expression.

When the *ACAN*-to-*COL2A1* relative gene expression was assessed ($2^{-\Delta CtACAN-\Delta CtCOL2A1}$), AD-MSCs stimulated with GDF6 demonstrated the highest ratio of 75:1, whereas BM-MSCs demonstrated a ratio of 29:1 (Figure 2C). Cells treated with TGF-β demonstrated the lowest ratio overall at 4:1 for AD-MSCs and 0.7:1 for BM-MSCs.

Novel NP marker expression in type I collagen hydrogels

Treatment of BM-MSCs with TGF-β and GDF5 caused no change in *KRT8*, *KRT19*, or *CAXII* and a downregulation of *KRT18*, *FOXF1*, and *T* gene expression compared with controls (Figure 2A). Conversely, treatment with GDF6 significantly upregulated *KRT8*, *18*, *19*, *CAXII*, and *T*, with no change noted in *FOXF1* compared with controls. Culture of AD-MSCs with GDF6 resulted in significant upregulation of all novel marker genes compared with the control, and in the case of *KRT8*, *KRT18*, *KRT19*, and *T* expression, was significantly higher than that that seen in AD-MSCs cultured with either TGF-β or GDF5 (Figure 2B). Comparison between cell types showed that expression levels were consistently upregulated to a greater extent in AD-MSCs than in BM-MSCs.

SGAG content

AD-MSCs in type I collagen hydrogels showed significant increases in the sGAG/DNA content within the constructs after stimulation with TGF-β (265.00 μg ±27.71) and GDF6 (243.53 μg ± 13.87), whereas BM-MSCs displayed significant increases only after TGF-β stimulation (215.59 μg ± 28.74) compared with controls (Figure 3A). AD-MSCs consistently demonstrated higher levels of sGAG/DNA compared with BM-MSCs, significantly so in the case of GDF6 stimulation (149.60 μg ±17.05 in BM-MSCs versus 243.53 μg ± 13.87 in AD-MSCs).

The sGAG released into the media over 14 days (Figure 3B) was highest in AD-MSCs treated with GDF6 (103.69 μg ± 8.5 μg), although BM-MSCs and AD-MSCS treated with either TGF-β or GDF6 consistently demonstrated significant increases in released sGAG compared with the control.

The combined total sGAG/DNA from both construct and media showed that AD-MSCs treated with GDF6 produced the most sGAG (3,228.62 μg ± 185.98), and this was significantly higher than the control group (1,703.74 μg ± 72.89), or after treatment with either TGF-β (2,414.88 μg ± 180.79) or GDF5 (2,512.97 μg ±

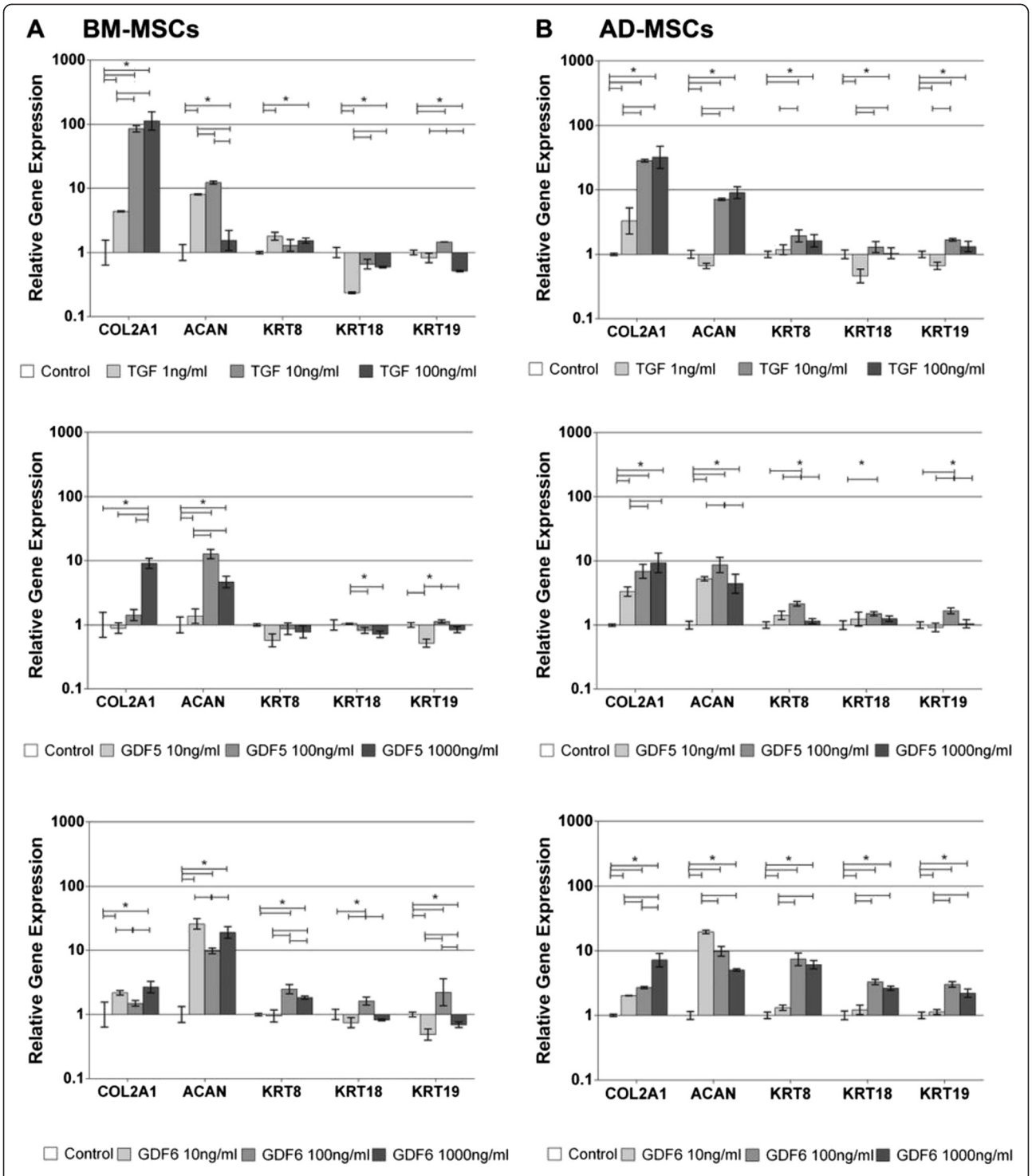

Figure 1 Quantitative real-time PCR analysis of gene expression in response to varying concentrations of growth factors. (A) BM-MSCs and **(B)** AD-MSCs were seeded in type I collagen gels and stimulated with varying concentrations of TGF-β, GDF5, or GDF6 for 14 days. Relative gene expression was normalized to mean housekeeping-gene expression and cells without growth-factor stimulation and plotted on a log scale. $N = 3$; data represent mean ± SEM. *$P < 0.05$.

134.44). Likewise, BM-MSCs synthesized the most sGAG after GDF-6 treatment (2,799.28 μg ±92.33), although this was lower than that produced by AD-MSCs.

Safranin-O staining of type I collagen hydrogels (Figure 3D) demonstrated a more-widespread distribution of sGAG within the GDF6-stimulated AD-MSC

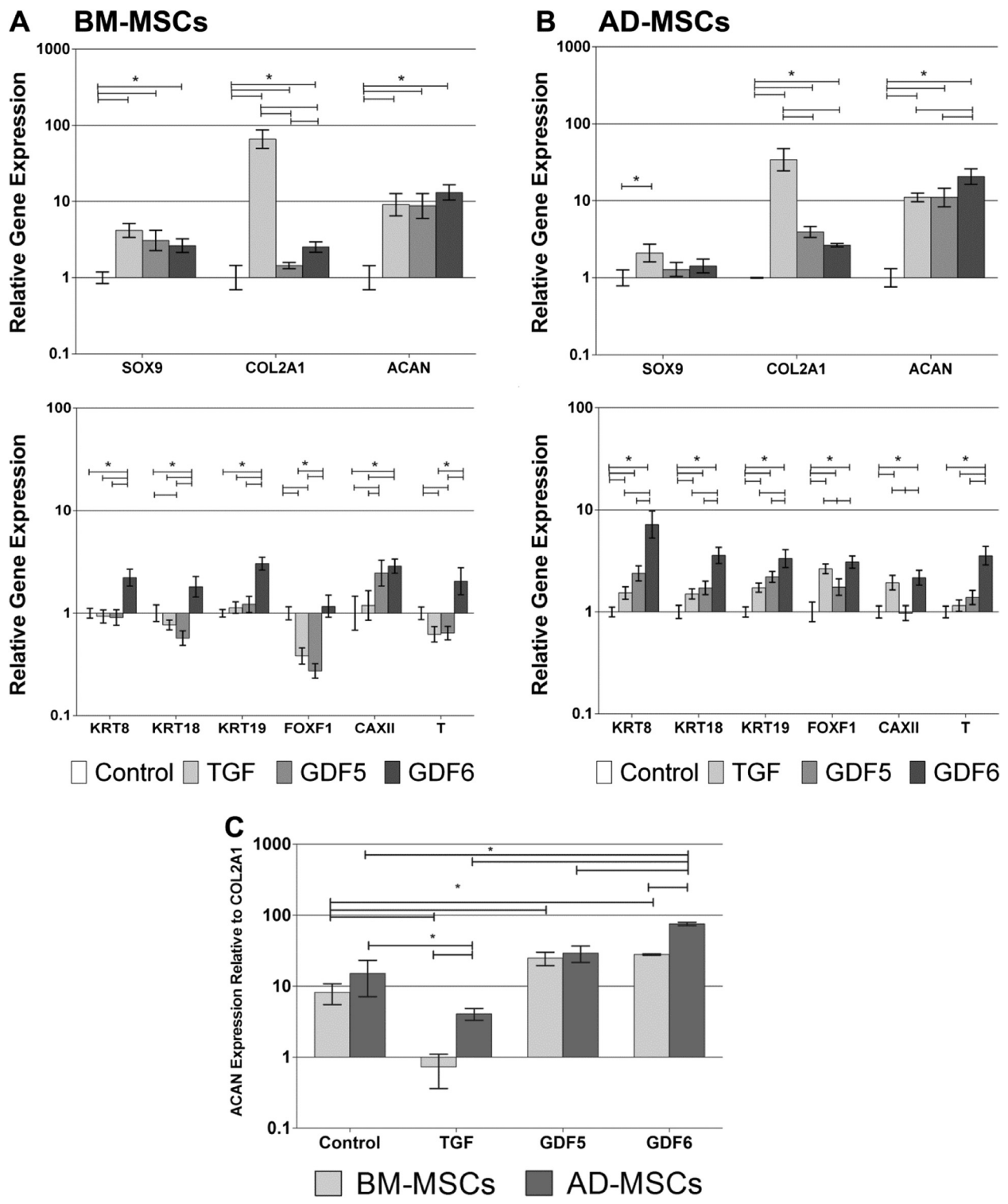

Figure 2 Quantitative real-time PCR analysis of gene-expression changes in response to growth factor stimulation. (A) BM-MSCs, and **(B)** AD-MSCs were cultured for 14 days in type I collagen hydrogels and stimulated with optimal concentrations of TGF-β, GDF5, or GDF6. Relative gene expression was normalized to mean housekeeping-gene expression and cells without growth factor stimulation and plotted on a log scale. **(C)** Aggrecan-to-type II collagen gene expression ratio in BM and AD-MSCs after culture in type I collagen hydrogels for 14 days with either no growth factor, or optimal concentrations of TGF-β, GDF5, or GDF6. Relative gene expression was normalized to mean housekeeping-gene expression and plotted on a log scale. $N = 7$; all data represent mean ± SEM. $^*P < 0.05$.

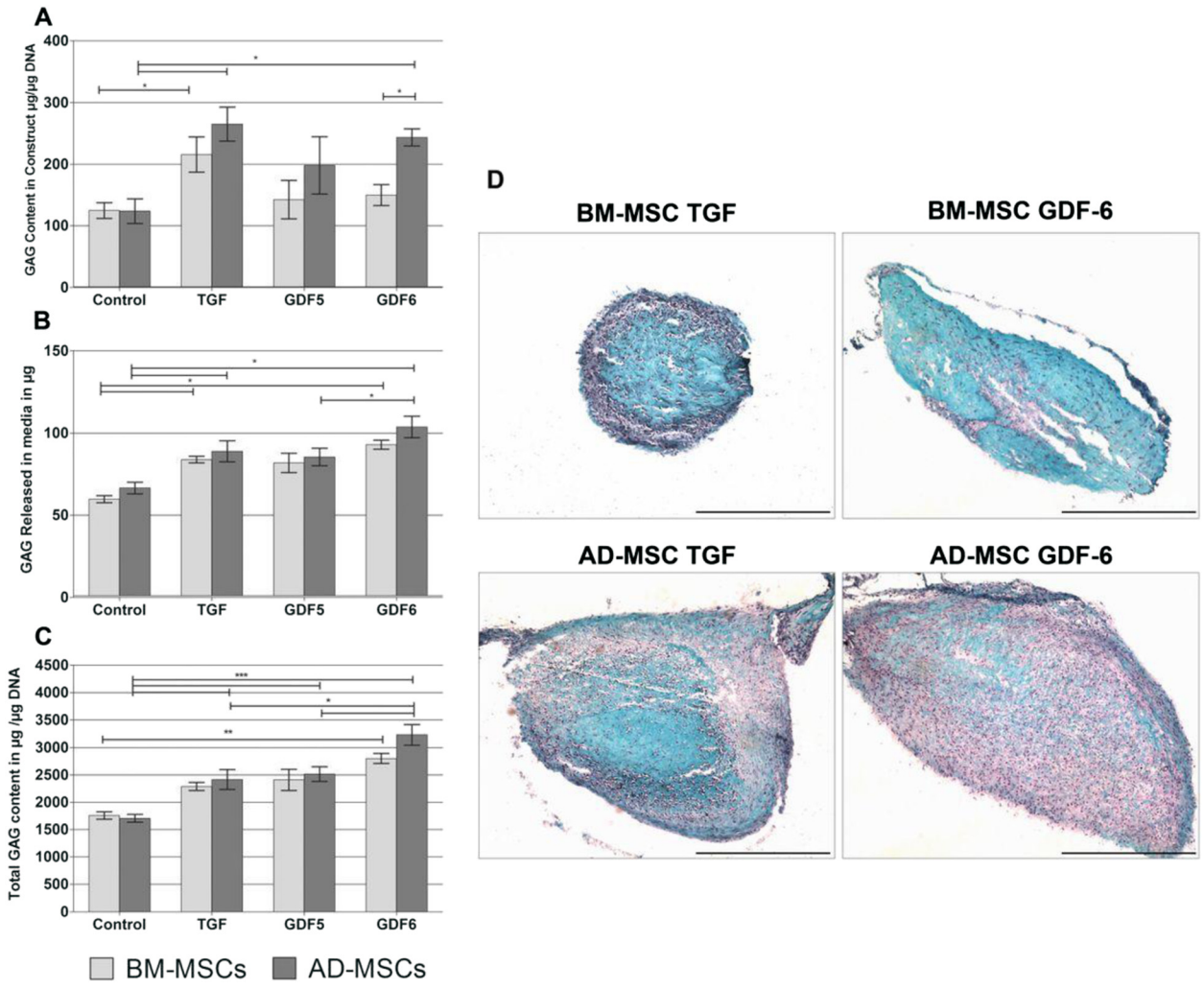

Figure 3 Analysis of sGAG production by BM and AD-MSCs in response to growth-factor stimulation. BM and AD-MSCs were seeded in type I collagen hydrogels and cultured in the absence or presence of TGF-β, GDF5, or GDF6. **(A)** DMMB quantification of sGAG retained within gel constructs, normalized to DNA content within the construct. **(B)** DMMB quantification of sGAG released cumulatively into the media throughout the culture period. **(C)** Quantification of total sGAG content in the construct and media normalized to DNA content within the construct at day 14. $N = 3$, data represent mean ± SEM. *$P < 0.05$. **(D)** Safranin O staining of MSC-seeded collagen gels demonstrating deposition of sGAG throughout the constructs, with AD-MSCs stimulated with GDF6 having the highest and most homogeneous sGAG deposition. Scale bars, 500 µm.

constructs compared with TGF-β-stimulated constructs. BM-MSCs treated with TGF-β showed staining confined to the periphery of the construct only, whereas AD-MSCs treated with either TGF-β or GDF6 demonstrated a more-homogeneous distribution throughout the construct.

Fibrillar collagen content and local stiffness

Fibrillar collagen deposition by BM-MSCs was independent of growth factor species (Figure 4; TGF-β, 15.4% ± 0.6%; GDF6, 16.0% ± 1.07%). In contrast, exposure to exogenous TGF-β and GDF6 induced significant differences in the deposition of fibrillar collagens by AD-MSCs (Figure 4; TGF-β, 19.5% ± 0.9%; GDF6, 16.2% ± 0.7%). These MSC source and growth factor-related differences in fibrillar collagen content were, in turn, correlated with the mean acoustic wave speed (and hence stiffness) of the tissue constructs. Whereas mean acoustic wave speed in TGF-β- and GDF6-treated BM-MSC constructs was growth factor independent (Figure 5; TGF-β, 1,629 ms^{-1} ± 8 ms^{-1}; GDF6, 1,642 ms^{-1} ± 17 ms^{-1}), acoustic-wave speed was significantly higher in TGF-β-treated AD-MSC seeded constructs compared with their GDF6-treated counterparts (Figure 5; TGF-β, 1,644 ms^{-1} ± 1 ms^{-1}; GDF6, 1,599 ms^{-1} ± 4 ms^{-1}).

MSC differentiation in pellet culture

To control for any influence of the reconstituted type I collagen hydrogels on differentiation, MSCs were cultured in three-dimensional pellets. Levels of conventional NP marker-gene expression (Figure 6A, B) were similar to

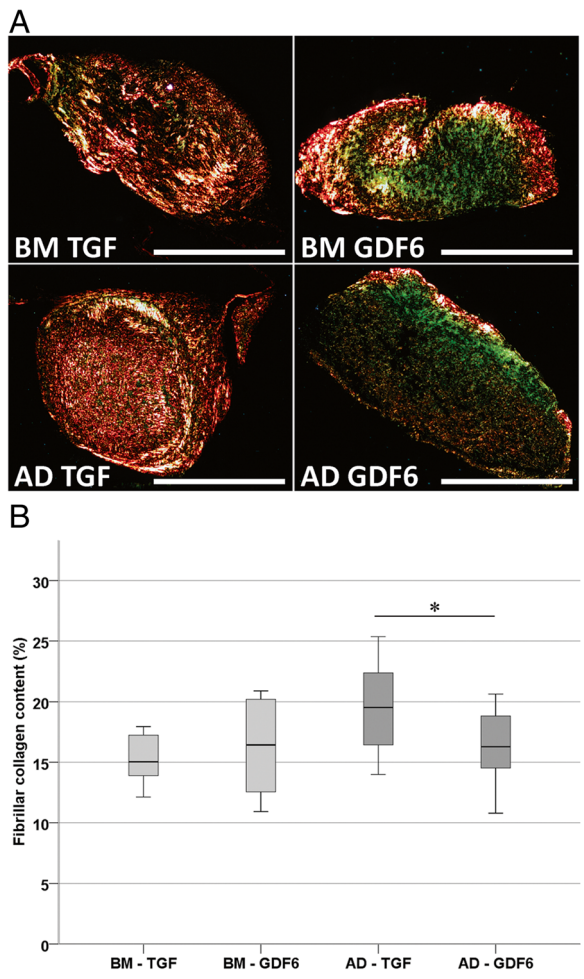

Figure 4 Fibrillar collagen content visualized by using polarized light microscopy of picrosirius red-stained sections. **(A)** Picrosirius red staining of MSC-seeded type I collagen hydrogels stimulated with TGF-β or GDF6, demonstrating enhanced fibrillar collagen deposition (red and green stains) in AD-MSC-seeded constructs stimulated with TGF-β compared with GDF6-stimulated constructs. Scale bar, 500 μm. **(B)** Quantification of percentage fibrillar collagen content in BM-MSC- and AD-MSC-seeded constructs after stimulation with TGF-β or GDF6. AD-MSC-seeded constructs stimulated with TGF-β demonstrated a significantly higher percentage of fibrillar collagen content compared with GDF-6-stimulated constructs; $N = 3$.

that seen previously, with AD-MSCs showing the highest upregulation of *ACAN* after GDF6 stimulation, whereas TGF-β induced the largest increase in *COL2A1* expression in both cell types. BM-MSCs demonstrated either no change or a downregulation of novel NP marker genes after TGF-β or GDF5 stimulation, with GDF6 causing significant upregulation of *KRTs 8*, *18*, and *19*, *FOXF1*, *CAXII*, and *T* (as with type I collagen hydrogels). In AD-MSCs, GDF6 caused a significant upregulation of all marker genes, with increases in *KRT8*, *18*, *19*, *CAXII*, and *T* being significantly higher after GDF6 stimulation than with either TGF-β or GDF5.

The ratio of *ACAN*-to-*COL2A1* in BM-MSCs and AD-MSCs was higher in both GDF5 and GDF6 groups compared with either controls or TGF-β-treated cells, with no significant difference identified between the two cell types after stimulation with any of the growth factors (Figure 6C).

Total GAG/DNA from both pellets and accumulated media showed that AD-MSCs treated with GDF6 had the highest total value (3,556.31 μg ± 133.06), and this was significantly higher than both the control (2,206.34 μg ± 267.54), and after treatment with either TGF-β (2,540.32 μg ± 32.78) or GDF5 (2,886.65 μg ± 225.76) (Figure 6D).

Discussion

Given the similarities in gene-expression profiles between articular chondrocytes and NP cells, specifically expression of *SOX-9*, type II collagen, and aggrecan, researchers have increasingly investigated the potential of MSCs to regenerate the IVD. However, to date, studies have applied methods more commonly used to induce chondrogenesis, specifically, culture in a 3D environment and differentiating media containing TGF-β and thereafter using ECM gene and protein expression as outcome measures to depict an NP-like tissue.

However, the differences in matrix composition between articular cartilage and NP tissue, together with recent phenotypic profiling studies comparing their native cells, suggest that these outcome measures are insufficient to define the end-stage differentiated cell and that more-detailed analyses are needed. Given the increased understanding of the NP cell phenotype, unique phenotypic markers can now be used to define accurately the lineage-specific MSC differentiation toward NP-like cells. This has allowed alternative culture systems, in particular, comparison of different growth factors, to be investigated with the aim of optimizing MSC discogenic differentiation and ensuring synthesis of an ECM with appropriate biochemical and biomechanical properties.

Members of the TGF-β superfamily are potential candidates for driving discogenic differentiation, with a recent study showing that GDF5 induces differentiation of MSCs *in vitro* to a more-IVD-like phenotype than TGF-β [17-19]. Given that we previously demonstrated expression of GDF5 and GDF6 by human NP cells [16] and that both AD-MSCs and BM-MSCs can differentiate to NP-like cells [6], here we aimed to investigate whether GDF6 may be a more-appropriate stimulus for MSC discogenic differentiation and production of an NP-like ECM than either TGF-β or GDF5.

Stimulation of both AD-MSCs and BM-MSCs with GDF6 resulted in increased expression of novel NP phenotypic marker genes *KRT8*, *18*, and *19*, *FOXF1* and *CAXII*, compared with either TGF-β or GDF5, particularly

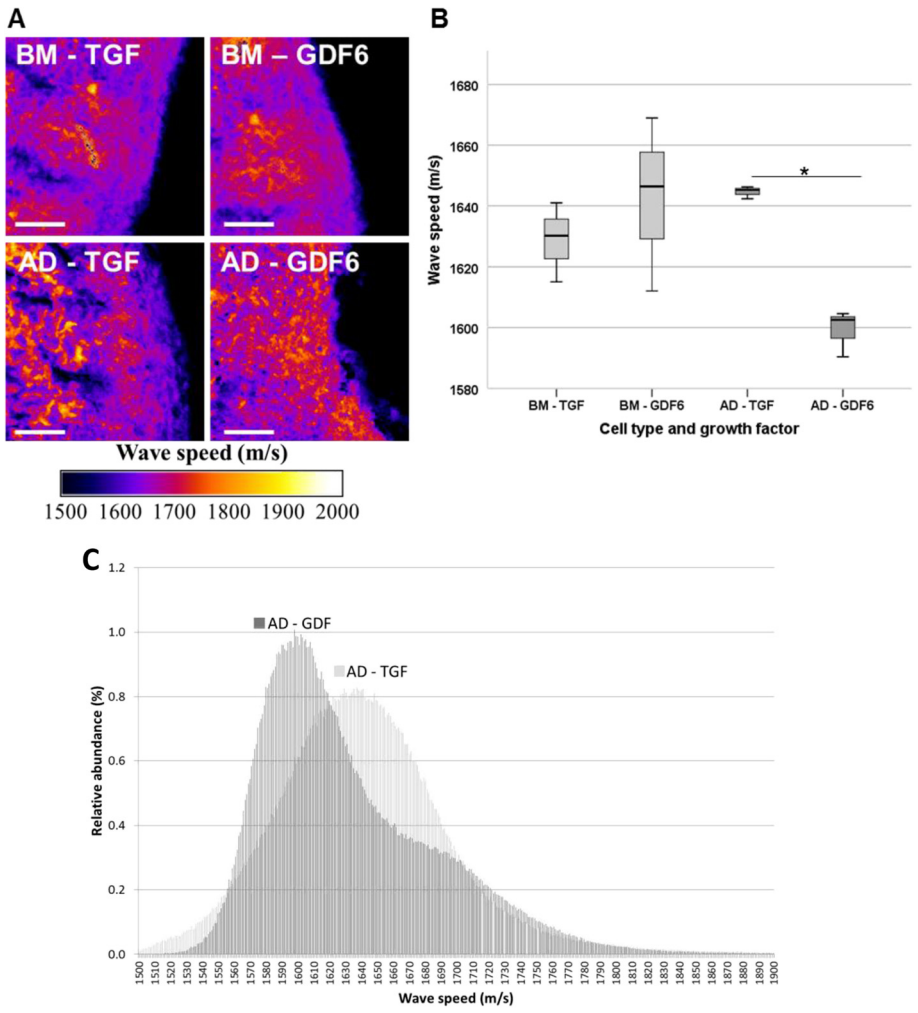

Figure 5 Mean acoustic wave speed (a surrogate measure of tissue stiffness) assessed with scanning acoustic microscopy. (A) Acoustic wave-speed distribution maps of BM-MSC- and AD-MSC-seeded type I collagen hydrogels stimulated with TGF-β or GDF6. Scale bar, 50 μm. **(B)** Quantification of wave speed in BM-MSC- and AD-MSC-seeded constructs after stimulation with TGF-β or GDF6. GDF6 stimulation of AD-MSCs resulted in a significantly decreased acoustic-wave speed compared with TGF-β-stimulated constructs, suggesting that GDF6-stimulated AD-MSC produced a less-stiff ECM. $N = 3$. $^*P < 0.05$. **(C)** Wave-speed distribution in AD-MSC-seeded constructs after stimulation with either TGF-β or GDF6. The GDF6-stimulated construct shows significantly reduced mean wave speed of 1,599 ms^{-1} compared with the TGF-β-stimulated counterpart, 1,644 ms^{-1}.

in AD-MSCs. Given that this panel of markers has been identified as NP specific and previously used to depict appropriate differentiation [6,9] , the observed increases in gene expression suggest that both AD-MSCs are BM-MSCs are capable of discogenic differentiation, which is particularly enhanced by GDF6.

We also investigated the expression of the notochordal and mesodermal marker brachyury (*T*), which has previously been shown to be expressed by adult NP cells [9] and demonstrated the greatest induction of gene expression after GDF6 stimulation, again particularly in AD-MSCs. Importantly, these findings were consistent with both cell types in both type I collagen hydrogel and pellet cultures, suggesting that the biomaterial did not influence differentiation, with growth-factor choice having the predominant effect on discogenic differentiation.

The molecules aggrecan and type II collagen are key components of the IVD ECM, with a higher aggrecan-to-type II collagen ratio (both at the gene transcription [17] and protein [8] level being indicative of an NP-like, rather than articular cartilage-like phenotype/matrix). As expected [32,33], stimulation of both BM-MSCs and AD-MSCs with TGF-β resulted in the highest *COL2A1* gene expression and lowest *ACAN*-to-*COL2A1* ratio. When combined with the decrease or small upregulation of novel NP marker genes in BM-MSCs and AD-MSCS, respectively, and the increased expression of *SOX-9* (major transcription factor for chondrogenesis), the data

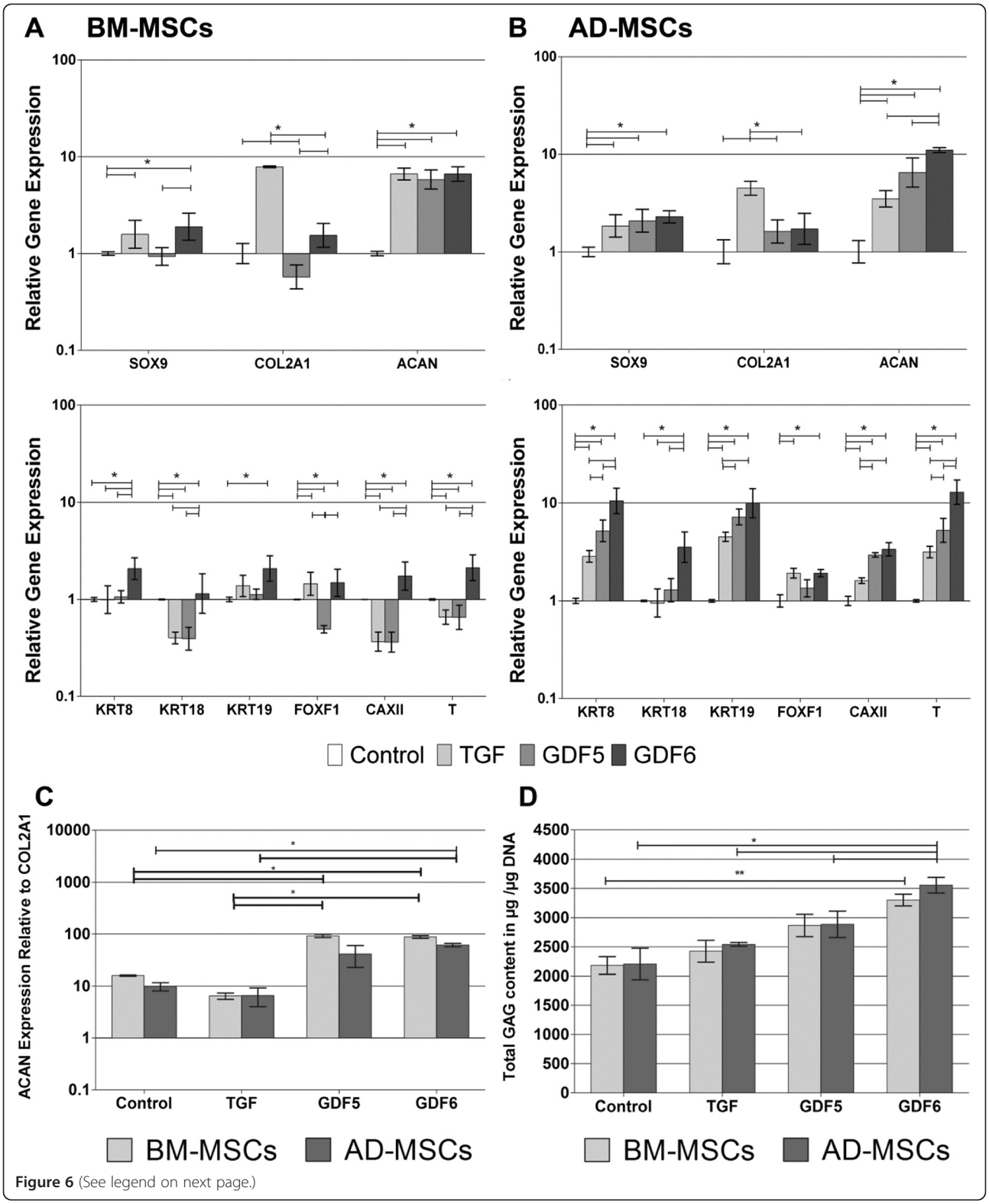

Figure 6 (See legend on next page.)

(See figure on previous page.)
Figure 6 Analysis of BM and AD-MSC response to growth-factor stimulation in pellet culture. Quantitative real-time PCR analysis of gene-expression changes in **(A)**, BM-MSCs and **(B)**, AD-MSCs in pellets in the absence or presence of TGF-β, GDF5, or GDF6. Relative gene expression was normalized to mean housekeeping-gene expression and cells without growth-factor stimulation and plotted on a log scale. **(C)** Aggrecan-to-type II collagen gene-expression ratio in BM and AD-MSCs after culture in type I collagen hydrogels for 14 days with either no growth factor, TGF-β, GDF5, or GDF6. Relative gene expression was normalized to mean housekeeping-gene expression and plotted on a log scale. **(D)** DMMB quantification of sGAG content within pellets and cumulative release into media over 14 days normalized to DNA content of the pellet at day 14. For all analyses, $N = 3$; data represent mean ± SEM. $^*P < 0.05$.

suggest that TGF-β is driving differentiation more toward a chondrocyte-like phenotype. Conversely, as was previously reported, GDF5 promoted *ACAN* gene expression, and resulted in an increased *ACAN*-to-*COL2A1* ratio compared with TGF-β stimulation [17,18]. Although stimulation of BM-MSCs with GDF6 resulted in a similar response to that of GDF5, AD-MSCs stimulated with GDF6 produced significantly higher levels of *ACAN* and demonstrated the highest *ACAN*-to-*COL2A1* ratio, indicative of an NP-like phenotype. Importantly, this gene-expression analysis (as assessed by using both conventional and novel NP markers, as well as *ACAN*-to-*COL2A1* ratio) has shown that GDF6 promotes discogenic differentiation of both BM-MSCs and AD-MSCs, with gene-expression changes being greatest in AD-MSCs, suggesting that these cells may be more able to differentiate to an NP-like phenotype.

Further to characterize these differences between the differentiated cell populations and to ensure that changes in gene expression were reflected at the protein level, analysis of sGAG synthesis was assessed. Cells under all conditions synthesized detectable levels of sGAG, with significant increases in retained sGAG (normalized to DNA) seen after TGF-β stimulation in both BM-MSCs and AD-MSCs, and after both TGF-β and GDF6 stimulation in AD-MSCs. A substantial amount of sGAG was also released into the media by all cells, with significant increases again being seen in both cell types after stimulation with either TGF-β or GDF6. Whereas the majority of newly synthesized sGAG was not retained within the constructs, similar findings have been observed in other comparable studies [19,34]. This may be due to the fiber density of the matrix produced, with differences in collagen synthesis or remodeling of the collagen hydrogel altering matrix retention.

However, when total sGAG synthesis was analyzed and normalized to DNA content, significantly more sGAG was synthesized by AD-MSCs after stimulation with all three growth factors, with AD-MSCs stimulated with GDF6 producing the most sGAG. Interestingly, GDF5 did not result in significant increases in sGAG synthesis in either cell type, a finding that has been reported for BM-MSCs previously [18]. As with the gene-expression profile, DMMB analysis revealed similar results after pellet culture, with GDF6-stimulated BM- and AD-MSCs synthesizing the largest amount of sGAGs. Interestingly, safranin-O staining of the collagen constructs also highlighted differences, whereas AD-MSCs stimulated with either TGF-β or GDF6 demonstrated more-intense safranin O staining than BM-MSCs, supporting the DMMB analysis on retained sGAG.

Additionally, a homogeneous GAG distribution was observed throughout the construct compared with the more-focal/discrete staining in BM-MSC constructs. Overall, given that GDF6-stimulated AD-MSCs produce the highest levels of sGAG and the most homogeneous matrix deposition, this cell type and stimulation may be the more-appropriate choice for regeneration of the PG-rich NP, whereas TGF-β may promote a more-articular cartilage-like matrix.

Although the majority of studies to date have relied on molecular and biochemical methods to characterize the ability of tissue-construct systems to mimic the target tissues, the micro- and hence macromechanical behavior of the construct is likely to influence the efficacy of any resulting therapy. Therefore, in this study, we quantified the acoustic-wave speed [23] of tissue-construct cryosections (which is proportional to the square root of the material's Young modulus (stiffness)) [35]. Having previously used SAM to localize age-related changes in vascular stiffness [24], here we demonstrate that a refined version of this technique (MLPA) is able to distinguish cell- and cytokine-specific effects on the resultant micromechanical behavior of tissue constructs. Furthermore, these effects are in concordance with our other findings that AD-MSC-seeded constructs treated with GDF6 showed decreased fibrillar collagen and increased proteoglycan deposition when compared with their TGF-β-treated counterparts.

AD-MSCs are thought to be better candidates for cell therapy because of their ease of access, limited donor-site morbidity, and high proliferation rate. Importantly, this study demonstrated differences in regenerative potential for IVD application between BM-MSCs and AD-MSCs, with the data suggesting that AD-MSCs are more able to undergo discogenic differentiation and produce an appropriate PG-like matrix. It was previously reported that AD-MSCs have a reduced capacity to differentiate to a chondrogenic lineage compared with BM-MSCs [36] because of differences in receptor expression (specifically, TGF-β receptor I [36]) compared with BM-MSCS. As

such, the differential effects of the exogenous growth factors used here (with TGF-β stimulating more of a chondrogenic phenotype and GDF-6, an NP- like phenotype and matrix) may be due to differences in cell-signaling pathways despite all being members of the TGF-β superfamily. TGF-β3 is recognized by type II (TGFRII) and type I surface receptors (ALK5, ALK1), which in turn facilitate the Smad 2/3 signaling pathway.

Conversely, GDF5 and GDF6 use BMPRII, ActRIIa, ALK3, and ALK6 receptors activating the alternative Smad 1/5/8 pathway [37]. Activation of these distinct signaling pathways may then lead to different downstream signals, which may explain the more-chondrogenic nature of TGF-β3 stimulation. GDF5 and GDF6 are 82% homologous in the highly conserved active C-terminal (mature signaling) domain [38] and are thus likely to operate by similar ligand/receptor interactions. However, recent evidence reporting differential effects of these factors on mouse calvarial osteogenesis [39] would suggest that these growth factors may have distinct signaling effects, despite similar receptor use, which could also account for the differential effects seen here, although elucidation of the signaling mechanisms is beyond the scope of this article.

Conclusion

The phenotype of differentiated cells, together with the ECM composition and micromechanics of tissue-engineered constructs, must be extensively characterized to ascertain that an appropriately functioning tissue is formed. In this study, we demonstrated differentiation of MSCs to an NP-like phenotype and formation of appropriate NP ECM components. Interestingly, AD-MSCs treated with GDF6 produced a less-stiff, PG-rich matrix, which may be more indicative of the native healthy NP ECM.

Abbreviations

AD-MSC: Adipose-derived mesenchymal stem cell; BM-MSC: bone marrow-derived mesenchymal stem cell; BMP: bone morphogenic protein; DMMB: dimethylmethylene blue; ECM: extracellular matrix; GDF5: growth differentiation factor 5; GDF6: growth differentiation factor 6; IVD: intervertebral disc; LBP: low back pain; NP: nucleus pulposus; PG: proteoglycan; SAM: scanning acoustic microscopy; sGAG: sulfated glycosaminoglycan; TGF: transforming growth factor.

Competing interests

All authors state that no conflict of interests exists.

Authors' contributions

LEC, Conception and design, collection and/or assembly of data, data analysis and interpretation, manuscript writing. JCM, conception and design, collection and/or assembly of data, data analysis and interpretation, manuscript writing. MJS, conception and design, data analysis and interpretation, manuscript writing. BD, data analysis and interpretation, critical revision, final approval of manuscript. SMR, co-investigator for securing funding, conception and design, data analysis and interpretation, manuscript writing, final approval of manuscript. JAH, secured funding, conception, and design, data analysis and interpretation, manuscript writing, final approval of manuscript. All authors read and approved the final manuscript.

Acknowledgements

We gratefully acknowledge The University of Manchester for funding a Faculty of Medical and Human Sciences PhD studentship to LEC. The Research Councils UK (RCUK) is acknowledged for funding a fellowship (grant EP/E500048/1) to SMR. BD and MJS acknowledge the support of the Medical Research Council grant G1001398 (Quantifying age-related changes in the mechanical properties of tissues). Technical support for this project (Sonal Patel) was funded by the National Institute for Health Research Manchester Musculoskeletal Biomedical Research Unit. The views expressed in this publication are those of the authors and not necessarily those of the NHS, the National Institute for Health Research, or the Department of Health.

Author details

[1]Centre for Tissue Injury and Repair, Institute of Inflammation and Repair, Faculty of Medical and Human Sciences, The University of Manchester, Oxford Road, Manchester M13 9PT, UK. [2]Wellcome Trust Centre for Cell-Matrix Research, Faculty of Life Sciences, The University of Manchester, Manchester, UK. [3]School of Materials, Faculty of Engineering and Physical Sciences, The University of Manchester, Manchester, UK. [4]NIHR Manchester Musculoskeletal Biomedical Research Unit, Central Manchester University Hospitals NHS Foundation Trust, Manchester Academic Health Science Centre, Nowgen Building, 29 Grafton Street, Manchester M13 9WU, UK.

Received: 14 November 2013 Accepted: 25 February 2014
Published: 12 March 2014

References

1. Cheung KM, Karppinen J, Chan D, Ho DW, Song YQ, Sham P, Cheah KS, Leong JC, Luk KD: **Prevalence and pattern of lumbar magnetic resonance imaging changes in a population study of one thousand forty-three individuals.** *Spine (Phila)* 2009, **34:**934–940.
2. Roughley PJ: **Biology of intervertebral disc aging and degeneration: involvement of the extracellular matrix.** *Spine (Phila)* 2004, **29:**2691–2699.
3. Adams MA, Roughley PJ: **What is intervertebral disc degeneration, and what causes it?** *Spine (Phila)* 2006, **31:**2151–2161.
4. Pittenger MF, Mackay AM, Beck SC, Jaiswal RK, Douglas R, Mosca JD, Moorman MA, Simonetti DW, Craig S, Marshak DR: **Multilineage potential of adult human mesenchymal stem cells.** *Science* 1999, **284:**143–147.
5. Richardson SM, Curran JM, Chen R, Vaughan-Thomas A, Hunt JA, Freemont AJ, Hoyland JA: **The differentiation of bone marrow mesenchymal stem cells into chondrocyte-like cells on poly-L-lactic acid (PLLA) scaffolds.** *Biomaterials* 2006, **27:**4069–4078.
6. Minogue BM, Richardson SM, Zeef LA, Freemont AJ, Hoyland JA: **Characterization of the human nucleus pulposus cell phenotype and evaluation of novel marker gene expression to define adult stem cell differentiation.** *Arthritis Rheum* 2010, **62:**3695–3705.
7. Sive JI, Baird P, Jeziorsk M, Watkins A, Hoyland JA, Freemont AJ: **Expression of chondrocyte markers by cells of normal and degenerate intervertebral discs.** *Mol Pathol* 2002, **55:**91–97.
8. Mwale F, Roughley P, Antoniou J: **Distinction between the extracellular matrix of the nucleus pulposus and hyaline cartilage: a requisite for tissue engineering of intervertebral disc.** *Eur Cell Mater* 2004, **8:**58–64.
9. Minouge BM, Richardson SM, Zeef LA, Freemont AJ, Hoyland JA: **Transcriptional profiling of bovine intervertebral disc cells: implications for identification of normal and degenerate human intervertebral disc cell phenotypes.** *Arthritis Res Ther* 2010, **12:**R22.
10. Bailey AJ: **Molecular mechanisms of ageing in connective tissues.** *Mech Ageing Dev* 2001, **122:**735–755.
11. Akhtar R, Sherratt MJ, Cruickshank JK, Derby B: **Characterizing the elastic properties of tissues.** *Mater Today (Kidlington)* 2011, **14:**96–105.
12. Sherratt MJ: **Tissue elasticity and the ageing elastic fibre.** *Age (Dordr)* 2009, **31:**305–325.
13. Karsenty G, Wagner EF: **Reaching a genetic and molecular understanding of skeletal development.** *Dev Cell* 2002, **2:**389–406.
14. Settle SH Jr, Rountree RB, Sinha A, Thacker A, Higgins K, Kingsley DM: **Multiple joint and skeletal patterning defects caused by single and double mutations in the mouse Gdf6 and Gdf5 genes.** *Dev Biol* 2003, **254:**116–130.
15. Asai-Coakwell M, French CR, Ye M, Garcha K, Bigot K, Perera AG, Staehling-Hampton K, Mema SC, Chanda B, Mushegian A, Bamforth S, Doschak MR, Li G, Dobbs MB, Giampietro PF, Brooks BP, Vijayalakshmi P, Sauvé Y, Abitbol M,

Sundaresan P, van Heyningen V, Pourquié O, Underhill TM, Waskiewicz AJ, Lehmann OJ: **Incomplete penetrance and phenotypic variability characterize Gdf6-attributable oculo-skeletal phenotypes.** *Hum Mol Genet* 2009, **18:**1110–1121.

16. Le Maitre CL, Freemont AJ, Hoyland JA: **Expression of cartilage-derived morphogenetic protein in human intervertebral discs and its effect on matrix synthesis in degenerate human nucleus pulposus cells.** *Arthritis Res Ther* 2009, **11:**R137.
17. Gantenbein-Ritter B, Benneker LM, Alini M, Grad S: **Differential response of human bone marrow stromal cells to either TGF-β (1) or rhGDF-5.** *Eur Spine J* 2011, **20:**962–971.
18. Stoyanov JV, Gantenbein-Ritter B, Bertolo A, Aebli N, Baur M, Alini M, Grad S: **Role of hypoxia and growth differentiation factor-5 on differentiation of human mesenchymal stem cells toward intervertebral nucleus pulposus like cells.** *Eur Cell Mater* 2011, **21:**533–547.
19. Peroglio M, Eglin D, Benneker LM, Alini M, Grad S: **Thermoreversible hyaluronan-based hydrogel supports in vitro and ex vivo disc-like differentiation of human mesenchymal stem cells.** *Spine J* 2013 (in press).
20. Feng G, Wan Y, Balian G, Laurencin CT, Li X: **Adenovirus-mediated expression of growth and differentiation factor-5 promotes chondrogenesis of adipose stem cells.** *Growth Factors* 2008, **26:**132–142.
21. Tassabehji M, Fang ZM, Hilton EN, McGaughran J, Zhao Z, de Bock CE, Howard E, Malass M, Donnai D, Diwan A, Manson FD, Murrell D, Clarke RA: **Mutations in GDF6 are associated with vertebral segmentation defects in Klippel-Feil syndrome.** *Hum Mutat* 2008, **29:**1017–1027.
22. Wei A, Williams LA, Bhargav D, Shen B, Kishen T, Duffy N, Diwan AD: **BMP13 prevents the effects of annular injury in an ovine model.** *Int J Biol Sci* 2009, **5:**388–396.
23. Zhao X, Akhtar R, Nijenhuis N, Wilkinson SJ, Murphy L, Ballestrem C, Sherratt MJ, Watson RE, Derby B: **Multi-layer phase analysis: quantifying the elastic properties of soft tissue and live cells with ultra-high-frequency scanning acoustic microscopy.** *IEEE Trans Ultrason Ferroelectr Freq Control* 2012, **59:**610–620.
24. Graham HK, Akhtar R, Kridiotis C, Derby B, Kundu T, Trafford AW, Sherratt MJ: **Localised micro-mechanical stiffening in the ageing aorta.** *Mech Ageing Dev* 2011, **132:**459–467.
25. Strassburg S, Richardson SM, Freemont AJ, Hoyland JA: **Co-culture induces mesenchymal stem cell differentiation and modulation of the degenerate human nucleus pulposus cell phenotype.** *Regen Med* 2010, **5:**701–711.
26. Purmessur D, Schek RM, Abbott RD, Ballif BA, Godburn KE, Iatridis JC: **Notochordal conditioned media from tissue increases proteoglycan accumulation and promotes a healthy nucleus pulposus phenotype in human mesenchymal stem cells.** *Arthritis Res Ther* 2011, **13:**R81.
27. Shen B, Bhargav D, Wei A, Williams LA, Tao H, Ma DD, Diwan AD: **BMP-13 emerges as a potential inhibitor of bone formation.** *Int J Biol Sci* 2009, **5:**192–200.
28. Livak KJ, Schmittgen TD: **Analysis of relative gene expression data using real-time quantitative PCR and the 2(−Delta Delta C(T)) method.** *Methods* 2001, **25:**402–408.
29. Farndale RW, Buttle DJ, Barrett AJ: **Improved quantitation and discrimination of sulphated glycosaminoglycans by use of dimethylene blue.** *Biochim Biophys Acta* 1986, **883:**173–177.
30. Richardson SM, Hughes N, Hunt JA, Freemont AJ, Hoyland JA: **Human mesenchymal stem cell differentiation to NP-like cells in chitosan-glycerophosphate hydrogels.** *Biomaterials* 2008, **29:**85–93.
31. Graham HK, Trafford AW: **Spatial disruption and enhanced degradation of collagen with the transition from compensated ventricular hypertrophy to symptomatic congestive heart failure.** *Am J Physiol Heart Circ Physiol* 2007, **292:**H1364–H1372.
32. Li Z, Kupcsik L, Yao SJ, Alini M, Stoddart MJ: **Chondrogenesis of human bone marrow mesenchymal stem cells in fibrin-polyurethane composites.** *Tissue Eng Part A* 2009, **15:**1729–1737.
33. Clouet J, Grimandi G, Pot-Vaucel M, Masson M, Fellah HB, Guigand L, Cherel Y, Bord E, Rannou F, Weiss P, Guicheux J, Vinatier C: **Identification of phenotypic discriminating markers for intervertebral disc cells and articular chondrocytes.** *Rheumatology* 2009, **48:**1447–1450.
34. Buckley CT, Kelly DJ: **Expansion in the presence of FGF-2 enhances the functional development of cartilaginous tissues engineered using infrapatellar fat pad derived MSCs.** *J Mech Behav Biomed Mater* 2012, **11:**102–111.
35. Turner CH: **The elastic properties of trabecular and cortical bone tissues are similar: results from two microscopic measurement techniques.** *J Biomech* 1999, **32:**437–441.
36. Hennig T, Lorenz H, Thiel A, Goetzke K, Dickhut A, Geiger F, Richter W: **Reduced chondrogenic potential of adipose tissue derived stromal cells correlates with an altered TGF beta receptor and BMP profile and is overcome by BMP-6.** *J Cell Physiol* 2007, **211:**682–691.
37. Mazerbourg S, Sangkuhl K, Luo CW, Sudo S, Klein C, Hsueh AJ: **Identification of receptors and signalling pathways for orphan bone morphogenetic protein/growth differentiation factor ligands based on genomic analyses.** *J Biol Chem* 2005, **280:**32122–32132.
38. Williams LA, Bhargav D, Diwan AD: **Unveiling the bmp 13 enigma: redundant morphogen or crucial regulator?** *Int J Biol Sci* 2008, **4:**318–329.
39. Clendenning DE, Mortlock DP: **The BMP ligand Gdf6 prevents differentiation of coronal suture mesenchyme in early cranial development.** *PLoS One* 2012, **7:**e36789.

doi:10.1186/ar4505
Cite this article as: Clarke *et al.*: Growth differentiation factor 6 and transforming growth factor-beta differentially mediate mesenchymal stem cell differentiation, composition, and micromechanical properties of nucleus pulposus constructs. *Arthritis Research & Therapy* 2014 **16:**R67.